C.R-171986

STS84-0013

6.4 PERCENT SCALE MODEL SSV SRM/SSME IGNITION OVERPRESSURE VERIFICATION TESTING FOR WESTERN TEST RANGE:
TEST PROGRAM AT MSFC

MARCH 1984

CONTRACT: NAS 9-14000

IRD NO.: TM-474D

WBS: 10.2.1

(NASA-CR-171986) THE 6.4 PERCENT SCALE
MCDEL SSV SRM/SSME IGNITION OVERFRESSURE

N87-70572

VERIFICATION TESTING FOR WESTERN TEST RANGE:
TEST FROGRAM AT MSFC (Rockwell

International Corp.) 332 p Avail: NTIS

Unclas 00/25 0085572

PREPARED BY:

N. S. Dougherty

A. C. Mansfield

APPROVED BY:

H. Wiener, Project Manager Flight Systems Development

F. S. Laspesa, Supervisor

Airloads Evaluation Shuttle Aerodynamics Murray F. Moore

Director of Engineering Huntsville Operations



`			
			<u>.</u>

STS84-0013

6.4 PERCENT SCALE MODEL SSV SRM/SSME IGNITION OVERPRESSURE VERIFICATION TESTING FOR WESTERN TEST RANGE:
TEST PROGRAM AT MSFC

MARCH 1984

CONTRACT: NAS 9-14000 IRD NO.: TM-474D

WBS: 10.2.1

PREPARED BY:

N. S. Dougherty

A. C. Mansfield

APPROVED BY:

H. Wiener, Project Manager Flight Systems Development

F. S. Laspesa, Supervisor

Airloads Evaluation Shuttle Aerodynamics Murray F. Moore

Director of Engineering Huntsville Operations



			and the
			-

PREFACE

Rockwell has prepared this test data report for tests performed by NASA Marshall Space Flight Center's (MSFC) Test Laboratory at the Acoustic Model Test Facility, Test Stand 116, Redstone Arsenal, Alabama. The report has been prepared under Contract Number NAS 9-14000, IRD No. SE-501D, WBS 10.2.1.

On-site support of the tests including preparation of test requirements, test article geometric and instrumentation verification, test data check/validation/transmittal, and test documentation and reporting were provided by Rockwell International Corporation. The tests were performed at the request of NASA's Johnson Space Center (JSC) under auspices of the Shuttle Ignition Overpressure Working Group comprised of NASA Headquarters, Kennedy Space Center (KSC), JSC, MSFC, the USAF Shuttle Activation Task Force (SATAF) and Space Division (SD), Rockwell International Corporation, Martin Marietta Corporation, and Aerospace Corporation. The working group is chaired by J. A. Wood of JSC.

ABSTRACT

A test program was performed at MSFC to obtain data on the SRM and SSME ignition overpressure environment for Space Shuttle Launches from WTR. The program included a total of seventeen "hot-firing" verification tests and utilized the 6.4 - percent scale model vehicle and launch mount/exhaust duct system with scaled launch mount sound suppression water sprays. environment in model scale was defined using 93 surface - mounted Up to 100 additional model operational overpressure sensing gages. measurements per test defined the test conditions at model SRM and SSME ignition. Test techniques and conditions, instrumentation, model geometric details, data processing and special data manipulations with example results are given for a complete documentation of this test program. Twenty final data packages are appendaged, constituting a complete set of all the overpressure data acquired including reprocessed data from four SRM overpressure screening tests performed earlier. Data were acquired for the first Vandenberg launch baseline configuration with water troughs for SRM overpressure suppression, for a contingency SRB duct - extension muffler for SRM overpressure suppression if the first launch data show it to be needed, and at varied water flow rates for determining the launch mount water effectiveness. More than 95 percent of the data were recovered per test resulting in a comprehensive data set from this test program.

TABLE OF CONTENTS

SECT	ION	TITLE	PAGE
1.0		INTRODUCTION	1-1
2.0		TEST PROGRAM	2-1
	2.1 2.2 2.3 2.4	Overall Program/Procedure	2-2 2-6
3.0		MODEL GEOMETRIC DETAILS	3-1
	3.1 3.2 3.3 3.4 3.5 3.6 3.7	Model Vehicle	3-1 3-6 3-16 3-31 3-66
4.0		DATA RECORDING/PROCESSING	4-1
	4.1 4.2 4.2.1 4.2.2 4.2.3	Typical Time Histories	4-3 4-3 4-6
5.0		RESULTS AND DISCUSSION	5-1
	5.1 5.1.1 5.1.2 5.2 5.3 5.3.1 5.3.2	Model SSME Ignition Data	5-1 5-27 5-31 5-31 5-47 5-63
6.0		SUMMARY OF RESULTS	6-1
		REFERENCES	6-3
		APPENDICES	A-1
		A. "Off-line" Development of the Contingency Muffler	A-1
		B. SRM Model Ignition Excessive Delay	B-1
		C. Spike in Model SRM Chamber Pressure	C-1

ILLUSTRATIONS

Figure		Page
2.4-1	Schematic Diagram of the Model Sound Suppression Water Flow System	2-11
2.4-2	Automatic Sequence Logic Diagram for Single-Model SRM Tests	2-12
2.4-3	Automatic Sequence Logic Diagram for SSME-Only Tests	2-12
2.4-4	Automatic Sequence Logic Diagram for the Full-Model Test	2-13
2.4-5	Water Accumulation Depth Versus Gallons Passed in the Model SRB Exhaust Ducts	2-15
2.4-6	Water Accumulation Depth in Each Model SRB Exhaust Duct as a Function of Time (Full-Model Test)	2-16
2.4-7	Photograph of Water Pooling in the LH Model SRB Exhaust Duct	2-16
2.4-8	Water Accumulation Depth in the LH Model SRB Exhaust Duct as a Function of Time (Single-Motor Test)	2-17
3.1-1	Model Test Arrangement Pitch-Type Tests	3-2
3.1-2	Model Test Arrangement Lateral-Type Tests	3-4
3.1-3	Model SSV Positioning Over the Model Launch Mount	3-5
3.2-1	Model SRM Thiokol TE-M-416 8.31-KS-11,000 Tomahawk Motor	3-7
3.2-2	Typical Model- and Full-Scale SRM Chamber Pressure Ignition Transients	3-7
3.2-3	Enhanced - Performance SRM Nozzle Simulation	3-8
3.2-4	Model SRM Nozzle Extension Mounting Details	. 3-9
3.3-1	Model SSME's	3-12
3.3-2	Model- and Full-Scale SSME Chamber Pressure Ignition Transients	. 3-14
3.4-1	Model SRB and SSME Exhaust Duct Configurations in the 1976 Tests	. 3-17

ILLUSTRATIONS - (CONTINUED)

Figure		Page
3.4-2	SRB Exhaust Ducts Present Configuration	3-18
3.4-3	SRB Exhaust Duct and Pier Details	3-19
3.4-4	Model SSME Exhaust Duct Present Configuration	3-22
3.4-5	ISS "Dog-House" Cover Modification to the Model Launch Mount	3-26
3.4-6	Work Platform Chain Hoist Cover to the Model SSME Exhaust Hole	3-29
3.4-7	Launch Mount Sound Suppression System Water Layout	3-30
3.4-8	Model Launch Mount Water Spray Pattern	3-32
3.4-9	Mdoel Water Nozzle Flow Calibration Data	3-33
3.5-1	Model SRM Chamber Pressure Measurement Location Detail	3-35
3.5-2	Model SRM Case Strain Measurement Locations	3-36
3.5-3	Model SRM Nozzle Exit Static Pressure Measurement Installation	3-37
3.5-4	Overpressure Measurement Locations on the Model Vehicle and Splitter Plate	3-40
3.5-5	Overpressure Measurement Locations on the Model Facility	3-45
3.5-6	Typical Overpressure Measurement Installations on the Model Orbiter Close-up Views	3-49
3.5-7	Model Orbiter Fuselage and Model External Tank Rings of Measurements (Single-Model SRM Tests)	3-53
3.5-8	"Dough-nut" Radiation Baffle for Model Vehicle Measurements	3-67
3.6-1	Geometric Details of the Contingency Muffler	3-68
3.6-2	Overpressure Measurement Locations Inside the Model SRB Exhaust Duct Muffler	3-72

ILLUSTRATIONS - (CONTINUED)

Figure		Page
3.7-1	Water Trough Configuration Details Original Design	3-74
3.7-2	Model Water Trough Installation Single-Motor Tests	3-77
3.7-3	Water Trough Configuration Details Present Design	3-82
3.7-4	Model Water Trough Installation Full-Model Test Configuration	3-84
4.1-1	Overpressure Data Recording Schematic Diagram	4-2
4.2-1	Data Processing Flow Schematic Diagram	4-4
4.2-2	Typical Overpressure Data Plots Model Orbiter Cargo Bay	4-11
4.2-3	Typical Computed Differential Pressure Plot Model Orbiter Cargo Bay	4-12
4.2-4	Typical Distribution of Differential Pressure Peak Amplitude Model Orbiter Cargo Bay "C" Ring	4-13
4.2-5	Example of Filtering Influence on Model SRM Chamber Pressure Rise Data	4-16
4.2-6	Example of Filtering Influence on Model SRM Case Strain Rise Data	4-17
4.2-7	Example of Filtering Influence on an Overpressure Measurement a Low Signal/Noise Case	4-18
4.2-8	Example of Filtering Influence on an Overpressure Measurement a High Signal/Noise Case	4-19

ILLUSTRATIONS (CONTINUED)

Figure		Page
4.2-9	Example of Filtering Influence on a Differential Pressure Computation One Measurement Having Low Signal/Noise	4-20
4.2-10	Example of Filtering Influence on a Differential Pressure Computation Both Measurements Having Higher Signal/Noise	4-22
5.1-1	Typical Tomahawk Motor Chamber and Pyrogen Pressure Transient	5-2
5.1-2	Model SRM Ignition Transient Data Test 5	5-4
5.1-3	Model SRM Ignition Transient Data Test 7	5-9
5.1-4	Typical Computed Model SRM Chamber Pressure and Case Strain Rise Rate Histories Test 6	5-15
5.1-5	Computed Model SRM Chamber Pressure and Case Strain Rise Rate Histories Test 10	5-18
5.1-6	Model SRM Ignition Transient Data Test 8	5-21
5.1-7	Computed SRM Chamber Pressure and Case Strain Rise Rate Histories Test 8	5-24
5.1-8	Model SSME Ignition Transient Data Test 30	5-28
5.3-1	Baseline Model Test Geometry Elevation View	5-34
5.3-2	Baseline Model Test Geometry Plan View	5-36
5.3-3	Example Model SRM Overpressure Data Test 16	5-4 8
5.3-4	Example Model SRM Overpressure Data Test 7	5-50
5.3-5	Example Model SRM Overpressure Data Test 10	5-53
5.3-6	Example Model SRM Overpressure Data Test 8	5-55
5.3-7	Example Model SRM Overpressure Data Test 9	5-57

ILLUSTRATIONS (CONCLUDED)

Figure			Page
5.3-8	Example Model	SRM Overpressure Data Test 12	5-59
5.3-9	Example Model	SRM Overpressure Data Test 14	5-61
5.3-10	Example Model	SRM Overpressure Data Test 15	5-64
5.3-11	Example Model	SRM Overpressure Data Test 40	5-65
5.3-12	Example Model	SSME Overpressure Data Test 40	5-70
5.3-13	Example Model	SSME Overpressure Data Test 30	5-75
5.4-1	Example Model	Muffler Internal Pressure Data Test 8	5-79
5.4-2	Example Model	Muffler Internal Pressure Data Test 9	5-86

TABLES

Table		Page
2.1-1	SRM Overpressure Screening Tests	2-3
2.2-1	SRM Overpressure Verification Tests	2-5
2.3-1	SSME Overpressure Verification Tests	2-8
3.2-1	Tomahawk Motor Performance Characteristics	3-11
3.3-1	Model SSME Performance Characteristics	3-15
3.4-1	Model Launch Mount Water Spray Nozzles Reorientation	3-25
3.4-2	Model Launch Mount Water Spray System Design Parameters	3-30
3.5-1	Overpressure Measurement Locations	3-56
4.2-1	Data Processing Historical Track	4-7
4.2-2	Data Reduction Equations for Single - SRM Test Differentials	4-8
4.2-3	Data Reduction Equations for Dual - SRM and SSME Test Differentials	4-9
5.1-1	Maximum Rise Rate Values in Model SRM Chamber Pressure and Case Strain	5-14
5.2-1	Model SRB Exhaust Duct Water Flowrates at Model SRM Ignition	5-32
5.2-2	Model SSME Exhaust Duct Water Flowrates at Model SSME and SRB Ignition	5-33
5.3-1	Single-Model SRM Overpressure Data Pitch-Type Tests	5-37
5.3-2	Single-Model SRM Overpressure Data Lateral-Type Tests	5-40
5.3-3	Dual-Model SRM Overpressure Data Full-Model Test	5-43
5.3-4	Model SSME Overpressure Data	5-44
5.4-1	Overpressure Data on the Model Muffler Interior Walls	5-93

This page was intentionally left blank.

1.0 INTRODUCTION

				-
1				

1.0 INTRODUCTION

1

Seventeen Space Shuttle Solid Rocket Motor (SRM) ignition overpressure tests using the 6.4 - percent scale model were performed at NASA MSFC to define the environment for the vehicle during launches from Western Test Range (WTR). The simulations of the SRM ignitions were accomplished by the use of Tomahawk solid rocket motors during the tests. generated by the model Space Shuttle Main Engines (SSME's) was also eva-The model vehicle and instrumentation were of the same configuration as used previously with the Eastern Test Range (ETR) Kennedy Space Center Launch Complex 39 mobile launch platform/exhaust system model, Reference 1. The launch mount/exhaust ducting configuration of the Western Test Range (WTR) Space Launch Complex 6 (SLC-6) facility was modeled. These WTR tests were conducted in three phases: early screening (four SRM tests in May-June 1982), SRM verification (twelve SRM tests in February through April 1983), and SSME verification (three tests in June 1983). There was also a full-model (dual SRM's plus SSME's) test in September The SRM screening and verification tests were single-model SRM firings making use of a splitter plate as the most cost-effective and reliable means to achieve test objectives. The one dual SRM-plus-SSME's test provided both SSME and SRM data and was part of the five-test acoustic verification test series for WTR.

The SRM screening phase, Reference 2, revealed SRM ignition overpressure (IOP) levels comparable to those for STS-2 and subsequent flights. An SRB exhaust duct overpressure (DOP) was found to exist which is predicted from the model data to be greater than ETR. The DOP presents a potential problem for Shuttle payloads launched from WTR. The SRM verification phase was conducted after an off-line development program at MSFC to identify a suitable "fix" for the SRM DOP. The off-line tests are described in this report. They resulted in the proposed duct-extension-type muffler device for both SLC-6 SRB exhaust ducts that was evaluated in the verification test phase as a contingency if the first launch data from WTR show mufflers are necessary. Verification tests were performed with and without the proposed muffler to define the baseline overpressure environment (without

mufflers) and the degree of suppression with mufflers. Water troughs over the SRB exhaust openings (holes) to control IOP, similar to those which are part of the SRM overpressure suppression "fix" at ETR, are a part of the baseline configuration for WTR following verification in these scale-model tests. The baseline configuration in this report means the launch facility configuration as planned for the first launch: 100 percent design flow-rate sound suppression water and water troughs over the SRB exhaust holes similar to those in use at ETR.

Emphasis was placed on defining the baseline facility launch environment. The last single-motor test in the SRM verification phase was performed, however, without sound suppression water sprays and without water troughs or mufflers. Three of the SRM screening tests had been performed with reduced sound suppression water flow, one of which was with water troughs. Flowrates tested in the screening phase included 25 and 50 percent of the baseline design. Environment verification for WTR also required the SSME ignition overpressure data. There were three SSME ignition overpressure tests, with the baseline sound suppression water flow rate. The full-model test with dual SRM's had an SSME start without the water (completely dry) giving a wet versus dry SSME overpressure comparison.

This report provides a detailed description of the scale-model test program, the test article configuration and instrumentation, and data reduction methodology. The report describes all of the basic test data acquired. Appendaged to this report are twenty final data packages, already transmitted to all Ignition Overpressure Working Group member agencies in microfiche form, which contain the raw overpressure data plots and tabulations from all of the tests -- all final engineering unit data, checked and released by Rockwell International in direct support to MSFC.

2.0 TEST PROGRAM

,			
ı			

2.1 Overall Program/Procedure

SRM and SSME ignition overpressure environments were measured in twenty separate "hot-firing" tests. There had been four SRM overpressure screening tests which are described in Reference 2. There were twelve SRM overpressure verification tests. There were three SSME overpressure verification tests with SSME sound suppression water. There was one full-model test with dual SRM's but with the model SSME's started dry before bringing "On" the SSME water flow. The basic test procedure was to define the baseline facility launch environment (first Vandenberg Launch) and then to define the environment with the duct overpressure suppression muffler.

The four SRM screening tests and twelve SRM verification tests utilized a single LH model SRM with LH SRB duct and SSME duct water flows "On". Single-SRM tests were performed with and without splitter plate which had been found to provide a reliable and cost-effective means for acquiring data under conditions simulating simultaneous left-right SRM ignition and simulating non-simultaneous SRM ignition during the ETR test program (see Reference 1). The test procedure and instrumentation were essentially the same as used in the ETR tests so that the scale model data would be directly relatable. Vehicle pitch-axis forcing function data (simultaneous SRM ignition case) were acquired with the splitter plate. Vehicle lateralaxis forcing function data were acquired with the splitter plate removed. Use of special differencing equations with time skewing in lateral forcing - function development provided means to investigate effects of nonsimultaneous SRM ignition. The full-model test took place with whatever model SRM ignition simultaneity happened to occur. It was four msec and out-of-specification (equivalent to 62.5 msec full scale). The full-model test environment was useful to the overall program objectives but less usethan if the simultaneity had been one msec or less (within Inability to control 0.064 - scale model SRM ignition simultaneity within one msec had been the reason for using the single-SRM procedure, the splitter plate giving reflections as if two SRM's were present and ignited perfectly simultaneously.

The SRM screening test configurations summary from Reference 2 is repeated in Table 2.1-1. Sound suppression water flowrate variation was investigated in these four tests. Water troughs were added in the fourth screening test at the 50-percent design flow rate. The splitter plate (which divides the model through the Z axis into left and right halves) was used for all four screening tests.

The overpressure instrumentation placement on the model vehicle in the verification tests duplicated that from ETR tests for emphasis on defining vehicle pitch-axis and lateral-axis loading from overpressure wave passage over the model vehicle with simultaneous ignition of both SRM's. Additional instrumentation on the model SSV provided data on shell-model loading. Overpressure instrumentation in both SRM ducts and in the SSME duct provided data on the overpressure wave development within the ducts during all tests.

Minor test program startup problems were experienced and overcome in the screening test phase having to do with the fact that time also scales by 0.064. These were in regard to sound suppression water sequencing for scale-model tests and the pre-ignition water accumulation depth in the bottom of the SRB exhaust duct. It was necessary to scale the depth of water accumulated in the duct for each flow rate condition. The prediction for scaled water depth in the LH model SRB exhaust duct was 1.9 inches maximum for 100 percent design flow (29.7 inches full scale), from full-scale projected facility operation computations of water "On" sequence time, the use of preprimed water manifolds, and the water system volumes involved. The water "On" sequencing was within specification for all the verification tests performed.

2.2 SRM Verification Tests

The 100-percent design sound suppression water flowrate for SSME's and SRB's was used for the eleven verification tests with water sprays "On". The simulation of SSME duct water sprays made the model simulation more complete. Test 16 was performed with no sound suppression water (completely dry) and without water troughs to obtain a measure of the effectiveness of the water sprays in suppressing the overpressure.

TABLE 2.1-1 SRM OVERPRESSURE SCREENING TEST MATRIX

EXHAUST DUCT WATER ACCUMULATION DEPTH, IN. *	1.8	0.8	3.3	0.8
WATER SPLITTER ROUGHS PLATE	YES	YES	YES	YES
WATER TROUGHS	ON	ON	ON	YES
WATER FLOW TEST RATES NUMBER (Percent of Design)	100	20	25	90
TEST NUMBER		2	ю	4

* OBTAINED KNOWING THE MODEL SRB EXHAUST DUCT GEOMETRY FROM INTEGRATION OF WATER FLOWMETER DATA.

The verification test matrix is shown in Table 2.2-1. Tests identified as "pitch-type" tests had instrumentation placement emphasis in the model vehicle pitch axis and used the splitter plate. Tests identified a "lateral-type" had instrument placement emphasis in the lateral axis, had a "dummy" RH model SRM, and the splitter plate was removed. The LH SRM overpressure waves were allowed to spread across the full-model vehicle in the "lateral-type" tests. The final test (Test 40) was with dual-model SRM's, model SSME's, and the full-model as a complete system -- vehicle and launch facility -- baseline case, with the water troughs over both the LH and RH SRB exhaust openings.

Seven of the SRM verification tests were thus performed with the splitter plate, being pitch-axis tests the same as the four screening tests. Five single-SRM tests were performed with the splitter plate removed in order to obtain the "lateral-axis" test data. Four of these single-motor tests were performed with the contingency muffler: two pitch and two lateral. All tests with the muffler had the water troughs installed.

Model facility operation was within specified conditions for all the verification tests with model SRM ignition occurring in all eleven single-motor tests 1.1 ± 0.1 sec after Water Valves Open Command and the water flowrates being fully established, and SSME ignition came 1.0 \pm 0.1 sec after the SSME water valve opened in the three SSME tests. There was one test ano-The water drain valve on the model SRB exhaust duct was inadvertently left open during one single-model SRM test (Test 10). There was only slight variation test-to-test in SRB duct pre-ignition water accumulation level in the verification test phase. The time from SRB Water Valves Open Command to dual-motor SRB Ignition Command in the full-model test was 1.2 sec, with all of the water flows within specification, from SSME water valve open command to SSME ignition again 1.0 sec likewise within specification. The model water trough installation and vehicle/launch facility geometry were essentially constant every test, repair/refurbishment to the duct and SRB haunches refractory coating being applied to correct routine damage caused by the SRM and SSME plume inpingement and heating after every test.

TABLE 2.2-1 SRM OVERPRESSURE VERIFICATION TEST MATRIX

MUFFLER	ON.	0	NO	YES	YES	NO	ON.	ON.	ON	YES	YES	ON	NO.
EXHAUST DUCT WATER ACCUMULATION DEPTH, IN. * *	2.3	2.3	2.3	2.3	2.3	2.3	2.3	2.3	2.3	2.3	2.3	2.3	3.2 LH/2.9 RH
SPLITTER PLATE	YES	YES	YES	YES	YES	YES	ON	NO	NO	ON	NO	YES	ON
WATER TROUGHS	YES	YES	YES	YES	YES	ON	YES						
WATER FLOW RATE (Percent of Design)	100	100	100	100	100	100	100	100	100	100	100	0	100
TEST TYPE	РІТСН	РІТСН	РІТСН	РІТСН	РІТСН	РІТСН	LATERAL	LATERAL	LATERAL	LATERAL	LATERAL	РІТСН	FULL*
TEST NUMBER	2	9	7	80	6	10	11	12	13	14	15	16	40

Full-Model, SSME's operating, dual-SRM ignition and operation, pitch and lateral data combined.

** Based on computations from flowmeter integrations.

Long delays in beginning of chamber pressure rise occurred in the Tomahawk motors used in Tests 11 and 13 like that which had been experienced in Test 3. The same type of anomalous spiking in motor chamber pressure seen in earlier Screening Test 4 occurred during every verification test except Test 7 and occurred in one motor but not the other in Test 40.

The spikes in chamber pressure always occurred well after the overpressure waves had been generated and gone, and there is no indication of compromise to the overpressure objectives of these tests. All the evidence in the data about the model chamber pressure spike anomaly is documented.

2.3 SSME Verification Tests

SSME ignition overpressure required investigation, like the SRM overpressure, with the WTR launch mount/exhaust duct configuration. A data base exists with the ETR configuration in the launches to date and in the Main Propulsion Test Article (MPTA) test firings of full scale SSME's at the National Space Technology Laboratory (NSTL), Mississippi. The scale-model SSME tests were performed knowing that the model SSME ignition transient does not simulate the full-scale SSME ignition transient and the model SSME's would ignite nearly simultaneously rather than with the programmed staggered start in an actual launch sequence.

The model SSME's were operated with LO $_2$ lead at ignition and LO $_2$ override at shutdown in the propellant valve sequencing. This was to minimize any possibility of free GH $_2$ accumulation and occurrence of detonation - type "pops". The overpressure developed was a more controlled ignition overpressure (without random GH $_2$ "pops"), associated with the initial rise in model SSME chamber pressure.

The SSME - only check firings established procedures for model operating conditions that would make the ignition characteristics repeatable. The principal variable affecting the model SSME overpressure was the LO $_2$ feed line pre-chill temperature. It was varied between - 200°F and - 260°F. At the coldest pre-chill temperatures, ignition was erratic and sometimes the model engines would not ignite. At slightly warmer temperatures, the model

engines sometimes experienced "hardstart" with very large ignition overpressures. At still warmer temperatures near -200° F, model engine ignition was smoother and more reliable, and the ignition overpressure was still large enough to measure pressure differentials across the model Orbiter planform as well in the lateral plane if non-symmetrical wave production between the three model engines occurred. The -200° F LO₂ line pre-chill was selected for these verification tests.

There were three model SSME test firings with the SSME exhaust duct sound suppression water flow. The water flow rate was at 100 percent design. A fourth test of the full model, SSME's and dual-model SRB's (Test 40) was also performed; overpressure data were being acquired during model SSME ignition as well as during the dual-model SRM ignition. Test 40 was performed for acquisition of acoustic data as well. The model SSME's were ignited first and burned 8.2 sec before the model SRM's were ignited. The SSME sound suppression water was turned on 4.0 sec after SSME ignition in Test 40, and the model SSME start was dry. The reason for delayed activation of the SSME water spray was to minimize the pre-SRM ignition water depth in the SRB exhaust ducts for a closer simulation of that which will be in a full-scale launch. The West wall sprays of the SRB primary holes of the model launch mount are manifolded together the same as in full scale. This amount of West wall water spray that comes "On" with the SSME water flow pools in the bottom of each SRB duct before the rest of the SRB water sprays are turned "On". Acoustic data during model SSME - only operation was required during this test for 4.2 sec with SSME water sprays "On" before model SRM ignition and the slight compromise in scaling preignition SRB duct water depths was made to acquire the needed acoustic data.

The matrix of the four SSME overpressure tests performed is shown in Table 2.3-1. There were several additional SSME checkout firings preparatory to these tests. During one checkout firing, the SSME sound suppression water supply pressure was inadvertently set about 5 psi higher than the maximum model design in Test 33, with the result that the water shutoff valve leaked through. The water supply pressure had been just enough against the valve cylinder closing pressure to bring the valve slightly off its seat. The water level in the SSME duct at ignition was estimated to be one-third

TABLE 2.3-1 SSME OVERPRESSURE VERIFICATION TEST MATRIX

EXHAUST DUCT WATER ACCUMULATION DEPTH, IN. *	1.5	1.5	1.5	0
WATER FLOWRATE (PERCENT OF DESIGN)	100	100	100	0
TEST	SSME's - only	SSME's - only	SSME's - only	FULL*
TEST	30	31	32	40

* Full-Model with SRB's ignited after 8.2 sec of SSME's - only operation

** Based on computations from flowmeter integrations

to one-half full. There was very strong water blowback all over the model vehicle for about one second after ignition as the SSME duct was pressurized at SSME ignition. The water blew some 12 feet or more in all directions out the top of the SSME exhaust hole. This checkout firing served to show that control over SSME duct pre-ignition water accumulation depth was important in the model operation, established the upper limit for SSME water supply pressure, and resulted in use of remote television monitoring prior to test for assurance there would be no occurrence of inadvertent water leakage into either the SSME or the SRB exhaust ducts prior to test.

2.4 Model Operating Sequence

1_

For single-model SRM overpressure verification tests, the model launch mount water sprays were turned "On" nominally 1.1 sec prior to SRB Ignition Command (T_0). Both the LH SRB and SSME exhaust duct sprays were operated for best simulation of launch conditions. The simulation included time-scaling of sound suppression water "On" time before ignition so that the pre-ignition water accumulation depth in the LH SRB duct would be properly scaled.

There are eleven separate water supply valves and manifolds in the model launch mount sound suppression water system. The valve pit is located approximately at the scaled distance from the model launch mount as the full-scale so that line lengths and volumes are nearly simulated. The model SRM ignition sequence was fully automatic in single-motor screening and verification tests once the Water Valves Open Command was issued. The water pre-bleed procedure to each manifold like that which will be done prior to a launch in full scale was employed on the model. The problem of late priming of a given water manifold experienced in the screening test phase was overcome by requiring that each water manifold pressure as well as flowrate be within approximately 90 percent of design before SRB Ignition Command. (For the SRM screening phase, only the flowrates were used in the automatic ignition sequencing.) Use of both the flowrates (measured by turbine-type flowmeters) and the manifold pressures (measured

close to the water injection points) eliminated any further occurrence of ignition without fully established water flow in the SRB and SSME exhaust ducts. The water flow start-up transients were repeatable at the 100-percent design flowrate condition and the pre-ignition water accumulation depth in the LH SRB exhaust duct was close to proper scale for every single-model SRM overpressure verification test performed.

A schematic diagram of the model sound suppression water flow system is shown in Figure 2.4-1. For the single-model SRM tests, the LH SRB and SSME water was supplied from a common source. For the dual-model SRM Test 40, the SRB water and SSME water came from separate sources. Both the LH and RH SRB duct water sprays were brought "On" after SSME ignition in the SSME overpressure Tests 30, 31 and 32 and full-model Test 40. Tests 30, 31 and 32 like Tests 33 and 34, served as full launch mount water system sequence runs preparatory to Test 40. Use of separate sources for SSME and SRB water eliminated perturbations in SSME flow when the much larger SRB flows were initiated. The automatic sequence logic used for the single-model SRM tests is shown in Figure 2.4-2. The sequence used for SSME - only overpressure Tests 30, 31 and 32 was likewise automatic requiring SSME water flowrate and manifold pressure to be satisfied before SSME Ignition Command could be issued. The logic diagram is shown in Figure 2.4-3. The sequence used for Test 40 is shown in Figure 2.4-4. Eleven flowrates and eleven manifold pressures all had to be satisfied by relay closures in queue in staggered SSME and SRB water flows start. In order to set upper limits on SSME and SRB duct water accumulation levels, time-delay relays were started at Water Valve Open Commands to inhibit the respective ignition commands if flows and pressures were not satisfied in specified time. Additionally, relay closures were required indicating that all three model SSME chamber pressures were at 800 - psig minimum before SRB Ignition Command could be issued in Test 40. For reasons of safety, the SSME chamber pressures were also scanned to be in excess of 600 psig, assuring the pressure rise to have taken place, within 1.6 sec after SSME Ignition Command. Otherwise, there would be a Low Chamber Pressure Cutoff command to prevent excessive unburned propellant accumulation if the model SSME's engines failed to ignite. Also, there were automatic cutoff provisions on

Note: Eleven individual flows and pressures OK required for "green light."

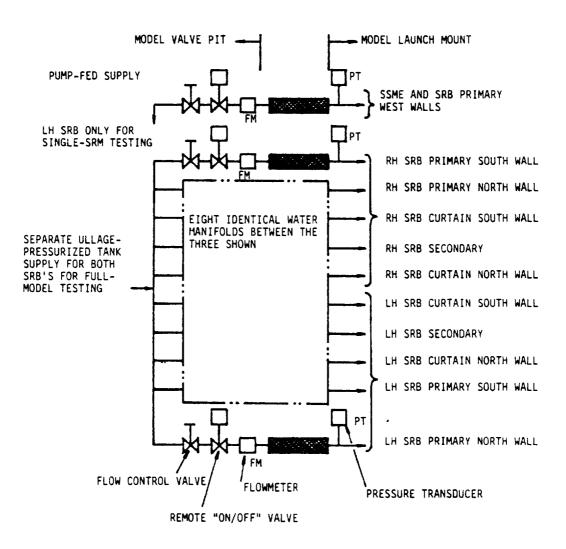


Figure 2.4-1 Schematic Diagram of the Model Sound Suppression Water Flow System

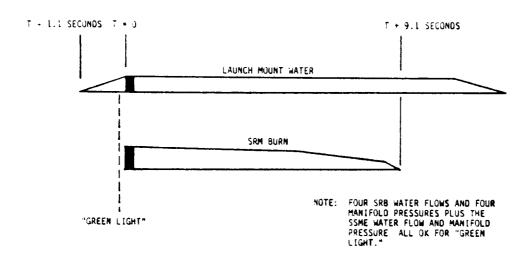


Figure 2.4-2 Automatic Sequence Logic Diagram for Single-Model SRM Tests

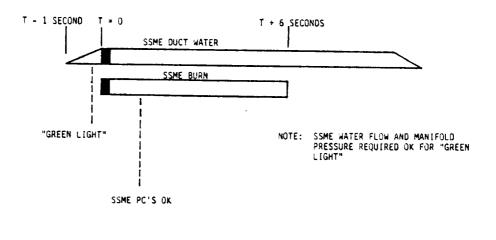
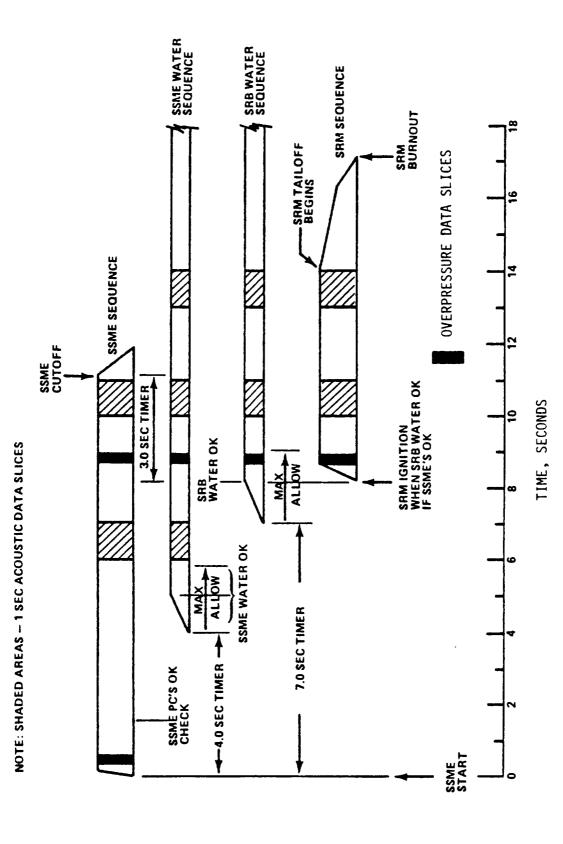


Figure 2.4-3 Automatic Sequence Logic Diagram for SSME-Only Tests

OVERPRESSURE DATA SLICE



Automatic Sequence Logic Diagram for the Full-Model Test Figure 2.4-4

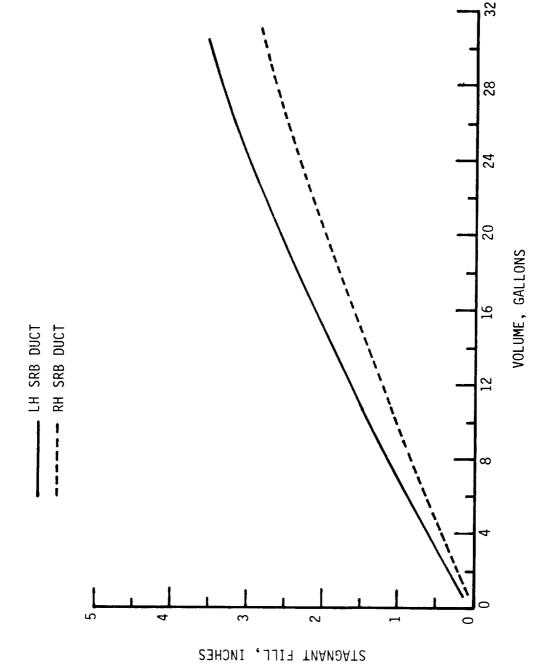
Œ

el SSME that would cut off all three if injector or thrust chamber atures exceeded safe operating limits. All model SSME healthitoring systems requirements had to be satisfied before SRB Ignition ommand could be issued.

The full-model operating sequence shown in Figure 2.4-4 gave SRB Ignition Command nominally 1.2 - 1.3 sec after SRB Water Valves Open Command, the time to achieve steady flows in both the RH and LH SRB ducts being 0.1 - 0.2 seconds longer than that for the LH SRB duct alone in the single-motor tests. This sequence for acquiring both acoustic and overpressure data in the full-model test was a slight compromise for the SRB overpressure simulation regarding the pre-ignition water accumulation levels in the LH and RH SRB exhaust ducts.

The method for estimating the pre-SRB ignition water accumulation depth in each model SRB exhaust duct was to integrate the flowmeter data to indicate gallons passed as a function of time. The relationship between standing water depth and gallons passed in each model SRB duct was calculated from the duct geometry and is shown in Figure 2.4-5. A typical history of the water accumulation depth in each model SRB duct as a function of time so calculated from flowmeter data integration for full-model testing is shown in Figure 2.4-6. Photographs of the water pooling in the LH SRB duct taken from high-speed motion-picture camera data from a sequence run prior to full-model testing are shown in Figure 2.4-7. For single-model SRM testing, the SSME water was brought "On" at the same time as the LH SRB duct water and there was no additional contribution from the SRB duct primary hole West wall sprays as in the full-model test. A typical history of calculated water accumulation depth in the LH model SRB duct for singlemodel testing is shown in Figure 2.4-8.

Test program conduct -- procedures and operating sequence -- were in accord with requirements initially set forth in Reference 3, amended with necessary updating for SRM verification after the screening tests as given in Reference 4,, and incorporating the SSME overpressure and dual-SRM overpressure investigations into the acoustic verification program as specified in Reference 5. Model launch facility geometry underwent certain changes



2-15

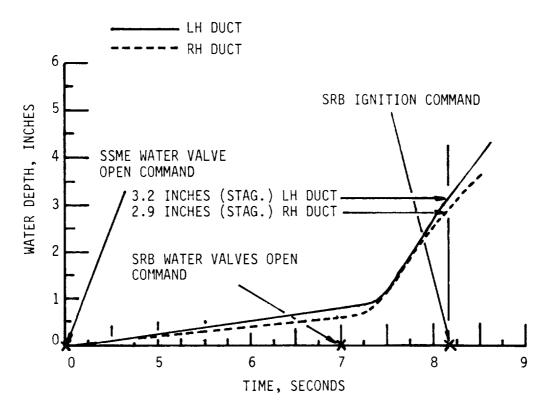


Figure 2.4-6 Water Accumulation Depth in Each Model SRB Duct as a Function of Time (Full-Model Test)

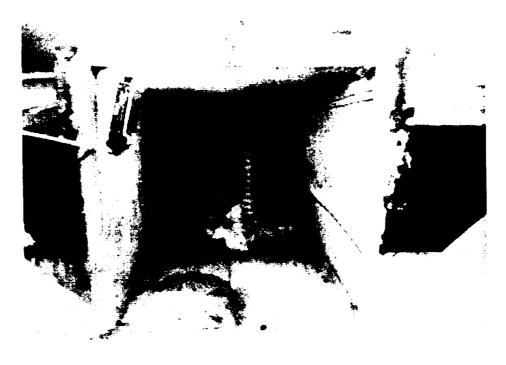


Figure 2.4-7 Photograph of Water Pooling in the LH Model SRB Exhaust Duct 2-16

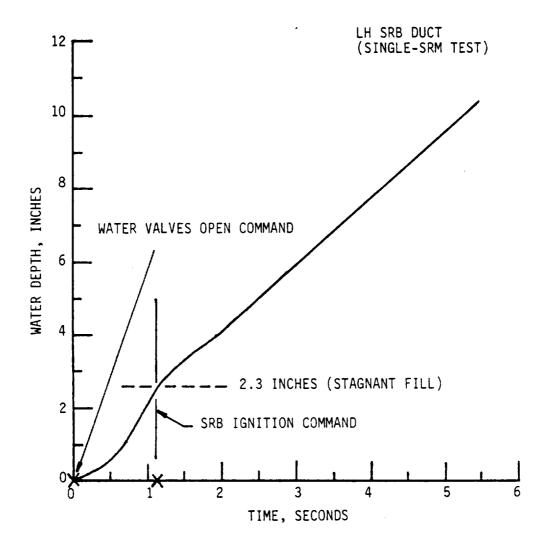


Figure 2.4-8 Water Accumulation Depth in the LH Model SRB Exhaust Duct as a Function of Time (Single-Motor Test)

in the period over which this program was conducted. This and the other documents referenced herein give a complete tracking since the initial requirements release of model geometry and changes. The acoustic release of model geometry and changes. The acoustic verification tests, Reference 6, completed all scheduled work with the 6.4 - percent scale model in support of preparations for the first Vandenberg launch.

3.0 MODEL GEOMETRIC DETAILS

	•	:	
•			
			ì
			مستنده

3.0 MODEL GEOMETRIC DETAILS

3.1 Model Vehicle

Basic geometry of the model vehicle is shown with and without the splitter plate in Figures 3.1-1 and 3.1-2. The model vehicle positioning over the launch mount is shown in Figure 3.1-3. The model Orbiter vertical stablizer was removed when the splitter plate was installed. Cylindrical pipes 3 1/2 in. in diameter simulated the cores of the two model SSME's in the pitch-type tests, the three model SSME's in the lateral-type tests. The model vehicle configuration was identical to that for the ETR tests of Reference 1, except the LH model SRM was fired instead of the RH and these tests used model SRM nozzle extensions simulating enhanced performance SRM's, with the High Performance Motor (HPM) nozzle. The model SSV, except for enhanced - performance nozzles, was the same as it was in previous WTR overpressure testing performed at MSFC in 1976, Reference 7, which did not utilize a splitter plate.

3.2 Model SRM

The Tomahawk model TE-M-416 motor is shown in Figure 3.2-1. The nozzle extensions on the model SRM's matched the HPM nozzle scaled length, diameter, and expansion ratio. Typical chamber pressure time histories through the ignition rise period are compared in full-scale time in Figure 3.2-2. The Tomahawk motor has a higher operating chamber pressure level and a slower (scaled) ignition rise rate than either the basic or the enhanced - performance full-scale SRM. This lower rise rate (by approximately a factor of three) must be accounted for in scaling the scale-model overpressure data to full scale as the actual overpressure levels on the model are lower than for a correctly-scaled rise rate.

A phenolic nozzle extension was bonded to each Tomahawk motor nozzle with epoxy resin simulating the length, exit area, and expansion ratio of the enhanced-performance or high-performance motor (HPM) SRM nozzle intended for use from WTR. These nozzle extensions, Figure 3.2-3, are reusable motor-to-motor and were machined to HPM specification from larger exten-

FIGURE 3. 1-1 MODEL TEST ARRANGEMENT -- PITCH-TYPE TESTS

İ. .__

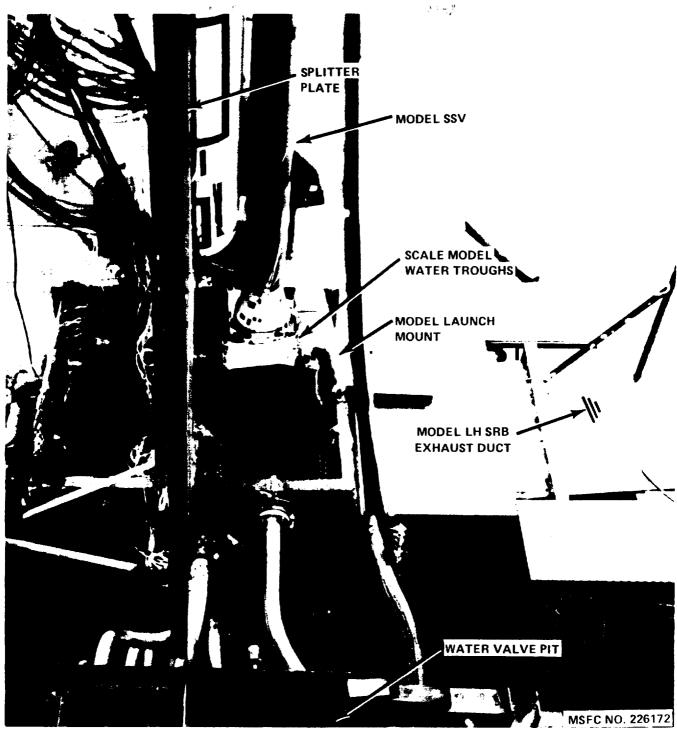
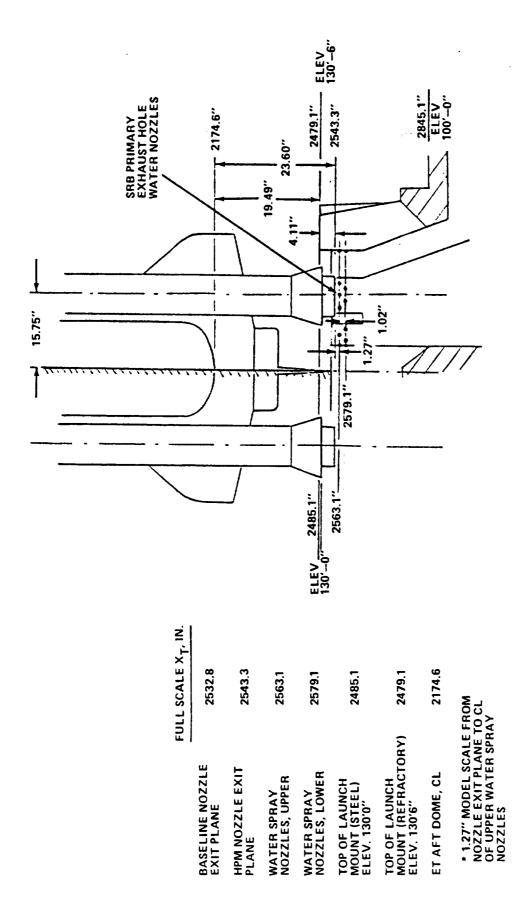


FIGURE 3.1-1 (CONCLUDED)

FIGURE 3. 1-2 MODEL TEST ARRANGEMENT --LATERAL-TYPE TESTS





sions that were available for Tomahawk motors. Epoxy filler was used to blend the interior conical shape of each extension to that of the basic nozzle, Figure 3.2-4. The nozzle extensions were drilled to accept static pressure instrumentation near the nozzle exit plane.

Performance characteristics of the Tomahawk motor with the HPM-simulation nozzle extension are shown in Table 3.2-1 compared to the full-scale hpm prediction at $68^{\circ}F$.

3.3 Model SSME's

The Model SSME's (Figure 3.3-1) are LO_2/GH_2 - burning rocket engines generating scaled thrust at scaled mass flowrate. They have water-cooled thrust chambers using coaxial - jet injectors like full-scale SSME's and have close-to-scale external exit diameters and lengths, although only 8:1 expansion ratio and less-than-scale internal exit diameters. Liquid oxygen and gaseous hydrogen are pressure fed through common propellant valves to the three model engines. Ignition is accomplished by mixing the propellants in the presence of a high voltage spark igniter at the center of the injector operating at 120 sparks/second.

The model SSME's operate at nominally 900 psia chamber pressure with a mixture ratio of 4.3 for safe and reliable operation (much lower than full scale). Typical model- and full-scale SSME chamber pressure rise rates are compared on the full-scale time basis in Figure 3.3-2. The model engines use a $40\text{-msec}\ \text{LO}_2$ lead and override at shutdown to minimize free GH $_2$ preignition accumulation for safety purposes. The initial rise in chamber pressure is to about 800 psia with a more fuel-rich mixture needed for smooth ignition near 4.0. Chamber pressure builds slowly with LO $_2$ chilldown and LO $_2$ density increase over about 7 seconds burn time until nominal operating conditions at 900 psia are achieved. Performance characteristics of the model SSME's are shown Table 3.3-1 compared to the actual SSME scaled by 0.064 at 100 percent power level.

The model SSME thrust chamber lengths, angular orientation (thrust vector) and exit plane distance from the model Orbiter aft heat shield are closely

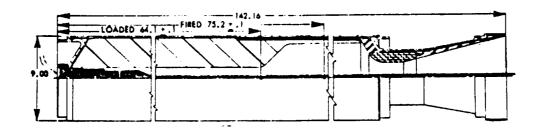


FIGURE 3. 2-1 MODEL SRM
-- THIOKOL TE-M-416 8. 31-KS-11, 000 TOMAHAWK MOTOR

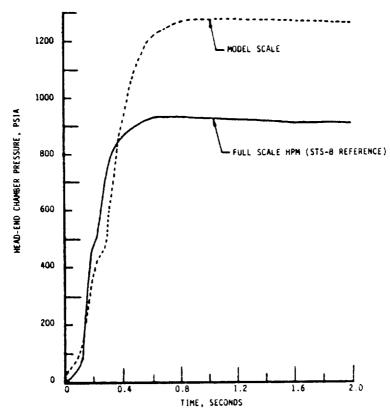


FIGURE 3. 2-2 MODEL AND FULL SCALE SRM CHAMBER PRESSURE IGNITION TRANSIENTS

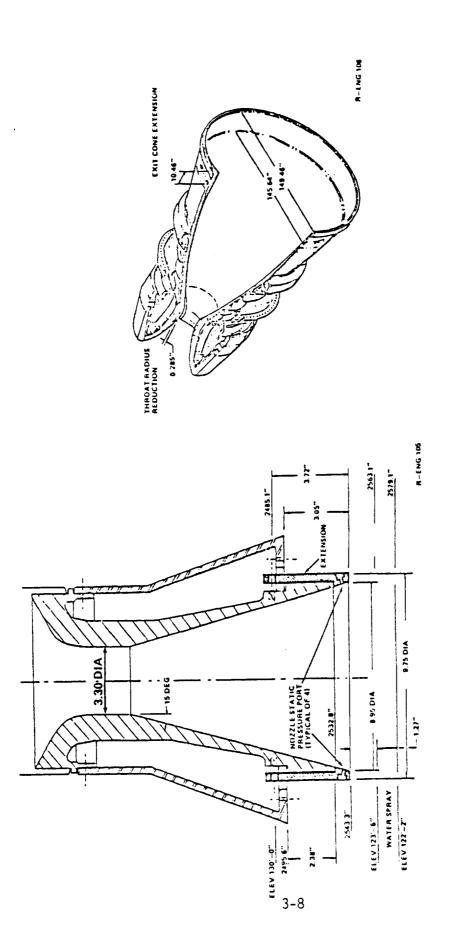


FIGURE 3. 2-3 ENHANCED-PERFORMANCE NOZZLE SIMULATION

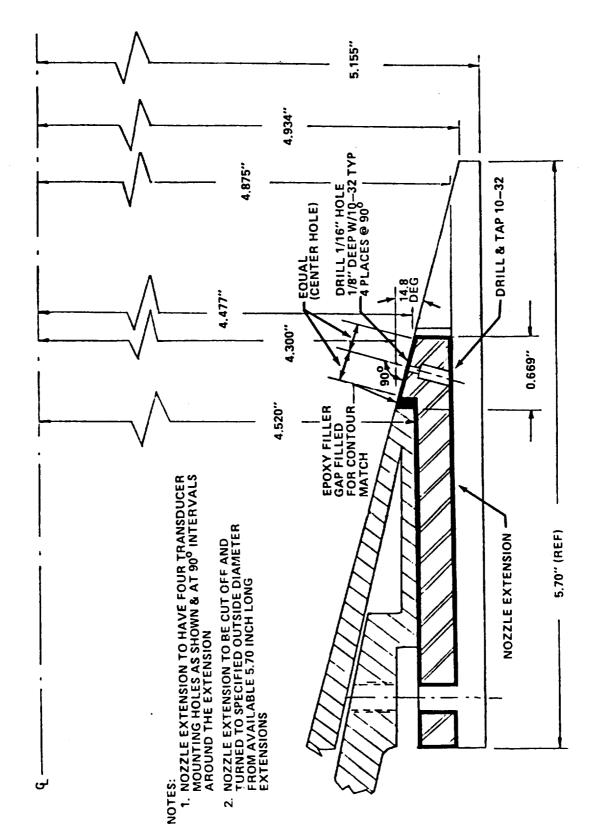


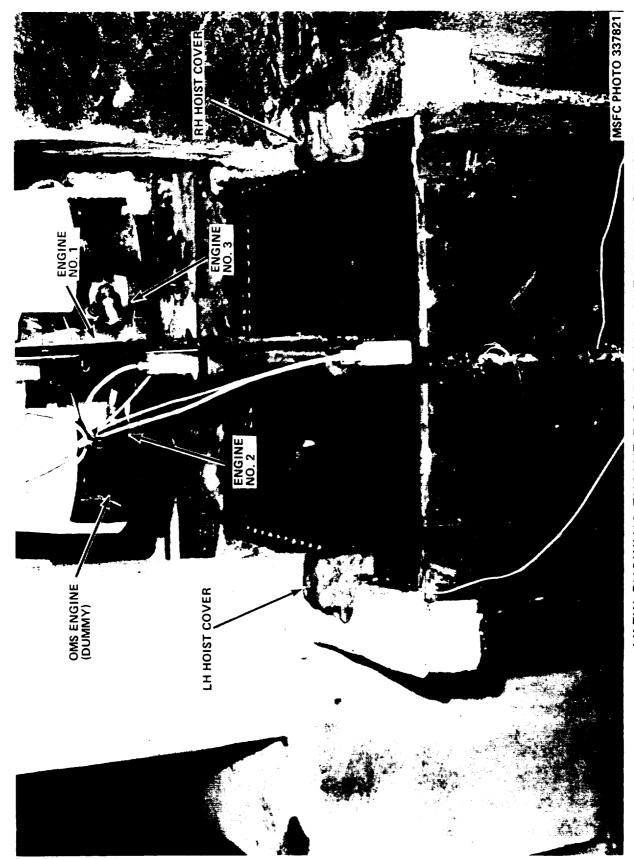
FIGURE 3. 2-4 MODEL SRM NOZZLE EXTENSION MOUNTING DETAILS



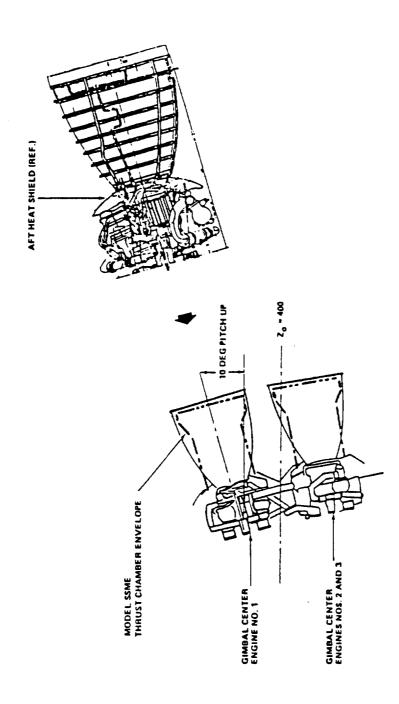
FIGURE 3. 2-4 (CONCLUDED)

TABLE 3.2-1 TOMAHAWK MOTOR PERFORMANCE CHARACTERISTICS

PARAMETER	MODEL ACTUAL @ 2-SEC AFTER IGNITION	HPM @ 2-SEC (0.064 SCALED)	
Sea Level Thrust, 1bf	10,775	12,288	
Sea Level Specific Impulse, sec	223.1	251.4	
Mass Flow Rate, 1bm/sec	48.3	48.87	
Chamber Pressure, psia	999	897.7	
Chamber Temperature, °R	6,413	6,151	
Ratio of Specific Heats	1.16	1.138	
Throat Area (Initial), ft ²	0.0594	0.0648	
Exit Area (HPM Nozzle), ft ²	0.437	0.500	
Expansion Ratio	7.36	7.72	
Exit Half Angle, Deg	15	6	
Exit Pressure, psia	21	17.14	
Exit Mach Number	2.82	2.949	
Exit Velocity, ft/sec	6,919	7,874	
Chamber Pressure Rise Rate (Nominal), psi/sec	50,000	140,000	



a. VIEW SHOWING ENGINE POSITIONING OVER EXHAUST HOLE FIGURE 3.3-1 MODEL SSME'S



b. ENVELOPE COMPARISON WITH FULL SCALE FIGURE 3.3-1 (CONCLUDED)

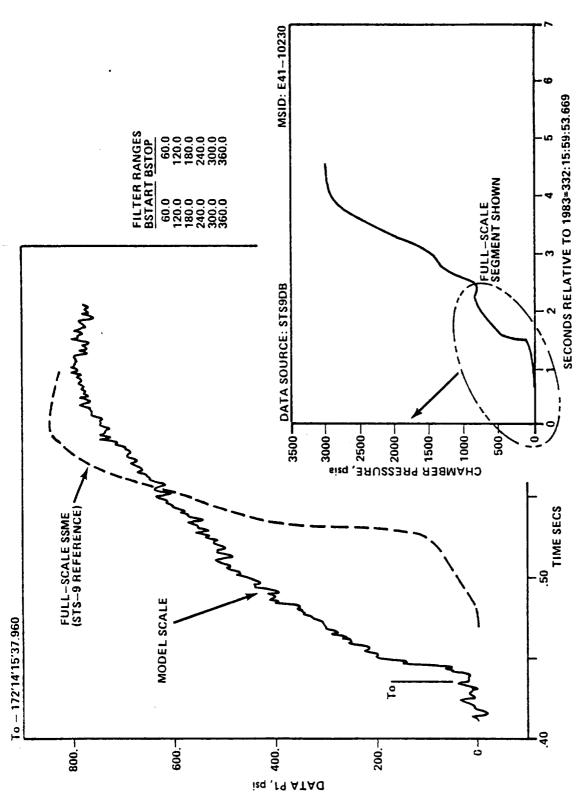


FIGURE 3.3-2 MODEL - AND FULL-SCALE SSME CHAMBER PRESSURE IGNITION TRANSIENTS

TABLE 3.3-1 MODEL SSME PERFORMANCE CHARACTERISTICS

PARAMETER	MODEL ACTUAL @ STEADY CONDITIONS	FULL-SCALE @ 100% POWER LEVEL
Sea Level Thrust, 1bf	1527.1	1543.8
Sea Level Specific Impulse, sec	382.9	361.1
Mass Flow Rate, 1bm/sec	3.988	4.265
Chamber Pressure, psia	903	3006
Chamber Temperature, °R	5530	6295
Mixture Ratio	4.3	6.0
Ratio of Specific Heats	1.26	1.26
Throat Area, ft ²	0.00786	0.00238
Exit Area, ft ²	0.0668	0.1839
Expansion Ratio	8.5	77.0
Exit Half Angle, Deg	20	5.4
Exit Pressure, psia	12	5.35
Exit Mach Number	3.325	4.234
Exit Velocity, ft/sec	12,540	13,473

scaled to full-scale SSME's without gimbal. The exit diameters are small by approximately a factor of three and the area ratios by nearly an order of magnitude.

3.4 Model Launch Mount/Exhaust Ducts

Initial overpressure tests with this model launch mount, Reference 7, were of a development nature and incorporated several variations on launch mount shape, SRB haunch, and sound suppression water spray arrangement. The model SRB exhaust ducts had a divergent cross section and large horizontal-floor exit open channels (apron areas) as seen in Figure 3.4-1. The small support pier in each SRB duct was not a part of the haunch structure as it is now. The WTR model facility was modified to its present configuration by altering the water spray pattern, incorporating a larger pier into the Northeast and Southeast haunches, alteration of the area between the SRB holes to an elevation of 125'-3", and conversion to the 8-deg upramped duct floor with the 15-deg upramped discharge as shown in Figure 3.4-2 (full-scale configuration).

The location for the start of the 8-deg ramp in the duct ceiling was inadvertently not changed before the screening test series (see the dashed line in Figure 3.4-3). It remained as it was in Figure 3.4-1 for the screening tests and the off-line muffler development tests and was changed to the proper geometry giving 50-ft full-scale square cross section for the veri-(The start of the upramp in the RH duct had remained the fication tests. same for the 50-ft square constant-area cross section.) An alteration in the SSME exhaust duct geometry from the original configuration tested in Reference 3 was made as shown in Figure 3.4-4. This alteration brought the SSME duct geometry up to the as-built configuration and consisted of closure of the then - contemplated air entrainment port and shortening of the vertical pier where the SSME expands to double its width and begins the The roof-line correction in the LH model SRB exhaust duct 15-deg upramp. and the SSME duct air entrainment port closure were the only geometric changes to the model facility between the screening and single-SRM verification test series.

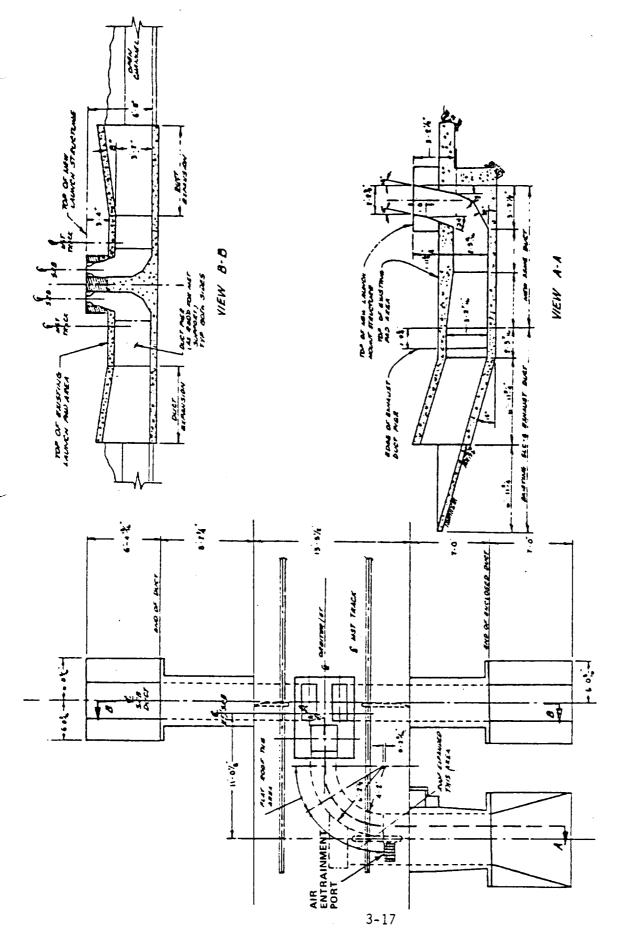


FIGURE 3.4-1 MODEL SRB AND SSME EXHAUST DUCT CONFIGURATIONS IN THE 1976 TESTS

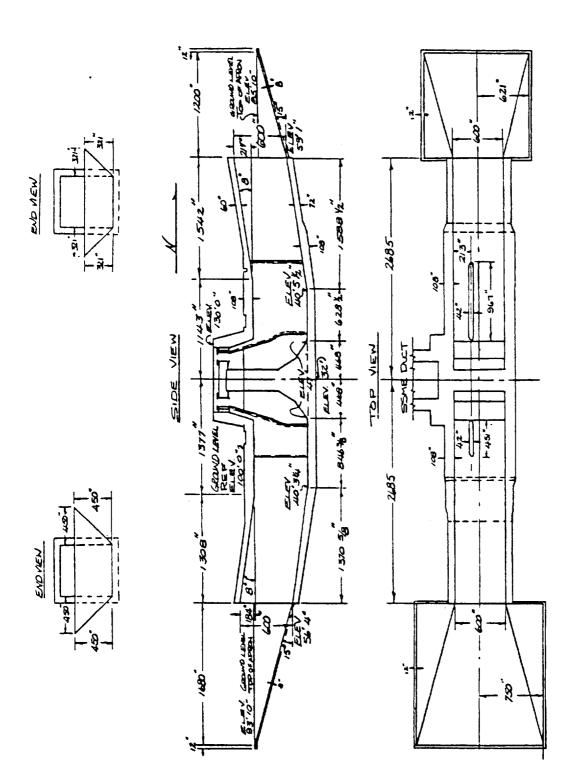
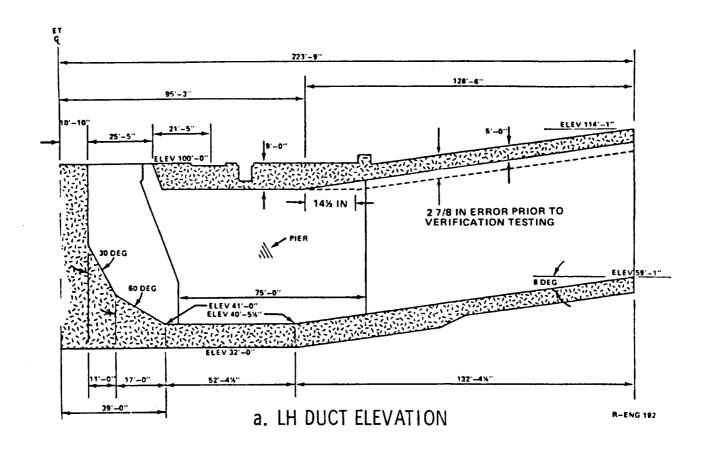


FIGURE 3.4-2 SRB EXHAUST DUCTS -- PRESENT CONFIGURATION

1



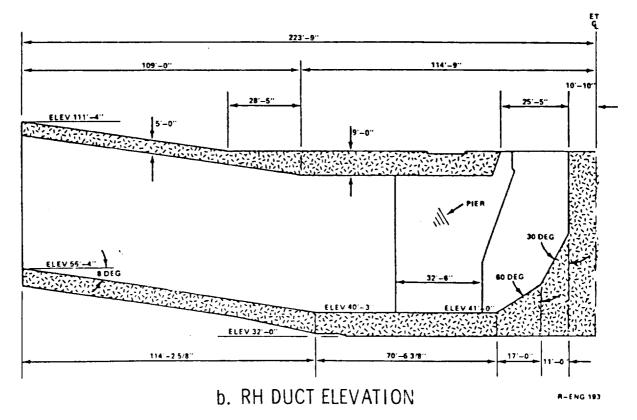
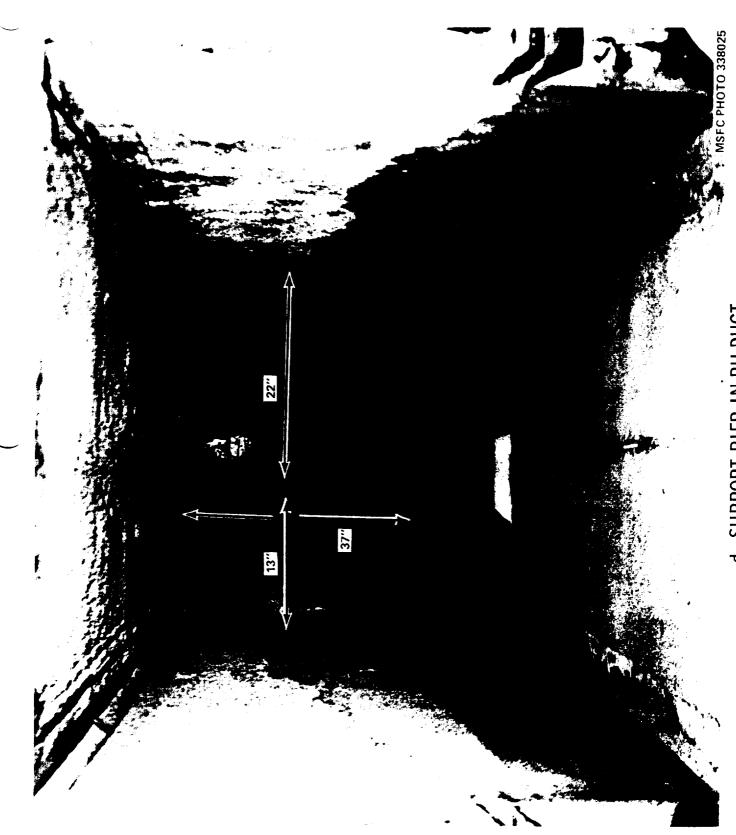
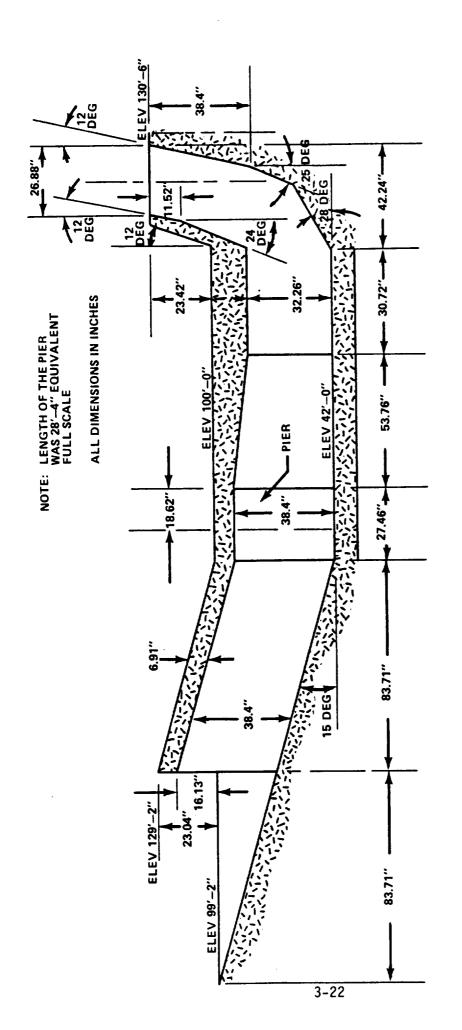


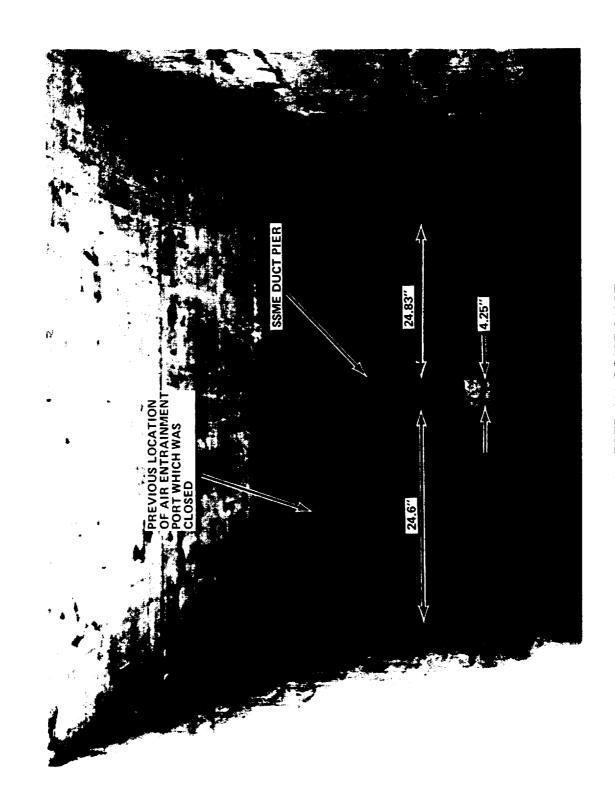
FIGURE 3.4-3 SRB EXHAUST DUCT AND PIER DETAILS







a. DUCT ELEVATION FIGURE 3. 4-4 MODEL SSME EXHAUST PRESENT DUCT CONFIGURATION



Two other model launch mount geometry changes were made in August 1983 after the three SSME - only ignition overpressure tests and before the final full-model test (Test 40). These were: (1) addition of the ET Ice Suppression System (ISS) "dog-house" cover in the Elev. 125'-3" area of the launch mount between the SRB exhaust holes shown in Figure 3.4-5 which will represent a modification to be made to the "as-built" full-scale launch mount, and (2) addition of two Orbiter work platform chain hoist covers between the two tail service masts on the North and South walls of the SSME exhaust hole shown in Figure 3.4-6. The "dog-house" cover, raising the 125'-3" elevation area on the launch mount to approximately 131', and the Orbiter work platform chain hoist covers were not present in the single-model SRM verification tests; the configuration was as shown in Figure 3.4-5c.

The sound suppression system water nozzles are vee-jet type on the model launch mount except for scarfed nozzles in the SRB primary exhaust hole, the development of which was discussed in Reference 2. The water nozzle spacing, flowrates, protrusions, and spray angles are all scaled on the model. The water discharge velocities match the full-scale. The spray turn-down on the model delineated in Table 3.4-1 was in effect for both the screening and verification tests. The full-scale launch mount has been constructed with spray nozzles oriented horizontally.

The full-scale launch mount sound suppression water system has been redesigned so that its spray pattern will be similar to the spray patterns as tested on the sub-scale model.

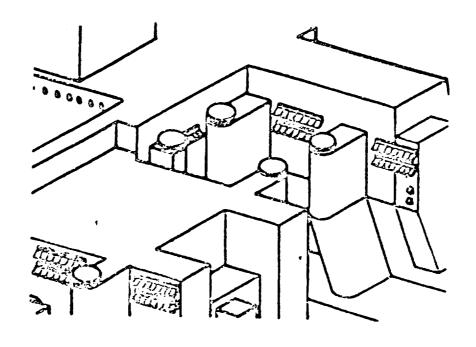
The launch mount sound suppression water system plan layout is shown in Figure 3.4-7. The nozzle layout was implemented in detail on the model except for the few nozzles marked in Figure 3.4-7 that were intentionally plugged for best spray impingement pattern without splash. Model water system scaling data are given in Table 3.4-2. (The manifold symbol coding in Table 3.4-2 refers to the callouts in Figure 3.4-7.) The basic design intent for the model launch mount water sprays was $(0.064)^2$ scaled flowrate and matched injection velocity for every nozzle spray bank.

TABLE 3. 4-1 MODEL LAUNCH MOUNT WATER SPRAY NOZZLES REORIENTATION

NOZZLE LOCATION	BEFORE	AFTER
SRB PRIMARY	HORIZONTAL	DOWN 360
SRB CURTAIN	HORIZONTAL	DOWN 30°
SRB SECONDARY HOLE	UP 10 ⁰	DOWN 10°
ORBITER (SSME) HOLE	UP 10 ⁰	DOWN 30°

^{*}NOZZLE TYPE CHANGE FROM VEE-JET TO SCARFED SPLASH-HEAD CONFIGURATION

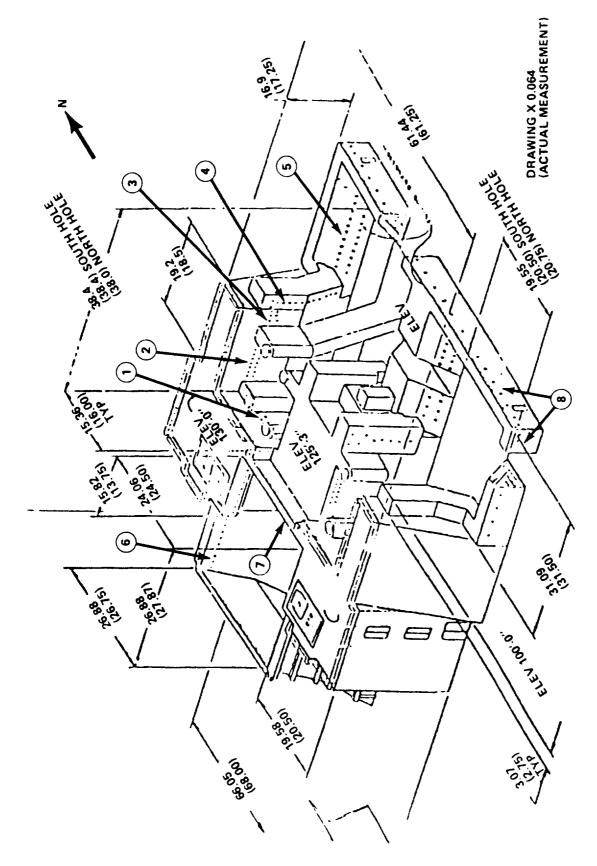
FULL SCALE DEFLECTOR PLATE CONCEPT FOR SRB PRIMARY AND CURTAIN SPRAYS



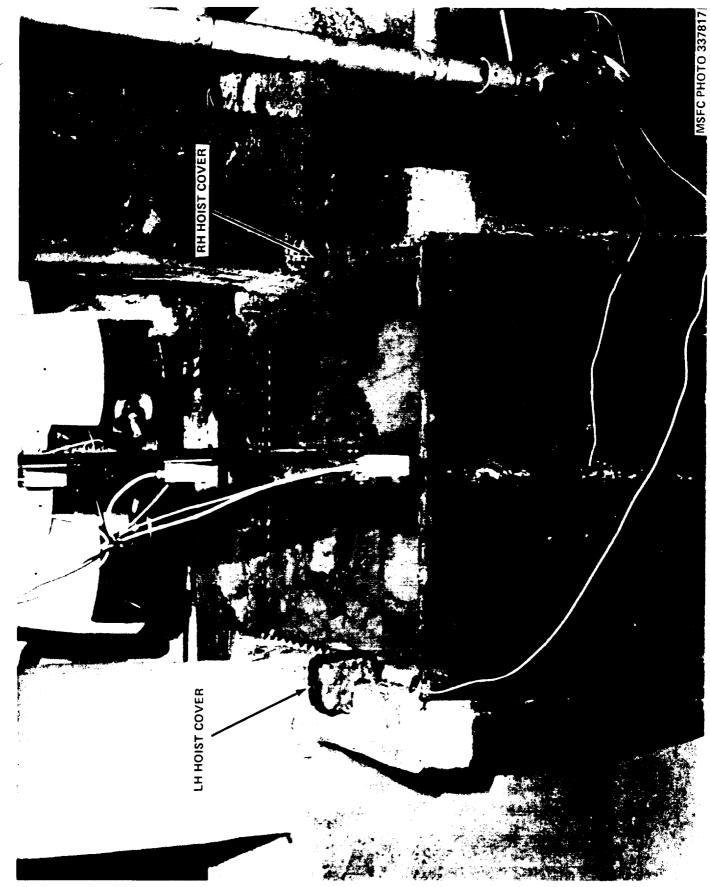


a. TEST 40 CONFIGURATION - 3/4 VIEW FIGURE 3. 4-5 ISS "DOG-HOUSE" COVER MODIFICATION TO THE MODEL LAUNCH MOUNT

b. TEST 40 CONFIGURATION - END VIEWFIGURE 3. 4-5 (CONTINUED)



c. GEOMETRY FOR SRM-ONLY AND SSME'S -ONLY VERIFICATION TESTS FIGURE 3.4-5 (CONCLUDED)



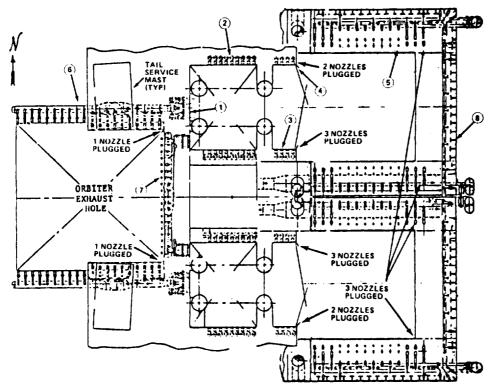


FIGURE 3.4-7 LAUNCH MOUNT SOUND SUPPRESSION WATER SYSTEM LAYOUT

R-ENG 123

TABLE 3.4-2 MODEL LAUNCH MOUNT WATER SPRAY SYSTEM DESIGN PARAMETERS

	FULL SCALE		MODE	MODEL SCALE		
	GPM	1bm/sec	ft/sec	<u>GPM</u>	1bm/sec	
w }	28,000	3887	60	114.7	15.92	0
N .	58,200	8080	60	238.4	33.10	Ø
s	58,200	8080	60	238.4	33.10	2
lB Curtain						<u> </u>
Curtain E Horiz.	25,000	3471	60	102.4	14.21	3
Curtain E Horiz.	25,000	3471	60	102.4	14.21	3
Curtain S Vert.	64,800	8996	60	265.4	36.85	3
Curtain N Vert.	64,800	8996	60	265.4	36.85	<u> </u>
RB SECONDARY HOLE						
N	48,600	6747	50	199.1	27.64	(5)
\$	48,600	6747	50	199.1	27 .64	<u> </u>
RB TOTALS						
	421,200	58,475		1725.3	239.52	ــــــــــــــــــــــــــــــــــــــ
SME HOLE N, S, and E ote: North, Sout	122,000	16,938	60	1 499.7	69.38	(and ()

3-30

Photographs of the model launch mount water spray pattern are shown in Figure 3.4-8. (The model SSME's are operating in both photographs.) The water spray manifolds and some of the model water nozzles were made of carbon steel. Routine maintenance was required to keep the nozzles free of rust and scale. The water flows could generally be held from 90 to 105 percent of design test-to-test. Typical flowrate - versus - nozzle inlet pressure calibration data for each type of model water nozzle used are shown in Figure 3.4-9. A hand-operated throttling valve was used to set the desired flowrate on each manifold, left in a fixed position for all tests once calibrations were completed. A constant water supply reservoir pressure guaranteed the desired water flowrates and injection velocities.

3.5 Instrumentation

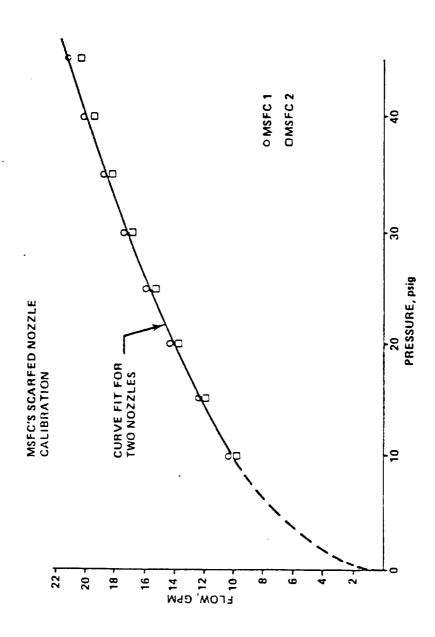
The complement of instrumentation included a close-coupled Kulite Type XTS-1-190-1000 strain-gage pressure transducer to measure the model SRM ignition transient pressure, two epoxy-bonded hoop-tension strain gages on the model SRM motor case to measure strain rate transients proportional to the internal combustion pressure, and two nozzle exit static pressure transducers to measure the SRM nozzle starting transient pressure. model SRM combustion pressure and strain rate instrument location and mounting details are shown in Figures 3.5-1 and 3.5-2. Model SRM nozzle exit static pressure measurement installation details are shown in Figure 3.5-3. During one acoustic verification test (Test 42) that followed the overpressure testing program which was at elevation above the model launch pad, the nozzle exit static pressure measurements were repeated to obtain an "on-pad" versus - "off-pad" comparison for possible asymmetric nozzle separation analysis. Model SSME combustion chamber pressure measurements were not dynamically close-coupled, the transient response was slightly inferior to that of the model SRM chamber pressure measurements.

There were up to 93 surface-mounted Kulite Type XCS-190-5SG strain-gage pressure transducers per test to measure incident overpressure at selected locations on the model vehicle, in the model exhaust ducts, and on the splitter plate. The two nozzle exit static pressure transducers on each





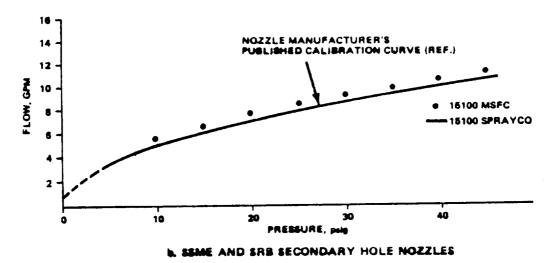
FIGURE 3. 4-8 MODEL LAUNCH MOUNT WATER SPRAY PATTERN
3-32



到 作品 智 赞新

a. SRB PRIMARY HOLE NOZZLES FIGURE 3.4-9 MODEL WATER NOZZLE FLOW CALIBRATION DATA

DATA POINTS ARE MSFC'S CALIBRATION DATA FROM ONE NOZZLE (TYP)



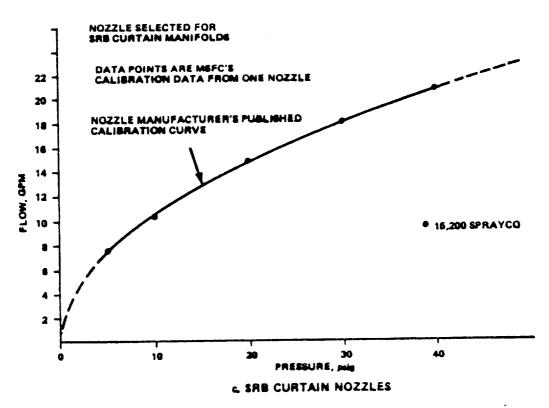


FIGURE 3.4-9 (CONCLUDED)
3-34

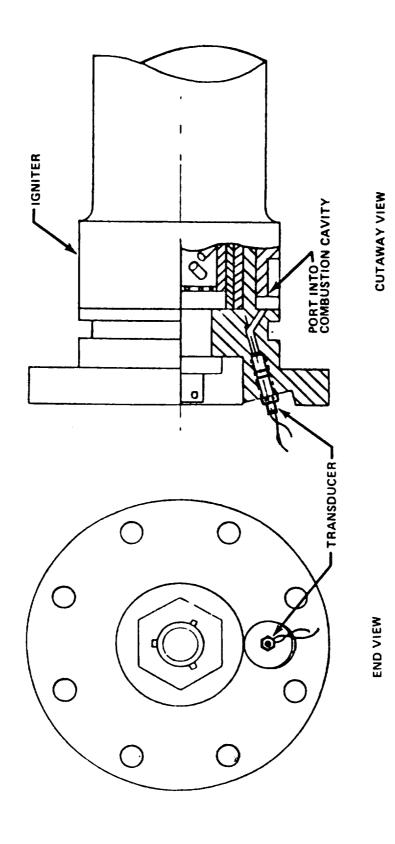
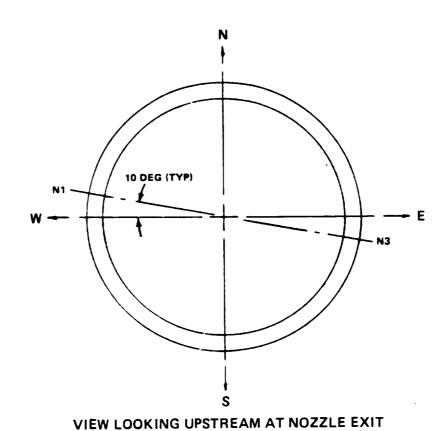


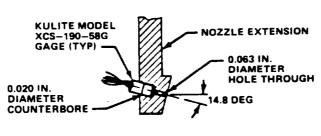
FIGURE 3. 5-1 MODEL SRM CHAMBER PRESSURE MEASUREMENT LOCATION DETAILS



FIGURE 3.5-2 MODEL SRM CASE STRAIN MEASUREMENT LOCATIONS

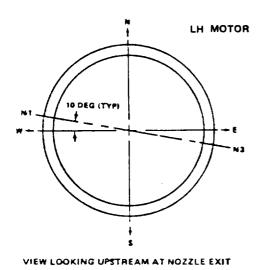


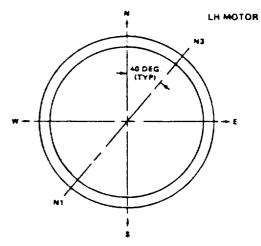
1



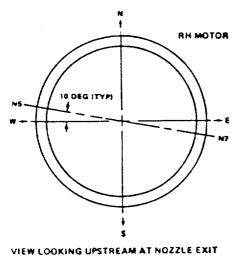
a. LH SRM -- SINGLE-MOTOR TESTS 5, 6, 7, AND 16

FIGURE 3.5-3 MODEL SRM NOZZLE EXIT STATIC
PRESSURE MEASUREMENT INSTALLATION





VIEW LOOKING UPSTREAM AT NOZZLE EXIT



N6 10 DEG (TYP)

RH MOTOR

b. DUAL - MOTOR TEST 40

c. DUAL - MOTOR TEST 42
(AT 84 FT EQUIVALENT ELEVATION ABOVE THE PAD)

VIEW LOOKING UPSTREAM AT NOZZLE EXIT

FIGURE 3.5-3 (CONCLUDED)

model SRM were also Kulite Type XCS-190-5SG, close coupled to measure the dynamic characteristics of the starting flow transient inside the model SRM nozzle. The overpressure measurement locations are shown in Figure 3.5-4 and -5 and are detailed in Table 3.5-1. Two measurements added in Test 40 at USAF/SATAF request called FH1 and FH2 denote locations to measure the environment for the Fan House at SLC-6 located almost directly out from the LH SRB duct discharge apron. Their locations are indicated in Figure 3.5-5g, approximately 500 ft out from the ET centerline on full-scale. The density of measurement locations on the model Orbiter and ET was increased for the verification tests as delineated in Reference 4 to enable definition of shell-model forcing functions. Close-up photographs of selected overpressure measurements on the model Orbiter are shown in Figure 3.5-6.

1

Measurements of overpressure incident on the model Orbiter were arranged in pairs on the wings, elevons, body flap, and vertical stabilizer and in rings approximately every 30 deg around the model Orbiter fuselage and approximately every 45 deg around the model ET. The Orbiter fuselage and ET ring sections with their respective measurement locations are shown in (The model Orbiter lines differ slightly from the full-Figure 3.5-7. scale mold lines which is the reason that some of the measurement points fail to lie precisely on the full-scale cross sections shown.) two measurements 180 deg apart at the location of the model SRB thermal curtain (aft heat shield) and one external and parallel to the SRB nozzle There were five pairs of measurements on the model SRB case There were three of only. pitch tests 180-deg apart for Orbiter aft heat shield. overpressure measurement on the model remaining measurements were distributed throughout the exhaust duct, open air above the exhaust duct oriented toward the duct exit, on splitter plate, and on the interior surfaces of the contingency muffler.

Certain measurement locations were added or deleted test-to-test for best use of the limited number of data channels available (98 maximum) and are so noted in Table 3.5-1. For instance, measurement locations were densified at the exhaust discharge end in some tests to better define the DOP wave exiting the duct and measurements were placed inside the scale-model muffler in two tests to define the dynamic pressure environment

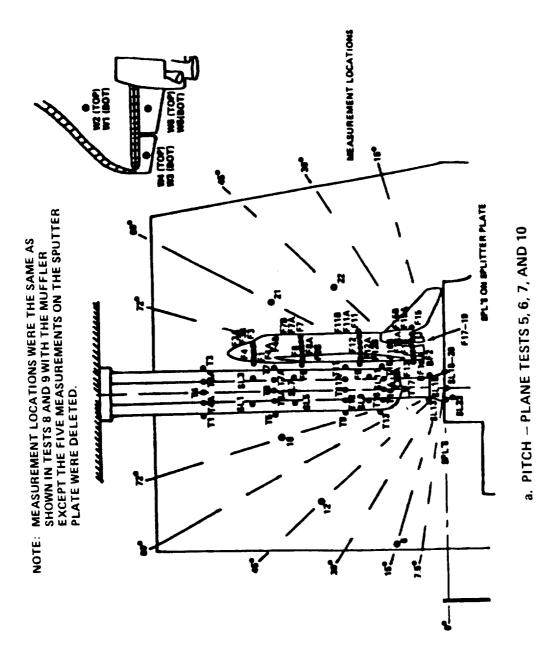
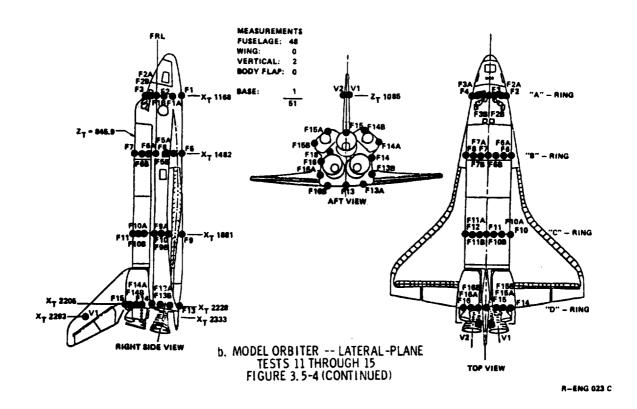
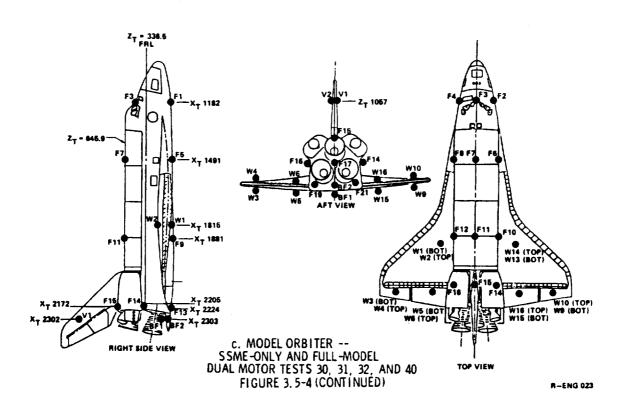
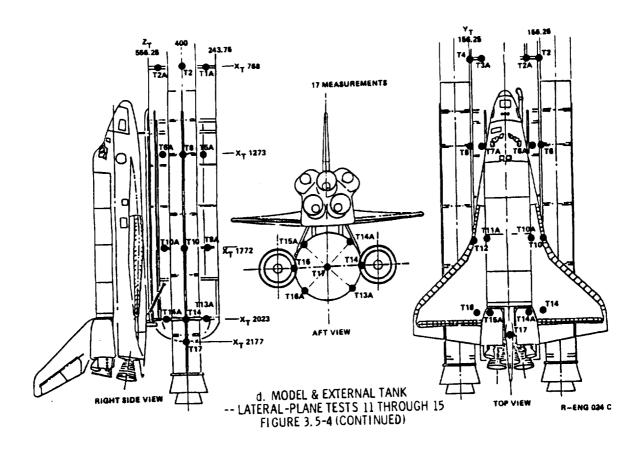
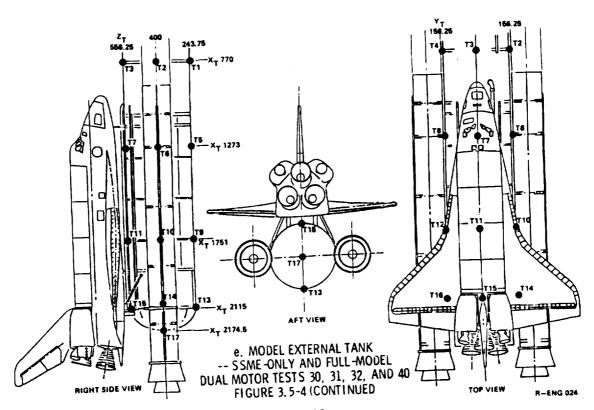


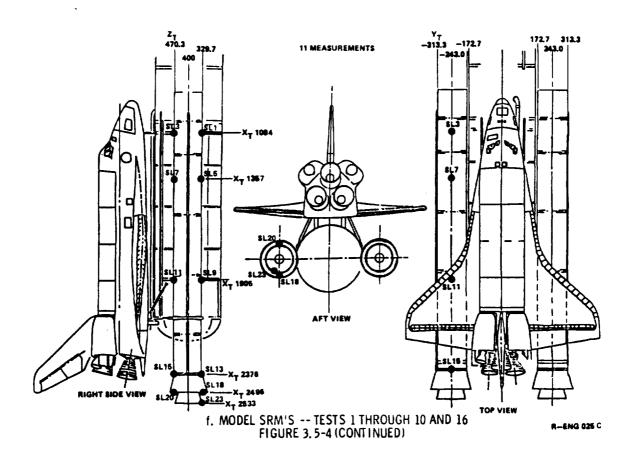
FIGURE 3.5-4 OVERPRESSURE MEASUREMENT LOCATIONS
ON THE MODEL VEHICLE AND SPLITTER PLATE

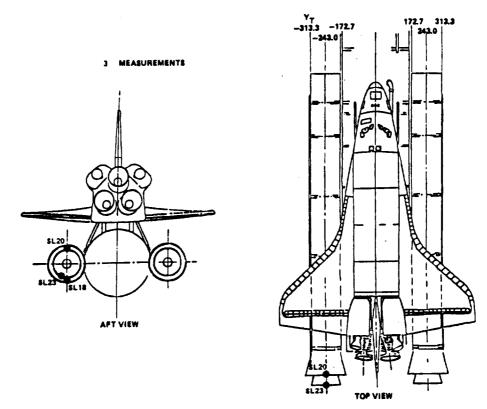






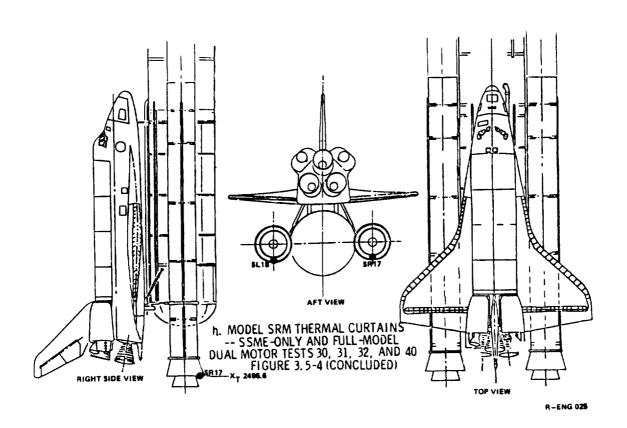


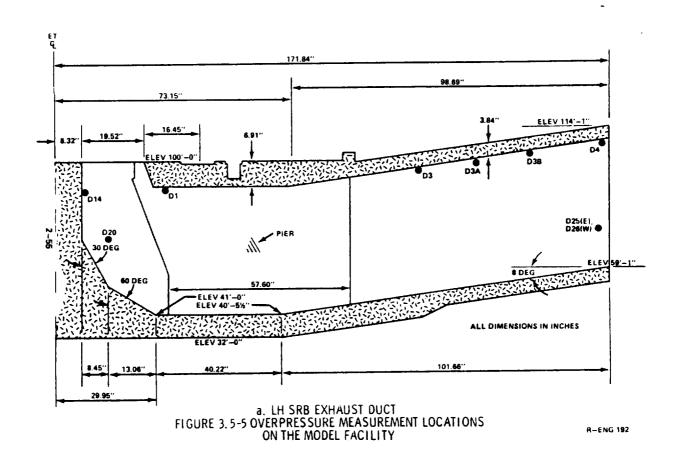


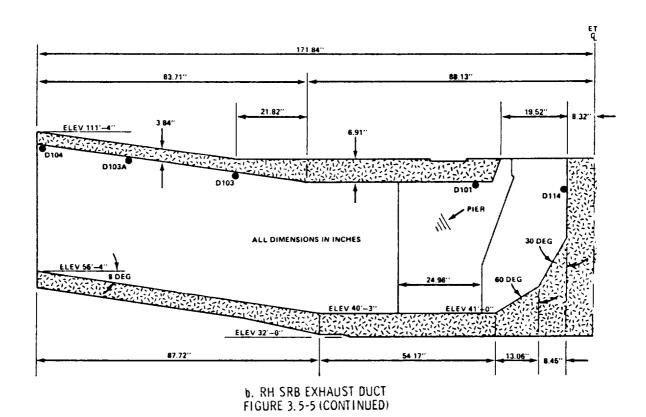


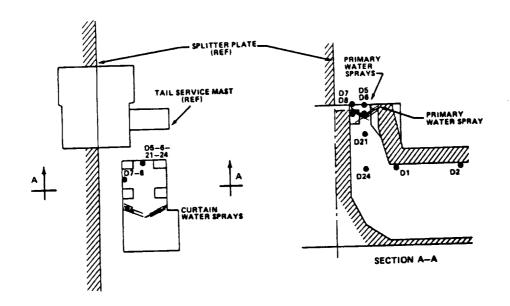
g. MODEL SRM THERMAL CURTAIN -- TEST 11 THROUGH 15 FIGURE 3.5-4 (CONTINUED)

3-43



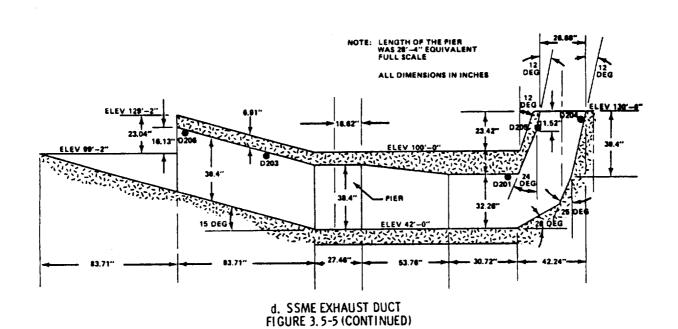




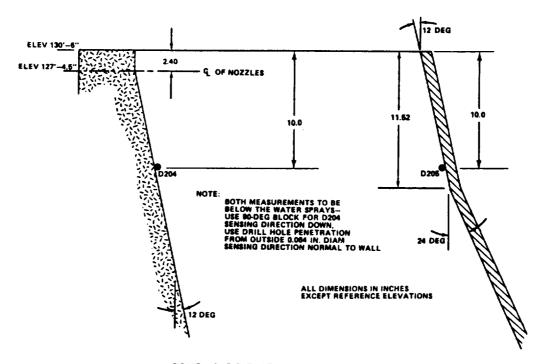


c. MODEL SRB PRIMARY EXHAUST HOLE FIGURE 3.5-5 (CONTINUED)

R-ENG 147



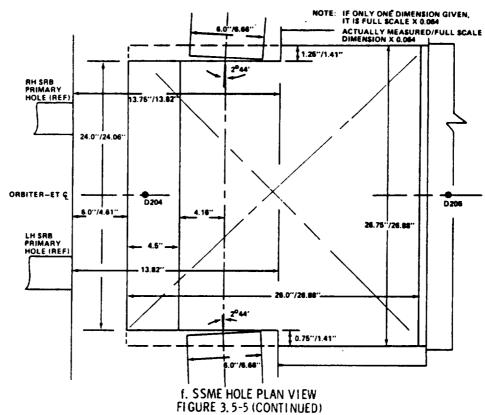
3-46



€_

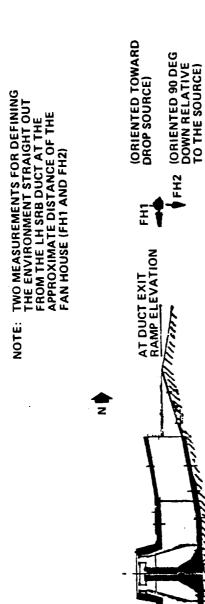
e. SSME HOLE ELEVATION (LOOKING SOUTH) FIGURE 3. 5-5 (CONTINUED)

R-ENG 197



3-47

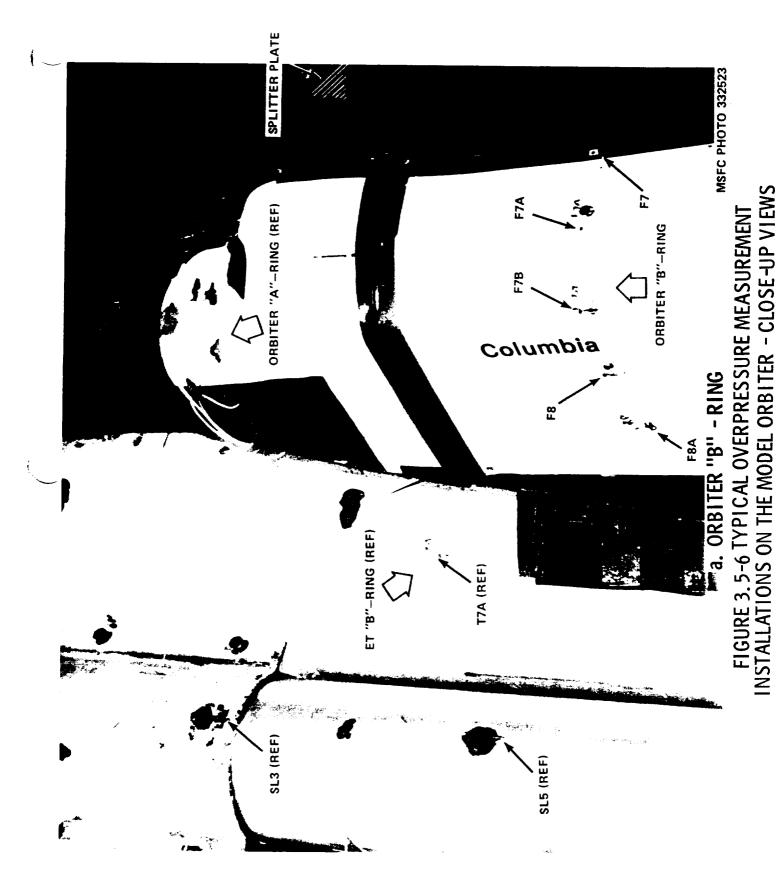
R-ENG 198



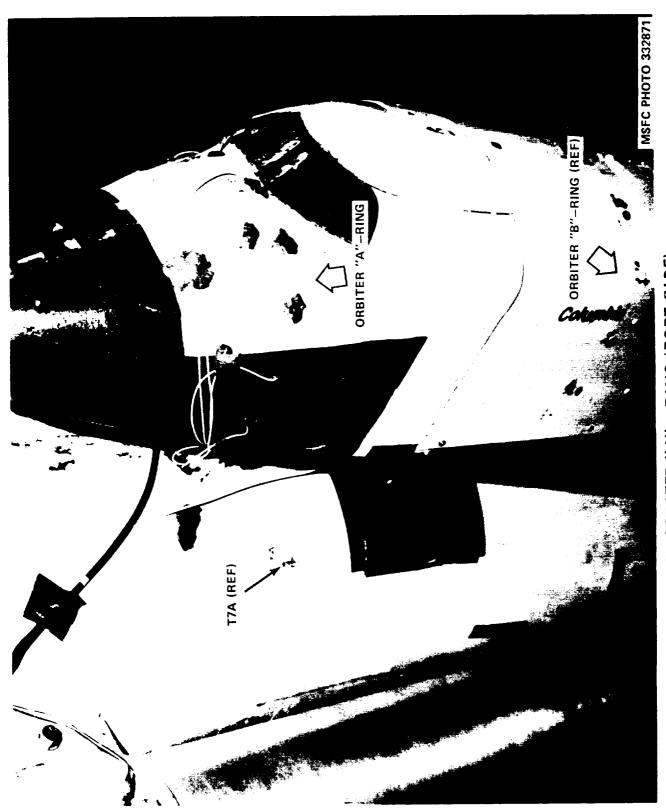
g. LOCATIONS FOR FAN HOUSE ENVIRONMENT FIGURE 3.5-5 (CONCLUDED)

FH1, FH2

500' EQUIV FULL SCALE ON THE SRB DUCT CENTERLINE



3-49



b. ORBITER "A" - RING (PORT SIDE)FIGURE 3. 5-6 (CONTINUED)

d. ORBITER "D" - RING FIGURE 3.5-6 (CONCLUDED)

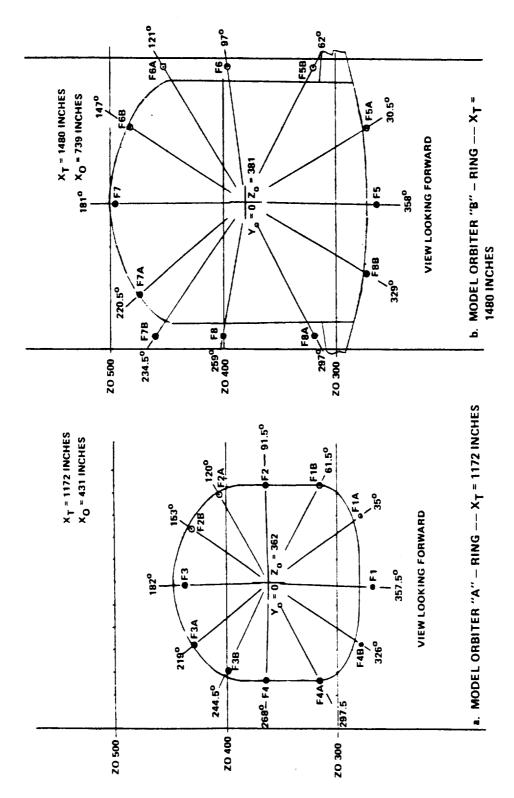


FIGURE 3.5-7 MODEL ORBITER FUSELAGE AND MODEL EXTERNAL TANK RINGS OF MEASUREMENTS (SINGLE - MODEL SRM TESTS)

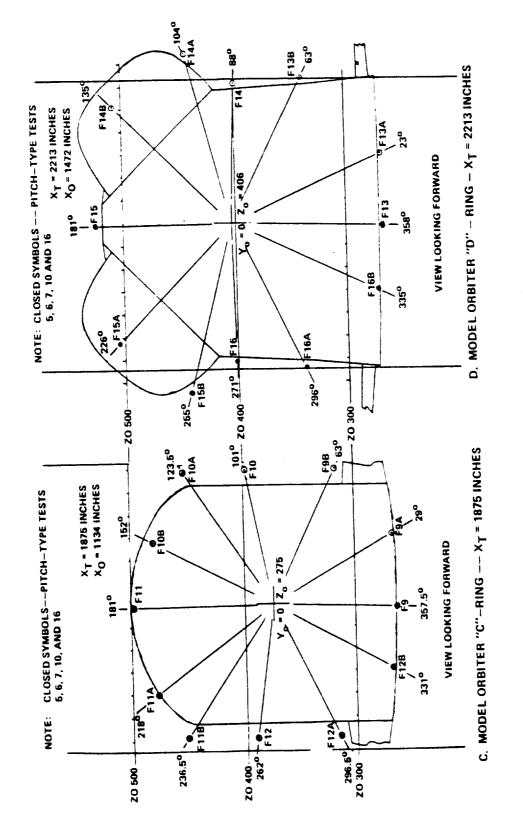
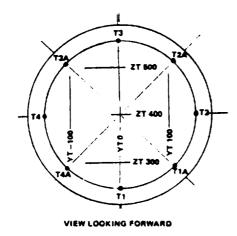
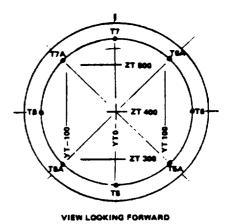


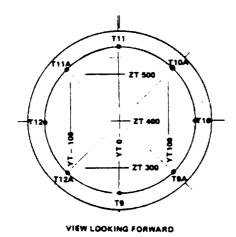
FIGURE 3.5-7 (CONTINUED)

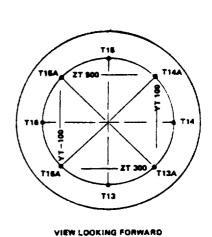
NOTES: 1. CLOSED SYMBOLS — PITCH-TYPE TESTS 6, 6, 7, 10 AND 16
2. MEASUREMENTS T1 AND T3 WERE DELETED
FOR LATERAL-TYPE TESTS 11 THROUGH 16





e. MODEL EXTERNAL TANK "A" - RING --XT = 771 INCHES f. MODEL EXTERNAL TANK "B" - RING -- XT = 1273 INCHES





g. MODEL EXTERNAL TANK "C" - RING --- X_T = 1751 INCHES h. MODEL EXTERNAL TANK AFT DOME "D" -- RING --- X_T = 2116 INCHES

FIGURE 3.5-7 (CONCLUDED)

TABLE 3-5-1 OVERPRESSURE MEASUREMENT LOCATIONS

a. PITCH-TYPE SRM TESTS

	FULL	SCALE, INC	HES	MODEL S	CALE, INC			HEAT/	
SENSOR	XT	YT	ZŢ	X	Y	z	ORIENTATION	LIGHT	TESTS
NUMBER	'							PROTECTION	
				- 1	1	1			
Orbiter		1	1		1		_		- 10 16
F1	1171.7	-3.9	604-7	12.65	-0.25	13-10	- Z	None	5-10,16
F3	1172.5	-2.3	775.0	12.70	-0.15	24.00	+Z	None	5-10, 16
F3A	1172.5	-57.0	767.2	12.70	-3-65	23.50	+Z;-Y	None	5-10, 16
F38	1172.5	-78-1	734.4	12.70	-5.00	21.40	+Z;-Y	None	5-10,16
F4	1173-3	-85.9	696.9	12.75	-5.50	19.00	-Y	None	5-10,16
F4A	1172-5	-85.9	653-1	12.70	-5.50	16 - 20	-Z;-Y	None	5-10,16
F48	1172.5	-54.7	614.8	12.70	-3.50	13.75	-Z;-Y	None	5-10,16
F5	1479.5	-1.7	599.2	32. 35	-0-11	12.75	- Z	None	5-10, 16
F7	1481.9	-2.8	829.7	32.50	0.18	27.50	+Z	None	5-10,16
F7A	1481-9	-81.3	810.2	32.50	-5.20	25.25	+Z;-Y	None	5-10,16
F7B	1479.5	-117.2	796.9	32. 35	-7.50	25.40	-Y	None	5-10,16
F8	1479.5	-117.2	737-5	32. 35	-7.50	21.60	-Y	None	5-10,16
F8A	1479-8	-117-2	656 - 3	32. 37	-7.50	16.40	- Y	None	5-10,16
F88	1479.7	-62.5	607-8	32. 36	-4.00	13.30	- Z	None	5-10,10
F9	1872-5	-4.2	599.2	57.50	-0 • 27	12.75	- Z	D	5-10,10
F11	1876.4	-2.8	835.6	57.75	-0.18	27.88	+Z	D	5-10,1
F11A	1874-1	-80.2	814.8	57.60	-5.13	26.55	- Y	D	5-10,1
F11B	1874.1	-117.2	788.3	57.60	-7.50	24.85	- Y	D	5-10,1
F12	1877.9	-117.2	728.9	57.85	-7.50	21.05	- Y	D	5-10,1
F12A	1878.3	-117.2	653.9	57.87	-7.50	16.25	- Y	D	5-10,1
F128	1876-4	-58.6	603-1	57.75	-3.75	13.00	- Y	ם	5-10,1
F13	2212.3	-3.9	603-1	79.25	-0.25	13.00	- Z	D	5-10,1
F 15	2212.37	1	860.9	79.25	-0.15	29.50	+Z	D	5-10,1
F15A	2219.1	-104.7	841.4	79.68	-6.70	28.25	+Z;-Y	D	5-10,1
F 15B	2216.3	-149.2	778.9	79.50	-9.55	24.25	- Y	D	5-10,1
F 16	2212.3	-121-1	737.5	79.25	-7.75	21.60	-Y	D	5-10,1
F 16A	2211.9	-126.6	675.0	79.22	-8-10	17.60	-Y	D	5-10,1
F 16B	2213-2	-58.6	607.8	79.30	-3.75	13.30	- Z	D	5-10,1
F17	2275.2	-1.6	704.7	8 3 . 2 7	-0.10	19.50	+X;+Z	1	5-10,1
F18	225 3.8	-82.0	733.6	81.90	-5.25	21.35	+X;+Z	D	5-10,1
F 19	2274.8	-113-3	633-6	83.25	-7.25	16.87	+X;+Z	D	5-10,1
BF1	2356.9	-6.7	608.8	88.50	0.43	13-36	- Z	D	5-10,1
BF 2	2356-1	-8.6	604.7	88.45	-0.55	13-10	+Z	D	5-10,1
W1	1943.9	-195.3	647.0	62.07	-12.50	15.81	- Z	D	5-10,1
W 2	1934-1	-187-5	654.8	61.44	-12.00	16.31	+Z	D	5-10,1
W3	2150.9	-377.0	647.0	75.32	•	15.81	- Z	D	5-10,1
W4	2150.9	-398.4	654.8	75.32		16.31	+Z	D	5-10,
W5	2170.5	-201.3	647.0	76.57	3	15.81	- z	D	5-10,1
W6	2174.4	-220.8	654.8	76.82	1	16.31	+Z	D	5-10,1
#U	1 *****		1			ł		<u> </u>	

TABLE 3-5-1 OVERPRESSURE MEASUREMENTS LOCATIONS (CONTINUED)

a. PITCH-TYPE SRM TESTS

	FULL	SCALE, II	ICHES	MODEL	SCALE, IN	ICHES		HEAT/	
SENSOR	X _T	YT	ZŢ	X	Y	Z	ORIENTATION	LIGHT	TESTS
NUMBER	<u>'</u>	<u> </u>						PROTECTION	
ET	İ						•		
T1	770.6	-1.6	243.8	-13-02	-0.10	-10.00	- Z	None	5-10,16
T3	770-6	-1.6	556.3	-13-02	-0.10	10.00	+Z	None	5-10,16
T3A	770-6	-113.3	513.3	-13.02	-7.25	7.25	+Z;-Y	None	5-10,16
T4	770.6	-156.3	400.0	-13.02	-10.00	0	-Y	None	5-10,16
T4A	770.6	-113.3	286.7	-13-02	-7.25	-7.25	-Z;-Y	None	5-10,16
T5	1272.7	-1.6	243.8	19.11	-0.10	-10.00	- Z	None	5-10,16
T 7	1272.7	-1.6	556.3	19.11	-0.10	10.00	+Z	None	5-10,16
T7A	1272.7	113-3	513.3	19.11	-7.25	7.25	+Z;-Y	None	5-10,16
T8	1272.7	-156.3	400.00	19.11	-10.00	0	-Y	None	5-10,16
TBA	1272.7	-113.3	286.7	19.11	-7.25	-7.25	-Z;-Y	None	5-10,16
T9	1750-8	-1.6	243-8	49.71	-0-10	-10.00	- Z	None	5-10,16
T11	1750.8	-1.6	556.3	49.71	-0.10	10.00	+Z	None	5-10,16
TIIA	1750-8	-113.3	513.3	49.71	-7.25	7.25	-Z;-Y	D	5-10,16
T12	1750-8	-156.3	400.0	49.71	-10.00	0	-Y	ס	5-10,16
T12A	1750-8	-113.3	286.7	49.71	-7.25	-7.25	-Z;-Y	D	5-10,16
T13	2115.5	-1.6	243-8	73-05	-0.10	-10.0	- Z	D	5-10,16
T 15	2115.5	-1.6	556.3	73.05	-0.10	10.0	+Z	D	5-10,16
T 15A	2115.5	-113.3	513.3	73.05	-7.25	7.25	+Z;-Y	ם	5-10,16
T16	2115.5	-156.3	400.0	73-05	-10.00	0	-Y	D	5-10,16
T16A	2115.5	-113.3	286.7	73-05	-7.25	-7.25	-Z;-Y	Ð	5-10,16
T17	2174.5	-4.2	400.0	76.83	-0.27	0	+X		5-10,16
									5-10,16
LH SRM									5-10,16
P4	314.1	-371-1	400.0	-42.24	-23.75	0	+X	N/A	5-10,16
SG 2	456.6	-317.2	400.0	-33.12	-20.30	0	Ноор	N/A	5-10,16
SG4	2145.2	-317.2	400.0	74.95	-20.30	0	Ноор	N/A	5-10,16
N1	25 35 . 5	-273.4	470.3	99.93	-17.50	4.50	Radial	P	5-10,16
N3	25.55.5	-210.9	329.7	99.93	-13-50	-4.50	Radiai	Р	5-10,16
SL 1	1084.4	-246-1	325.8	7.06	-15.75	-4.75	+X	None	5-10,16
SL3	1084.4	-246.1	474.2	7.06	-15.75	4.75	+X	None	5-10,16
SL5	1356.9	-246-1	325.8	24.50	-15.75	-4.75	+X	None	5-10,16
SL7	1356.9	-246-1	474.2	24.50	-15.75	4.75	+X	None	5-10,16
SL9	1904.7	-246-1	325.8	59.56	-15.75	-4.75	+x	D	5-10,16
SL11	1904.7	-246.1	474.2	59.56	-15.75	4.75	+X	D	5-10,16
SL13	2375.5	-246-1	325.8	89.69	-15.75	-4.75	+X	D	5-10,16
SL 15	2375.5	-246.1	474.2	89.69	-15.75	4.75	+X	D	5-10,16
SL 18	2495.6	-329.0	400.0	97.38	-21-06	0	+X	D	5-10,16
SL 20	2495.6	-329.1	400.0	97.38	-10-05	0	+X	ם	5-10,16
SL 23	2543.8	-246.1	485.9	100.46	-15.75	5.50	+X	D	5-10,16
		[1	Í			!		

TABLE 3-5-1 OVERPRESSURE MEASUREMENTS LOCATIONS (CONTINUED)

a. PITCH-TYPE SRM TESTS

1	FULL :	SCALE, INC	HES	MODEL	CALE, INC	nes		HEAT/	
SENSOR	XT	YT	Z _T	x	Y	Z	ORIENTATION	LIGHT PROTECTION	TESTS
NUMBER								PROTECTION	
		[l		1				
Splitter		1	1		\$	į.		1	
Plate	2177•3	0	-806.4	77.01	0	-77.21	-Y	D	5-10,16
SPL6	1624.7	0	-471.7	41.64	ō	-55.79	-Y	D	5-10,16
SPL12	1324.1	o l	18.8	22.40	0	-24.40	- Y	D	5-10,16
SPL 18	1303-8	o l	1089.1	21.10	0	44.10	- Y	D	5-10,16
SPL 21	1713.1	ŏ	1182.8	47.30	0	50.10	- Y	ם	5-10,16
SPL 22	1/1301	ľ			1	1			
SRB		ĺ	ĺ	}	j	}			
Exhaust				}		1			
Duct	ĺ			1	j	Ī		1 _	
01	2965.8	-568.0	390 - 2	127 - 47	-36.5	-0.63	- Z	В	5-10-16
D2	2965.8	-923.4	384.4	127.47	-59.10	-1.00	- Z	В	5-10-16
03	2887.7	-1708-8	400-0	122-47	-109.36	0	+X	В	5-10.16
D 3A	28 22-5	-2157.3	400.0	118.30	-138.07	0	+X	P	16
D. 3 B	2788.8	-2410-2	400.0	116.4	-154.25	0	+X	P	16
D.3C	3187.7	-2180.6	495.8	141.67	-139.56	6.13	- Z	Р	16
0.30	28 22.5	-2173-0	3.4	118.30	-139.07	-25.38	+X	P	16
DΣ	3187.7	-2165.2	-92.2	141-67	-138.57	-31.50	+Z	Р	16
D4	ł	i i)		В	5-7
D4*	275915	-2623-6	400	114.24	-167-91	0	+X	P	8-10, 16
D5	2431.1	-253.6	493.8	93.25	-16-23	6.00	+X	В	5,6,7,10,
D6	2587.3	-253.9	493.8	103.25	-16.25	6.00	+X	В	5,6,7,10,
D7	24.35 - 1	-118.8	390 - 2	93.57	-7.60	-0.63	+X	В	5,6,7,10,
D8	2588.4	-117.2	388.3	103-32	-7.50	-0.75	+X	В	5,6,7,10,
021	2743.6	-23.6	493-8	113-25	-15 - 23	6.00	+X	В	5,6,7,10,
D 24	2899.9	-241.9	493.8	123.25	-15.48	6.00	+X	В	5,6,7,10,
025	3297.8	-26万.6	495.8	148.72	-168-68	6.13	- Z	8	5-7
025*	3063.6	-2620.5	495.8	133-73	-167.71	6-13	- Z) R	8-10,6
026	3301.6	-26.35.9	-92.2	148.96	-168.70	-31.50	+Z	В	5-7
026*	3055.8	-2623-6	-92.2	133-23	-167.91	-31.50	+Z	P	8-10,6
027	2891.7	-2914.1	909.8	122.73	j.	32-63	- Z	D	5-10,6
0.28	2891.7	-2910.9	-516-1	122.73	ł	-58.63	+Z) 0	5-10,6
01	2253.3	-1703-1		81.87		0	- Y	D	5-10,6
02			{ !		1		- Y	D	10
•			([-Y	D	10,16
03							_,		

TABLE 3.5-1 OVERPRESSURE MEASUREMENTS LOCATIONS (CONTINUED)

a. PITCH-TYPE SRM TESTS (CONCLUDED)

	FULL	SCALE, IN	CHES	MODEL	SCALE, IN	CHES		HEAT/	
SENSOR	X _T	YT	ZŢ	X	Y	Z	ORIENTATION	LIGHT	TESTS
NUMBER			,					PROTECTION	
MUFFLER									
D 29	2555.5	-2621.9	-18.0	101.21	-167.80	-26.75	+x	Р	8,9
0.30	2588.8	-2621.9	521.1	103-34	-167.80	7.75	- Z	Р	8,9
031	2757.0	-2952.0	-78.4	114-11	-188-93	-30.62	+Z	P	8,9
033	2484.2	-2953.9	-18.0	96.65	-189.05	-25.75	+X	P '	8,9
034	2484.2	-2953.9	216.4	96.65	-189.05	-11.75	+X	P	8,9
D35	2484.2	-2953.9	421.4	96-65	-189.05	1.37	+X	P	8,9
D36	25 15 . 9	-2952.0	521.1	98.68	-188.93	7.75	- Z	Р	8,9
0.37	2757.0	-2951.9	521.1	114-11	-188.92	7-75	- Z	P	8,9
D 3 8	2977.0	-2952.0	521.1	128.19	-188.93	7.75	- Z	P	8,9
039	2425.6	-3168-8	216.4	92.9	-202.80	-11.75	+X	P	8,9
D40	2425.6	-3168.8	421.4	92.9	-202.80	1.37	+X	P	8,9
D42	2640.5	-3164-1	521.1	106.65	-202.50	7.75	- Z	Р	8,9
D43	2589.7	-3164.1	521.1	103-40	-202.50	7.75	- Z	P	8,9

TABLE 3-5-1 OVERPRESSURE MEASUREMENTS LOCATIONS (CONTINUED)

b. LATERAL-TYPE SRM TESTS

	FULL S	CALE, INC	HES		SCALE, INC			HEAT/	TECTE
SENSOR	X _T	YT	ZT	X	Y	Z	ORIENTATION	LIGHT	TESTS
NUMBER								PROTECTION	
			1	1	1				
Orbiter	1	1				13.10	- Z	None	11-15
F1	1171-7	-3.9	604-7	12.65	-0.25		-Z;+Y	None	11-15
F1A	1171.7	58.6	614-8	12.65	3-75	13.75	-Z;+Y	None	11-15
F 18	1170.6	85.9	684-4	12.58	5.50	19.00	+Y	None	11-15
F2	1170-9	85.9	696.9	12.60	5.50	22.00	+Z;+Y	None	11-15
F 2A	1171.7	78-1	743.8	12.65	5.00	23.50	+Z;+Y	None	11-15
F 2B	1171.7	万•2	767.2	12.65	2.25	24.00	+Z	None	11-15
F3	1172.5	-2.3	775.0	12.70	-0.15		+Z;-Y	None	11-15
F3A	1172.5	-57.0	767.2	12.70	-3.65	23.50		None	11-15
F 38	1172.5	-78.1	734.4	12.70	-5.00	21.40	+Z;-Y -Y	None	11-15
F4	1173-3	-85.9	696.9	12.75	-5.50	19.00		None	11-15
F4A	1172-5	-85.9	653-1	12.70	-5.50	16 - 20	-Z;-Y -Z;-Y	None	11-15
F4B	1172.5	-54.7	614.8	12.70	-3.50	13.75	-2;-1 -Z	None	11-15
F5	1479.5	-1.7	599.2	32. 35	-0.11	12.75		None	11-15
F5A	1479-1	64.8	507.8	32.32	4-15	13.30	-Z;+Y -Z	None	11-15
F5B	1479.5	117-2	656.3	32. 35	7.50	16.40	-2 +Y	None	11-15
F6	1479.8	117.2	732.8	32. 37	7.50	21.30		None	11-15
F6A	1480.3	117.2	789-1	32.4	7.50	24.90	+Y	None	11-15
F68	1479.5	64-1	818-8	32.35	4 10	26.80	+Z;+Y	D	11-15
F7	1481.9	-2.8	829.7	32.50	-0.18	27.50	+Z	1	11-15
F7A	1481.9	-81.3	810.2	32.50		26.25	+Z;-Y	D	11-15
F7B	1479.5	-117.2	796.9	32. 35	-7.50	25.40	- Y	D	11-15
F8	1479-5	-117-2	737.5	32. 35	-7.50	21.60	-Y	Į.	11-15
F8A	1479.8	-117.2	656.3	32. 37	-7.50	16.40	-Y	D	11-15
F88	1479.7	-62.5	607.8	33.36	-40.0	13-30	-Z)	11-15
F9	1872-5	-4-2	599.2	57.50	1	12.75	-Z	D	11-15
F9A	1874-1	60.6	603-1	57.60	ı	13.00	- Z	D	11-15
F98	1874-1	117.2	653-9	57.60	*	16.25	+Y	D	11-15
F10	1874-1	117.2	735.0	57.60	,	21.44	+Y	D	11-15
FIOA	1875.6	117.2	789-2	57.70		24.91	+ Y	0	11-15
F10B	1875.6	54.7	817.3	57.70		26.71	+Z;+Y	D	11-15
FII	1876.4	-2.8	835.6	57.75	•	27 - 88	+Z	D	11-15
FIIA	1874 - 1	-80-2	814.8	57.60		26.55	+Z;-Y	D	1
F118	1874.1	-117.2	788 - 3	57.60		24.85	-Y	D	11-15
F12	1877-9	-117.2	728.9	57.85	*	21.05	- Y	0	11-15
F12A	1878-09	-117.2	653.9	57.87	,	16.25	-Y	D	11-15
F128	1876-4	-58.6	603-1	57.75	,	13.00	-z	D	11-15
F13	2212.3	-3.9	603-1	79.25	1	13.00	-Z	D	11-15
F13A	2212.3	58.6	604.7	79.25	1	13-10	-z	D	11-15
F138	2211.6	125.6	675.0		,	17.60	+Y	D	11-15
F14	2216.3	121.1	735.9	79.50	7.75	21.50	+Y	D	11-15
F14A	2211.6	148.4	779.7	79.20	9.50	24.30	+Y;-Z	D	11-15
F14B	2213-1	100.9	843.8	79.30	6.46	28.40	+Z;-Y	D	11-15
		1	i	L	1				

TABLE 3.5-1 OVERPRESSURE MEASUREMENTS LOCATIONS (CONTINUED)

b. LATERAL-TYPE SRM TESTS

SENSOR NUMBER	× _T	YT							
,		''	Z _T	X	Y	Z	ORIENTATION	LIGHT PROTECTION	TESTS
F15	2212.3	-2.3	860.9	79.25	-0.15	29.50	+Z	D	
F 15A	2219.1	-104.7	841.4	79.68	-6.70	28.25	+Z;+Y	D	11-15
F 158	2216.3	-121.1	778.9	79.50	-9.55	24.25	+Z;-Y	D	11-15
F16	2212.3	-121.1	7.70.5	79.25	-7.75	21.60	-Y	D	11-15
F16A	2211.9	-126.6	675.0	79.22	-8.10	17.60	-Y	D	11-15
F 16B	2213-1	-58.6	607.8	79.30	-3.75	13-30	-z	D	11-15
F 18	225 3.8	-82.0	733.6	81.90	-5.25	21.35	+X;+Z	. D	11-15
F20	225 3.8	80.5	735.9	81.90	5. 15	21.50	+X;+Z	D	11-15
F21	225 3.8	113.3	642.2	81.90	7.25	15.50	+X;+Z	D	11-15
Vertical				!					
V1	2292.5	1.6	1083.6	84.38	0.10	43.75	+Y	D	11-15
V2	229 2.5	-1.6	1096 • 1	84.38	0 - 10	44.55	- Y	D	11-15
1			;						
ET	ł		'					}	
T1A J	770.6	113-3	286.7	-13.02		-7.25	-Z;+Y	D	11-15
T2 }	770.6	156 - 3	400.0	-13.02	10.00	0	+Y	D	11-15
T2A	769.4	113-3	513.3	-13.10	7.25	7.25	+Z;+Y	D	11-15
T3A	770.6	-113.3	513.3	-13.02	-7.25	7.25	+Z;-Y	D	11-15
T4	770.6	-156.3	400.0	-13-02	-10.00	0	- Y	D	11-15
T4A	770•6	-113-3	286.7	-13.02	-7.25	7.25	-Z;-Y	D	11-15
T5A	1273.0	113-3	286.7	19.13	7.25	-7.25	-Z;+Y	D	11-15
T6	1273.3	156.3	400.0	19.15	10.00	0	+Y	D	11-15
T6A	1273.3	113.3	513.3	19.15	7.25	7.25	+Z;+Y	D	11-15
T7A	1272.7	-113.3	513.3	19.11	-7.25	7.25	+Z;-Y	D	11-15
T8	1272.7	-156-3	400.0	19.11	-10.00	0	-Y	D	11-15
TBA	1272.7	-113.3	286.7	19.11	-7.25	-7.25	-Z;-Y	D	11-15
T9A	1750.6	113.3	286.7	49.70	7.25	-7.25	-Z;+Y	D	11-15
T10	1750-8	156-3	400.0	49.71	10.00	0	+Y	D	11-15
TIOA	1750.8	113-3	513.3	49.71	7.25	7.25	+Z;+Y	D	11-15
TIIA	1750.8	-113.3	513.3	49.71	-7.25	7.25	+Z;-Y	D	11-15
T12	1750.8	-156.3	400.0	49.71	-10.00	0	-Y	D	11-15
T12A	1750.8	-113.3	286.7	49.71		-7.25 -7.25	-Z;-Y	D	11-15
T13A	2114.7	113.3	286.7	73.0	7.25	-7.25	-Z;+Y	D	11-15
T14	2115.5	156.3	400.0	73-05	10.00	0	+Y	D	11-15
T14A	2115.5	113.3	513.3	73-05	7.25	7.25	+Z;+Y	D	11-15
T15A	2115.5	-113.3	513.3	73-05	-7.25	7.25	+Z;-Y	D	11-15
T16	2115.5	-156.3	400.00		-10.00	0	-Y	D	11-15
T16A	2115.5 2174.5	-113.3 -4.2	286.7 400.0	73-05 76-83	-7.25 -0.27	-7•25 0	-Z;-Y +X	D	11-15 11-15

TABLE 3-5-1 OVERPRESSURE MEASUREMENTS LOCATIONS (CONTINUED)

b. LATERAL-TYPE SRM TESTS (CONCLUDED)

	FULL S	SCALE, INC	HES	MODEL S	CALE, INC	HES		HEAT/	
SENSOR	XT	YT	ZT	х	Y	Z	ORIENTATION	LIGHT	TESTS
NUMBER								PROTECTION	
_H SRM			1						
P4	314.1	-371-1	400.0	-42.24	-23.75	0	+X	None	11-15
SG 2	456.6	-317.2	400.0	-33-12	-20.30	0	Ноор	N/A	11-15
SG4	2145.2	-317.2	400.0	74.95	-20.30	0	Ноор	N/A	11-15
SL 18	2495.6	-329.1	400.0	97.38	-21.06	0	+X	D	11-15
SL 20	2495.6	-329.1	400.0	97.38	-10.05	0	+X	D	11-15
SL 23	2543.7	-246.1	485.9	100.46	-15.75	5.50	+X	D	1 1-15
SR8			ł	1				ĺ	
Exhaust			ł	1					
Duct	2965.8	-568.0	390.2	127.47	-36.35	-0.63	- Z	В	11-19
D1 D2	2965.8	-923.4	384.4	127.47	-59.10	-1.00	- Z	В	
-	2887.7	-1708.8	400.0	122.47	-109.35	0	+X	В	11-1
D3	28 22.5	-2157-3	400.0	118.30	-138.07	0	+X	Р	11-1
D3A	2788.8	-2410-2	400.0	116.14	-154.25	0	+X	P	11-1
0.38	3187.7	-2180.6	495.8	141.67	-139.56	6.13	- Z	Р	13-1
D3C D3D	28 22.5	-2173.0	3.4	118.30	-139.07	-25.38	+X	P	13-1
030 03E	3187.7	-2165-2	-92.2	141.67	-138.57	-31.50	+Z	Р	13-1
03E D4#	2759.1	-2682.0	400.0	114.24	-167.91	0	+X	Р	11-1
D 4 -	2431.1	-253.6	493.8	93.25	-16.23	6.00	+X	В	11-1
D6	2587.3	-253.9	493.8	103-25	-16.25	6.00	+X	В	11-1
D7	2436.1	-118.8	390 - 2	93.57	-7.60	-0.63	+X	В	11-1
D8	2588.4	-117.2	388.3	103-32	-7.50	-0.75	+X	В	11-1
D21	2743.6	-253.6	493-8	113-25	-16-23	6.00	+X	В	11-1
D21	2899.8	-241.9	493.8	123.25	-15.48	6.00	+X	В	11-1
0.2 4 0.25*	3063.6	-2620.5	-495.8	133-73	-167.71	6.13	- Z	Р	11-1
026*	3055.8	-2623.6	-92.2	133-23	-167-91	-31.50	+Z	В	11-1
0.27	2891.7	-2914-1	909.8	122.73	1 1	32.63	- Z	D	11-1
D 28	2891.7	-2910.9	-516.1	122.73	1 1	-58.63	+Z	D	11-1
026	205101							1	1

TABLE 3-5-1 OVERPRESSURE MEASUREMENTS LOCATIONS (CONTINUED)

c. SSME AND FULL-MODEL TESTS

	FULL	SCALE, IN	ICHES 1	MODEL	SCALE, II	NCHES 1		HEAT/ 2	
SENSOR	X _T	YT	ZT	X	Y	Z	ORIENTATION	LIGHT	TESTS
NUMBER	· '	'	'	(1	1	i	PROTECTION	
						 			
Orbiter	1			l		1	Í	İ	
F1	1171.7	-3.9	604.7	12.65	-0.25	13.10	- z	None	30-32,40
F2	1170.9	85.9	696.9	12.60	5.50	19.00	+Y	None	30-32,40
F3	1172-5	-2.3	775.0	12.70	-0.15	24.00	+Z	None	30-32,40
F4	1173.3	-85.9	696.9	12.75	-5.50	19.00	-Y	None	30-32,40
F5	1479.5	-1.7	599.2	32.35	-0.11	12.75	- -Z	None	30-32,40
F6	1479.8	117.2	732.8	32. 37	7.50	21.30	+Y	None	30-32,40
F7	1481.9	-2.8	832.0	32.50	-0.18	27 - 65	+Z	None	30-32,40
F8	1479.5	-117.2	737.5	32.35	-7.50	21.60	-Y	None	30-32,40
F9	1872.5	-4.2	599.2	57.50	-0.27	12.75	- z	D	30-32,40
F10	1874.1	117.2	735.0	57.60	7.50	21.44	+Y	D	30-32,40
F11	1876.4	-2.8	835.6	57.75	-0.18	27.88	+Z	D	30-32,40
F12	1877.9	-117.2	728.9	57.85	- 7.50	21.05	- Y	D	30- 32, 40
F13	2212.3	-3.9	603.1	79.25	-0.25	13.00	- z	ם ו	30-32,40
F14	2216.3	121.1	735.9	79.50	7.75	21.50	+Y	D	30-32,40
F 15	2212-3	-2.3	860.9	79.25	-0.15	29.50	+Z	ا ۵	30-32,40
F16	2212.3	-121.1	737.5	79.25	-7.75	21.60	-Y	D	30-32,40
F17	2267.0	-1.6	704.7	82-75	-0.10	19.50	+X;+Z	D	30-32,40
F 19	225 3.8	-113.3	663.6	81.90	-7.25	16.87	+X;+Z	D	30-32,40
F21	225 3.7	113.3	642.2	81.90	7.25	15.50	+X;+Z	D	30-32,40
BF1	2356-1	-5.5	604.7	88.45	-0.35	13-10	+Z	D	30-32,40
BF2	2356.9	-6.7	608.8	88.50	-0.43	13.36	- z	ם	30-32,40
W1	1943.9	-195.3	647.0	62.07	-12.50	15-81	- Z	D	30-32,40
W2	1934-1	-187.5	654.8	61.44	-12-00	16.31	+Z	D	30-32,40
W3	2150.9	-377.0	647.0	75.32	-24.13	15.81	- Z	D	30-32,40
W4	2150.9	-398.4	654.8	75.32	-25.50	16.31	+Z	D	30-32,40
W5	2170.5	-201.3	647.0	76.57	-12.88	15.81	- Z	D	30-32, 40
W6	2174.4	-220.8	654.8	76.82	-14.13	16 - 31	+Z	D	30-32,40
W9	2157.7	378.9	619.8	75.75	24.25	14.07	- z	ם	30-32,40
W10	2157.7	398.4	629.5	75.75	25.50	14.69	+Z	D	30- 32, 40
W13	2011-3	240.3	619.8	66.38	15 • 38	14.07	- Z	D	30-32, 40
W14	2011-3	259.7	629.5	66.38	16.62	14.69	+Z	D	30-32,40
W 15	2179-1	217.5	619•8	77-12	13-94	14.07	- Z	D	30-32,4 0
W16	2179•1	198-3	629.5	77-12	12.69	14.69	+Z	D	30-32, 40
V 1	229 2.5	1.6	1083.6	84-38	0.10	43,75	+Y	D	30-32,40
V2	229 2.5	-1.6	1096-1	84.38	-0.10	44.55	- Y	D	30-32, 40
								İ	
ET			ļ						
T1	770.6	-1.6	24 3.8	-13.02	-0.10	-10.00	- Z	None	30-32,40
T2	770.6	156.3	400.0	-13-02	10.0	0	+Y	None	30- 32, 40
Т3	770.6	-1.6	556.3	-13-02	-0.10	10-00	+ Z	None	30-32,40
T4	770.6	-156.3	400.0	-13-02	-10.0	0	-Y	None	30-32,40
T5	1272.7	-1.6	243.8	19.11	-0.10	-10.00	- Z	None	30-32,40
T6	1273.3	156.3	400.0	19.15	10.0	0	+Y	None	30-32,40
Т7	1 27 2 • 7	-1.6	556.3	19.11	-0.10	10.00	+ Z	None	30-32,40

TABLE 3.5-1 OVERPRESSURE MEASUREMENTS LOCATIONS (CONTINUED)

c. SSME AND FULL-MODEL TESTS

Į.	FULL S	CALE, INC	HES <u>1 [</u>	MODEL S	CALE, INC			HEAT/ 2	TECTO
SENSOR NUMBER	XT	YT	Z _T	X	Y	Z	ORIENTATION	LIGHT PROTECTION	TESTS
No. sex									
тв	1272.7	-156-3	400.0	19-11	-10.0	0	- Y	None	30-32,40
T9	1750-8	-1.6	243-8	49.71	-0.10	-10.00	- Z	None	30-32,40
T10	1750-8	156-3	400.0	49.71	10.0	0	+Y	D	30-32,40
T11	1750.8	-1.6	556-3	49.71	-0.10	10.00	+Z	None	30-32,40
T12	1750-8	-156.3	400.0	49.71	-10-0	0	- Y	D	30-32,40
T13	2115.5	-1.6	243.8	73-05	-0.10	-10.00	- Z	D	30-32,40
T14	2115.5	156-3	400.0	73-05	10.0	0	+Y	D	30-32,40
T15	2115.5	-1.6	556.3	73.05	-0.10	10.00	+Z	D	30-32,40
T16	2115.5	156-3	400.0	73.05	-10.0	0	-Y	D	30-32,40
T17	2174.5	-4-2	400.0	76.83	-0-27	0	+X	D	30-32,40
SSME's									
P1				ĺ				-	30-32,4
P2				1			-	-	30-32,4
P3							•	-	30-32,4
SRB's				ļ				-	30-32,4
P4	314-1	-371 - 1	400.0	-42.24	-23.75	0	-	_	30-32,4
P5	314-1	371-1	400.0	-42.24	23.75	0	-	_	30-32,4
SG2	456.6	-317-2	400.0	-33-12	-20-30	0	Ноор	_	1
SG8	456.6	317.2	400.0	-33-12	20.30	0	Ноор	_	30-32,4
SL18	2495.6	-329.0	400-0	97.38	-21.06	0	+X	D	30-32,4
SR17	2495.6	246.1	310-2	97.38	15.75	-5.75	+X	D	30-32,4
LH SRB			j	1	j				
DUCT	ļ.					0.67	- Z	8	30-32,4
Dt	2965.8	-568.0	390-2	127.47	-36-35	-0.63	+X	P	30-32,4
03	2887.7	-1708-8	400.0	122-47	-109-36	0	+X	P	30-32,4
D4	2759.1	-2623-6	400.0	114-24	-167.91	0		В	30-32,
D14	2969.7	-125.0	71 - 1	127.72	-8.00	-21.05	+X	8	30-52,
FAN HOUSE							+Y	D	40
FH1	2849.0	-9375.0	400.0	120-0	-600.0	0	+X	D	40
FH2	2849•0	-9375.0	400.0	120.0	-600.0	J	**		
RH SR8									
DUCT			400.0	127.47	36.35	0	-z	В	30-32,
0101	2965.8	568.0	400.0		109.36	0	+x	P	30-32,
D103	2906.3	1708-8	400.0	123.66	138.07	Ö	+x	Р	30-32,
D103A	2843.2	2157.3	400.0	119.62	167.91	0	+X	P	30-32,
D104	2777.7	2623.6	400.0	115.43	ł	-21.05	+x	В	30-32,
D114	2969-7	125.0	71 • 1	127.72	-8.00	-21.00	1 '^	1	1

TABLE 3.5-1 OVERPRESSURE MEASUREMENTS LOCATIONS (CONCLUDED)

c. SSME AND FULL-MODEL TESTS (CONCLUDED)

	FULL	SCALE, IN	CHES 1	MODEL :	SCALE, INC	CHES 1		HEAT/ 2	
SENSOR NUMBER	X _T	Υ _T	Z _T	х	Y	Z	ORIENTATION	LIGHT PROTECTION	TESTS
SSME DUCT									
D 201	3037+1	0	1306-3	132.03	0	58.0	- Z	B	30- 32, 40
D 20 3	2864.7	1708-8	2344.0	121.00	109.36	124.42	X;+Y	P	
D 204	2635.4	0	640.2	106.32	0	15 . 37	X;+Z	В	
D 205	2635.4	0	1054.4	106.32	0	41.88	X;-Z	P	
D 206	2739.7	2623-6	2344.0	105 - 25	167.91	124.42	X;+Y	P	

NOTES: 1. The model scale coordinate system used herein is referenced to the model ET centerline at the elevation of the Model Orbiter -- X increases positively going aft, Y increases positively toward the Model Orbiter right wing, Z increases positively to the Model Orbiter verifical stabilizer. The full scale ET coordinate system is used and is related to the model coordinate system as follows:

$$X_T = (X + 62.34)/0.064$$
 $Y_T = Y/0.064$ $Z_T = (Z + 25.6)/0.064$

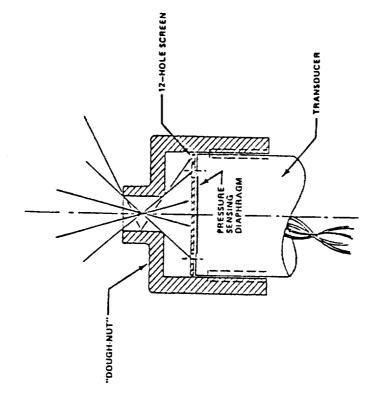
- 2. Symbols denoting sensor mounting requirements for heat/light protection are as follows:
 - Code "D" denotes the "dough-nut" device added to the transducer
 - Code "B" denotes sensor installation in an aluminum 90-deg block fixed to the duct wall
 - Code "P" denotes a penetration hole through the duct wall steel and Fondu Fyre from the outside with the transducer being screened into a tapped counterbore.

it must sustain if incorporated in full scale at SLC-6. The "dough-nut" heat/light protective device used on these measurements so identified in Table 1 is shown in Figure 3.5-8. The drillhole penetrations for model SRM nozzle exit static pressure measurements and for the model exhaust ducts and the muffler were of essentially the same configuration and had the same protective effect as the "dough-nut".

Sound suppression water system supply pressures and flow rates were measured to record conditions at the time of test through the full 9-sec burn duration and the starting transient conditions which led to the pre-ignition water flows and water accumulation depths in the SRB and SSME exhaust ducts. The model SRM and SSME chamber pressures, SRM case strains and nozzle exit pressures, and all other SSME performance parameters were recorded over the full burn duration for test-to-test correlation of model performance. There were some 100 measured and computed performance parameters for operation of the model SSME's. However, only the SSME starting transient chamber pressures are documented for the purposes of this report. The ambient environment temperature was recorded every test and the wind speed and direction were also recorded during the full-model test (Test 40).

3.6 Contingency Muffler

The proposed muffler configuration tested in this verification program, Figure 3.6-1, was derived from off-line development tests using a "popper" acoustic source and 6.4-percent scale duct hardware. Its development from the "off-line" work performed is discussed in Appendix A. It has constant 50-ft square cross section at the same upramp angle as the 15-deg SRB duct sloped exit apron where it would be installed at SLC-6 and is rigidly sealed to the duct exit plane. The muffler's horizontal length would be 45 ft. Its roof is closed, and there are slotted vents on each vertical side wall giving an open area that is approximately 60 percent of the basic duct's 2500 ft 2 exit plane area. Internal overpressure measurement locations used to obtain data upon which to base the full-scale muffler design are shown in Figure 3.6-2. The muffler wall thickness was 1 1/4 inches model scale.



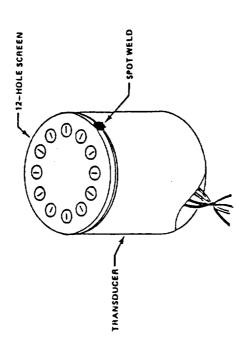
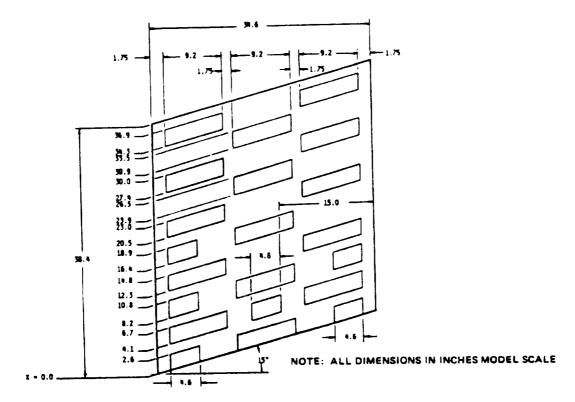


FIGURE 3, 5-8 "DOUGH-NUT" RADIATION BAFFLE FOR MODEL VEHICLE MEASUREMENTS



SLOT DIMENSION DETAILS

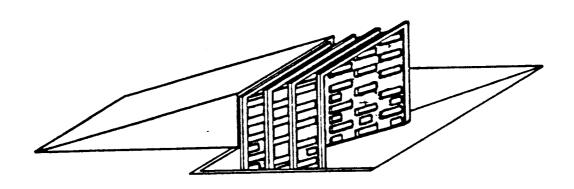
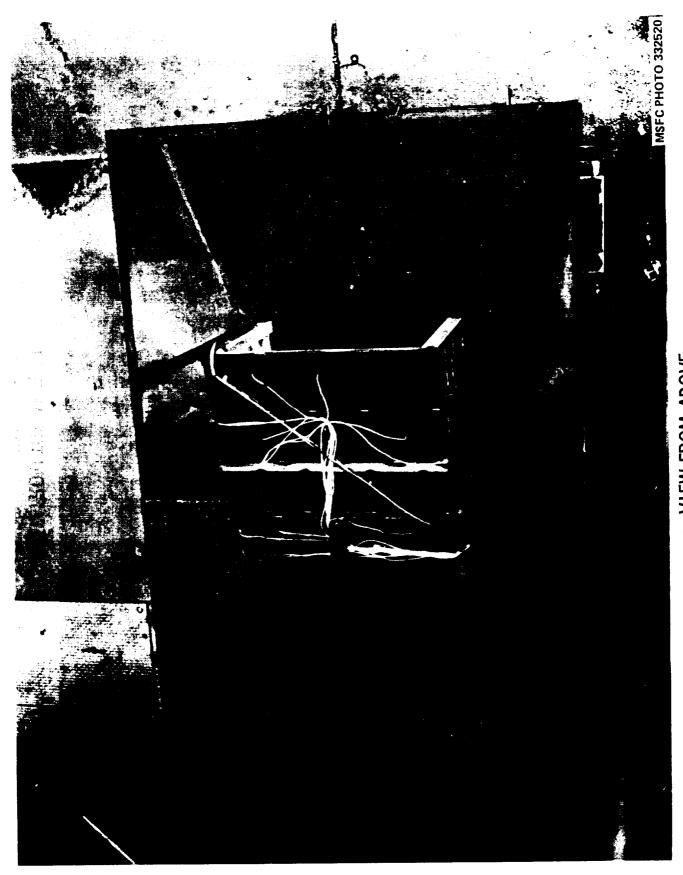
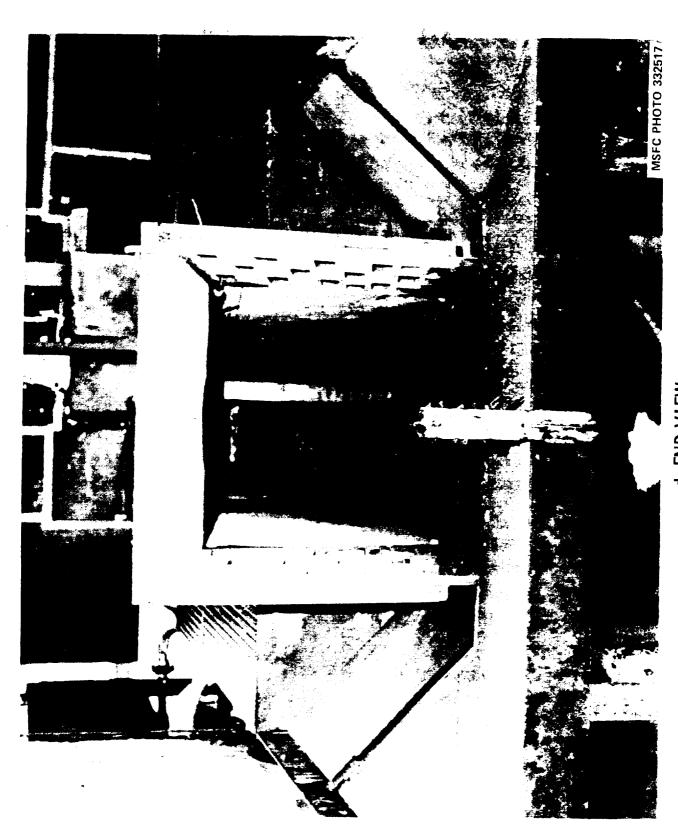


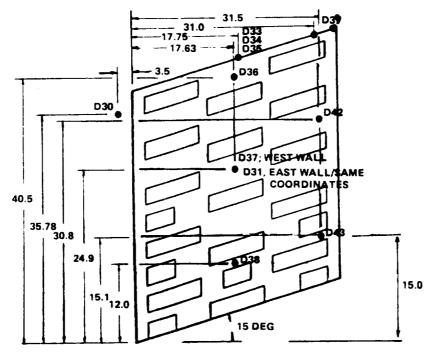
FIGURE 3.6-1 GEOMETRIC DETAILS OF THE CONTINGENCY MUFFLER







3-71



SIDE WALL COORDINATE LOCATIONS

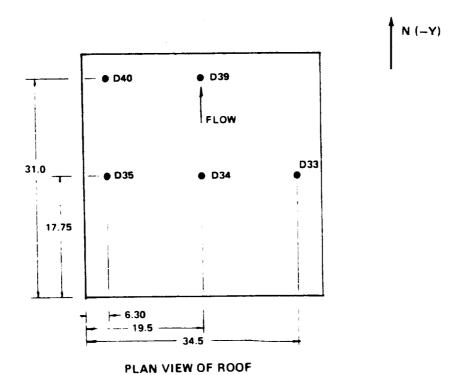


FIGURE 3. 6-2 OVERPRESSURE MEASUREMENT LOCATIONS INSIDE THE MODEL SRB EXHAUST DUCT MUFFLER

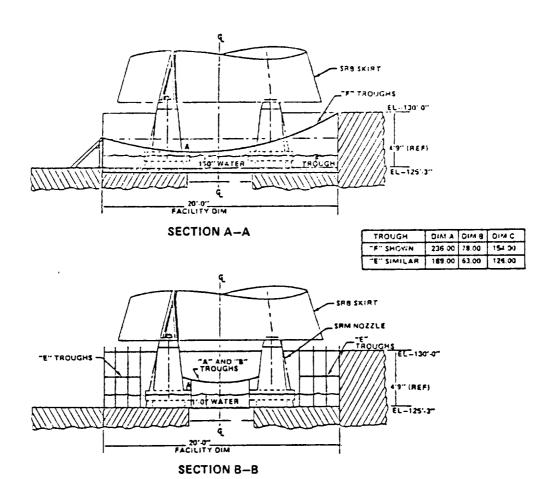
The scale-model muffler made of steel allows four columns for support from the duct exit plane to its discharge equally spaced between the slots. The porous open area and slot shapes were designed in the effort to reduce the strength of the DOP impacting the vehicle.

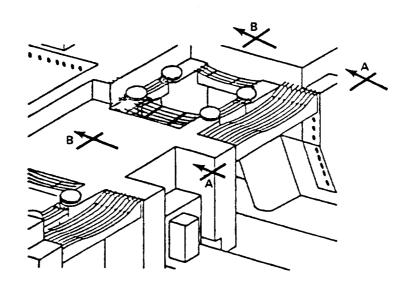
3.7 Water Troughs

1

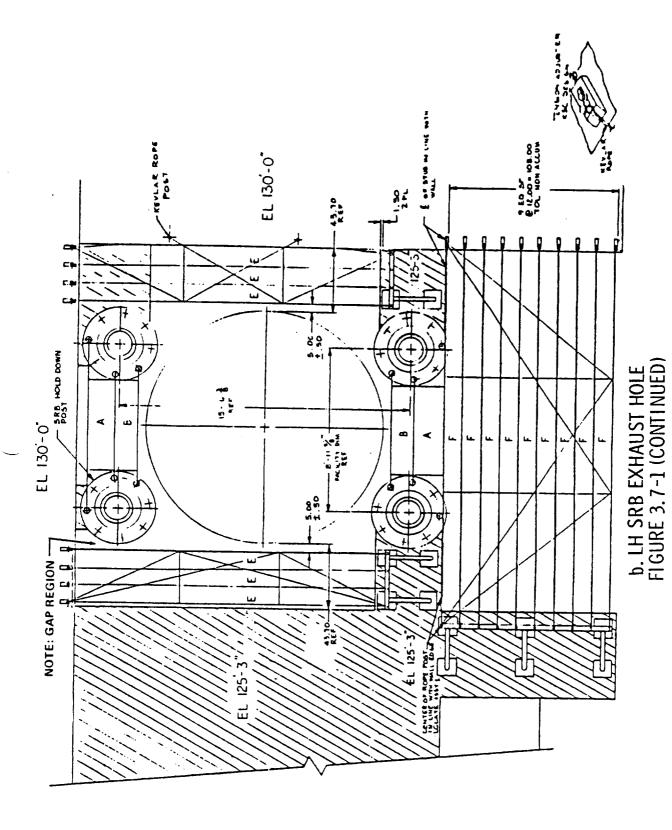
The water troughs are to be fabricated from nylon and held in place with kelvar ropes. They are designed to burn away and the water they contain to flash immediately after vehicle liftoff. The trough catenary tension is such that when filled with water they will hold water at a constant depth forming a standing water barrier to block upward - traveling SRM ignition overpressure waves over all of the SRB opening area at Elev. 125'-3" in each SRB hole except for nominally 53.5 ft² around the HPM nozzle. The troughs as tested on the model launch mount were designed to be able to hold a scaled 2 ft standing depth of water; they were tested, however, at an equivalent 1 ft standing depth, the same as at KSC's LC-39. The troughs butt against side wall and haunch refractory surfaces and were sealed against these model surfaces using zinc chromate putty.

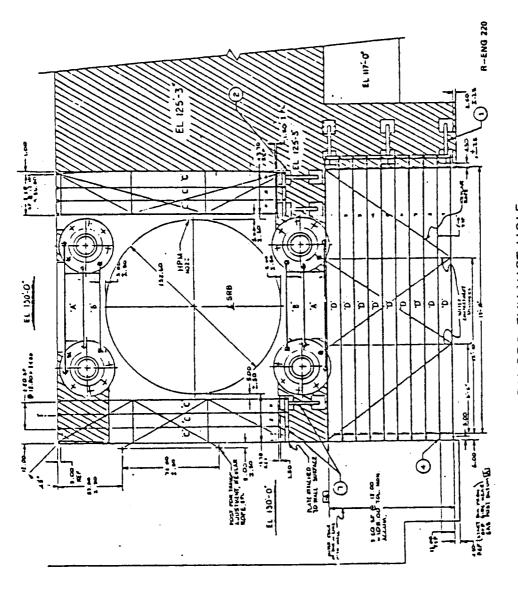
Water trough configuration details are given in Figure 3.7-1 as they were orginally conceived for the scale-model tests. They were tested in this original configuration in the single-motor verification tests. Model water trough installation details for single-model SRM tests are shown in Figure 3.7-2. A design modification was implemented for the full-model test (Test 40) dealing with the inboard corners of each SRB primary hole between the small SRB hold down posts on each West wall and the ET. As seen in Figure 3.7-1, the original design had longer "E" troughs (LH SRB hole designation) on the inboard side, called "E modified", than those on the outboard side, called "E". There remained a gap between the "E modified" troughs and the West wall hold down post with the original trough design layout. That gap (out to the same standoff distance as the "B" trough into the primary hole, moving Eastward from the wall) was simply filled with zinc chromate putty on the model during the single-motor tests to get the desired scaled 53.5 ft² open area. By August 1983, a provision for closure of the unwanted gap





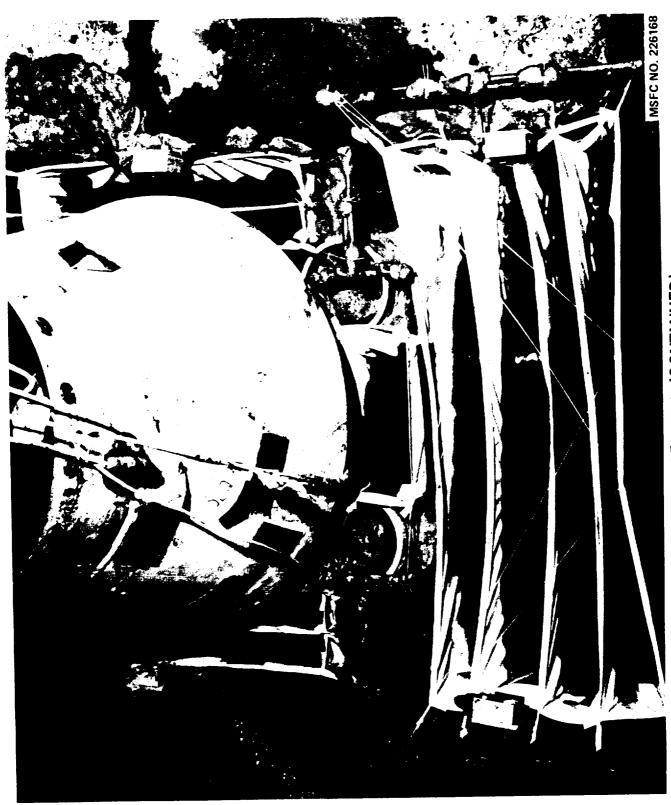
a. CONCEPTUAL LAYOUT
FIGURE 3.7-1 WATER TROUGH
CONFIGURATION DETAILS -- ORIGINAL DESIGN



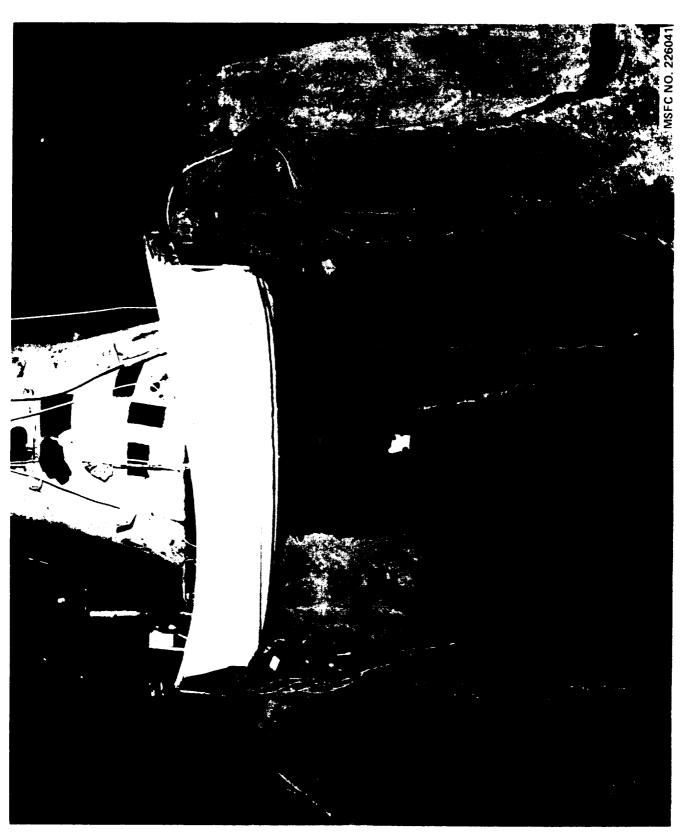


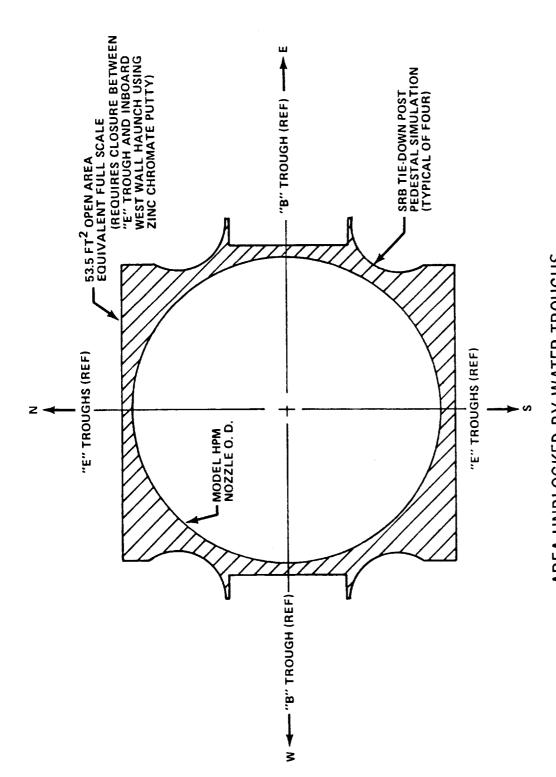
c. RH SRB EXHAUST HOLE FIGURE 3.7-1 (CONTINUED)

FIGURE 3. 7-2 MODEL WATER TROUGH INSTALLATION -- SINGLE MOTOR TESTS



3-78





AREA UNBLOCKED BY WATER TROUGHS FIGURE 3. 7-2 (CONCLUDED)

was decided upon, constituting the design modification. This provision was to add a steel plate at Elev. 125'-3" in the Southwest corner of the LH hole (Northwest corner of the RH hole) filling that gap between the small West wall hold down post and the inboard wall. In a plan view, the modified design looks like that shown in Figure 3.7-3, the hold down post planform becoming like the other three in each SRB hole. Then "E" troughs of length spanning the haunch planform separation distance East-to-West instead of "E modified" troughs spanning all the way to the West wall will be used on both the inboard and outboard sides of the hole. These troughs must butt against the new plate to form a seal. The modified configuration was tested in Test 40. The installation is shown in Figure 3.7-4. Great care was exercised in every test to simulate the water trough installation details as closely as possible and maintain the unblocked open area around the model SRM nozzle at the scaled 53.5 ft² as indicated in Figure 3.7-2d.

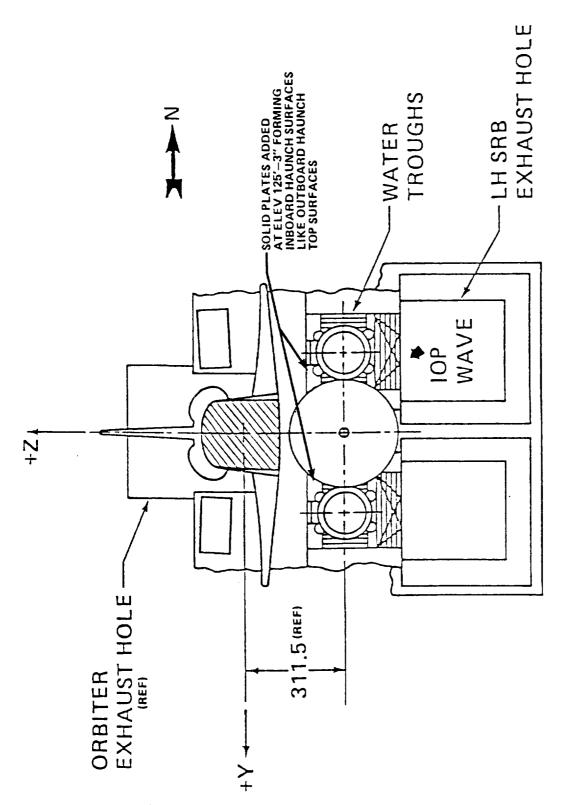


FIGURE 3.7-3 WATER TROUGH CONFIGURATION -- PRESENT DESIGN



3-83



3-84

4.0 DATA RECORDING/PROCESSING

		sum t
		-
		-

4.0 DATA RECORDING/PROCESSING

4.1 Recording

The overpressure data channels including model SRM chamber pressure, case strain, and nozzle exit static pressures were recorded on two FM multiplex tape recorders with 0-to-16kHz frequency response. Pitch- and lateral-pair overpressure sensors to be differenced during data processing were arranged to be on the same recorder so that they would be time correlated.

The facility measurements, i.e. water system flows and pressures, model SSME operational parameters, were recorded on a digital system unit (DSU) scanning each measurement at 25 samples/sec. The model SRM internal pressure and case strain measurements and the model SSME chamber pressures were parallel recorded on the DSU and on the FM multiplex system.

Both of the overpressure tapes and the DSU had event markers indicating the time of SRB Ignition Command, which is reference time zero (T_0) . The DSU had a time event marker for the Water Valves Open Command. These events are marked by the symbol "X" on each time history plot generated from the DSU data.

Overpressure sensor and recording channel calibrations were described in full in Reference 2 and will not be repeated in this report. All calibration procedures were the same in the verification test series as those in the screening test series and the prior ETR testing, Reference 1. A typical overpressure data acquisition channel is traced through the signal conditioner and record amplifier in Figure 4.1-1 from the sensor (Kulite pressure transducer) to the recorder (FM multiplex) analog tape. Each signal conditioner is a Wheatstone bridge balance network. The sensitivity of each overpressure transducer in psi after appropriate multiplication with the record amplifier gain was recorded on the tape log sheet for each data channel.

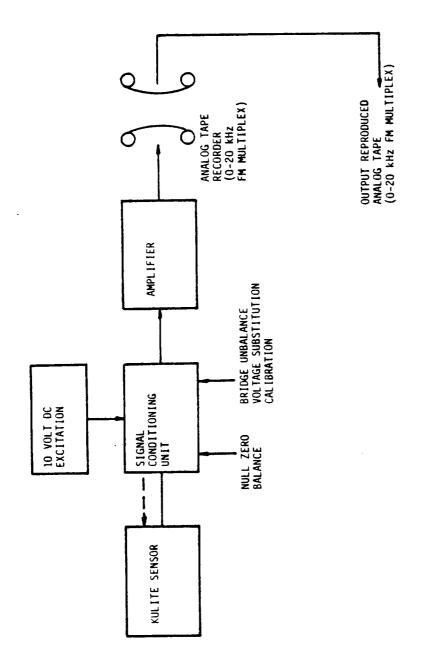


Figure 4.1-1 Overpressure Data Recording Schematic Diagram

}

4.2 Processing

ŧ

4.2.1 Data Flow

The data flow from the original analog tape record to the various output forms delivered as final, checked data is shown in Figure 4.2-1. The original analog tapes were retained at the test site by MSFC's Test Laboratory and are to remain there in storage at least until after the first Vandenberg launch. All data processing was performed on duplicate analog tapes provided by MSFC's Test Laboratory to MSFC's Computer Laboratory.

MSFC's Computer Laboratory first provided quick-look oscillogram records, low-pass filtered at 400 Hz (model scale), of every channel recorded on the analog tapes from every test. These oscillograms were used for corrective measures on any data channel faults before the next test, for a preliminary assessment of the test results, and for planning the final data processing. Rockwell International performed a quick check on all oscillogram records for MSFC, returned any data squawks found to MSFC's Test Lab, recommended record amplifier gain settings and picked exact time slices in the data records for the final digital processing.

MSFC's Computer Lab created a raw data tape through an analog/digital converter at 4,000 samples/sec with 400-Hz low-pass filtering containing every data channel recorded on the analog tapes. Approximately 3 sec of data were digitized and stored on the Raw Data tapes encompassing the model SRM ignition transient, including a period of at least one second prior to T_0 . The FMEUC program (the acronym has significance only to MSFC's Computer Lab) applied the scale factors derived from the sensor sentivities log, applied the identification labels for each data channel, and stored the calibration header information with the approximately 3 sec of data stored on the Raw Data tape. The output of the FMEUC program was Engineering Unit Data tapes, as yet without any filtering except for the 400-Hz low pass. The Engineering Unit Data tapes were in Test Users Tape (TUT tape) format.

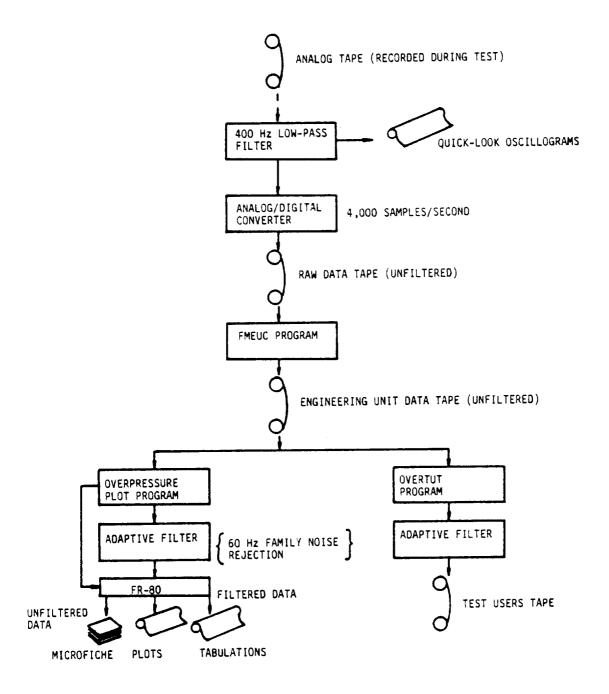


Figure 4.2-1 Data Processing Flow Schematic Diagram

The Overpressure Program selected the prescribed time intervals for plotting (250-msec of the SRM or SSME ignition transient, 100-msec expanded of just the overpressure wave generation and passage across all measurement locations), performed special differencing computations, and generated CRT plots and tabulations. Time plots history were made of every measurement (delta pressure) over the 250-msec intervals. Plots and tabulations were made of every measurement and every special differencing computation (delta delta pressure) over the 100-msec intervals.

The plot routines had auto-range scaling, had zero suppression, and applied the appropriate header information. Plots and tabulations were made from special computations of model SRM chamber pressure rise rate ($P_{\rm C}$) and motor case strain rise rates (SG2 and SG4) over the 100-msec interval. Rockwell International performed check/validations of the microfiche and hardcopy plots and tabulations and returned data squawks on any measurement anomalies found to the Computer Lab. Very close data checking as to amplitude trends and wave occurrence times was necessary because the channel alinement on all tapes created was by manual patching input and the header information was by keypunch input. The dense spacing of measurements, particularly on the Orbiter and ET, made the data channels difficult to distinguish one from another without close examination and data check plotting for trends. After satisfying all squawks, an Engineering Unit Data tape was thus obtained for each test and one copy of the microfiche was retained by MSFC.

Signal/noise ratio had varied among the measurements during recording from test to test as overpressures on the scale model were generally small and scale up in full scale. Background electrical noise frequencies riding on the data fell across the range of overpressure data frequencies (some quite close to electrical noise frequencies) and altered the apparent overpressure waveforms. This was 60-Hz harmonic-family electrical noise. Overpressure amplitudes were smaller in the lateral-plane tests without the splitter plate and were, still smaller with the contingency muffler. The ability of MSFC's Test Laboratory to control the level of background noise varied from one day to another despite their concerted efforts to rid the data acquisition system of the noise. Filtering of the noise turned out to be critical.

The squawk/validation cycle was repeated until a set of fully-validated filtered microfiche and fully-validated filtered TUT tapes (selected tests only) was obtained. Twelve copies of microfiche were reproduced for release with this report, two of which were retained by Rockwell International, the remainder going to all Ignition Overpressure Working Group member agencies. One set of filtered and one set of unfiltered TUT tapes were provided to Rockwell International which, were used to compile the permanent data retention file at Rockwell's Seal Beach Scientific Computing Center. A second set of TUT tapes was provided to Martin Marietta Corporation, Denver, Colorado. Data from the filtered TUT tapes were used by Rockwell International to compute the forcing functions on the vehicle constituting the final output of the scale-model test program.

The scope of the data processing was large with most of the required manipulations to the scale-model data being done in the batch processing at MSFC. The time schedule on which all this processing took place is shown in Table 4.2-1. Quick-look data were available shortly after each test; Table 4.2-1 tracks production of the final data.

4.2.2 Typical Time Histories

The history of every measurement (delta pressure versus time) was provided to characterize the overpressure wave generation and propagation over the entire model, those on the model vehicle to characterize shell-model loadings. Selected pairings were taken on the model vehicle to produce pressure differentials (delta delta pressure versus time) across sections of model vehicle elements, e.g Orbiter, ET, each SRB. The pairings for differencing in pitch-type tests are listed in Table 4.2-2. The pairings for differencing in lateral-type tests are listed in Table 4.2-3. The form of the differencing equations (point-by-point at 4,000 samples/sec over the 100-msec time interval in each test) is given by

DEC ΝON 100 SEP Table 4.2-1 Data Processing Historical Track AUGUST JULY **SSME TESTS 30-32** JUNE ₩Ā SINGLE-SRM DATA PROCESSING FILTER DEVELOPMENT AND CHECK-OUT APRIL SINGLE-SRM TESTS 5-16 MARCH

TEST 42 DATA PROCESSING TEST 42 (SRM NOZZLE STATIC PRESSURES) TEST 40 DATA PROCESSING SSME DATA PROCESSING FULL-MODEL (DUAL SRM'S PLUS SSME'S) TEST 40

FINAL DATA PACKAGES COMPILED (MICROFICHE FORM)

TABLE 4. 2-2 DATA REDUCTION EQUATIONS FOR SINGLE-SRM TEST DIFFERENTIALS

DATA REDUCTION EQUATIONS FOR PITCH-PLANE DIFFERENTIALS

DATA REDUCTION EQUATIONS FOR LATERAL-PLANE DIFFERENTIALS All Delta Delta P's

# F1 - F3 # F48 - F3A # F48 - F3A # F128 - F11A # F128 - F11A # W1 - W2 # W3 - W6 # W5 - M6 # W5 - M6 # F8A - F7A # F8A - F7B # F13 - F15 # F13 - F15 # F14A - F15B # T1 - F3 # T1A - T1 # T1A - T1A # T1A - T1A													
	F1 - F F48 - F F4A - F	F9 F128 F12A	3	K3 -	BF1 .	F5 - F8B - F8A -	F13 - F168 - F16A -	11 144	15 - IHA -	19 - TH 112A - 111	11.3 116A -	51.1	- 515

DPLA = F4 - F2 DPLA1 = F4A - F1B DPLA2 + F4B - F1A DPLA3 = F3B - F2A DPLA4 = F3A - F2B	DPLB = FB - F6 DPLB1 = FBA - F5B DPLR2 = FBB - F5A UPLB3 = FB - F6A DPLB4 = F7A - F6B DPLC = F12 - F10 DPLC2 = F120 - F9B DPLC2 = F120 - F9B	FIIA - FIIA - FIIA - FIIA - FIIA - FIIB - FIIB - FIIS - FIIS - FIIA - FI	######################################

TABLE 4.2-3 DATA REDUCTION EQUATIONS FOR DUAL-SRM AND SSME TEST DIFFERENTIALS

DATA REDUCTION EQUATIONS FOR PITCH-PLANE DIFFERENTIALS

	All Delta Delta P's
OPA = F1 - F3	OPI = T1 - T3
DPB = F9 - F11	DPJ = T5 - T7
OPC = WL - W2	DPK = T9 - T11
OPO = W3 - W4	OPL # T13 - T15
DPE = W5 - W6	DPM = W9 - W10
OPF = 8F1 - 8F2	OPN = W13 - W14
DPG * F5 - F7	OPO = W15 - W16
DPH = F13 - F15	

NOTE: These differentials were computed for the SSME and SRB overpressure data slices.

DATA REDUCTION EQUATIONS FOR LATERAL-PLANE DIFFERENTIALS

All Delta Delta P's DPLA * F2 - F4 DPLB * F5 - F8 DPLF = T6 - T8 DPLC = F10 - F12 DPLD = F14 - F16 DPLO * V2 - V1

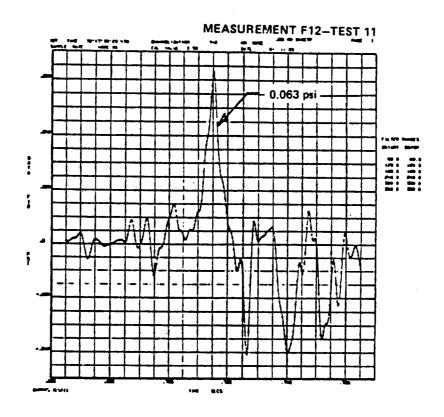
NOTE: These differentials were computed for the SSME and SRB overpressure

$$p_{X_{T},ij}(t) = p_{X_{T},j}(t) - p_{X_{T},j}(t)$$
 (pitch)
 $p_{X_{T},k}(t) = p_{X_{T},k}(t) - p_{X_{T},j}(t)$ (lateral)

for pitch- and lateral-type tests, respectively, at a particular section through the model element (at given χ_T) involved. Subscripts i and j represent ventral and dorsal measurements, respectively, used in a given pairing. Subscripts k and l represent port- and starboard- side measurements used in a given pairing.

Typical delta pressure data (a particular $p_{XT,k}(t)$ and a particular $p_{XT,1}(t)$) are shown in Figure 4.2-2. These measurements are one particular pair located on the port and starboard sides of the model Orbiter cargo bay on the "C"-ring. They were recorded in a lateral-type test -- Test 11. These data are final filtered data. The large positive peak in each delta pressure is the peak of the DOP wave, 0.063 psi for measurement F12 and 0.035 psi for measurement F10. The wave amplitude is larger on the port side than the starboard. It's arrival time is earlier on the port side, by little more than a millisecond. The computed difference between these two measurements (delta delta pressure) is shown in Figure 4.2-3. This difference was the result of the amplitude and phase difference between the two points of measurement. The peak positive delta delta pressure in Figure 4.2-3 was 0.037 psid.

The peak positive delta delta pressure during DOP wave passage in a given test (Test 11 example) form a distribution acting over the vehicle element centerplane, depicted by five pairings on each Orbiter ring. This peak positive distribution on the "C"-ring is shown in Figure 4.2-4. The lateral-component data without the splitter plate are those recorded in Test 11, the pitch-component data with the splitter plate being from Test 7. The dotted line profile on the RH side of the model Orbiter fuselage is assumed to equal that on the LH. The differential profiles were similarly obtained on the other three measurement rings on the model Orbiter, on the model Orbiter LH wing at its center of pressure and each elevon in pitch, on the model Orbiter vertical stabilizer in lateral and on four rings on the model ET.



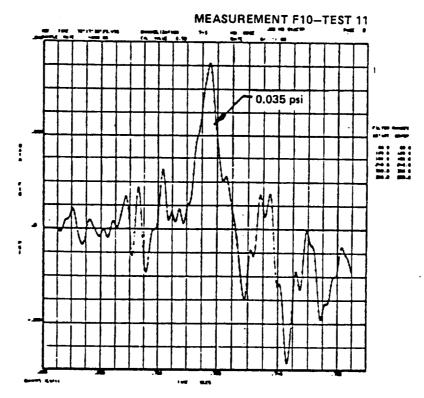
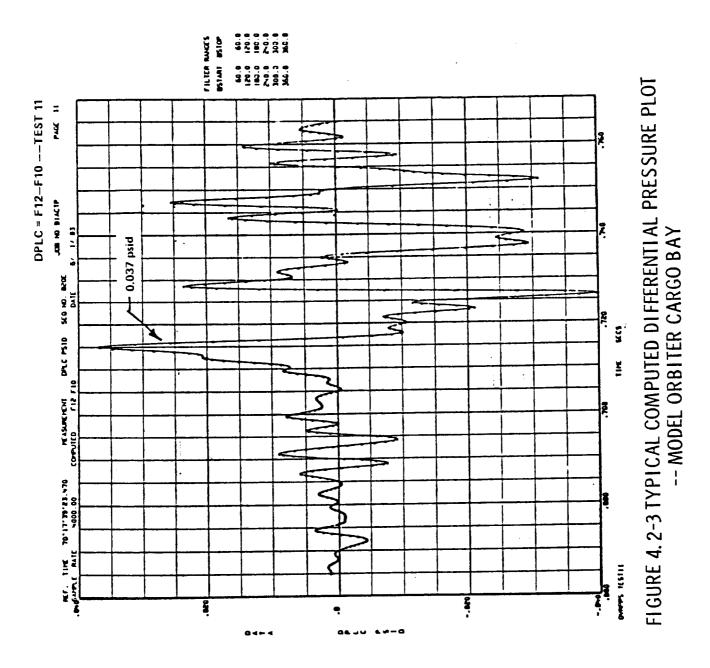


FIGURE 4.2-2 TYPICAL OVERPRESSURE DATA PLOTS
-- MODEL ORBITER CARGO BAY



4-12

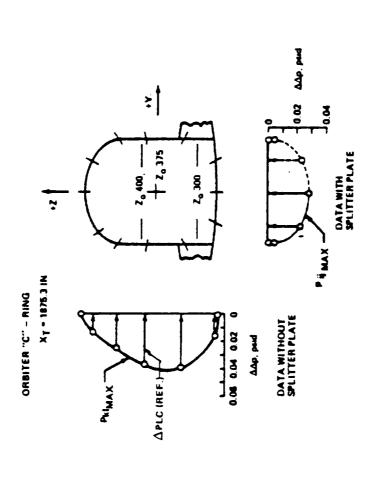


FIGURE 4.2-4 TYPICAL DISTRIBUTION OF DIFFERENTIAL PRESSURE PEAK AMPLITUDE -- MODEL ORBITER CARGO BAY "C" - RING

4.2.3 Adaptive Filter

The adaptive filter was applied to every data channel -- overpressure point sensor, SRM or SSME chamber pressure, SRM case strain, SRM nozzle exit pressure. The filter was actually a software addition to the basic data processing Overpressure Plot and Over TUT codes. It was adaptive in the respect that it removed 60, 120, 180, 240, 300 and 360-Hz components in each data signal completely only when their amplitudes exceeded a selected threshold percentage of the data level. It was based on the amplitude of the unwanted electrical noise component in the ambient background data that existed immediately before ignition. It was not a simple notch filter although it had bandwidth characteristics of a digital notch at each frequency -- no greater than 2 Hz bandwidth maximum for worst case (lowest) signal/noise ratio, usually sharper than 1 Hz bandwidth. It was designed not to remove an excess of the data signal. After the adaptive filtering, it applied a 400-Hz low pass digital cutoff (in addition to the first analog 400-Hz low-pass), removing any discretizing - induced high frequencies. The adaptive filter was a software innovation by MSFC's Computer Laboratory service contractor, New Technology, Inc., developed specifically for the purpose of this scale-model test program.

The bandwidth of the notch at each unwanted frequency was limited by the length of the data record being operated upon. The length chosen was 1 second after T_0 plus 1 second before ignition. This set the nominally 1 Hz notch. Within the time segment, the filter properties were best at the middle of the data record where the overpressure event occurred. After filtering, the specific segment of interest -- 250 msec and 100 msec expanded within that segment -- were selected for plotting, tabulating, and then the special data manipulations were performed.

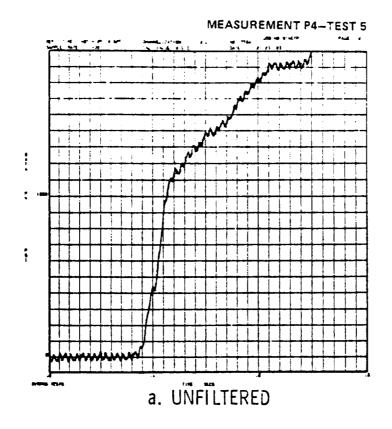
The filter operated in the frequency domain. The 2-sec data segment a 1-sec segment of noise before T_0 and 1-sec data segment after T_0 was Fourier transformed using the Fast Fourier Transform (FFT) algorithm and mean squared to form the power spectral density function (PSD), $\frac{-2}{p}$ (f).

The PSD was computed separately for the second half of the time segment that was overpressure data, $\frac{-2}{p}$ (f) data, and for the first half that ambient background noise, $\frac{-2}{p}$ (f) noise. The function

$$\binom{-2}{p}$$
 (f) data $-\frac{-2}{p}$ (f) noise)/ $\frac{-2}{p}$ (f) data

was then computed and compared with a selected threshold value of 0.6. If the absolute value of this function was 0.6 or greater at fn's 60 Hz in turn to 360 Hz, the value of $\frac{-2}{p}$ (f) data at those fn's was set equal to zero. If the absolute value was less than 0.6, the $\frac{-2}{p}$ (f) data were multiplied by the ratio computed. Then the $\frac{-2}{p}$ (f) data were sharply cut off at 400 Hz (giving marked improvement to derivatives and differentials) inverse Fourier transformed back to the time domain. This filter operating on the PSD function had no provision to handle phase information in the data. The chosen value of 0.6 for the threshold power setting was jointly arrived at by Rockwell International and New Technology, Inc, after trials on both high and low signal/noise ratio data. The 0.6 value was the best of the trials in its filtering effectiveness without introducing distinguishable distortion to the data.

Some examples of results obtained with the adaptive filter are given to illustrate the enhancement in data quality that was achieved. Model SRM chamber pressure rise histories are shown in Figure 4.2-5 before and after filtering, one that had high electrical noise and one where the noise had Model SRM case hoop strain data are shown in Figure 4.2-6 before and after filtering. The improvement is dramatic. An example of an overpressure measurement (delta pressure) with noise much larger than the data is shown in Figure 4.2-7. Data that would have been otherwise lost were recovered. An example of an overpressure measurement with low noise The improvement is subtle but none the less is given in Figure 4.2-8. important as the noise components add or subtract to the real pressure waves present changing apparent wave amplitudes and wave forms. The effect of excessive noise in one measurement used in a $p_{XT,ij}(t)$ computation (delta delta pressure) is shown in Figure 4.2-9. This differential would have been otherwise useless without filtering. Another p_{XT} ij(t) com-



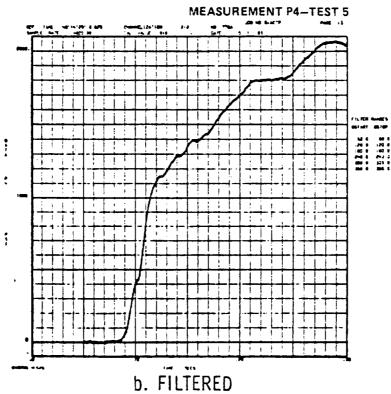
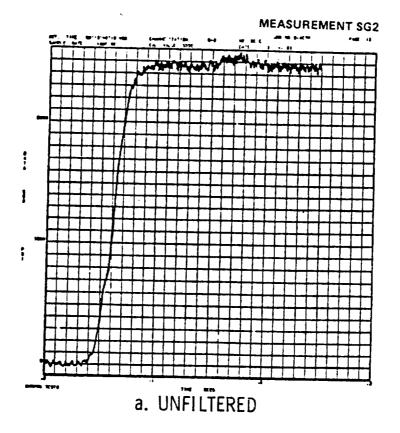


FIGURE 4. 2-5 EXAMPLE OF FILTERING INFLUENCE ON MODEL SRM CHAMBER PRESSURE RISE DATA



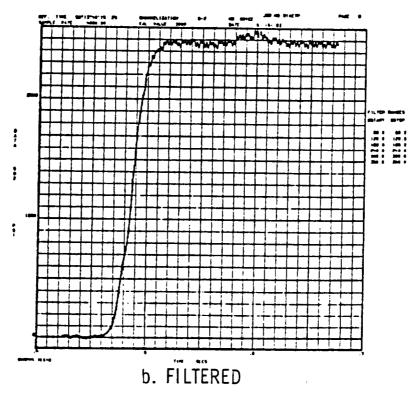
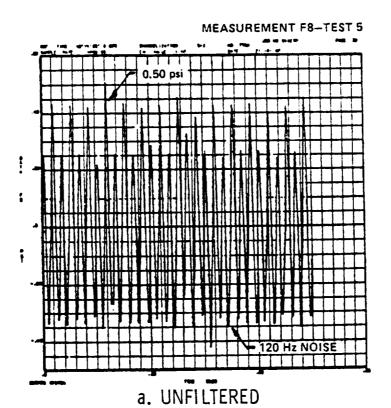


FIGURE 4. 2-6 EXAMPLE OF FILTERING INFLUENCE ON MODEL SRM CASE STRAIN RISE DATA



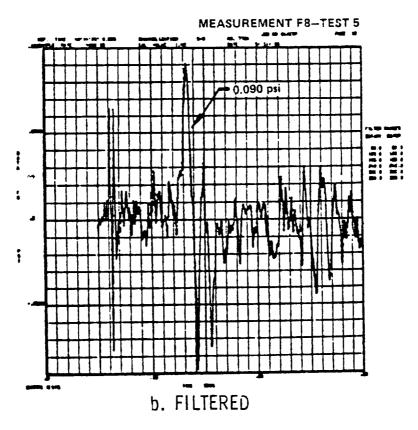
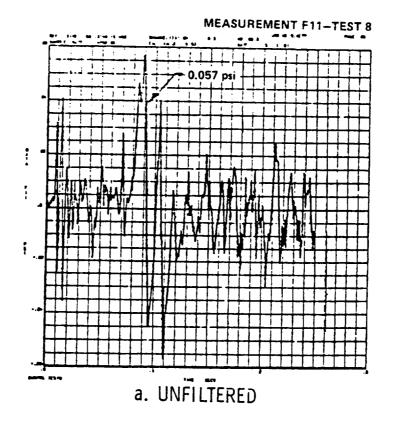


FIGURE 4. 2-7 EXAMPLE OF FILTERING INFLUENCE ON AN OVERPRESSURE MEASUREMENT -- A LOW SIGNAL/NOISE CASE



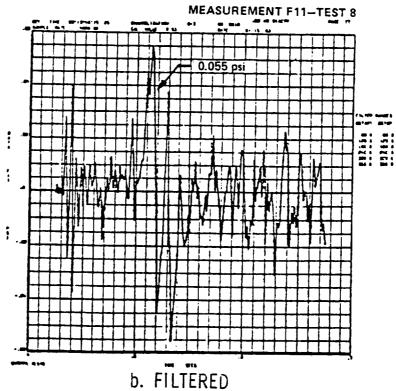
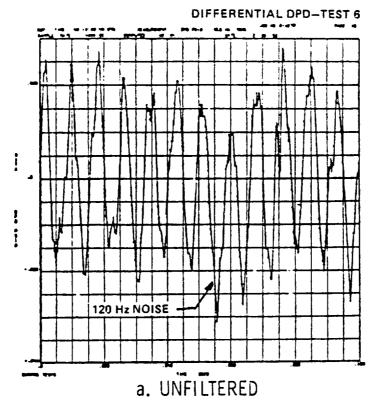


FIGURE 4. 2-8 EXAMPLE OF FILTERING INFLUENCE ON AN OVERPRESSURE MEASUREMENT -- A HIGH SIGNAL/NOISE CASE 4-19



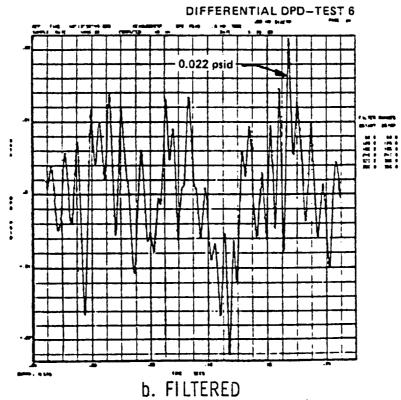
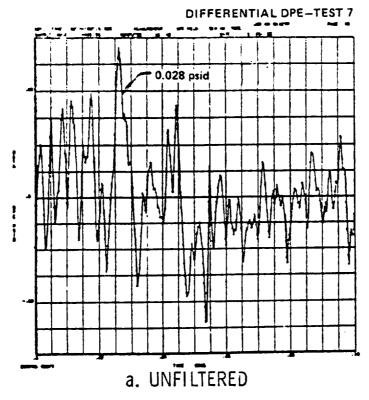


FIGURE 4.2-9 EXAMPLE OF FILTERING INFLUENCE ON A DIFFERENTIAL PRESSURE COMPUTATION -- ONE MEASUREMENT HAVING LOW SIGNAL/NOISE 4-20

putation where the noise was relatively small in both the i and j measurements used is shown in Figure 4.2-10 before and after filtering. The improvement is obvious.

The overpressure data from the four SRM screening tests presented in Reference 2 were unfiltered. The screening test data were reprocessed with the adaptive filter to make a complete data set from this test program. The final microfiche data 'packages appendaged to this report include the reprocessed SRM screening test data together with the SRM verification test data. The SSME overpressure test data were likewise filtered in the same manner as the SRM overpressure data.



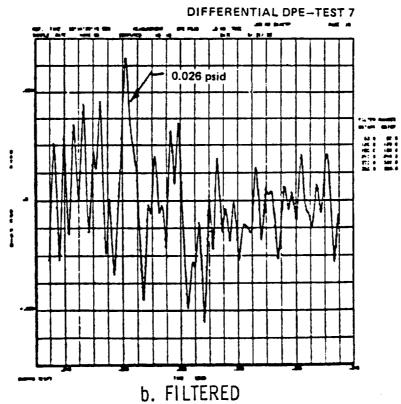


FIGURE 4. 2-10 EXAMPLE OF FILTERING INFLUENCE ON A DIFFERENTIAL PRESSURE COMPUTATION -- BOTH MEASUREMENTS HAVING HIGHER SIGNAL/NOISE 4-22

5.0 RESULTS AND DISCUSSION

		* ***
•		

5.1 Model SRM and SSME Ignition Transients

Overpressures generated and measured in these tests were the results of the sudden mass addition to the exhaust ducts as the model SRM's and SSME's ignited and the exhaust plumes suddenly expanded. The maximum rate of rise in the starting exhaust flow is proportional to the maximum slope in the chamber pressure versus time curve ($\dot{P}c_{max}$). Shortly after the wave motion -- pressure amplitude, frequency composition, and phase -- is influenced by the volume, length, and shape of the duct. The over-pressure is therefore dependent upon the motor/facility in combination and the timing of wave generation. Quantification of the ignition transient and timing of overpressure wave development is important to the quantification of the overpressure phenomena. This quantification included tracing model SRM head-end chamber pressure, head-end and nozzle-end motor case strain rise characteristics and the exhaust plume starting pressure characteristics at the nozzle exit.

5.1.1 Model SRM Ignition Data

The Tomahawk motor ignition system has a squib initiator, pellet basket, and pyrogen chain. A typical Tomahawk motor chamber pressure rise transient (typical of the motor but not of the present verification test series) is shown in Figure 5.1-1 together with a typical history of the pyrogen pressure. As hot exhaust products from the pyrogen ignite the propellant grain, flame spreads over the entire grain surface, exhaust gases begin to fill the combustion cavity volume, and chamber pressure builds to the equilibrium value where the mass flow rate expelled through the nozzle equals that generated in the steady combustion process. The steady mass flowrate generated is governed by the burning rate exponent of the propellant. Spikes occurred shortly after motor ignition in chamber that were not corroborated by motor case strain data, nozzle exit pressure data, or any overpressure sensing gage. They apparently stemmed from some measurement problem local to the chamber pressure sensing tube. They did not

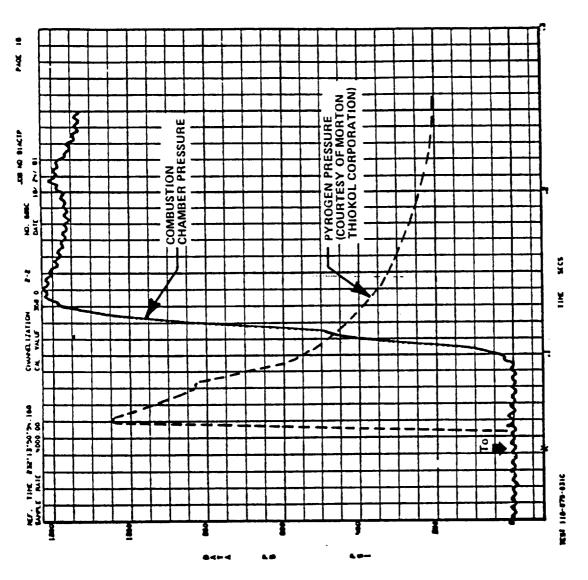


FIGURE 5.1-1 TYPICAL MODEL SRM CHAMBER AND PYROGEN PRESSURE HISTORIES

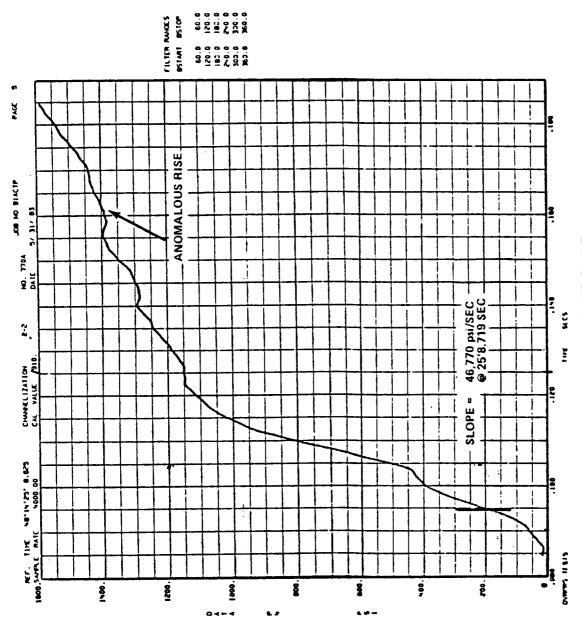
ì

compromise test objectives as they occurred well after the occurrence of $\dot{P}c$ $_{\text{max}}$.

Variations in the motor ignition system performance and in the surface conditions of the propellant grain can produce variations in the starting flow transient and thus in the ensuing overpressure. Examples of chamber pressure, motor case strain and nozzle exit static pressure data are presented for two tests in Figures 5.1-2 and 5.1-3. The values of Pc_{max} and SG_{max} obtained by machine computation are listed in Table 5.1-1. Typical derivative plots are given in Figure 5.1-4 and 5.1-5. There is a high-frequency oscillation riding over the mean rise data trend having an influence on the exact Pcmax determination. It is the first Pcmax that has been found to correlate the SRM ignition overpressure as indicated by the timing of the ensuing overpressure wave development. The head-end motor case strain has its maximum slope at the same time as the chamber pressure maximum slope. The nozzle-end motor case strain lags the head end with its maximum slope between the two peaks at the head end. The nozzle exit static pressures show the starting expansion wave leaving the nozzle at the same time as the maximum slope in the nozzle-end case strain and the saddle point in the head-end pressure and strain.

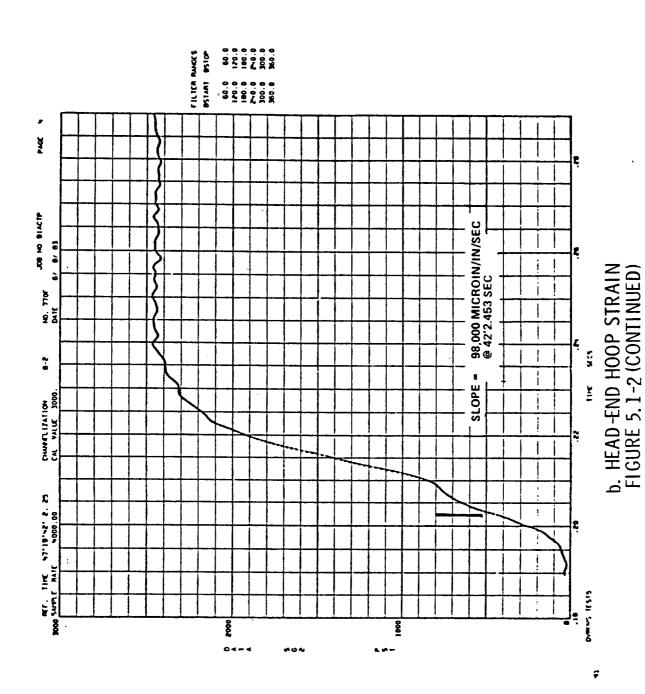
A yet more anamolous chamber pressure transient than that in Test 5 is illustrated in Figure 5.1-6. This occurred in Test 8 -- the anomalous spike and decay. (It occurred also in Tests 13 and 16.) There are larger high frequency oscillations in the head-end motor case strain in Test 8 than in either the Test 5 or Test 7 examples. The nominal Pc_{max} in the present WTR and the Reference 1 ETR test experience has been 50,000 psi/sec. It is noted in Table 5.1-1 that the Test 13 motor had the highest Pc_{max} of all and was considerably higher than 50,000 psi/sec.

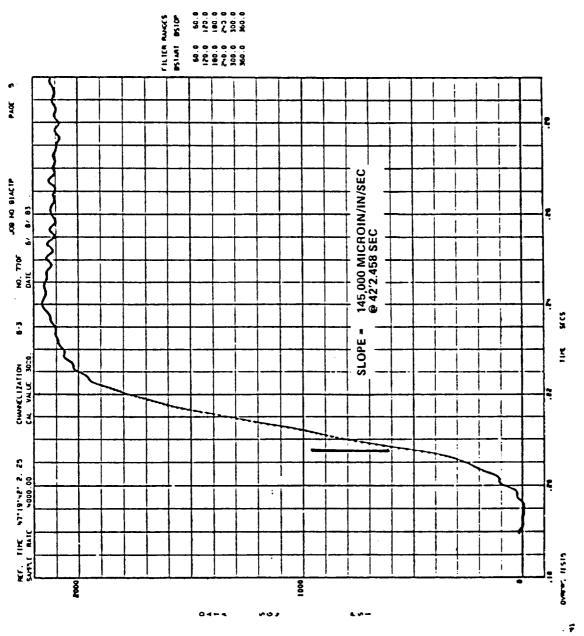
Nozzle exit static pressure histories shown are typical of the best quality data acquired in Tests 5 through 7. A sub-objective in making the SRM nozzle exit static pressures was to ascertain if they showed any sign of asymmetric plume development in any repeatable manner that might indicate asymmetric separation before the plume became fully developed and could such asymmetry be related to the SRB exhaust opening, water trough, and



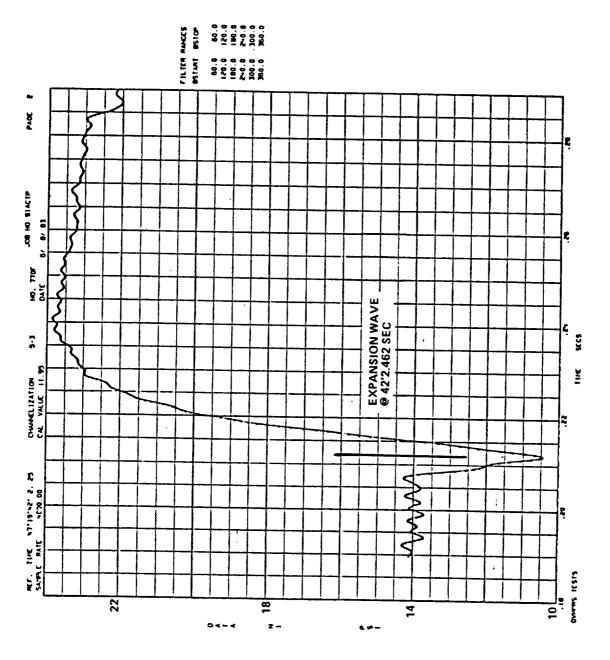
a. CHAMBER PRESSURE FIGURE 5.1-2 MODEL SRM IGNITION TRANSIENT DATA -- TEST 5

1

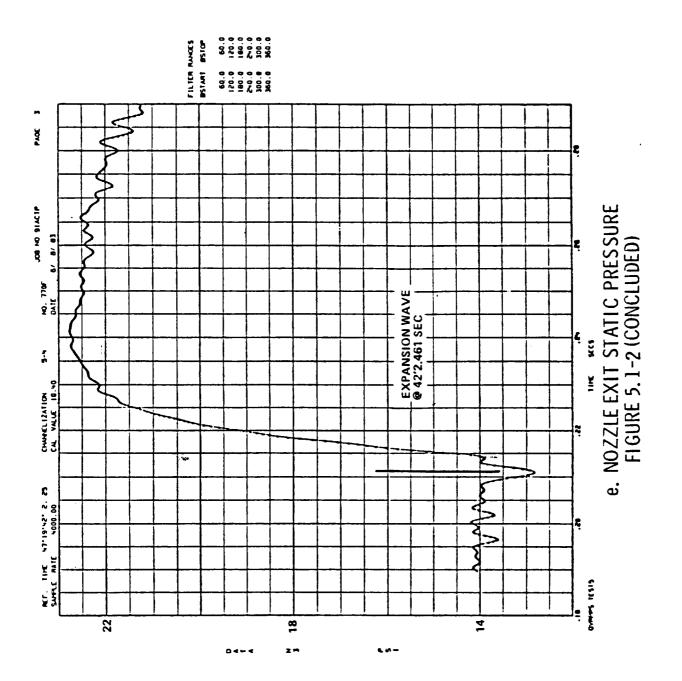


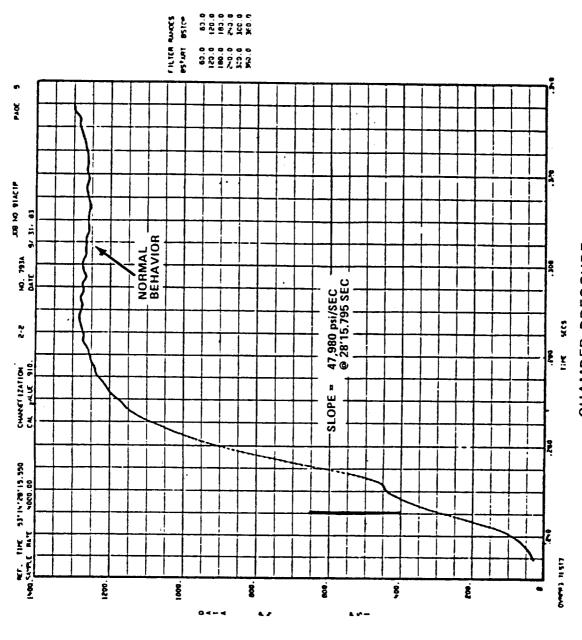


c. NOZZLE-END HOOP STRAIN FIGURE 5.1-2 (CONTINUED)



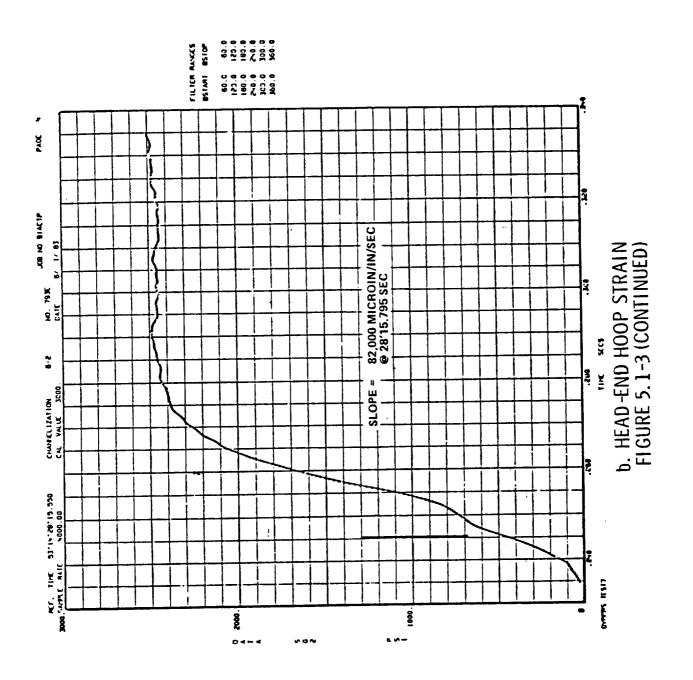
d. NOZZLE EXIT STATIC PRESSURE FIGURE 5. 1-2 (CONTINUED)

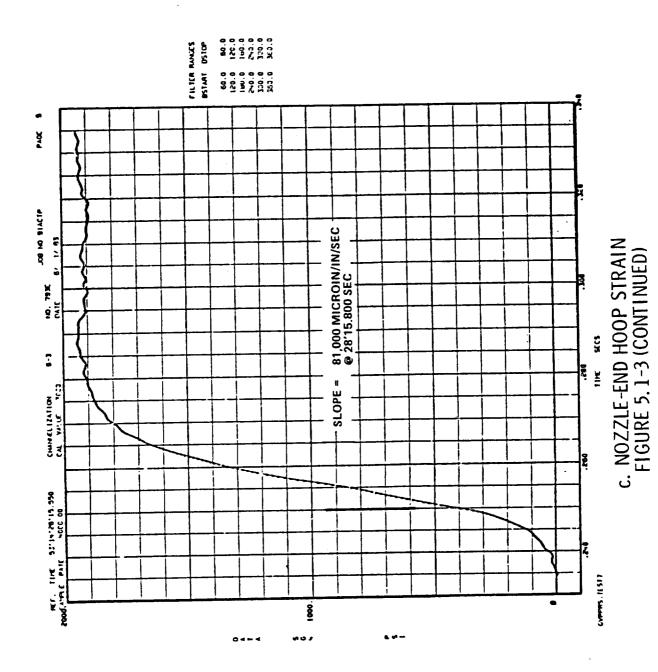




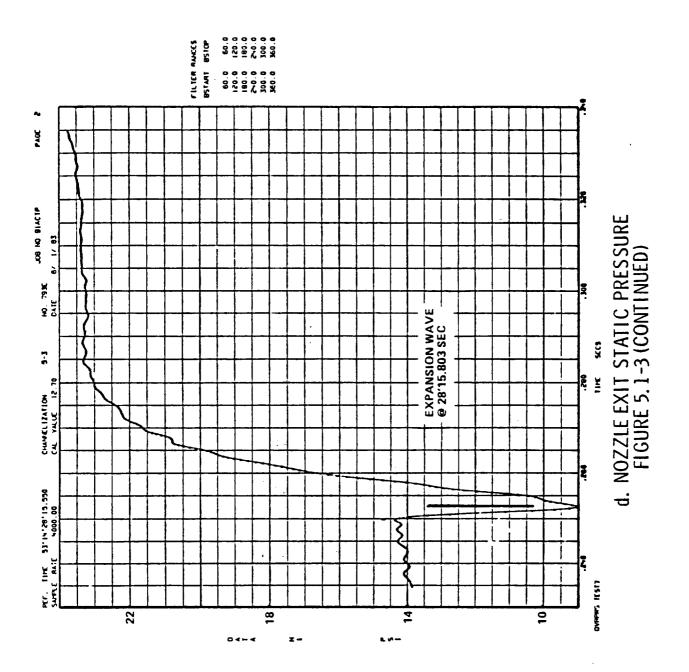
a. CHAMBER PRESSURE FIGURE 5.1-3 MODEL SRM IGNITION TRANSIENT DATA -- TEST 7

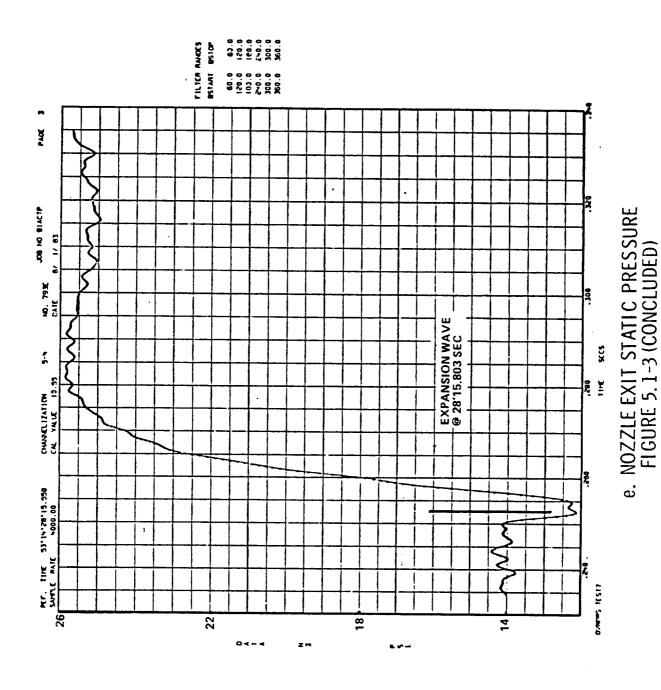
)





(_



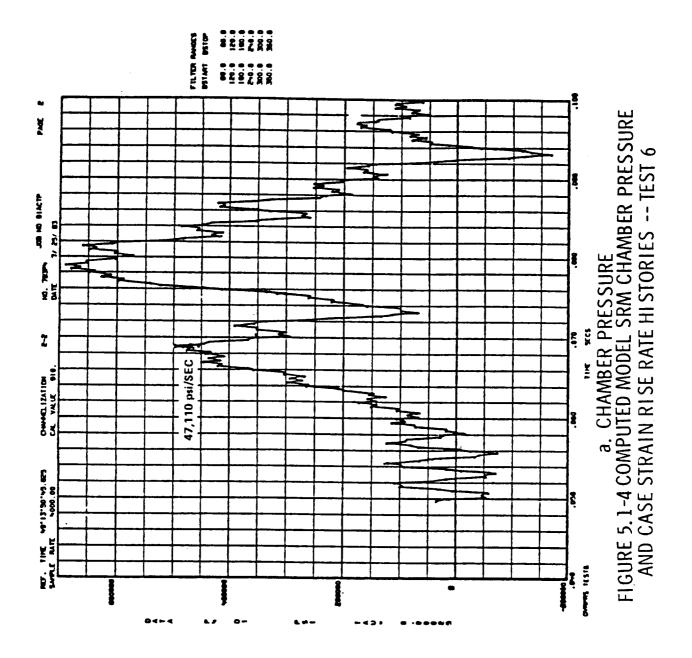


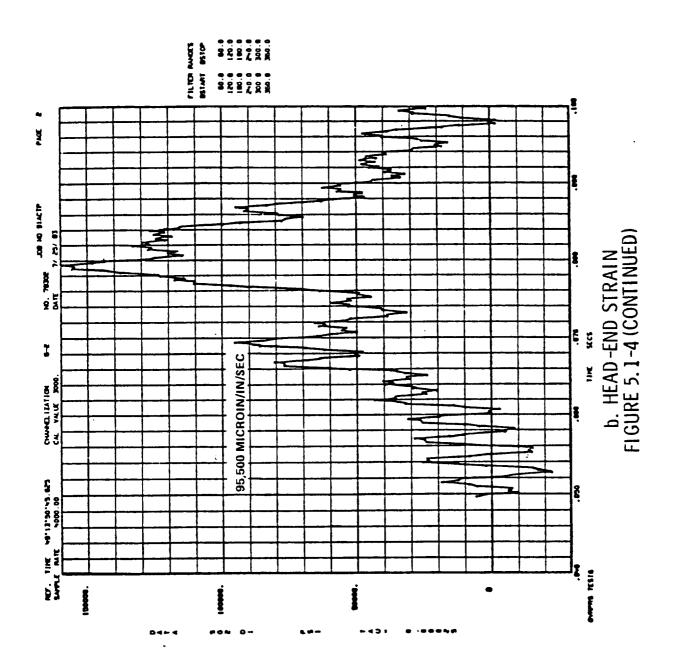
5-13

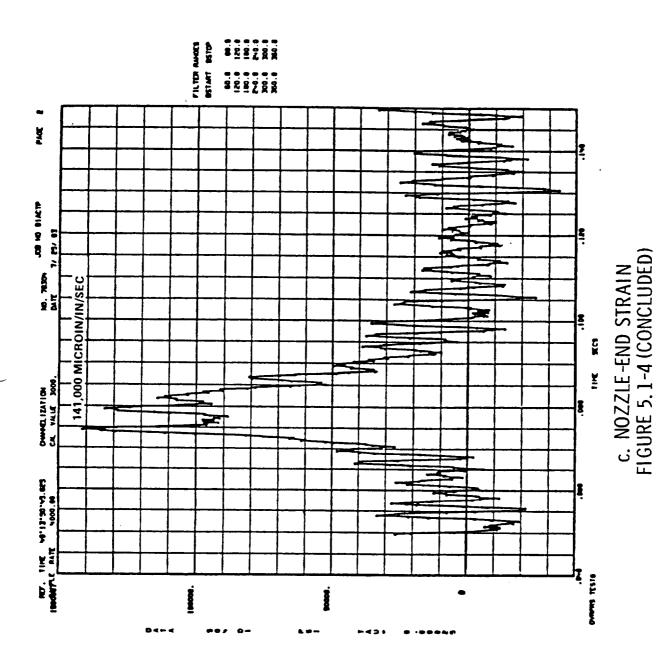
TABLE 5.1-1

MAXI	MUM KISE KAIE VALUES	MAXIMUM KISE KAIE VALUES IN PODEE SIN GIRABEN TIESSONE	
		HEAD-END ŚG _{max} ²	NOZZLE-END ŚG _{max} ²
TEST	Pcmax, ps1/sec	MICROIN/IN/SEC	MICROIN/IN/SEC
ער	46.770	98,000	145,000
- - -	47,110	95,500	141,000
	47,980	82,000	
. 00	51,420	80,000	141,000
σ	58.400	128,000	140,000
0	44,960	91,000	116,500
	66.440	65,500	64,000
12	46.930	83,000	84,000
3 -	78.210	150,000	113,000
7	49.620	94,000	000,18
- 2	60.230	115,000	107,000
16	49,290	117,000	93,000
	-		
40 RH		•	

NOTES: 1. THREE - POINT SLOPE METHOD DERIVATIVE ESTIMATE 2. NUMBERICAL DERIVATIVE EVERY JOINT



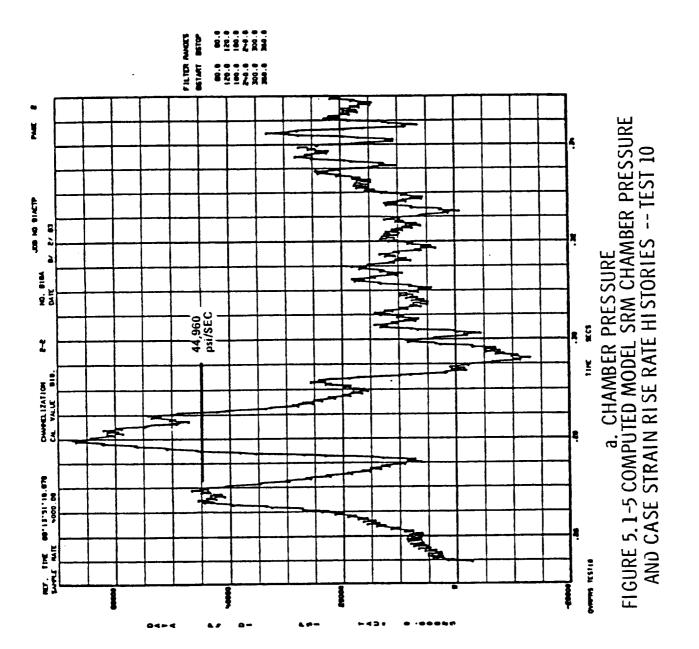


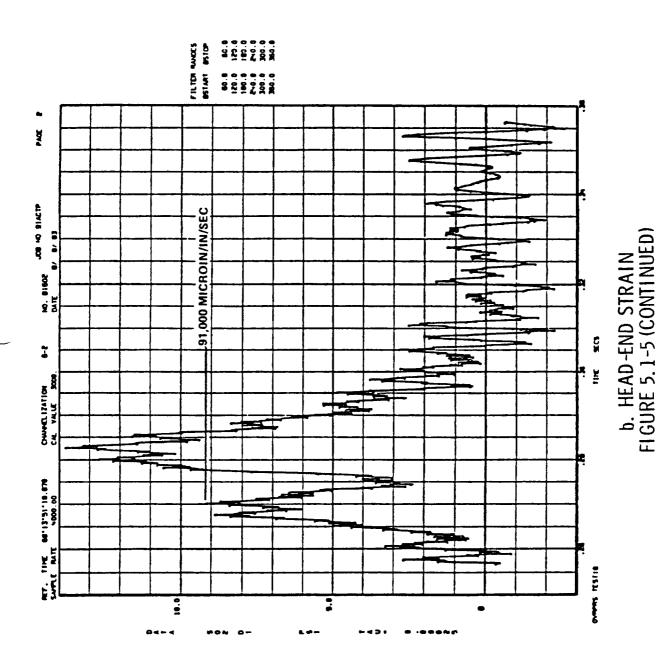


(

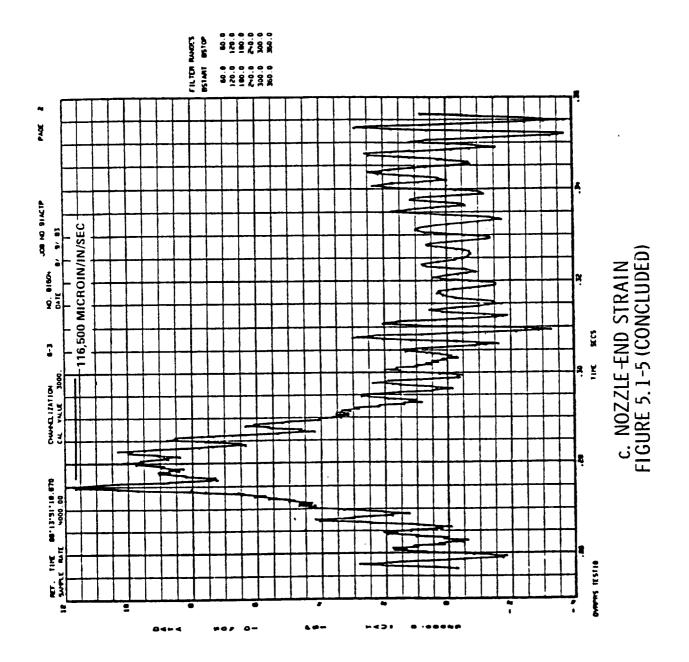
5-17

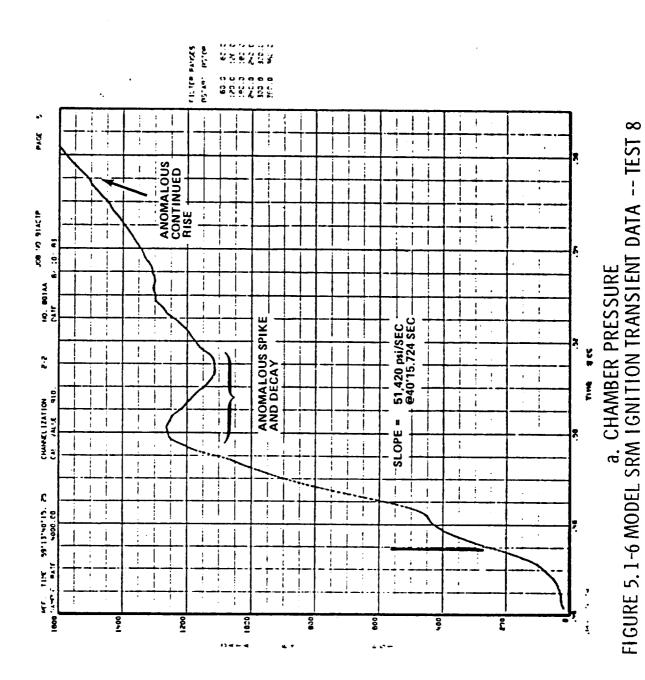
Ì



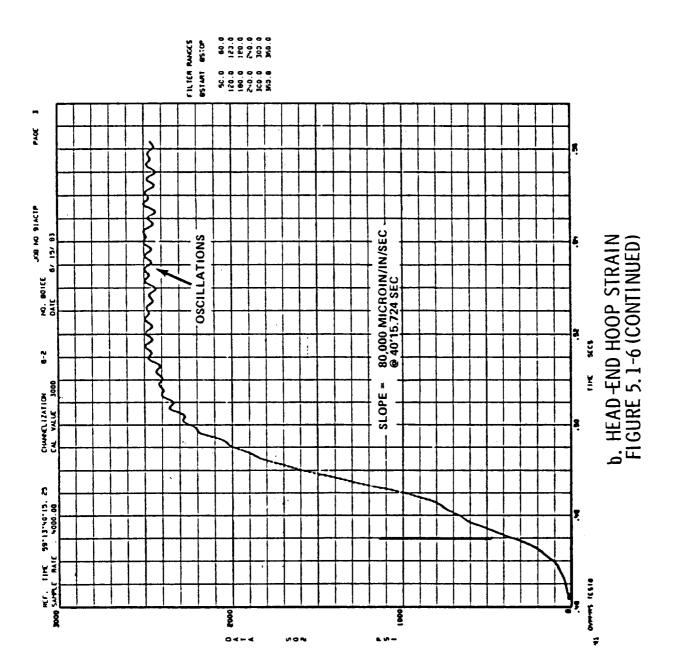


5-19

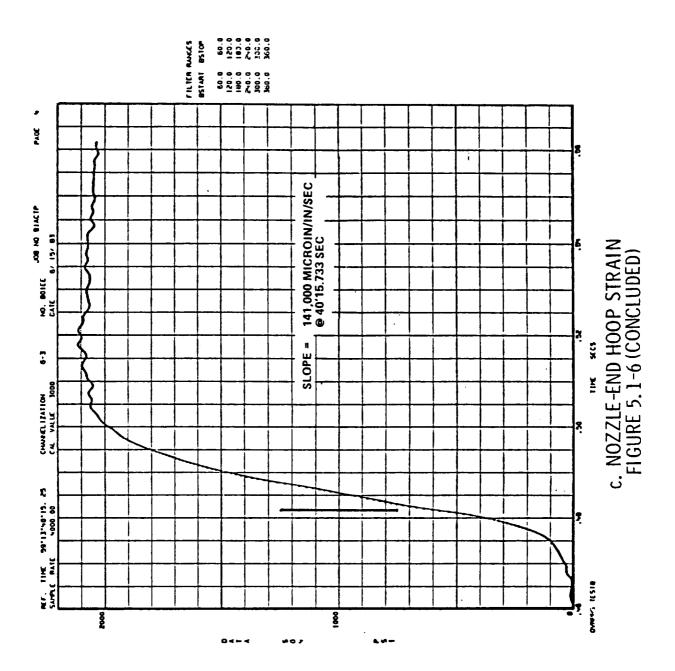




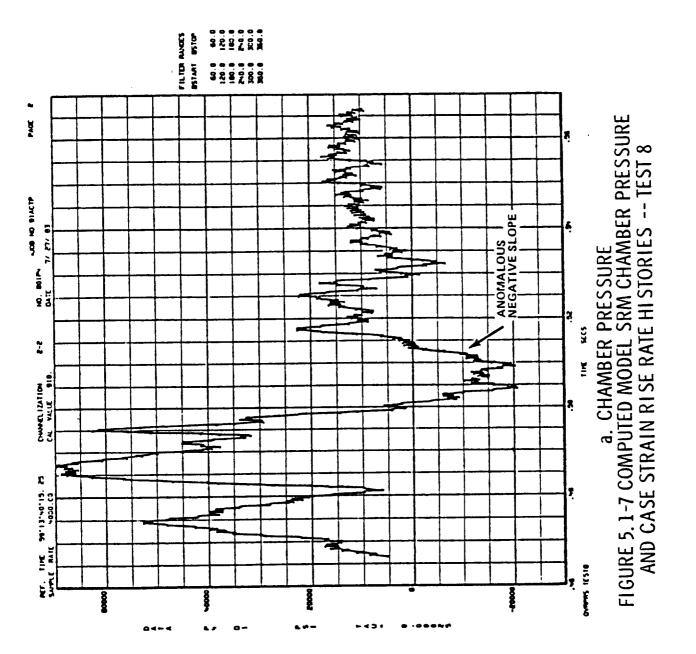
5-21

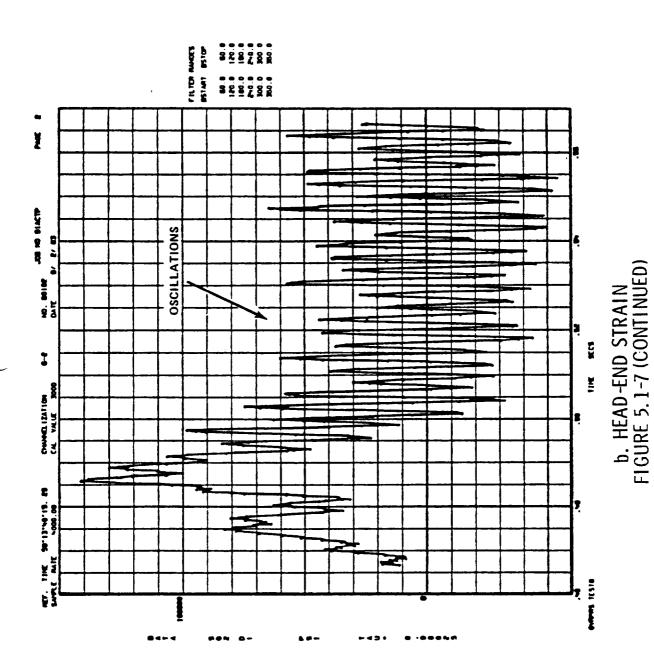


5-22



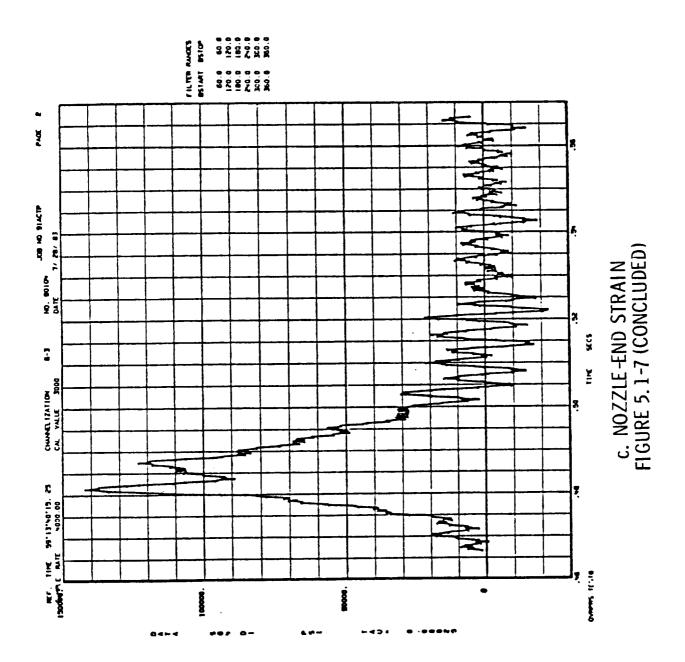
, in





į

5-25



5-26

water spray geometry. These nozzle exit static pressure measurements were added in Tests 40 and 42, Test 42 being an acoustic test at 84 ft simulated elevation above the model launch mount, and out of the influence of the model SRB exhaust hole geometry. The nozzle static pressure data acquired in Tests 40 and 42 were of poor quality traced to measurement sensing port irregularities that existed on the interior surface of the nozzle and to gas leakage around the transducers from improper seal. The diametrically opposed measurement pairs in no test ever showed an exactly matched pressure history that would be indicative of perfect symmetry in the expansion wave expulsion and plume attachment. Indications of asymmetry were not repeatable and were insufficient to deduce anything about facility geometry effects conclusively. There may well have been asymmetry; but the measurement port fidelity on the nozzle inside surface was never ideal because of inability to make a perfectly contoured surface with the epoxy filler joining the nozzle extension to the nozzle (see Figure 3.2-4). The nozzle exit static pressure data have been included in the final data packages but with reservations.

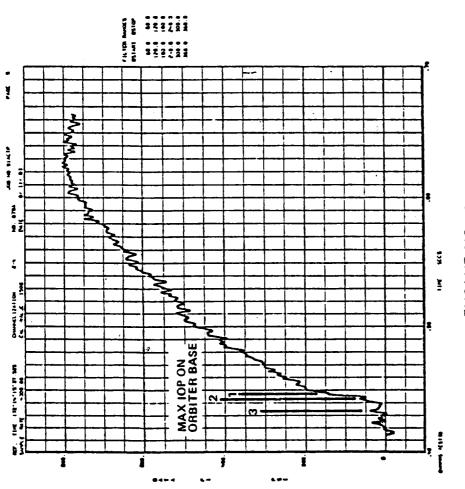
The model SRM's in Tests 11 and 13 exhibited long ignition delays to ignition rise. Details about the ignition transient data measured in these three tests are given separately in Appendix B. The large overshoot spikes after the ignition transient in the chamber pressure measurements from most of these tests are described in Appendix C. Chamber pressure was again normal after the spike in every test. The instances of long ignition delay and spiking in chamber pressure require elaboration to eliminate any confusion that might otherwise arise concerning these data.

5.1.2 Model SSME Ignition Data

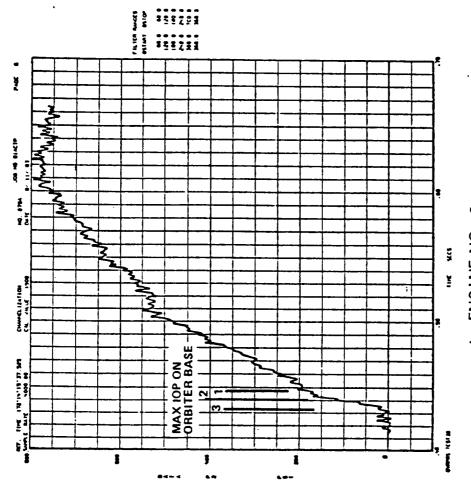
Typical model SSME chamber pressure ignition transient data are shown in Figures 5.1-8. The three model engines ignited nearly simultaneously in each test.

The maximum slope in each model SSME ignition transient occurs at the beginning of the rise transient. Timing of the SSME ignition overpressure wave development indicates the overpressure to be associated with this

Į

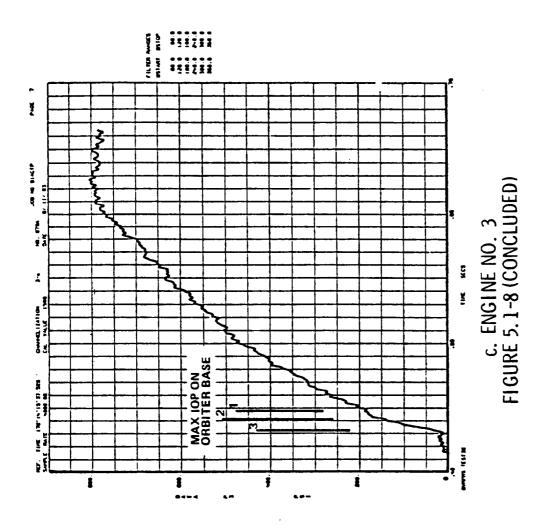


a. ENGINE NO. 1 FIGURE 5.1-8 SSME IGNITION TRANSIENT DATA -- TEST 30



! ._

b. ENGINE NO. 2 FIGURE 5. 1-8 (CONTINUED)



beginning of the rise transient. This origin of the model SSME overpressure is associated with the first ignition of propellants in each model SSME. The spark igniters are turned "On" first, then warm GO_2 enters the thrust chambers as the injector posts are initially warm, and ignition takes place as the warm GH_2 is issued through the coaxial jets when a combustible mixture of GO_2 and GH_2 is achieved in the presence of the spark.

5.2 Model Launch Mount Water Sprays

The sound suppression water acts on the starting flow into each exhaust duct and influences the overpressures generated. The total water flowrates into each active duct were all read from the DSU data at T_0 and are documented herein. The SRB duct flowrates at SRM ignition are shown in Table 5.2-1. The SSME duct flowrates at SRM and SSME ignition are shown in Table 5.2-2.

The actual SRB duct flowrates as seen in Tables 5.2-1 and 5.2-2 were slightly low for the single-SRM tests with the SSME and SRB flows supplied from the same source. Use of these separate source for the SRB water resulted in much closer SRB flowrate for the LH SRB duct in Test 40, slightly high for the RH duct. The SSME duct flow was close to the design value for every test. The total nominal 100-percent design water flowrate to the model launch mount is 3950.3 gpm, equivalent to 964,400 gpm full scale. (The 20,000 gpm peripheral spray around the outside of the full-scale launch mount on the Elev. 100 ft deck level was not simulated.)

5.3 Overpressure Data

A sketch of the baseline model geometry elevation view is shown in Figure 5.3-1. This elevation section through the LH SRB duct shows the full-scale equivalent dimensions. The SRM ignition overpressure (IOP) and duct overpressure (DOP) wave are separately identified by their timing and directions of propagation. The IOP waves arrive on the model vehicle first traveling upward from the top of the SRB exhaust hole. The DOP waves arrive on the model vehicle later traveling back from the end of the SRB

TABLE 5.2-1 MODEL SRB EXHAUST DUCT WATER FLOWRATES AT MODEL SRM IGNITION

PERCENT OF DESIGN,	92.0 92.0 92.6 91.6 94.3 91.9 89.6 94.4 94.2 91.1	PERCENT OF DESIGN, % 104.9
LH SRB TOTAL gpm	1586.6 1585.8 1597.1 1579.7 1626.4 1585.1 1546.7 1628.9 1626.0 1571.5 1562.8	RH SRB TOTAL gpm 1809.8
LH SRB PRIM W, 9pm	109.2 110.3 108.5 107.5 111.8 108.5 104.4 114.1 112.1 107.0 107.1	RH SRB PRIM W, gpm 119.1
LH SRB SECONDARY, gpm	367.2 373.1 374.5 373.7 381.1 373.7 369.6 380.7 383.3 370.9 368.1	RH SRB SECONDARY, gpm 395.3
LH SRB CURTAIN S, gpm	334.9 315.0 319.0 313.2 322.9 313.4 304.4 324.2 320.6 312.2 313.6	RH SRB CURTAIN S, gpm 390.0
LH SRB CURTAIN N, gpm	326.0 332.3 335.5 334.5 343.7 336.4 325.9 340.5 346.2 330.1 327.3	RH SRB CURTAIN N, gpm 375.4
LH SRB PRIM S,	220.7 220.4 225.5 220.3 220.3 220.7 217.6 229.2 227.7 220.3 218.5 -	RH SRB PRIM S, gpm 247.3
LH SRB PRIM N,	228.6 234.7 234.1 230.5 240.0 232.4 224.8 240.2 236.1 236.1 236.1	RH SRB PRIM N, gpm 282.7
TEST	5 7 7 8 9 10 11 11 13 14 16 16 40	TEST 40

TABLE 5.2-2 MODEL SSME EXHAUST DUCT WATER FLOWRATES AT MODEL SSME AND SRM IGNITION

TEST	MODEL SSM	E, gpm	PERCENT OF
	AT SSME IGN.	AT SRM IGN.	DESIGN, %
5 6 7 8 9 10 11 12 13 14 15 16	N/A N/A N/A N/A N/A N/A N/A N/A N/A N/A	475.7 480.6 472.6 468.3 486.9 472.6 454.8 497.2 488.2 466.0	95.2 96.2 94.6 93.7 97.4 94.6 91.0 99.5 97.7 93.3 93.3
30	523.6	N/A	104.8
31	511.3	N/A	102.3
32	507.4	N/A	101.5
40	-	530.4	106.1

N/A - Not Applicable

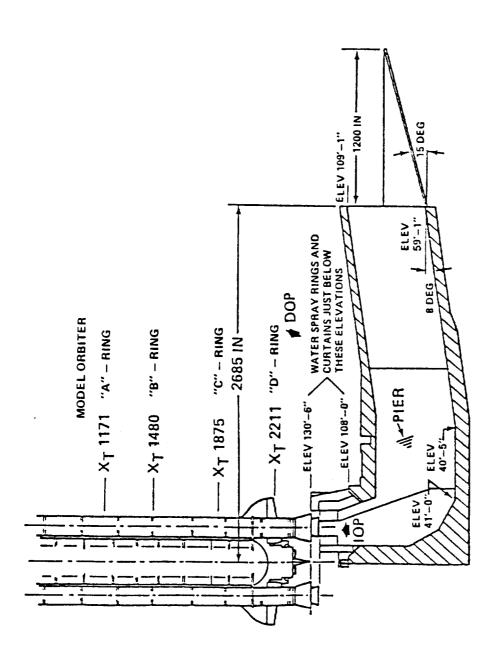


FIGURE 5.3-1 BASELINE MODEL TEST GEOMETRY -- ELEVATION VIEW

exhaust duct. The 311.5 in (full-scale) Z off-set of the Orbiter relative to the ET-SRB centerline as shown in Figure 5.3-2 gives pitch-axis loading components ventral-to-dorsal across the model Orbiter planform for both the IOP and DOP. The angle of the SSME exhaust and exhaust duct with the vertical away from the Orbiter tail gives expected pitch-axis components of SSME IOP across the Orbiter planform dorsal-to-ventral.

(.__

For the purposes of this report, all of the overpressure data in the twenty tests performed were checked for any instrument or data processing error in order to have a fully-validated set of overpressure data released as final data packages appendaged to this report. Any measurement found to have an unreconcilable fault and considered invalid has been so identified as being invalid and not included in the particular final data packages. A summary of peak positive delta pressures (the maximum value recorded on each measurement) is given for the SRM tests in Tables 5.3-1 through 5.3-3 and for the SSME tests in Table 5.3-4. There are a few instances noted in these tables where corrections are needed to the final data. These tables provide a general view of maximum overpressure level distribution over the entire vehicle/facility model in each test and the respective levels of model SRM and SSME overpressure. Only a small number of measurements were labelled invalid; the data recovery rate in these tests was over 95 per-The model SSME's were operating at model SRM ignition in Test 40, and it was necessary to identify the SRM overpressure against the SSME noise background. The background levels are listed in Table 5.3-3 to show the relative peak positive overpressure levels and background acoustic noise levels. In the 0-to-400 Hz band, the predominant SSME noise was in the 100 - 250 Hz range.

The SRM overpressure data contain an initial shock wave nominally 16 msec after T_0 of very large strength, sometimes with amplitude larger than the overpressure data. This shock is produced inside the Tomahawk motor igniter as the initiator fires and registers on every overpressure sensor. This shock, called the "igniter pulse", is part of the overall forcing time function; it has a long exponential decay time. The full-scale SRM has an igniter pulse as well. The igniter pulse was present in the model data and had to be contended with in setting record amplifier gains so as not to

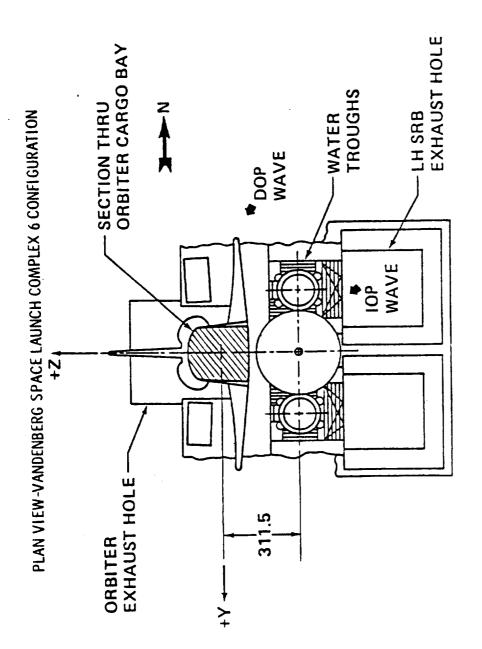


FIGURE 5.3-2 BASELINE MODEL TEST GEOMETRY -- PLAN VIEW

TABLE 5.3-1 SINGLE-MODEL SRM OVERPRESSURE DATA -- PITCH-TYPE TESTS

	PEAK AMPLITUDE (DELTA p), psi								
	BASEL		FURATION			TESTS	DRY TEST		
SENSOR	5	6	7	10	8	9	16		
ORBITER									
F1	0.074	0.069	0.081	0.049	0.056	0.064	0-180		
F3	0.067	0.063	0.079	0.048	0.050	0.058	0.160		
F3A	0.073	0.060	0.081	0.048	0.054	0.051	0-164		
F3B	0.070	0.068	0.077	0.048	0.049	0.059	0-167		
F4	INVALID	0.082	0.091	0.051	0.052	0.048	0.165		
F4A	0.074	0.063	0-075	0.049	0.053	0.061	0.172		
F4B	0.074	0.072	0.078	0.048	0.057	0.060	0.180		
F5	0•078	0+070	0.083	0.056	0.062	0.060	0.2184		
F7	0.050	0.068	0-084	0-052	0.062	0.060	0.180		
F7A	0.066	0.062	0.082	0.049	0.053	0.056	0.172		
F7B	0.086	0.067	0.080	0.053	0.057	0.055	0.178		
F8	0.091	INVALID	INVALID	0.069	0.057	0.057	0.240		
F8A	0.077	0.071	0.084	0.055	0.061	0.057	0-175		
F8B	0.067	0.059	0.074	0.053	0.055	0.056	0-215		
F9	0.093	0•070	0•099	0•070	0.075	0.052	0.520		
Fll	0.066	0.063	0.080	0.055	0.054	0.056	0.190		
F11A	0.066	0.063	0.076	INVALID	0.054	0.055	0.185		
F118	0.066	0.062	0.074	0.060	0.054	0.063	0.206		
F12	0.069	0.080	0.077	0.054	0.053	INVALID	0.214		
F12A	0.065	0.064	0.080	0.053	0.052	0.054	0.218		
F12B	0.093	0.061	0.099	0.068	0.070	0.053	0.510		
F13	0.082	0.062	0-110	0.059	0+065	0.059	0•490 ⁴		
F15	0.062	0.065	0.077	0.047	0.048	0.049	0.160		
F15A	0.059	0.059	0.075	0.048	0.047	0.048	0-151		
F15B	0.060	0.068	0.072	0.034	0.046	0.050	0.147		
F16	0.059	0.059	0.120	0.047	0.050	0.046	0.224		
F16A	INVALID	0.059	0.081	0.050	0.053	0.042	0.240		
F16B	INVALID	INVALID	INVALID	0.060	0.061	0.055	0.600		
F17	0.067	0.054	0.081	0.094	0.050	0.041	0.250		
F18	0.056	0.048	0.072	0.042	0.045	0.039	0.196		
F19	0.060	0.053	0.0784	0.048	0.053	0.040	0.260		
BF1	0.071	0.060	0.096	0.050	0.063	0.046	0.570		
BF2	INVALID	0.050	0.082	0.046	0.053	0.039	0.280		
W1	0.073	0.067	0.102	0.066	0.065	0.057	0.510		
W2	0.064	0.061	0.077	0.055	0.041	0,052	0.155		
W3	0.063	0.055	0.081	0.054	0.047	0.059	0.410		
W4	0.068	0.064	0.089	0.061	0.057	0.068	0.190		

TABLE 5.3-1 SINGLE-MODEL SRM OVERPRESSURE DATA -- PITCH-TYPE TESTS (CONTINUED)

• • • • •	PEAK AMPLITUDE (DELTA p), psi							
	BASEL	INE CONGI	FURATION	TESTS	MUFFLER	TESTS	DRY TEST	
SENSOR	5	6	7	10	8	9	16	
W5	0-065	0.060	0.095	0.058	0.059	0.060	0.430	
W6	0.052	0.061	0.082	0.050	0.048	0.047	0.186	
ΕT								
T1	0.062	0.067	0.080	0.047	0.047	0.056	0-190	
T3	0.062	0.060	0.081	0.036	0.049	0.048	0.150	
T3A	0.056	0.062	0.076	0.053	0.043	0.068	0.142	
T4	0.054	0.070	INVALIO	0.047	0.053	0.055	0.230	
T4A	0.059	0.071	0.077	0.044	0.047	0.056	0-237	
T5	0.075	0.074	0.080	0.057	INVALID	0.055	0.340	
T7	0.0563	0.0543	0.081	0.050	0.062	0.060	0.200	
T7A	0.076	0.066	0.083	0.050	0.063	0.062	0.190	
T8	0.071	0.062	0.071	0.051	0.062	0.060	0.270	
TBA	0.068	0.062	0.079	0.053	0.056	0.053	0.340	
Т9	0.056	0.055	0.098	0.056	0.067	0.088	0.500	
T11	0-100	0.072	0.093	0.068	0.072	0.062	0.430	
TIIA	0.092	0.062	0.088	0.066	0.068	0.060	0.420	
T12	0.078	0.066	0.063	0.061	0.064	0.049	0.430	
T12A	INVALID	0.066	0.101	0.057	0.064	0.045	0.520	
T13	0.062	0.063	0-117	0.056	0.064	INVALID	0.890	
T15	0.088	0.060	0.120	0.070	0.072	0.048	0.690	
T15A	0.074	0.062	0.109	0.060	0.041	0.058	0.490	
T16	0.074.	0.062	0.136	0.052	0.064	0.051	0.650	
T16A	0.061	0.065	0.108	0.056	0.044	0.057	0.760	
T17	0.084	0.070	0-112	0.055	0.064	0.052	INVALID	
LH SRB	0.058	0.063	0.073	0.051	0.053	INVALID	0.280	
SL1	0.068		0.073	0.055	0.052	0.061	0.200	
SL3	0.061	0.062	+	0.055	0.057	0.056	0.360	
SL5	0.065	0.065	0.085	0.052	0.064	0.057	0.249	
SL7	0.068	0.051	0.075	0.055	0.063	0.051	0.620	
SL9	0.059	0.059	0.096	0.057	0.084	0.035	0.460	
SL11	0.072	0.056	0.062			0.037	1.050	
SL13	0.047	0.053	0.090	0.046	0.045	+	0.620	
SL15	0.071	0.060	0.094	0.052	0.059	0.090	0.960	
SL18	0.050	0.050	0.060	0.040	0.040	0.050		
SL20	0.030	0.040	0.110	0.030	0.060	0.050	0.460	

TABLE 5.3-1 SINGLE-MODEL SRM OVERPRESSURE DATA -- PITCH-TYPE TESTS (CONCLUDED)

	PEAK AMPLITUDE (DELTA p), psi						
	BASEL	INE CONGI	FURATION	TESTS	MUFFLER	TESTS	DRY TEST
SENSOR	5	6	7	10	8	9	16
SL23	0-180	0.074	0-150	0.030	0.270	0.050	2.62
SPLITTER PLATE							
SPL6	0.039	0.040	0.064	0-038	N/A	N/A	0.350
SPL12	0.062	0.067	0.085	0.055	N/A	N/A	N/A
SPL18	0.071	0.082	0.093	0.058	N/A	N/A	N/A
SPL21	0.064	0.059	0.079	0.050	N/A	N/A	N/A
SPL22	0.062	0.063	0.084	0.048	N/A	N/A	N/A
LH SRB DUCT							
D1	2•36	3.80	3.98	2.50	3.30	3.70	4.80
D2	INVALID	5.40	8.00	3.49	4.30	6.30	6-45
D3	3.50	4.45	3.20	3-50	3.30	3.25	5.40
D3A	N/A	N/A	N/A	N/A	N/A	N/A	7.00
D3B	N/A	N/A	N/A	N/A	N/A	N/A	5.30
D3C	N/A	N/A	N/A	N/A	N/A	N/A	6.60
D30	N/A	N/A	N/A	N/A	N/A	N/A	6.55
D3E	N/A	N/A	N/A	N/A	N/A	N/A	6.95
D4	0.14	0.27	0.23	0-89	1.97	1.80	2.65
D5	0.04	0.04	0.11	0.15	N/A	N/A	0.73
D6	0.70	1.00	0.85	0.35	N/A	N/A	4.50
D7	0-11	0.13	0.11	0.25	N/A	N/A	0.80
D8	0.75	NIL	NIL	0.23	N/A	N/A	0.80
D21	1.00	0.90	1.00	0.48	N/A	N/A	5.50
D24	2.55	2.90	INVALID	1.85	N/A	N/A	5.50
025	2.50	2.40	3.00	1.56	2.16	2.10	4.05
026	2.45	2.60	3.60	1.18	2.45	1.95	2.76
D27	INVALID	0.34	INVALID	0.50	0.31	0.45	1.15
D28	0.23	0.25	0.295	0.48	0.21	0.23	INVALID
OUTSIDE AIR PATH							
01	0.071	0.095	0.112	0.07	0.060	0.057	0.195
	AL /A	N/ / A	NI /A	0.055	N/A	N/A	N/A
02	N/A	N/A	N/A	0.000	IN/ A	N/A	117/A

NOTES: 1. N/A denotes a measurement not made in a particular test.

- 2. NIL denotes value negligibly small on model SR8 base and at top of SR8 hole -- where aspiration influence is strong.
- 3. Data as published have a factor of two scale error from incorrect record amplifier setting.
- 4. Filtered data as published are invalid -- unfiltered data used.

TABLE 5.3-2 SINGLE-MODEL SRM OVERPRESSURE DATA -- LATERAL-TYPE TESTS

	PEAK AMPLITUDE (DELTA p), psi								
	BASE	LINE TEST	\$	MUFFLER	TESTS				
SENSOR									
	11	12	13	14	15				
ORBITER									
F1	0.044	0.040	0.045	INVALID	0.027				
F1A	0.037	0.033	0.042	0.020	0.024				
F18	0.037	0.033	0.039	0.020	0.024				
F2	0.039	0.031	0.039	0.021	0.023				
F2A	0.042	0.032	0.043	0.023	0.025				
F 28	0.035	0.032	0.040	0.024	0.026				
F3	0.041	0.032	0.053	0.022	0.030				
F3A	0.049	0.034	0.042	0.025	0.028				
F38	0.051	0.035	0.048	0.025	0.028				
F4	0.055	0.038	0.050	0.027	0.029				
F4A	0.056	0.037	0.049	0.026	0.029				
F48	0.054	0.036	0.049	0.027	0.029				
F5	0.047	0.030	0.041	0.024	0.026				
F5A	0.037	0.030	0.033	0.024	0.023				
F5B	0.036	0.029	0.038	0.022	0.023				
F6	0.039	0.028	0.039	0.024	0.025				
F6A	0.038	0.029	0.039	0.020	0.024				
F6B	0.040	0.028	0.041	0.020	0.023				
F7	0.047	0.033	0.043	0.023	0.027				
F7A	0.053	0.033	0.045	0.024	0.029				
F78	0.056	0.036	0.048	0.026	0.027				
F8	0.077	0.051	0.066	0.037	0.035				
F8A	0.062	0.041	0.054	0.028	0.027				
F88	0.047	0.031	0.044	0.024	0.026				
	<u> </u>	1							
F9	0.048	0.039	0.054	0.021	0.025				
F9A	0.043	0.033	0.044	0.020	0.021				
F98	0.033	0.026	0.037	0.020	0.021				
F10	0.036	0.026	0.038	0.021	0.023				
F10A	0.036	0.027	0.038	0.022	0.025				
F108	0.044	0.031	0.044	0.023	0.024				
FII	0.043	0.034	0.045	0.024	0.028				
F11A	0.053	0.038	0.044	0.022	0.028				
F118	0.059	INVALID	0.051	0.026	0.031				

TABLE 5.3-2 SINGLE-MODEL SRM OVERPRESSURE DATA -- LATERAL-TYPE TESTS (CONTINUED)

F12A F12B	11 0.063 0.063 0.053	12 0.041 0.045		MUFFLER	TESTS
F12 F12A F12B	0.063 0.063	0.041		14	4.5
F12A F12B	0.063 0.063	0.041		14	4.5
F12A F12B	0.063		0.050		15
F128		0.045	4	0.027	0.029
	0.053		0.050	0.027	0.030
F13		0.042	0.060	0.022	0.030
F13					
	0.039	0.035	0-040	0.016	0.023
F13A	0.033	0.035	0.037	0.017	0.023
F13B	0.035	0.028	0.037	0.0175	0.026
F14 ·	0.039	0.033	0.039	0.018	0.027
F14A	0.033	0-025	0.040	0.017	0.029
F14B	0.039	0.046	0.040	0.020	0.033
F15	0.049	0.032	0.040	0.020	0.024
F15A	0.051	0.035	0.043	0.023	0.027
F158	0.047	0.015	0.051	0.022	0.025
F16	0.051	0.042	0.053	0.021	0.026
F16A	0.054	0.041	0.049	0.024	0.027
F16B	0.038	0.041	0.053	0.021	0.024
F18	INVALID	0.034	0.046	0.019	INVALID
V1.	0.040	0.031	0.040	0.020	0.023
٧2	0.051	0.036	0.042	0.023	0.028
ET					
_					
TIA	0.044	0.029	0.043	0.023	0.025
T2	0.042	0.026	0.039	0.019	0.027
T2A	0.042	0.028	0.041	0.024	0.023
T3A	0.053	0.024	0.050	0.026	0.030
T4 (0.062	0.043	0.049	0.029	0.030
T4A	0.057	0.041	0.049	0.026	0.027
T5A	0.034	0.030	0.042	0.020	0.027
T6 (0.037	0.032	INVALID	0.020	0.027
T6A	0.037	0.030	0.041	0.019	0.025
T7A	0.057	0.032	0.054	0.028	INVALID
T8 (0.061	0.042	0.056	0.026	0.033
TBA (0.056	0.038	0.053	INVALID	0.034
T9A	0.040	0.032	0.045	0.023	0.030
T10 (0.033	0.028	0.043	0.018	0.027
T10A	0.027	0.029	0.037	0.019	0.025

TABLE 5.3-2 SINGLE-MODEL SRM OVERPRESSURE DATA -- LATERAL-TYPE TESTS (CONCLUDED)

	PEAK AMPLITUDE (DELTA p), psi									
İ	BASEL	INE TEST	S	MUFFLER	TESTS					
SENSOR										
	11	12	13	14	15					
T11A	0.060	0.039	0.058	0.025	0.031					
T12	0.058	0.043	0.058	0.026	0.028					
T12A	0.048	0.041	0.054	0.024	0.025					
T13A	0.035	INVAL ID	0.038	0.016	0.026					
T14	0.037	0.027	0.036	0.016	INVAL 10					
T14A	0.033	0.016	0.027	0.018	0.027					
T15A	0.049	0.032	0.042	0.018	0.017					
T16	0.040	0-041	0.055	0.020	0.026					
T16A	0.046	0.036	0.052	0.017	0.025					
T17	0.038	0.037	0.043	0.020	0.027					
	!				1					
LH SRB					1					
SL18	INVALID	0.086	INVALID	0.009	NIL					
SL20	INVAL 10	NIL	INVALID	NIL	NIL					
SL23	0.079	0.040	NIL	0.022	NIL					
	1									
LH SRB			1							
DUCT			1							
D1	4.203	3.10	6.70	2.99	5.10					
D2	4.60	4.45	8.55	4.12	6.48					
D3	3.88	2.85	4.60	3.33	3.80					
D3A	3.22	2.18	4.20	2.98	3.67					
D3B	2.26	1.58	3.08	3.594	2.85					
D3C	N/A	N/A	4.25	3.68	4.78					
030	N/A	N/A	4.30	2.754	3.75 ~					
D3E	N/A	N/A	4.40	2.72	3.28					
D4	1.08	0.78	1.45	1.73	2.09					
05	INVALID	0.05	N/A	N/A	N/A					
06	2.70	0.40	1.18	NIL	0.53					
D7	INVALID		N/A	N/A	N/A					
D8	1.00	0.27	N/A	N/A	N/A					
D24	6.55	2.98	5.80	INVALID	4.55					
D25	1.70	1.24	2.25	3.144	2.32					
026	1.52	0.86	1.78	2.454	1.78					
D27	0.44	0.31	0.65	0.23	0.31					
D28	N/A	N/A	N/A	N/A	N/A					
1 N/					particula					

- NOTES: 1. N/A denotes a measurement not made in a particular test.
 - 2. NIL denotes value negligibly small on model SRB base and at top of SRB hole -- where aspiration influence is strong.
 - 3. Data as published have a factor of two scale error from incorrect record amplifier setting.
 - 4. Data as published have a factor of ten scale error from incorrect record amplifier setting.
 - 5. Filtered data as published are invalid -- unfiltered data used.

TABLE 5.3-3 DUAL-MODEL SRM OVERPRESSURE DATA -- FULL-MODEL TEST

PEAK AMP	PLITUDE (DI	ELTA p), psi	PEAK AME	PLITUDE (D	ELTA p), psi	PEAK AMPL	ITUDE (DI	ELTA p), ps
SENSOR	TEST	1*	SENSOR	TEST	1*	SENSOR	TEST	1*
	40	BACKGROUND		40	BACKGROUND		40	BACKGROUN
ORBITER								
F1	0.100	0.03	W9	0.087	0.04	LH SRM		
F2	INVALID	INVALID	W10	0.083	0.04	SL 18	0.115	0.02
F3	0.100	0.03	W13	INVALID	INVALID			
F4	0.125	0.03	W14	0.078	0.03	RH SRM		
			W15	0.065	0.035	SR17	0.122	0.02
F5	0.099	0.035	W16	0.093	0.04			
F6	0.077	0.035				LH SRB		
F7	INVAL ID	INVALID	V1	0.115	0.08	DUCT		
F8	0.131	0.035	٧2	0.132	0.08	D1	4.35	0.4
			ET			D3	5.30	0.03
F9	0-111	0.04	TI	0.101	0.015	D4	2.00	0.03
F10	0.079	0.04	T2	0.074	0.015	D14	2.30	0.15
F11	0.103	0.05	T3	0.098	0.03			
F12	0.136	0.04	T4	0.134	0.03	RH SRB		
						DUCT		
F13	0.103	0.055	T5	0.110	0.02	D101	3.00	0.1
F14	0.100	0.06	T6	0.070	0.02	D103	5.45	0.05
F15	0.129	0.06	T7	0.085	0.03	D103A	4.10	0.05
F16	0.127	0.06	T8	0.137	0.03	D104	1.52	0.04
						D114	2.25	0.15
F17	0.141	0.14	T9	0.102	0.02			
F19	0.099	0.07	T10	0.087	0.03	FAN HOUSE		
F21	0.067	0.09	TII	0.110	0.03	LOCATION		
BF1	INVAL ID	INVALID	T12	0.152	0.03	FH1	0.55	0.02
BF2	INVALID	INVALID				FH2	0.14	0.015
			T13	0.122	0.03			<u> </u>
WI	CI JAVAL	INVALID	T14	0.098	0.04			
W2	INVALID	INVALID	T15	0.122	0.04			
W3	0.148	0.035	T16	0.161	0.04			
W4	0.1252	0.03	T17	0.120	0.05			
W5	0.150	0.05					- · - · · · · · · · · · · · · · · · · ·	
W6	0.138	0.06						

^{*} NOTES: 1. SSME acoustic noise background before SRM ignition (100 - 250 Hz range, predominantly 200 Hz).

^{2.} Data as published have a factor of two scaling error from incorrect record amplifier scaling.

TABLE 5.3-4 MODEL SSME OVERPRESSURE DATA

	PEAK AMPLITUDE (DELTA p), psi							
SENSOR	BAS	ELINE TEST		DRY TEST				
	30	31	32	40				
ORBITER								
F1	0.064	0.016	0.040	0.040				
F2	0.055	0.016	0.027	INVALID				
F3	0.048	0.019	0.028	0.033				
F4	0.052	0.017	0.024	0.031				
F5	0.098	0.032	0.044	0.034				
F6	0.061	0.023	INVALID	0.045				
F7	0.066	0.032	0.031	INVALID				
F8	0.082	0.033	INVALID	0.036				
F9	0.232	0.067	0.092	0.033				
F10	0.140	0.068	0.119	0.067				
F11	0.102	0.049	INVALID	0.088				
F12	0.065	0.028	INVALID	0.060				
		i -						
F13	0.137	0.047	0.098	0.053				
F14	0.117	0.035	0.090	0.098				
F15	0.084	0.031	0.066	INVALID				
F16	0.295	0.083	0.140	0.105				
	1							
F17	0.227	0.268	0-195	0.240				
F19	0.215	0.158	0-191	0.105				
F21	0.211	0.147	0.190	0.125				
BF1	0.290	0.071	0.205	INVALID				
BF2	0.239	0.072	0.161	INVALID				
	 	1						
WT	0.109	0.048	0.092	0-110				
W2 ·	0.138	0.033	INVALID	0.110				
W3	0.183	0.068	0.147	INVALID				
W4	0.140	0.056	0.130	0.123				
W5	0.183	0.065	0.153	0.050				
W6	0.198	0.055	0.158	0.081				
- "	+	1						
W9	0.134	0.061	0.113	0.055				
W10	0.147	0.053	0.126	0.054				
1,0	1 00147	1,,,,,,	1					

TABLE 5.3-4 MODEL SSME OVERPRESSURE DATA (CONTINUED)

	PEAK	AMPL I TUDE	(DELTA p),	, psi
SENSOR	B/	ASELINE TES	TS	DRY TEST
	30	31	32	40
		1		1
W13	0-140	0.053	0-113	0-140
W14	0.120	0.037	0.095	0.072
W15	0.175	0.056	0-148	0.040
W16	0.162	0.043	0+138	0.073
V1	0.113	0.048	0-100	0.095
V2	0.112	0.079	0.084	0.079
ET				
]
T1	0.044	0.013	0.038	0.021
T2	0.043	0.018	0.038	0.020
T3	0.051	0-013	0.057	0.038
T4	0.050	0.047	0.038	0.033
T 5	0.061	0-056	0.050	0.017
T6	0.048	0.015	0.033	0.018
T7	0.079	0.020	0.072	0.038
T8	0.050	0.017	0.042	0.035
			<u> </u>	L1
T9	0.070	0.026	0.054	0.020
T10	0.084	0.026	0.065	0.027
T11	0.060	0.060	0-139	0.023
T12	0.100	0.032	0.083	0.027
T13	0-136	0.051	0-101	0.043
T14	0.186	0.069	0-152	0.048
T15	0.179	0.056	0.138	0.043
T16	0.185	0.093	0.153	0.046
T17	0.233	0.096	0.193	0.057
LH SRM				
SL18	0.116	0.054	0.102	0.019

TABLE 5.3-4 MODEL SSME OVERPRESSURE DATA (CONCLUDED)

	PEAK	AMPLITUDE	(DELTA p)	, psi
SENSOR	6	SASELINE TE	STS	DRY TEST
	30	31	32	40
RH SRM		1		
SR17	0.184	0.075	0.153	0.017
SSME				ŀ
DUCT		1		
		1	1	
D201	-	0.58	0.63	0.570
D203	-	0.41	0.32	INVALID
D204	-	1.24	1.00	0.270
D205	-	0.82	1.50	0.430
D206	-	0.22	0.16	

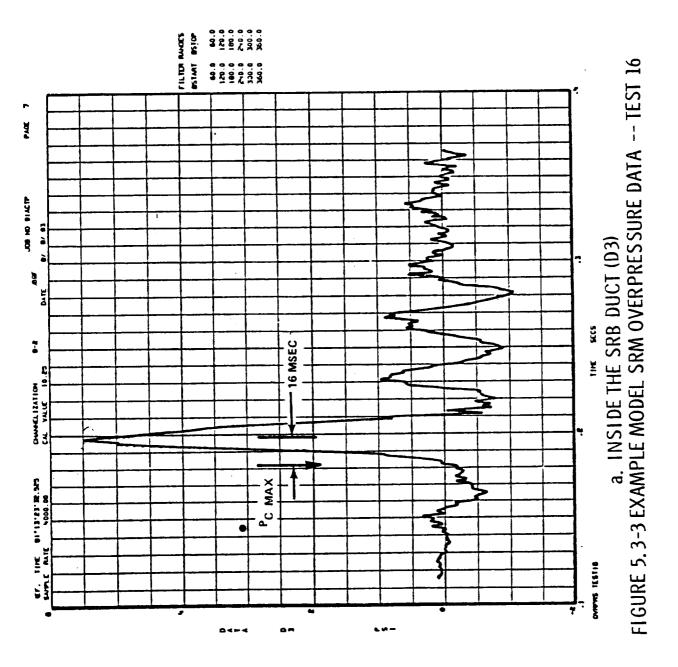
overrange a sensor's output at locations where the pulse amplitude was large. This is not to say that the igniter waves have no bearing on the overpressure results; accurate measurement of the model SRM igniter pulse strength was not a part of the present model investigation. A representative signature of the full-scale igniter pulse has been derived from flights to date (see Reference 8).

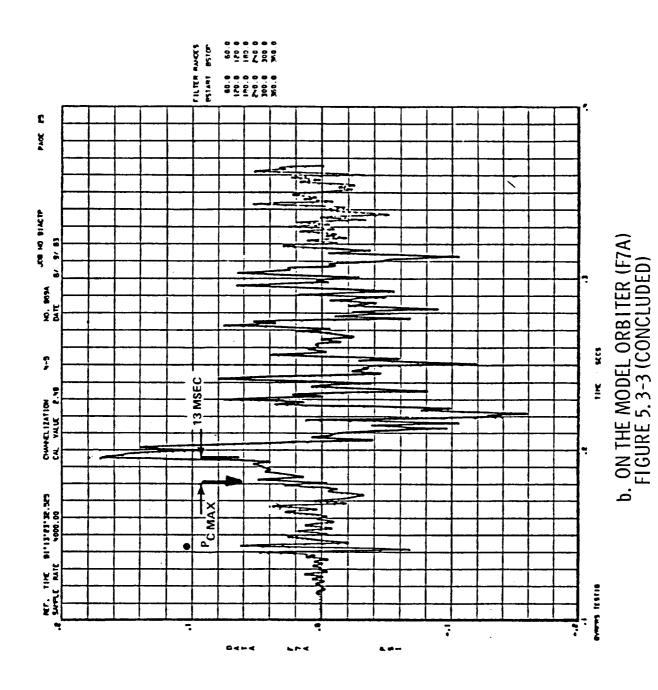
5.3.1 Example Model SRM Overpressure Data

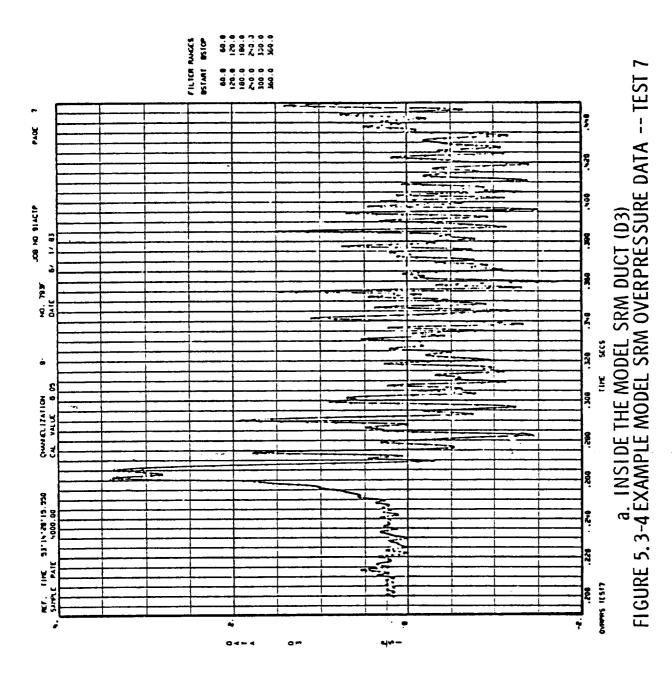
The data from the dry test (Test 16), two examples in Figure 5.3-3, showed a strong ignition overpressure wave emanating upward from the top of the SRB exhaust hole. An example pressure history inside the duct from Test 16 is shown in Figure 5.3-3a. The frequency of the oscillation inside the duct (measurement D3 providing the example) is approximately 30 - 31 Hz. The arrow on the figure denotes the time of occurrence of Pc_{max} . The The peak positive pressure at this measurement location about 80 percent down the duct length occurred 16 msec after the Pc_{max} . A measurement on the model Orbiter (F7A) is the example in Figure 5.3-3b and any other would serve equally as well. The peak positive amplitude is 0.17 psi. The wave arrived at measurement F7A slightly earlier than at measurement D3, 13 msec. The 30 - 31 Hz waveform is apparent in the F7A data; but there are higher frequencies as well, apparently second and third harmonics at 60 - 62 Hz and 120 - 124 Hz.

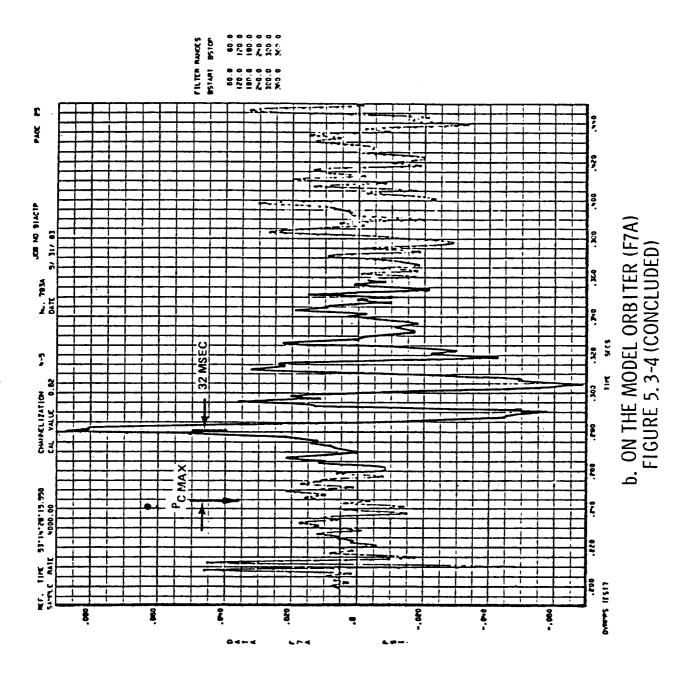
The overpressure wave timing in Test 6 started with Pc_{max} at IRIG time 50 min 45.694 sec and the maximum rise rate in nozzle-end case strain coming 5 msec later. The maximum nozzle-end case strain rise rate is coincident with the appearance of the nozzle starting expansion wave at the nozzle and was at 45.699 sec. The overpressure wave propagation time to measurement F7A was 30 msec after the expansion wave exited the nozzle, 45,729 sec. That was about 11 msec propagation time to the measurement D3 location in the duct, about 5 msec more to propagate on out the duct exit and begin expansion from the duct exit apron area, and about 14 msec back to measurement F7A.

The overpressure wave propagation time was a little less to measurement F7A in Test 7 as shown in Figure 5.3-4. It was 32 msec. A more distinct









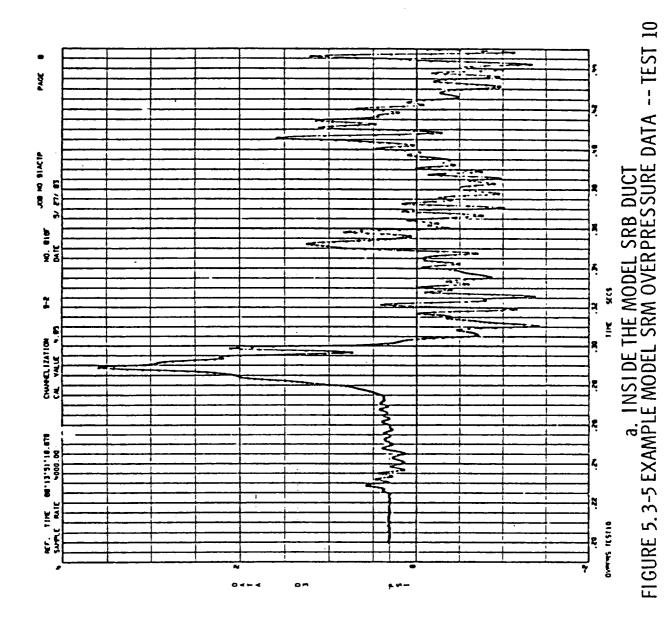
ringing pattern in the wave is evident in Test 7 than that which occurred in Test 6. Frequencies of 33 Hz and 66 Hz are evident in the duct overpressure (DOP) wave. The second rarefaction (negative peak) in the waveform shows the 33 Hz character as the second negative peak had larger amplitude than the first.

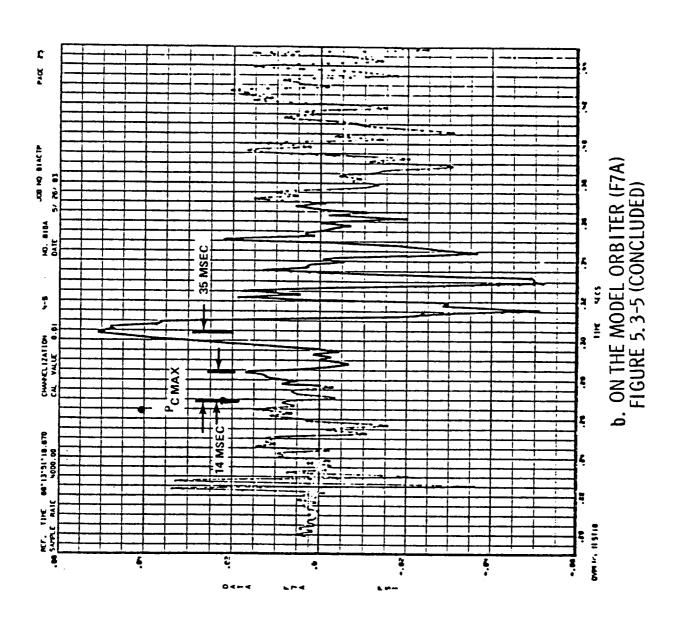
Test 10 was the third baseline configuration pitch-type test with the splitter plate. The DOP wave was smaller in amplitude as seen in Figure 5.3-5; it's arrival time at measurement F7A was 35 msec after Pc_{max} . There was a wave at 14 msec after Pc_{max} , the same time delay as the ignition overpressure (IOP) in Test 16. That wave is the ignition overpressure. The frequencies in the data at measurement F7A appear to be about 28 Hz and 66 Hz.

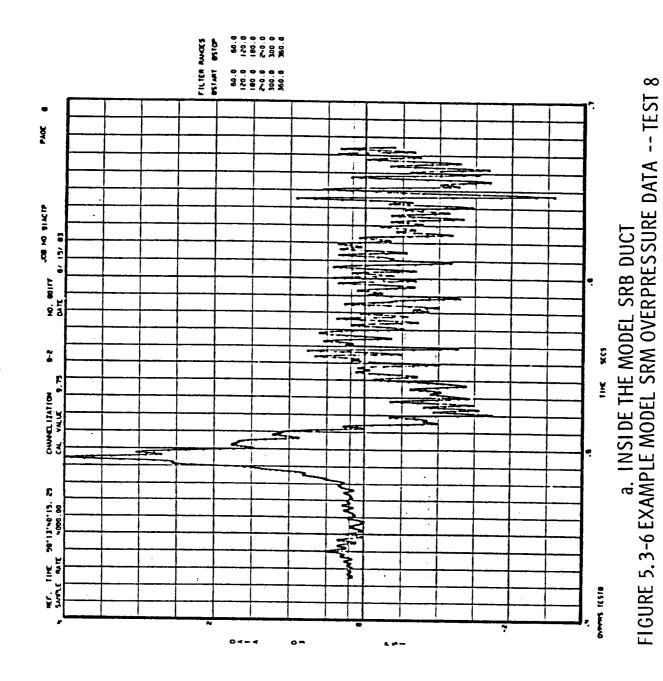
Tests 8 and 9 were pitch-type tests, with the splitter plate and with the muffler. The peak positive DOP amplitude was clearly smaller in Test 8 as seen in Figure 5.3-6 than in either Test 6 or 7 but about the same as in Test 10. These data have not been normalized for Pcmax variation. They are the data as measured. The wave arrival time was later with the muffler, 40 msec. The frequency content was about the same, 33 Hz and 66 Hz. The Test 9 example data are shown in Figure 5.3-7. The wave arrival time at measurement F7A was again 40 msec. The DOP waveform was slightly different, appearing to be comprised of predominantly 30 Hz and 66 Hz. The amplitude was slightly higher than in Test 8.

Test 12 was a lateral-type test, without the splitter plate, of the base-line configuration. The same example data are shown in Figure 5.3-8. The DOP amplitude at measurement F7A was roughly one-half that of Test 7, for example, without the doubling effect of the splitter plate. The wave arrival time was again 36 msec, nearly the same as in Test 6, 7 and 10. The frequency content was 30-33 Hz and 66 Hz. Data from Tests 11 and 13 in Appendix B use the same example, Orbiter measurement F7A, and are not presented here.

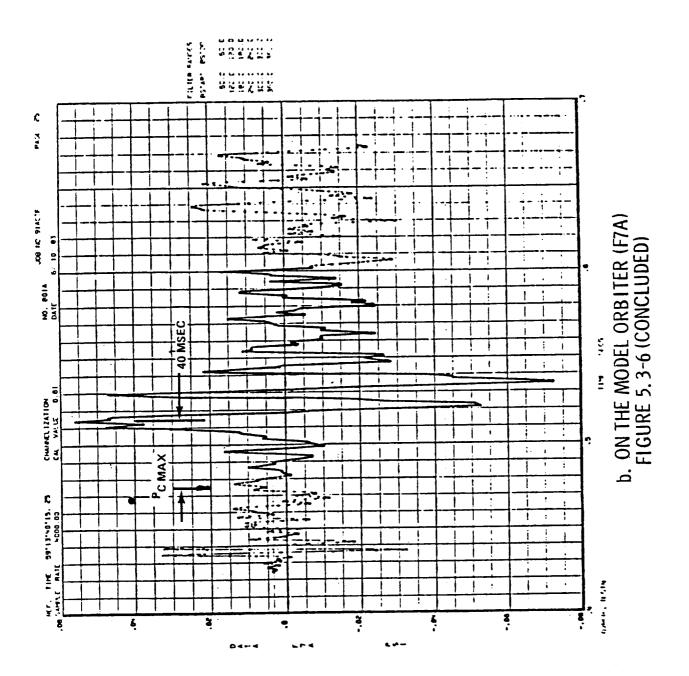
The two lateral tests with the muffler had considerably lower DOP amplitude than the other tests. The Test 14 example data are shown in Figure 5.3-9,

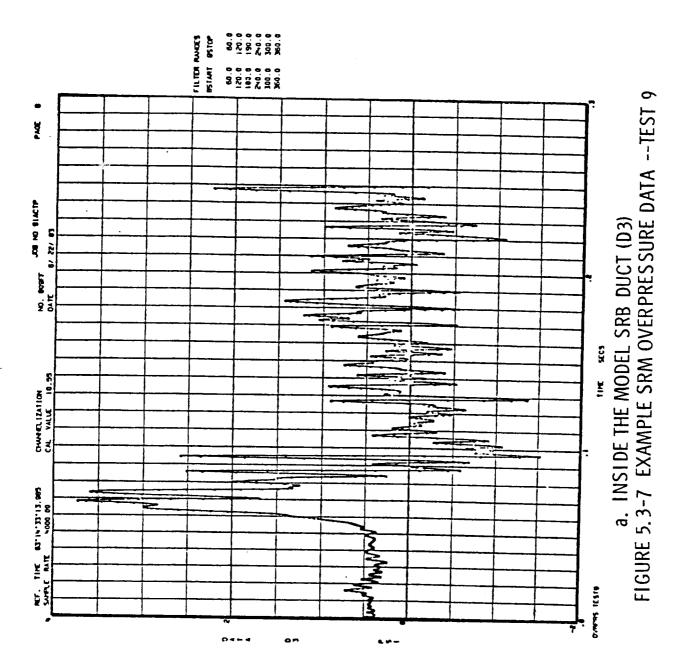


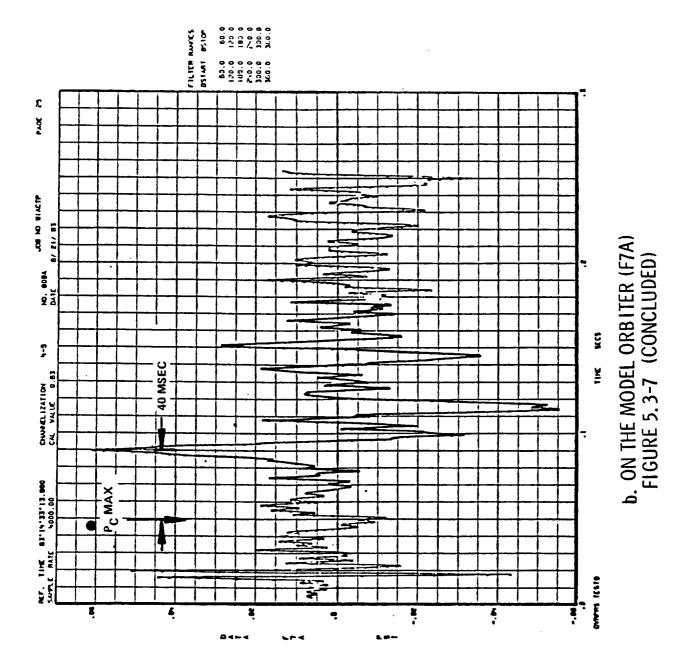


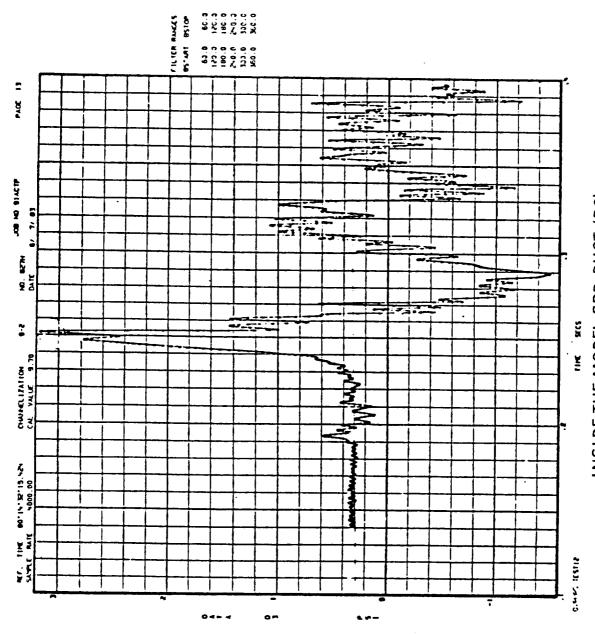


5-55

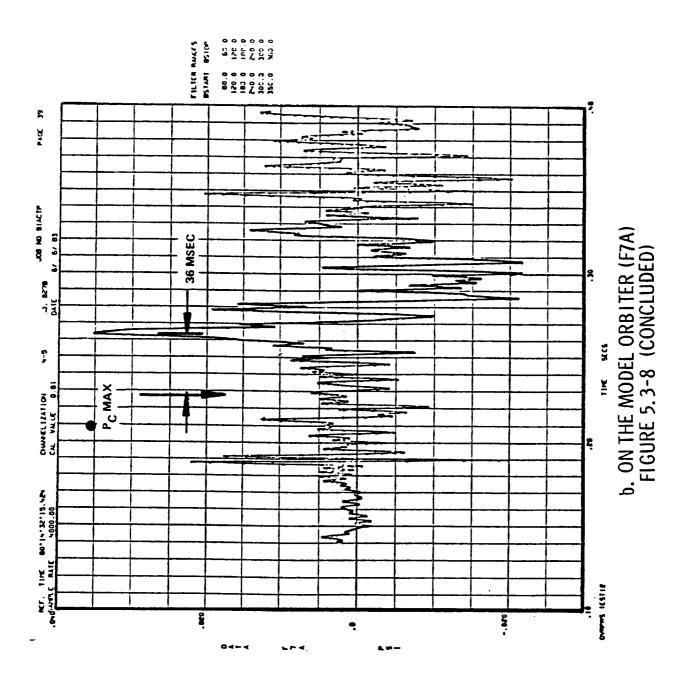


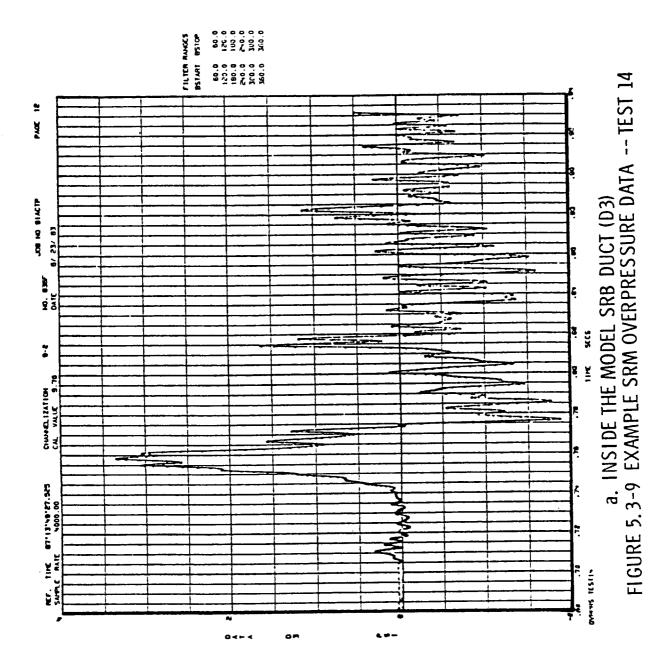


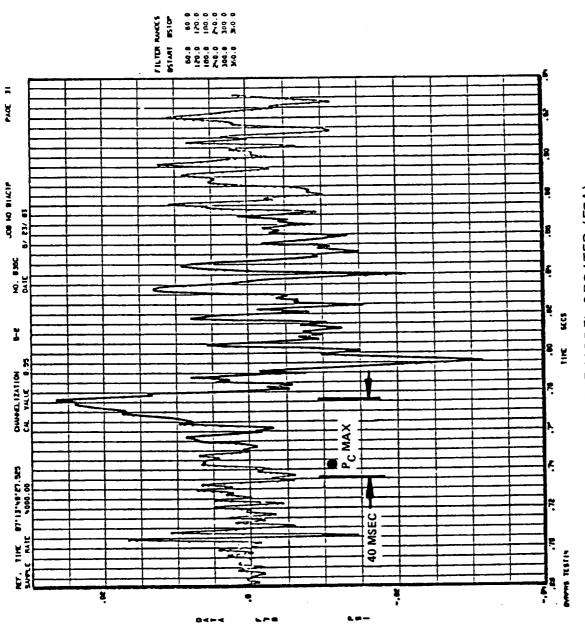




a. INSIDE THE MODEL SRB DUCT (D3) FIGURE 5.3-8 EXAMPLE SRM OVERPRESSURE DATA -- TEST 12







b. ON THE MODEL ORBITER (F7A)FIGURE 5.3-9 (CONCLUDED)

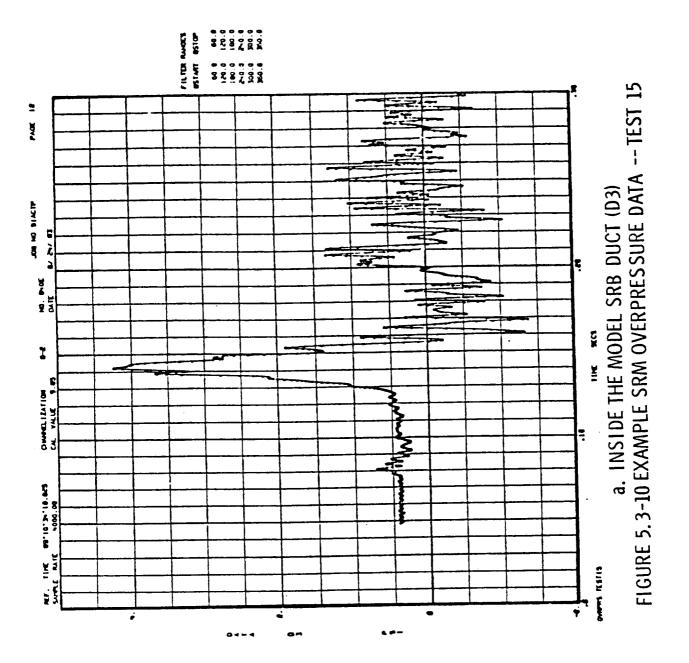
the Test 15 data in Figure 5.3-10. The wave propagation time to measurement F7A was again 40 msec in Test 14, 39 msec in Test 15. The frequencies were again about the same, 32 Hz and 64 Hz in Test 14, 66 Hz is evident in Test 15.

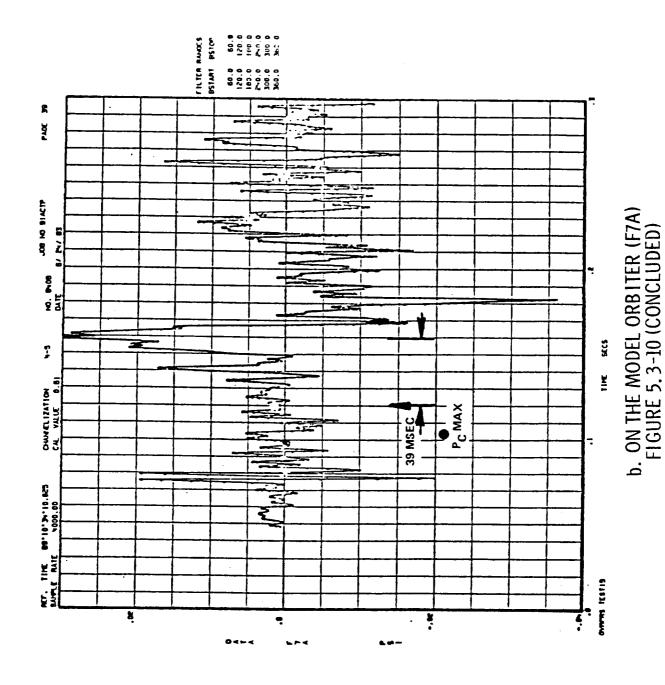
The last example to show is from the dual - SRM test (Test 40). Measurement F8 is the closest location to the F7A example used for all the single - SRM tests. Measurements at the same corresponding locations inside the LH and RH SRB ducts are shown. These data are shown in Figure 5.3-11. The amplitude of the DOP was largest of all in this dual - motor test. As seen in Table 5.3-3, the amplitudes were larger on the port sides of the model vehicle elements than on the starboard sides. The waveform of the mixed overpressure from the two ducts was about the same as in the single - motor tests; even though the non-simultaneity in model SRM ignition was out-of-specification.

These examples of waveform and timing from each SRM overpressure test show good test-to-test consistency in repeatability of the SRM overpressure phenomena as to frequency composition and propagation characteristics, even in the two instances of long model SRM ignition delay.

5.3.2 Model SSME Examples

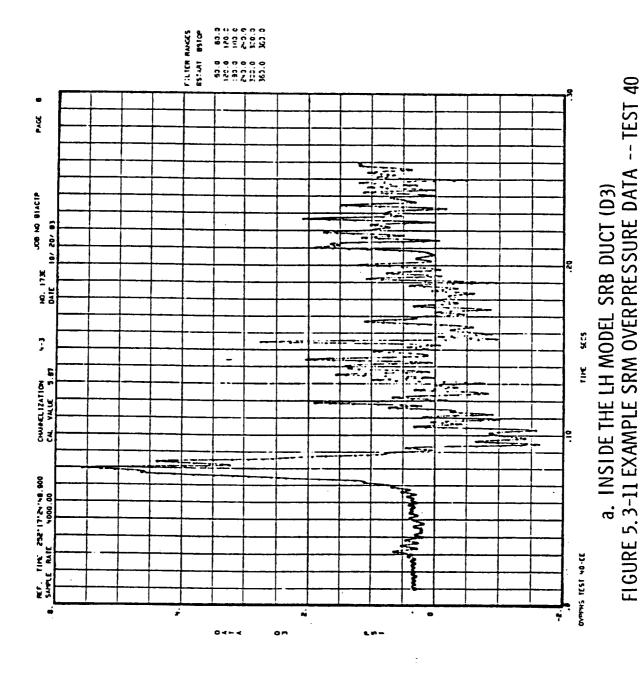
The dry start in Test 40 gave different SSME overpressure results than the three tests with the water. The three tests with the SSME water "On" are the ones to be used for the baseline environment analysis. The dry test data showed low-frequency pulses excited within the SSME duct to be propagated upward over the model vehicle. The pressures measured inside the duct and at two locations on the model Orbiter are shown in Figure 5.3-12, as examples of the dry test results. The duration of the pulses was longer than the data record length selected for these data plots; they miss the first ignition spike slightly on the model Orbiter examples. Analysis of the oscillogram data from the dry test showed almost negligible ignition spike amplitudes, and what is shown in Figure 5.3-12 is the only data of significant amplitude.

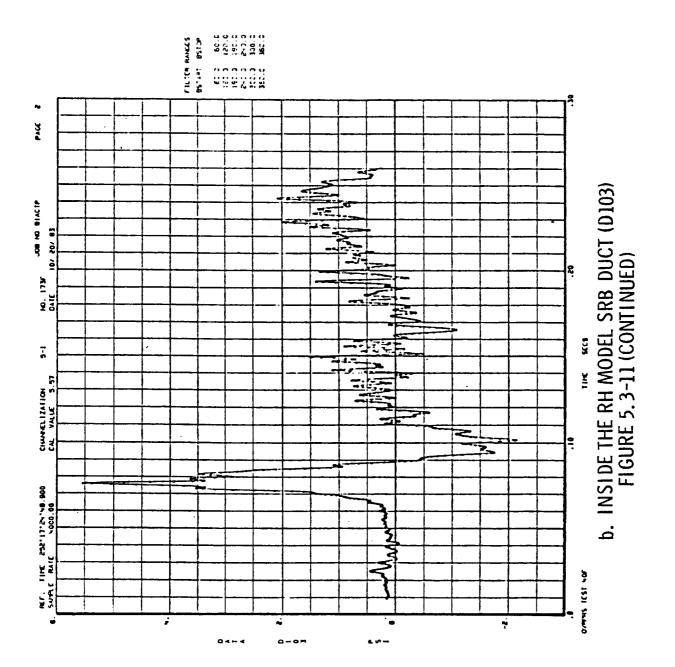


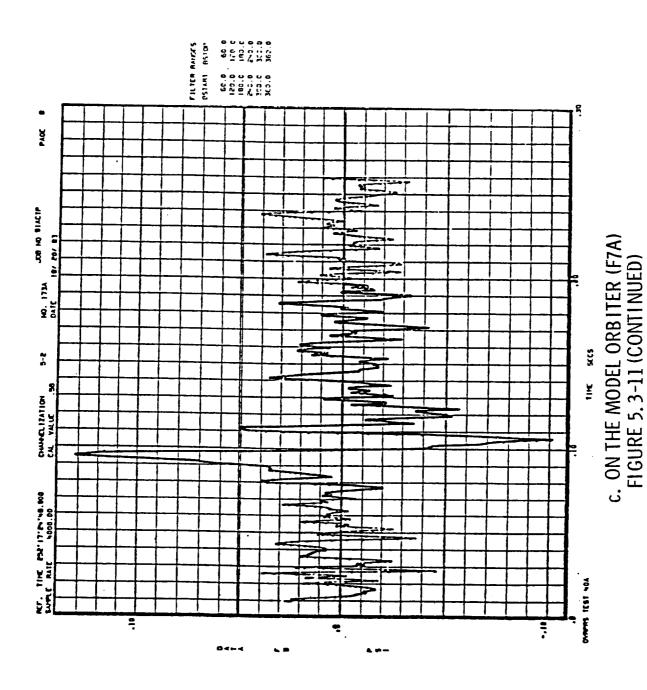


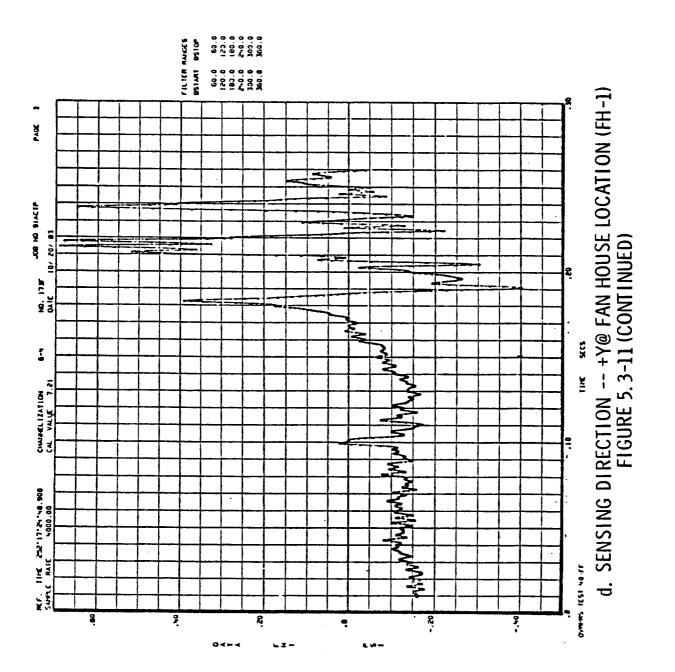
5-64 A

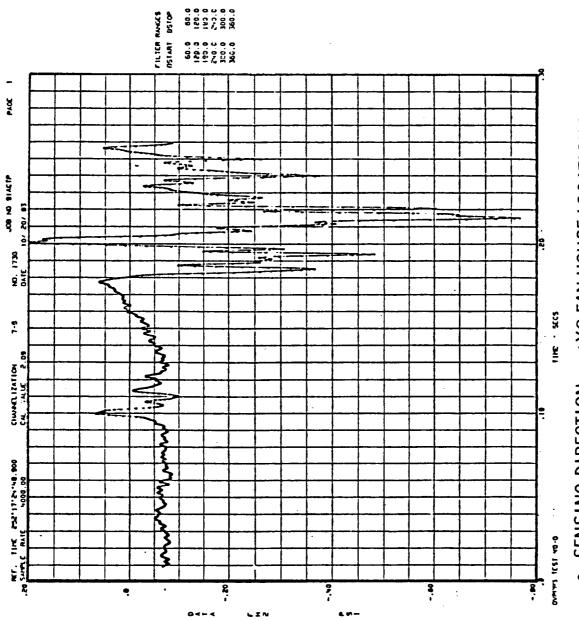
		<u>.</u>
		,



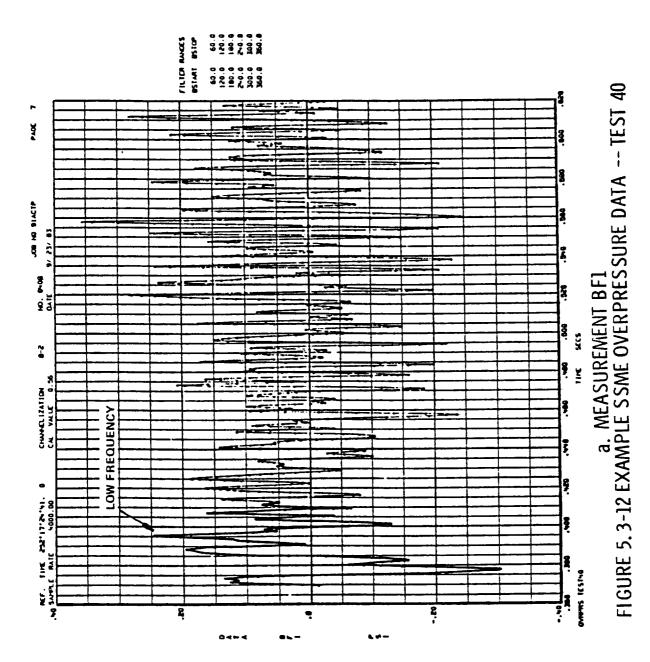




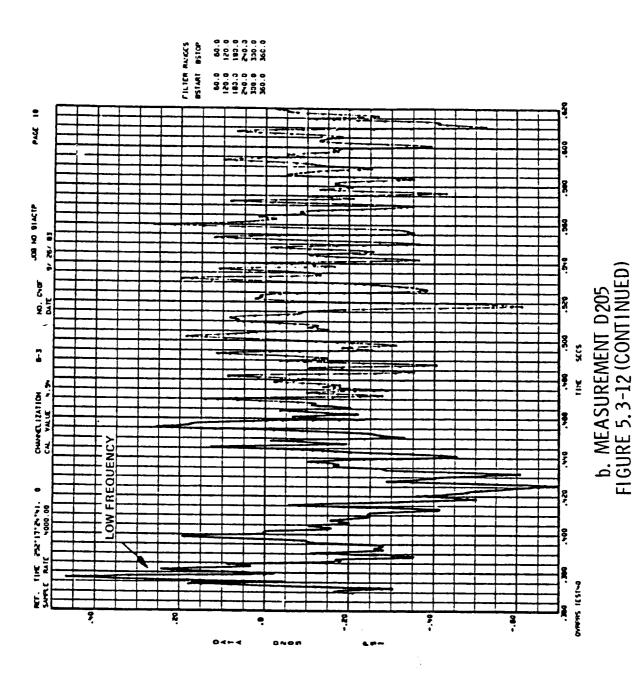




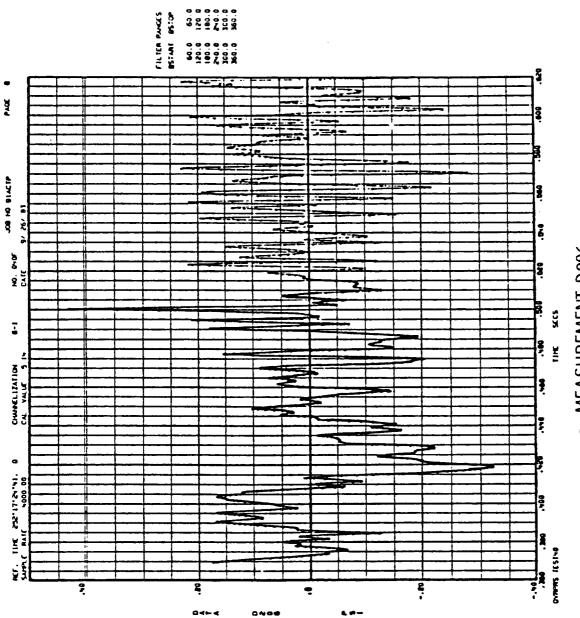
e. SENSING DIRECTION -- +X@ FAN HOUSE LOCATION (FH-2) FIGURE 5.3-11 (CONCLUDED)



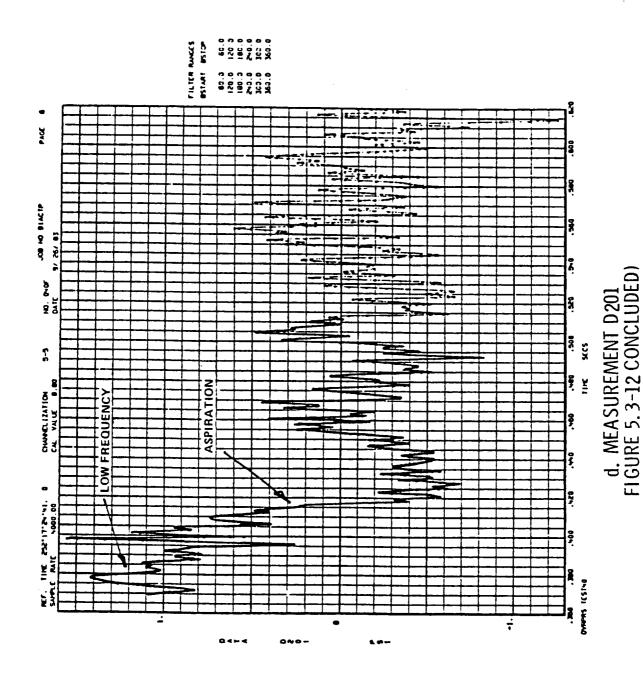
5-70



5-71



c. MEASUREMENT D206 FIGURE 5.3-12 (CONTINUED)



5-73

With the SSME water sprays "On", the only amplitudes of significance were associated with the first ignition spikes. Each model engine produces a distinct ignition spike as it ignites. The pressures measured within the SSME duct and at three selected locations on the model Orbiter are shown from Test 30 as the example of baseline SSME overpressure data in Figure 5.3-13. These data have relatively large amplitude (0.3 psi on the model Orbiter aft heat shield) but are comprised of relatively high frequencies. These waves propagated upward across the model vehicle and the full set of delta pressures and pitch- and lateral- delta delta pressures are presented in the final data packages from each SSME test that are appendaged to this report.

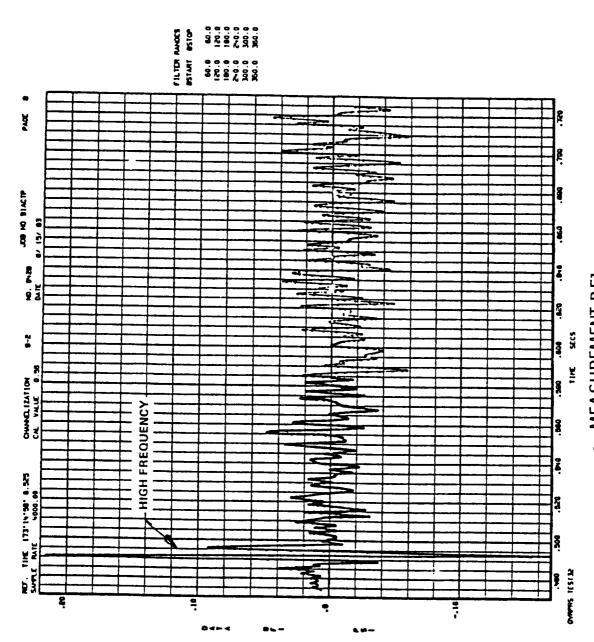
There was no indication of overpressure discharged from the SSME duct exit reaching the model SSV like the SRM duct overpressure.

The SSME ignition overpressure spikes measured for the baseline case with water sprays are larger in amplitude, although at higher frequencies, that the SRM overpressure. Their timing is associated with first ignition of the propellant mixture in each model SSME.

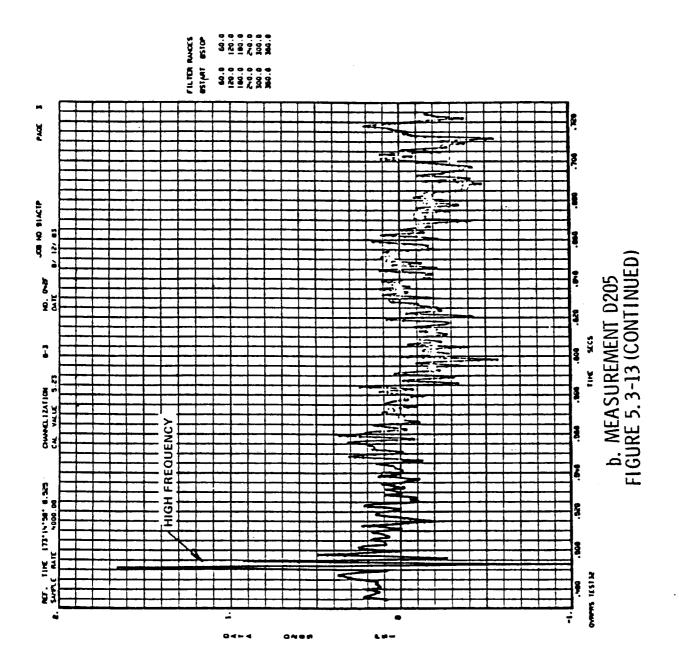
5.4 Model Muffler Internal Pressures

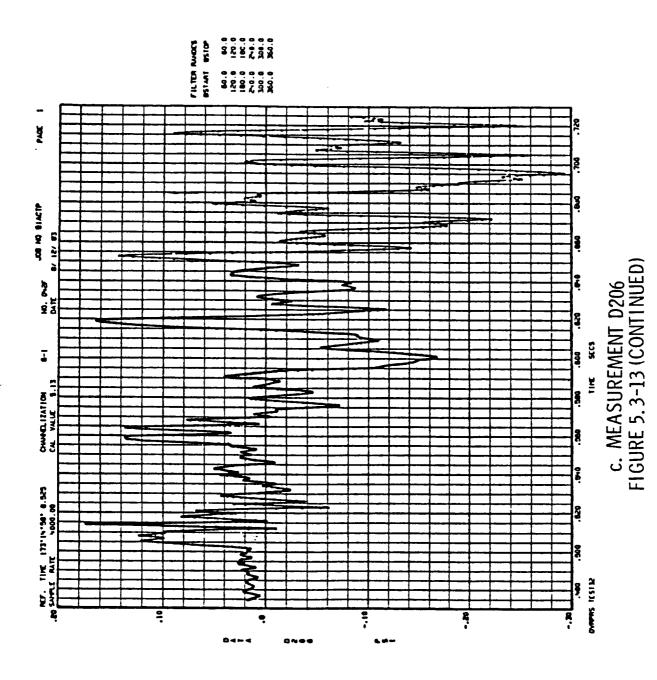
Internal overpressure measurements were made on the model muffler walls and at its entrance to obtain design loads data for the muffler implementation in full scale. These measurements were made in Tests 8 and 9.

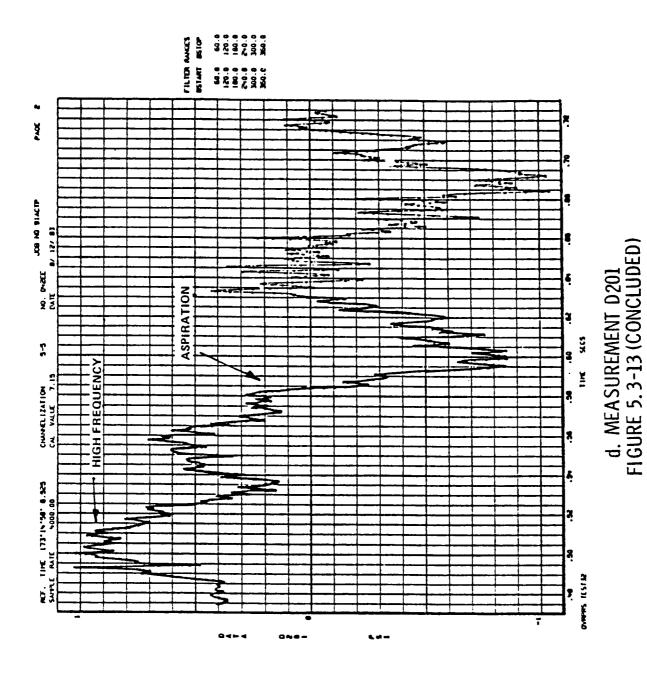
Example data from test 8 are shown in Figure 5.4-1, and from Test 9 are shown in Figure 5.4-2. As seen in Figures 5.4-1 and 5.4-2 these data were quite repeatable between the two tests. A summary of the peak positive overpressure amplitudes inside the muffler is given in Table 5.4-1.



a. MEASUREMENT BF1 FIGURE 5.3-13 EXAMPLE SSME OVERPRESSURE DATA -- TEST 32







5-78

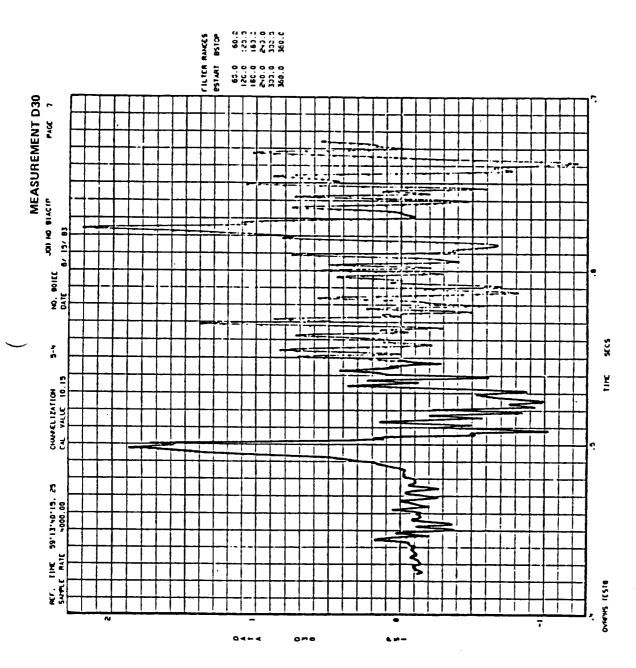


FIGURE 5.4-1 EXAMPLE MUFFLER INTERNAL PRESSURE DATA -- TEST 8

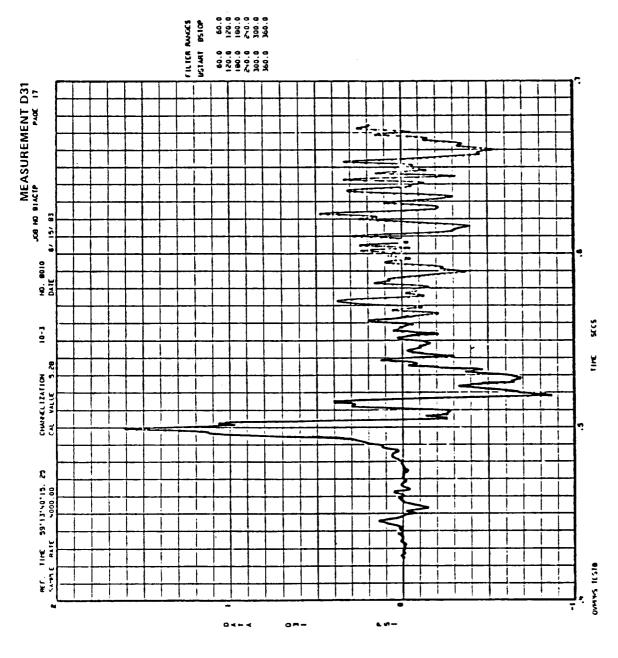
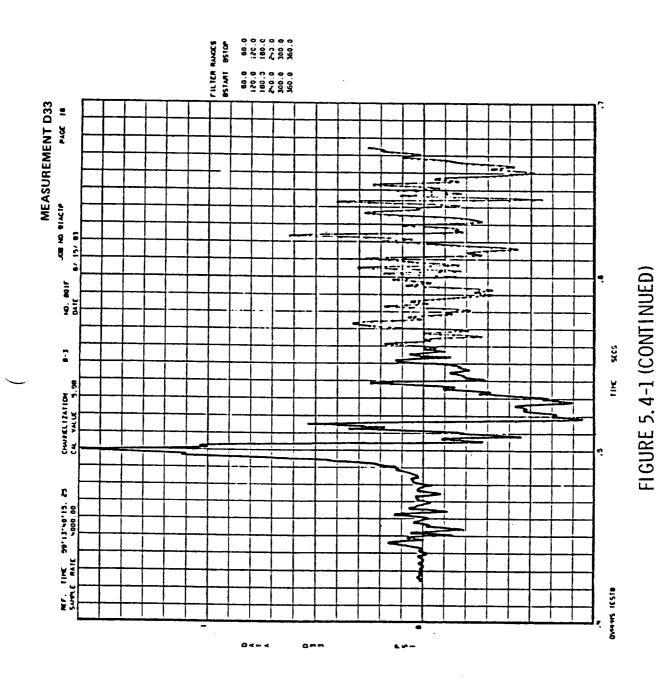
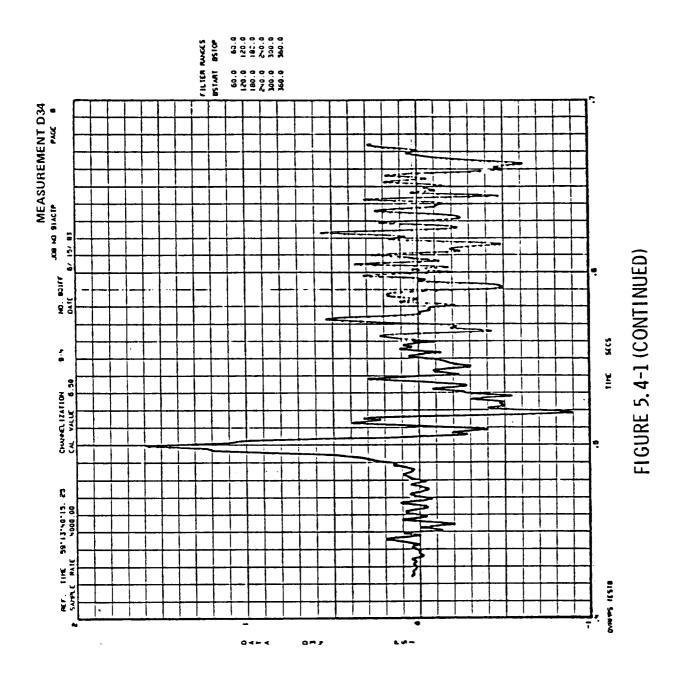


FIGURE 5.4-1 (CONTINUED)



5-81



5-82

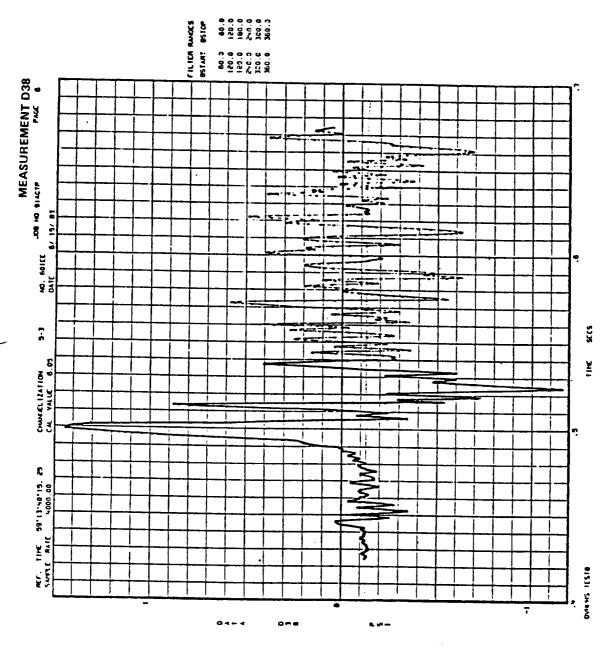
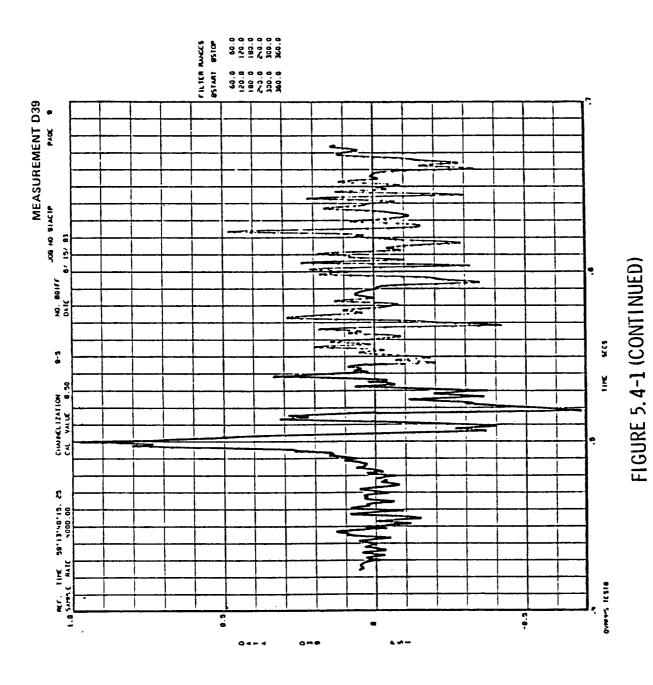


FIGURE 5.4-1 (CONTINUED)



5-84

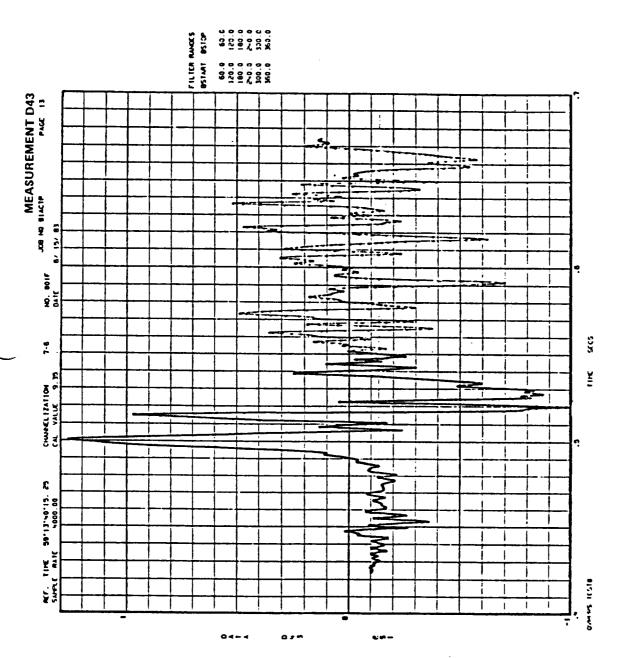


FIGURE 5.4-1 (CONCLUDED)

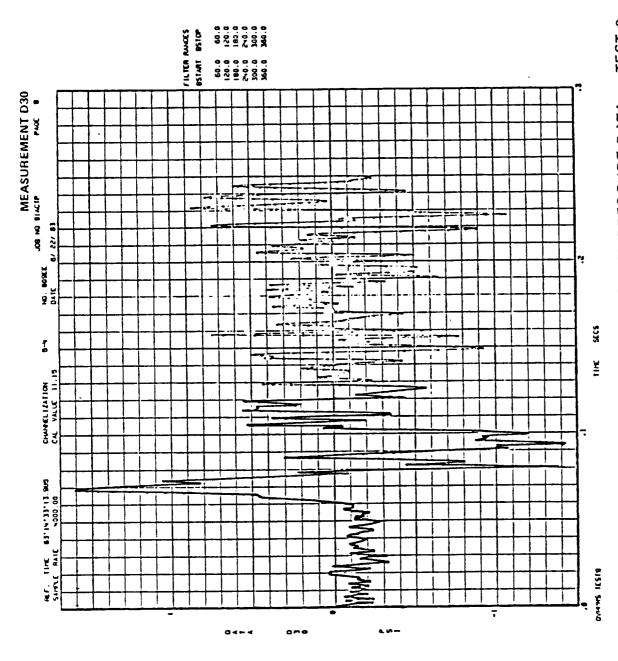


FIGURE 5.4-2 EXAMPLE MUFFLER INTERNAL PRESSURE DATA -- TEST 9

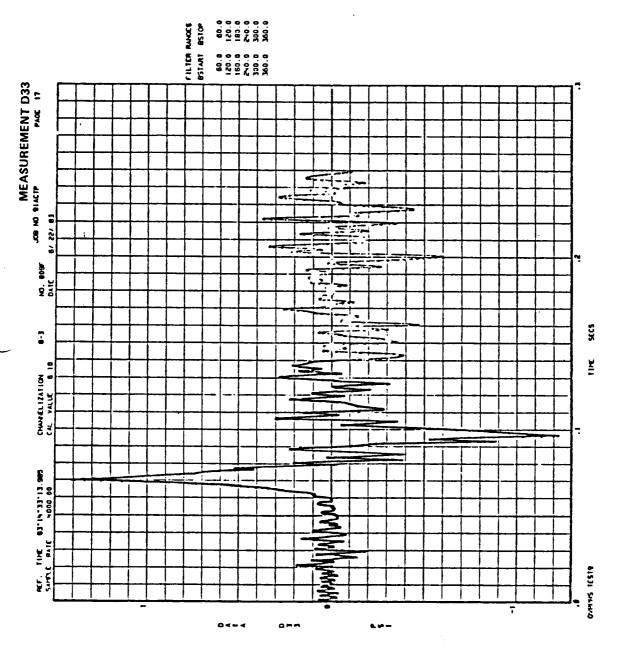
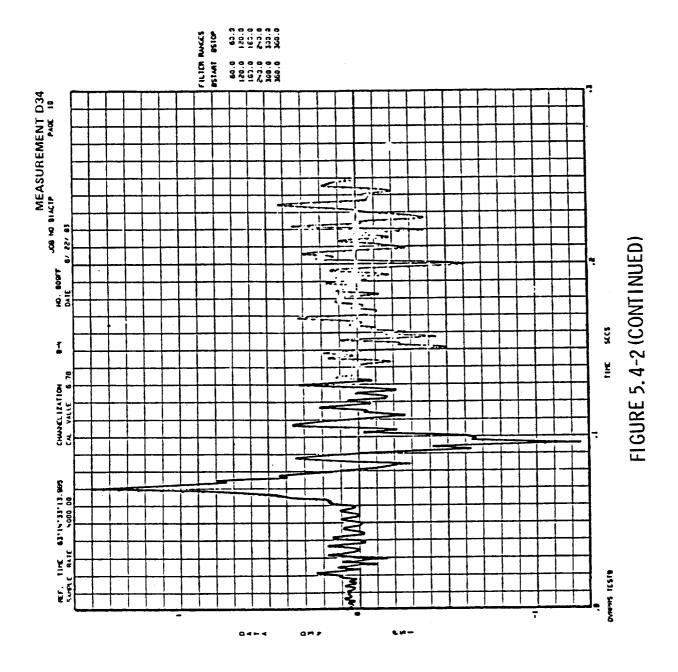
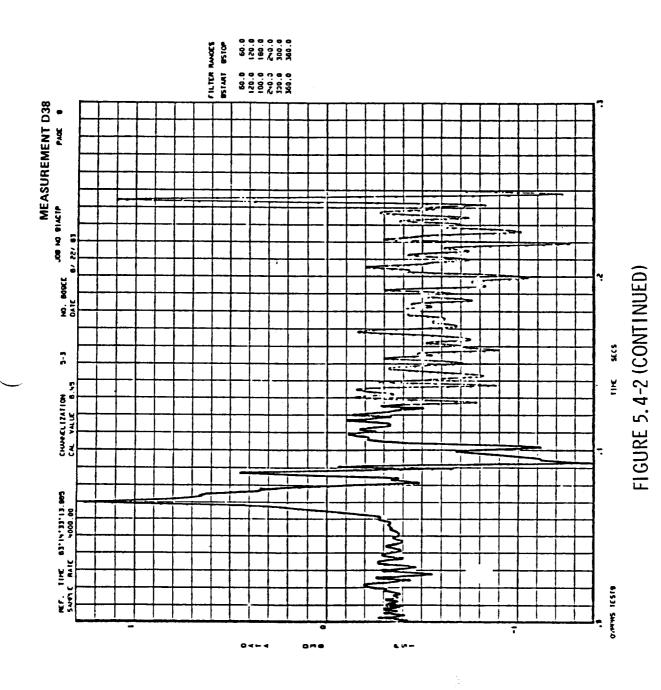
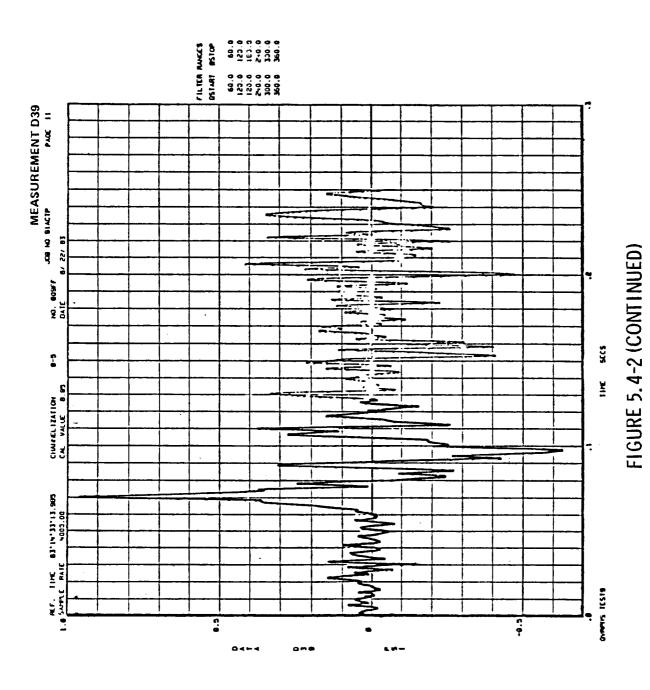


FIGURE 5.4-2 (CONTINUED)







5-90

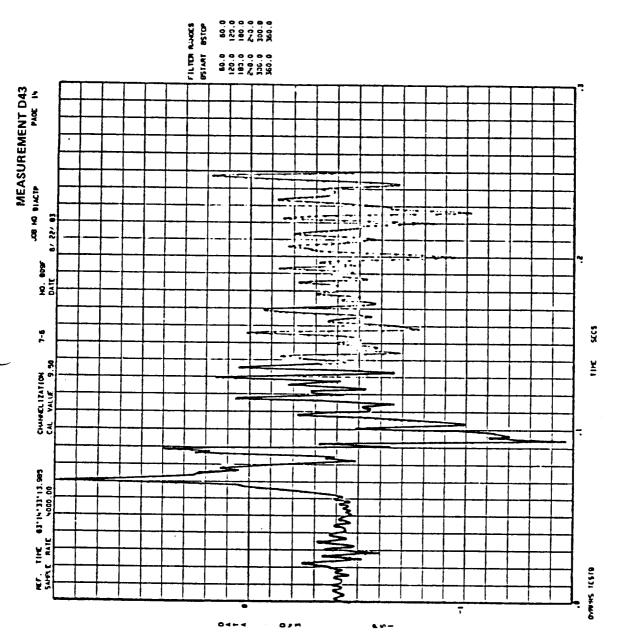


FIGURE 5.4-2 (CONCLUDED)

TABLE 5.4-1 OVERPRESSURE DATA ON THE MODEL MUFFLER INTERIOR WALLS

SENSOR		VE DELTA p, psi
NUMBER	TEST 8	TEST 9
D29	INVALID	1.90
D30	1.79	1.75
D31	1.61	INVALID
D33	1.59	1.40
D34	1.56	1.45
D35	1.78*	1.45
D36	1.47	1.40
D37	1.61	INVALID
D38	1.57	1.60
D39	0.98	0.92
D40	0.90	0.90
D42	1.18	1.18
D43	1.40	1.40

^{*}NOTE - DATA AS PUBLISHED HAD A FACTOR OF 2 SCALE ERROR DUE TO IMPROPER RECORD AMPLIFIER GAIN SETTING (CRT DATA INVALID)

				· .
•				
ı				
I				

THIS PAGE WAS INTENTIONALLY LEFT BLANK

		·

6.0 SUMMARY OF RESULTS

		-

6.0 SUMMARY OF RESULTS

Sixteen single-motor SRM ignition overpressure tests were performed using the 6.4-percent scale model SSV and WTR launch mount/exhaust duct system with scaled sound suppression water flows. The model launch facility simulated that geometry of the SLC-6 facility actually being constructed. A Z-axis splitter plate (dividing the model into left and right halves) provided simulation of simultaneous LH-RH SRM ignition and was used to obtain pitch-axis overpressure environment forcing function data on the SSV. The splitter plate was removed for some single-motor tests, and special data manipulations with left-right time skews were used to define lateral forcing functions over a range of possible LH-RH SRM non-simultaneity in ignition.

Four early screening tests provided data on sound suppression water effectiveness and the effectiveness of water troughs in suppressing the SRM overpressure. There was one later test without sound suppression water (completely dry) and no troughs. The significant finding from the early screening was a duct overpressure wave discharged from the end of each SRB duct and returning to the SSV with sufficient strength to pose a potential problem for the payloads to be launched from WTR. An off-line test program to select a suitable duct overpressure suppression device resulted in a 45-ft long (full-scale) duct extension muffler, and its effectiveness was evaluated in four verification tests after the off-line development work. Seven single-SRM verification tests performed without the muffler but with water troughs and 100-percent design launch mount sound suppression water provided SRM overpressure environmental verification data for the first launch from Vandenberg AFB. The mufflers remain a contingency if the first launch data show they are needed. SSME overpressure verification data were also acquired in three model SSME tests, but the model SSME ignition transients did not provide good simulation of the full-scale. A full-model test with model SSME's operating provided a dual-SRM overpressure verification with water troughs and 100-percent launch mount water with all the facility geometric detail practical that could be applied to the model. The LH-RH SRM ignition simultaneity, was out-of-specification in the fullmodel test, but the duct overpressure waveform was generally similar to that in single-SRM tests. The model SSME's were started with the SSME exhaust duct dry in the full-model test.

The dry SRM overpressure test produced a large ignition overpressure discharged upward from the top of the SRB exhaust ducts. This ignition overpressure was effectively suppressed by sound suppression water and water trough combination as the waves generated inside the SRB ducts were directed mainly out the duct exits. The duct extension muffler provided the anticipated reduction in the duct overpressure amplitude without appreciable shift in frequency content (no deleterious frequency components added).

All of the data are presented herein in the form of microfiche appendaged to this report.

REFERENCES

- 1. Dougherty, N. S. 6.4-Percent Scale Model SSV SRM Ignition Overpressure Testing for STS-2, Volume I: Model Tests at MSFC; Lai, S. Volume II: Results of Analysis. Space Systems Group, Rockwell International Corporation, STS 81-0665 (January 1982).
- 2. Dougherty, N. S. and D. A. Pinkleton. 6.4-Percent Scale Model SSV SRM Ignition Overpressure Screening Tests for Western Test Range. Shuttle Integration and Satellite Systems Division, Rockwell International Corporation, STS 82-0648 (January 1983).
- 3. Dougherty, N. S. Test Requirements for the 6.4-Percent Scale Thrust Augmented SSLV Acoustic/Overpressure Tests at MSFC. Space Systems Group, Rockwell International Corporation, STS 81-0322 (March 1981).
- 4. Dougherty, N. S. Requirements for 6.4-Percent Scale Model SSV SRM Ignition Overpressure Verification Tests for Western Test Range.

 Space Operations/Integration and Satellite Systems Division, Rockwell International Corporation, STS 82-0808 (December 1982).
- 5. Dougherty, N. S. 6.4-Percent Scale Model SSV Liftoff Acoustic Verification Test Requirements for WTR. Shuttle Integration and Satellite Systems Division, Rockwell International Corporation, STS 81-0322, Addendum C (April 1983).
- 6. Dougherty, N. S. 6.4-Percent Scale Model SSV Liftoff Acoustic Verification Testing for Western Test Range: Test Program at MSFC. Shuttle Integration and Satellite Systems Division, Rockwell International Corporation, STS 84-0014 (March 1984).
- 7. Trudell, R. W., R. F. Davis, K. Ando, and H. Tang. <u>DoD STS Final</u>
 Report for VAFB Launch Mount and Flame Ducts 6.4-Percent Model Test
 Program and Analyses. McDonnell Douglas Astronautics Company-East,
 Report MDC 31624 (December 1976).
- 8. Eastern Test Range Ignition Overpressure Operational Design Data.
 Shuttle Integration and Satellite Systems Division, Rockwell
 International Corporation, STS 83-0540 (October 1983).

THIS PAGE WAS INTENTIONALLY LEFT BLANK

APPENDIX A

"OFF-LINE" DEVELOPMENT OF THE CONTINGENCY MUFFLER

1			

APPENDIX A

"Off-line" Development Of The Contingency Muffler

Initial studies of how the duct overpressure (DOP) might be suppressed focused on control of the pressure amplitude upon discharge from each SRB duct exit. The distance of each duct exit plane from the ET centerline is 223 ft full scale. Protective barriers outside the duct upstream of the duct exit plane that might block the waves after their discharge to the open air were ruled out as likely too massive, too costly, and still possibly not effective.

Three concepts for DOP attenuation were advanced to the engineering feasibility/economic study stage. All three, in principle, would provide DOP attenuation at the SRB duct discharge locations. Two of them were considered as permanent additions to be installed and utilized in each Vandenberg launch. The third was proposed as a lower cost alternate to the capital cost of a permanent DOP suppression system. These concepts were:

- 1. A passive muffler device -- either within or an extension to the present SRB ducts -- integral to the facility.
- 2. A "waterfall" deluge over the end of each SRB duct -- with a quickrelease vertical drop of a sheet of water at least 8 inches thick from a water reservoir to be added at the end of each duct.
- 3. A thin membrane cover to be erected over the exit plane of each SRB duct that would be blown off at SRB ignition during each launch.

The second concept -- the "waterfall" deluge -- was not actually brought to the development test stage. Technical problems with creating a water sheet at the proper time in a launch countdown that required servicing and consummables for a new operating system seemed difficult when compared to a low maintenance, passive device like a muffler. A suitable muffler device -- the first concept -- was therefore sought with the third concept -- the membrane cover -- as a backup. A cost and availability study for the membrane structure and material ensued while development tests were being performed; this would be cost/flight versus the permanent muffler capital

costs and maintenance. The development tests were performed "off-line" at MSFC in accordance with Reference A-1 using a section of the LH SRB duct of the 6.4 - percent scale model, Figure A-1, with suitable overpressure instrumentation the same as in the sub-scale "hot-firing" tests and with high-speed color motion photography at 400 frames/sec. The attenuation goal for the these tests was 40 percent at the model SSV location.

This section of the model exhaust duct represented about one-half of the overall duct length and was easily removed from the rest of the model facility at a flanged joint. A wave approximating the DOP generated by the scale-model SRM (Tomahawk motor) could be generated inside the model duct section with the "popper" device, used in the early screening of ignition overpressure, IOP, suppression concepts for ETR, Reference A-2. The "popper" nozzle was centered in the model duct as shown in Figure A-2. The wave was generated using 100 grains of mild detonating fuse initiated by electrical current application to a dynamite cap initiator, Figure A-3.

The "popper" device is a Helmholtz resonator by design tuned to 67 Hz and integer-multiple harmonics thereof. The "popper" produced a strong wave, although highly directional, with a steep-fronted first rise and predominantly 67 Hz and 134 Hz frequency content as seen in open-air calibration data in Figure A-4. The duct section amplified the "popper" wave to amplitudes close to those that occurred with the Tomahawk motor. The duct section clearly resonated with frequencies that were odd-integer harmonics of approximately 30 Hz in the quarter-wave organ pipe mode (closed boundary condition at the "popper" end, open boundary condition at the duct exit end). The frequencies (f_n) predominant in the data were given by $f_n = \frac{na}{2 \text{ Leff}}$ where a is the speed of sound in ambient air and Leff was the

duct section length plus a small end correction. The leading edge of the wave propagated faster than the sound speed in ambient air. An exponentially - decaying standing wave continued for several cycles before it vanished with wave speed the speed of sound, a, in ambient air.

There were twelve overpressure measurements in the "off-line" test series -- four within the duct section to characterize the wave discharged, five

on a pole that was erected at the position where the model ET centerline would be in model scale, and three in the duct apron area. These measurement locations for the "off-line" tests are shown in Figure A-5 and Table A-1. All measurements outside the duct showed the same basic waveform as those measured within the duct for "baseline" tests (basic duct section without any candidate suppression device added). Typical data from measurements within the duct section, the end of the apron area, and at the simulated vehicle location are shown in Figure A-6. These data are from off-line Test 2 -- baseline configuration (no suppressive device installed.)

Two membrane cover configurations were tested -- one with the scaled equivalent areal density of 0.5 lbm/ft², the other with scaled areal density 0.25 lbm/ft². Both membranes in the model tests were made of aluminum sheet. The heavier membrane was 0.032-inch thick, the lighter membrane was 0.016-inch thick.

The membranes were mounted on aluminum hinges so that their motion under wave impact would be a rotation about the bottom hinge line followed by separation and deformation and/or fragmentation. The membranes were loosely fit to the duct exit plane around the vertical sides and top with nominally 1/8-inch gap. Membrane installation details are shown in Figure A-7. Both membranes blew off cleanly in test after rotational first movement as intended. The lighter membrane ripped away from its hinge. Posttest photos of each membrane are shown in Figure A-8. There was better attenuation with the higher membrane density; the data are shown in Figure A-9. However, the data showed a strong reflected wave returning within the duct back toward the "popper" and the membrane concept was abandoned, although it showed an attenuation at the model SSV location, because unwanted reflected waves could potentially impact the SSV with this concept.

Seven candidate muffler configurations were built and tested from 1/4-inch plywood. The high-speed motion picture data showed that they needed rigid bracing to prevent deformation under the overpressure wave loading. From these, the one actually built and tested in the "hot-firing" verification

test program was selected. It's performance in the "off-line" tests was close to but slightly below the 40-percent attenuation goal. The basis of selection was strongly predicated on a structural configuration that could be constructed economically at SLC-6 and on required muffler length. The muffler concepts selected for "off-line" test were all the duct-extension type. A solid duct extension was also tested to show the degree of attenuation by virtue of duct length increase alone versus that achieved with muffler action.

One muffler configuration (Configuration 1) had tapered slots of 45-ft equivalent full-scale length on both the vertical and top walls, Figure A-10. This muffler configuration was tested without bracing and exhibited large forced motion at the 30 Hz duct section fundamental organ-pipe frequency. It's performance in these tests was well below the goal at only 31 percent attenuation. This configuration had a horizontal roof (with "fingers" that extended into the water/exhaust plume region that would be issued from the duct in a firing of the model SRB). No attempt was made at optimizing the basic idea represented in Configuration 1; it was abandoned in favor of a more rigid framed, slotted-side wall type of muffler configuration.

There were six variations on the rigid-frame, slotted wall muffler configuration actually built and tested out of plywood. All had closed (solid) roofs. Two of these had a 30-ft full-scale equivalent length and are shown in Figures A-11 and A-12. One (Configuration 5) had vertical slots and a horizontal roof, a less costly configuration to construct for the 30-ft length from the standpoint of column supports for the roof between vertically-oriented slots. Its performance was only 18 percent attenuation, well short of the goal. The other (Configuration 4) had slots oriented with the exhaust flow at 15-deg with the horizontal. It's performance was only 16.5 percent attenuation, again short of the goal.

Four configurations of 45-ft equivalent full-scale length with 15-deg inclined solid roofs were built and tested. The test variable was the percent of porous open area afforded by the slots in the side walls and the distribution of the porosity over the muffler length. (The percent of

porous open area is defined herein as the total slot open area on the two side walls divided by the duct discharge cross-section area times 100, percent.) The basic design rule for the slots was to preserve approximately the same slot aspect ratio, i.e. slot length/width ratio, within the constraints of wall stiffening and proper support of the roof required of a full-scale design. The configurations of this basic concept for a muffler are identified as Configuration 2, 3, 6, and 7. Configuration 6 was actually a variation on Configuration 3 to place a column for roof support at the muffler center span. These four configurations represented conceptual designs to have 15-deg inclined slotted side walls and provisions for two, three, or four columns between slots, respectively. The configurations tested are shown in Figures A-13, A-14, A-15, and A-16.

Configuration 3 was not tested braced. It deformed in test under the overpressure loading. Configuration 6, with the center-span support columns was considered more structurally feasible and was selected for fully-braced test. The final selection came down to Configurations 2, 6, and 7. All were projected to have about the same costs for design and construction. A full-scale artists' conceptual rendering is shown in Figure A-17 of Configuration 6 in a reinforced concrete version. Either Configuration 6 or 7 could be built out of steel or concrete. Configuration 7 is depicted in a rendition of steel in Figure 3.6-1a. The case of 45 ft length and zero porosity was tested for the reference case by closing the side-wall slots of one muffler configuration with plywood as shown in Figure A-18.

Results of all the "off-line" tests are shown on the same comparative basis in Table A-2. The "knockdown" factors (degree of attenuation) were derived from a ratio of the average of the five measurements P8 through P12 at the simulated vehicle location with the respective candidate suppression device to the baseline average of the five measurements without.

Adjustments were applied to account for the test-to-test variation in "popper" wave strength and the coupled responses of the duct. They were done in two ways:

- 1. Using the amplitude of the duct internal measurement P2.
- 2. Using the average of the duct internal measurements P2 and P3. Computations were performed as follows:
 - The uncorrected "knock-down" factor is defined as

$$(KDF)_{m_{uncorr}} = \begin{bmatrix} i = 12 \\ \Sigma & p_i \\ i = 8 \end{bmatrix}_{m} / \begin{bmatrix} i = 12 \\ \Sigma & p_i \\ i = 8 \end{bmatrix}_{baseline avg}$$

where the subscript m indicates the individual test number and the subscript n the particular measurement number.

- The normalization (correction) factors N_1 and N_2 were calculated as $N_{1,m} = (p_2)$ baseline avg

and (p₂)_m

 $N_{2,m} = \frac{(p_2 + p_3)_{baseline avg}}{(p_2 + p_3)_m}$

The adjusted (normalized) "knock-down" factors were thus given by $(KDF)_{1,m_{ad,i}} = (N_{1,m}) (KDF)_{m_{uncorr}}$.

and

$$(KDF)_{2,madj} = (N_{2,m}) (KDF)_{muncorr}$$

Separate use of p_2 and the average of p_2 and p_3 in combination for normalization of knock-down factors provided increased confidence in the normalization upon comparison of $KDF_{1,m_{adj}}$ with $KDF_{2,m_{adj}}$.

The adjusted "knock-down" factors were converted to a percentage reduction in amplitude with the respective device. These percentage reductions were of the average peak positive overpressure amplitude measured at the simulated vehicle location.

Typical overpressure data (amplitude versus time) are shown for Configurations 2, 6, and 7 in Figures A-19, A-20, and A-21. They all have a similar waveform giving roughly 0.048 psi average peak positive amplitude at the simulated vehicle location. There was essentially the same half-period width (time from the leading edge of the first positive pulse to the zero crossing where the pressure begins its first negative, i.e. rarefaction excursion) with Muffler Configurations 6 and 7, but the half-period changed

about 19 percent with Muffler Configuration 2. This waveform change with Muffler Configuration 2 (seen in the average half-period time for all five measurements at the simulated vehicle location) made it less acceptable than other Configuration 6 or 7. A comparison of averaged amplitude attenuation results and half-period times for each of these three mufflers is There was no appreciable change in the shape of the given in Table A-3. overpressure waves (nor downshifting of frequencies to a lower range, no introduction of appreciable energy at higher frequencies). ferences of note -- other than the amplitude reduction -- was that the with each of these double-headed peak become positive Configurations.

Supplemental data are shown in Table A-4 documenting ambient temperature during each test with a calculation of the fundamental frequency of organpipe response for the baseline and each muffler configuration tested. straight duct extension case is shown also in the Table A-4. duct extension represented the extreme limit for a 45-ft long device added to the basic duct with a downshift in the fundamental frequency from 31 Hz to 22.7 Hz and, indeed, spectral analysis of the overpressure data acquired showed such frequency shift to have occurred in the test confirming organpipe resonant mode response of the duct and in the duct plus a straight extension to be present (see Test 18 frequency data). The odd-integer multiple harmonics were predominant as the open-closed boundary conditions The tuned "popper" frequencies lay close to what would be should dictate. the second and fourth harmonics of the baseline duct length and would have the duct without resonant amplification or continued passed through standing wave contribution.

Power spectral density (PSD) analyses were performed using a Hewlett-Packard 5451C wave analyzer on all the overpressure data over a 200-msec sampling time. They were performed also over reduced sampling times of 100 msec, 50 msec, and 20 msec, example data shown in Figure A-22. The reduced sampling - period examples were tried on Tests 3 and 6 which is the reason for showing Muffler Configuration 3 in the example. The penalty paid using 100 msec and 20-msec sampling time was in the effective frequency resolution of the discrete wave components being increased from 5 Hz

(1/0.200 sec) to 10 Hz (1/0.100 sec) for 100-msec and to 50 Hz (1/0.020 sec)sec) for 20-msec sampling, respectively. The 20-msec sampling (downshifted in Figure A-22b two decades) captures less than a full cycle of pressure and gives a power point only at every 50 Hz interval, inadequate to resolve the wave's frequency composition. High-pass and band-pass filtering was also applied in the time domain for further analysis of "popper" generated wave frequency content. The conclusions drawn from power spectral density analyses at the shorter sampling times were the same (no notable alteration in the spectra as the overpressure wave decayed over several fundamental frequency cycles), the spectra being comprised of harmonic duct modes and the two strongest "popper" frequencies -- 67 Hz and 134 Hz. The band-pass and high-pass filtering, isolating each of the various discrete frequency components one by one, showed continuation of the high frequencies over most of the 200-msec time. Spectral "knock-down" factors could thus be derived from 200-msec PSD's by comparing spectra with and without the respective suppression device installed.

It turns out that the "off-line" tests produced a baseline case over-pressure wave with about the same amplitude and frequency content as the "hot-firing" DOP wave with a harmonic family of discrete components making up both. The lowest fundamental frequency in the "hot-firing" data was approximately 32 Hz, fitting the entire duct length plus a nominal 6-percent end correction and the case of even mode number organ-pipe frequencies for a duct open at both ends. This lowest frequency in the "off-line" tests of nominally 31 Hz compares quite closely. The span of frequencies with the approximately half duct length in the "off-line" configuration was about the same as the span in the DOP from the actual "hot-firing" model test.

The "knock-down" factor, adjusted in the same manner as the peak positive composing "knock-down" factor using the measured internal duct overpressure was calculated at every 5 Hz bandwidth from the average power spectral density at the five simulated vehicle measurement locations. These "knock-down" factors as a function of frequency represent a sort of transfer function for each muffler configuration derived from the same measurements with and without that muffler. As seen in Table A-4, there were slight

increases in the effective duct length with the various mufflers, the reflection plane for establishing standing waves in the duct moving a different distance downstream with the particular distribution of porosity in "knock-down" factors for spectral muffler configuration. The Configurations 2, 6, and 7 are shown in Figure A-23. These data illustrate that all three mufflers operated effectively on the "popper" frequency components and duct modes 1 and 5 but not as well on the duct third and seventh harmonics near 89 Hz and 208 Hz which remained large. third harmonic downshifted in frequency with effective duct length increase by more than the 5 Hz discretizing interval of the ratio computations. 60 Hz family electrical noise evident in Figure A-23 did not compromise the Normalization of the frequencies by wave number would reduce the 89 Hz and 208 Hz spikes -- the plots are a function of the absolute frequency.

All factors considered, including the election of a four column structure for full-scale implementation, Configuration 7 was selected for "hotfiring" evaluation in the verification tests. Configurations 6 and 7 were both considered acceptable as to both attenuation and waveform. adjusted "knock-down" factors for the peak positive overpressure are shown for the various muffler configurations in Figure A-24 as a function of the porous open-area ratio. Both trend curves (P2 or P2 plus P3 adjusted) for 30-ft and 45-ft muffler configurations tend to indicate increasing "knockdown" with increasing porous open area up to the approximately 60 percent Normalization using N_2 would indicate the goal could be exceeded Normalization with N_1 would indicate the goal might with a 45-ft muffler. The lack of bracing in two just be reached at 60 porous open area. inbraced tests (of Configurations 2 and 3) appeared to reduce the muffling effectiveness while in other tests the inbraced results were nearly as good as the braced. The straight duct extension gave very little attenuation.

The 21-slot 45 ft duct-extension type muffler identified as Configuration 7 with the rectangular - prism slots would give about 35 percent DOP attenuation (average of the two tests -- normalization with N_1) on the 6.4 percent model, close to the goal. It turns out that the "hot-firing"

verification average of the two "popper" tests performed on Configuration 7.

Applying the same type of analysis from wave timing on the "popper" experimental setup shows an apparent wave source location for the baseline case very nearly the same as in the "hot-firing" tests with model SRM's, near the top and just beyond the duct exit plane, Figure A-25. Similar waveform peak amplitude, frequency composition, and wave propagation, timing between the "off-line" tests and the "hot-firing" tests lends credence to the results from the "off-line" testing approach. Non-repeatability in the "popper" source strength made normalization necessary and the results were slightly different regarding suppression effectiveness depending upon the method of normalization. Use of plywood construction for candidate muffler configuration screening permitted quick and cheap testing. Some of the non-repeatability in the "off-line" results is attributable to structural integrity of the plywood configurations. In general, the "off-line" program is viewed as having been successful in identifying a viable suppression device for the SRM duct overpressure.

REFERENCES

- A-1. Dougherty, N. S. 6.4 Percent Scale Model Test Requirements for "Off-Line" Investigation of WTR Overpressure "Fix" Concepts Using the "Popper" Source. Space Operations/Integration and Satellite Systems Division, Rockwell International Corporation, STS 81-0322 Addendum B, September 1982.
- A-2 Dougherty, N. S., and Mansfield, A. C. <u>Test Summary Report -- 6.4% -- Scale SRB Ignition Overpressure Screening of Suppression Concepts Using a Simulated "Popper" Source. Space Operations/Integration and Satellite Systems Division, Rockwell International Corporation, STS 81-0591, August 1981.</u>

ILLUSTRATIONS

Figure		Page
A-1	"Off-Line" Test Arrangement	A-17
A-2	"Popper" Installation Details	A-19
A-3	"Popper" Explosive Charge Details	A-20
A-4	"Popper" Calibration Data From Open-Air Testing	A-21
A-5	Overpressure Measurement Locations For "Off-Line" Tests	A-22
A-6	Typical "Popper" Overpressure Wave Data Inside The Duct Section	A-23
A-7	Candidate Duct Membrane Cover Installation Details	A-25
A-8	Post-Test Photographs of Membrane Covers	A-26
A-9	Duct Membrane Cover Test Overpressure Data	A-28
A-10	Candidate Muffler Configuration 1	A-30
A-11	Candidate Muffler Configuration 5	A-32
A-12	Candidate Muffler Configuration 4	A-34
A-13	Candidate Muffler Configuration 2	A-35
A-14	Candidate Muffler Configuration 3	A-37
A-15	Candidate Muffler Configuration 6	A-39
A-16	Candidate Muffler Configuration 7	A-40
A-17	Artist's Concept of a Full-Scale Configuration 6 Muffler in Concrete	A-42
A-18	Test Configuration of Solid-Wall Duct Extension (For Reference)	A-43
A-19	Overpressure Data Candidate Muffler Configuration 2	A-44
A-20	Overpressure Data Candidate Muffler Configuration 6	A-45

ILLUSTRATIONS (CONTINUED)

Figure		Page
A-21	Overpressure Data Candidate Muffler Configuration 7	A-46
A-22	Power Spectral Density Data Baseline and Muffler Configuration 3 Example	A-47
A-23	"Knock-Down" Factors as a Function of Frequency for the Candidate Muffler Configurations	A-48
A-24	"Knock-Down" Factors as a Function of Porosity for the Candidate Muffler Configurations	A-49
A-25	Apparent Wave Source Location Determined from Wave Arrival Timing at the Simulated Vehicle Location	A-50

TABLE A-1 "OFF-LINE" TEST INSTRUMENTATION LOCATIONS

SEMSOR	MODEL	HODEL SCALE, INCHES	NCHES	ORIENTATION	EXPECTED	33204	
NUMBER	X	>	7		KANGE, PSI	NOIES	
1	145.3	-72.9	-13.0	-Y (DOWNSTREAM)	12	ON "POPPER" - CONTROL (D)	<u> </u>
2	117.9	-109.0	0	7-	12	SAME AS 03	(8)
е	101.2	-171.3	0	7-	12	SAME AS D4 (1	(8)
*	110.9	-208.0	-13.0	Y (UPSTREAM)	m	BEYOND "MUFFLERS" (1	(0)
s	128.5	-198.3	26.4	7-	2	APRON WEST SIDE (<u> </u>
œ	128.5	-198.3	-52.4	Z	2	APRON EAST SIDE ((e)
7	81.8	-109.3	c	۲-	2	SAME AS DI	(a)
80	87.4	•	0)	9.0	SAME X AS BF1 ((0)
6	77.0	0	0	\ -	0.5	SAME X AS T17 ((0)
10	58.1	0	0	} -	0.5	SAME X AS F9 ((0)
11	33.1	0	0	λ- -	0.5	SAME X AS F5 (<u> </u>
12	-13.2	0	0	} -	0.5	SAME X AS T3 (<u> </u>

NOTES: 1. ALL SENSORS TO HAVE "DOUGH-NUT" (D) HEAT/LIGHT PROTECTION, EXCEPT AS WOTED.

2. ET COORDINATE SYSTEM USED (X = Y = Z = 0 ON ET CENTERLINE AT ORBITER MOSE ELEVATION MODEL SCALE).

3. SENSORS NOTED (B) HAVE EXISTING RIGHT ANGLE HEAT/LIGHT PROTECTION BLOCKS INSTALLED FROM PRIOR TESTS (PREVIOUSLY CALLED D3 AND D4).

TABLE A-2 PEAK POSITIVE COMPOSITE "KNOCK-DOWN" FACTORS

(0-T0-400Hz FILTERED DATA)

TEST CONFIGURATION	TEST NO.	AVERAGE PEAK POSITIVE AMPLITUDE (PSI) 1	KDF (UNCOR- RECTED) 2	N1 3	(KDF)1	N2 3	(KDF)2
BASELINE	1 2 3 10	0.057 0.069 0.068 0.059	DATA FR AVERAGE		NO. 1 NO	T USED	
2 (UNBRACED)	4 5 11	0.046 0.052 0.046	0.704 0.796 0.704	1.005 1.215 0.969	0.708 0.967 0.682	0.918 0.954 0.913	0.646 0.757 0.643
2	14	0.046	0.704	0.848	0.604	0.794	0.559
(STEEL BRACING)	15	0.038	0.582	1.163	0.684	0.987	0.574
3	6	0.054	0.827	1.180	0.975	1.084	0.896
	7	0.044	0.674	0.925	0.623	0.830	0.559
1	8	0.043	0.658	1.280	0.842	1.023	0.673
	9	0.047	0.720	1.197	0.861	0.987	0.710
STRAIGHT DUCT	13	0.074	1.133	0.866	0.981	0.786	0.889
EXTENSION	18	0.080	1.225	1.071	1.312	0.913	1.119
0.032" MEMBRANE 0.016" MEMBRANE	16 17	0.046 0.047	0.704 0.720	0.798 0.993	0.562 0.714		
4	19	0.072	1.103	0.857	0.944	0.769	0.848
	20	0.065	0.995	0.866	0.862	0.823	0.819
5	21	0.060	0.919	1.131	1.038	0.949	0.871
	22	0.066	1.011	0.904	0.914	0.753	0.761
6	24	0.0426	0.652	0.727	0.481	0.658	0.429
	25	0.0504	0.772	0.955	0.724	0.772	0.596
7	26	0.0484	0.741	0.754	0.545	0.683	0.506
	27	0.0478	0.732	0.993	0.717	0.821	0.601

NOTES: 1. AVERAGE PEAK POSITIVE AMPLITUDE (APPA) =

2. KDF (UNCORRECTED) = (APPA)TEST (APPA)BASELINE

3. NORMALIZATION FACTORS:

N1 = P2BASELINE, N2 = (P2 + P3)BASELINE,

P2TEST (P2 + P3)TEST

4. (KDF)₁ = (KDF) x N₁ (KDF)₂ = (KDF) x N₂

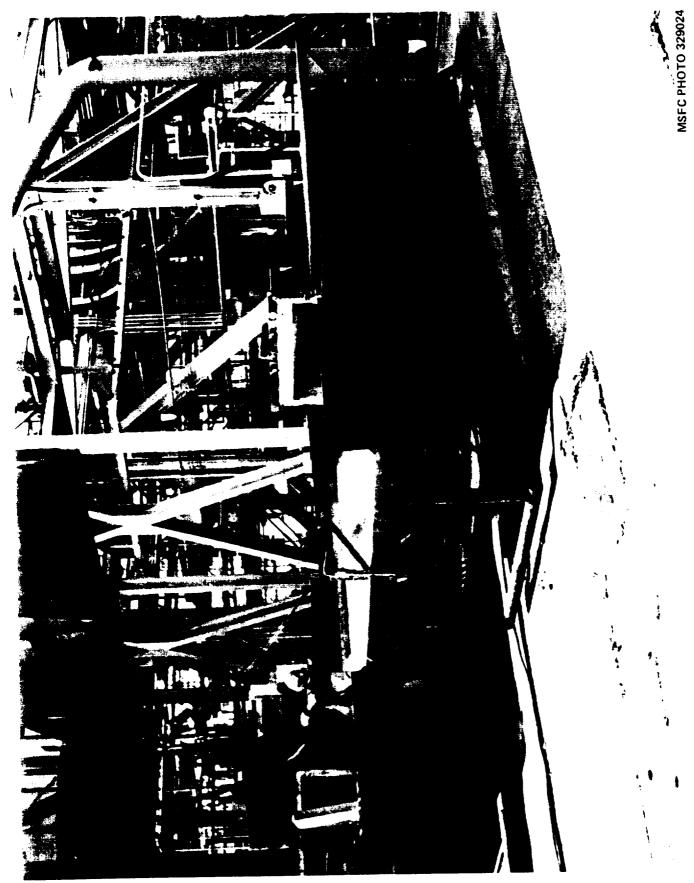
TABLE A-3 AMPLITUDE ATTENUATION AND HALF-PERIODS FOR MUFFLER CONFIGURATIONS 2, 6, AND 7

MUFFLER CONFIGURATION	AVERAGE AMPLITUDE ATTENUATION, PERCENT	AVERAGE CHANGE IN HALF-PERIOD WIDTH, PERCENT
2	35.6	19 (INCREASE)
6	39.4	NEGLIGIBLE
7	36.9	5 (INCREASE)

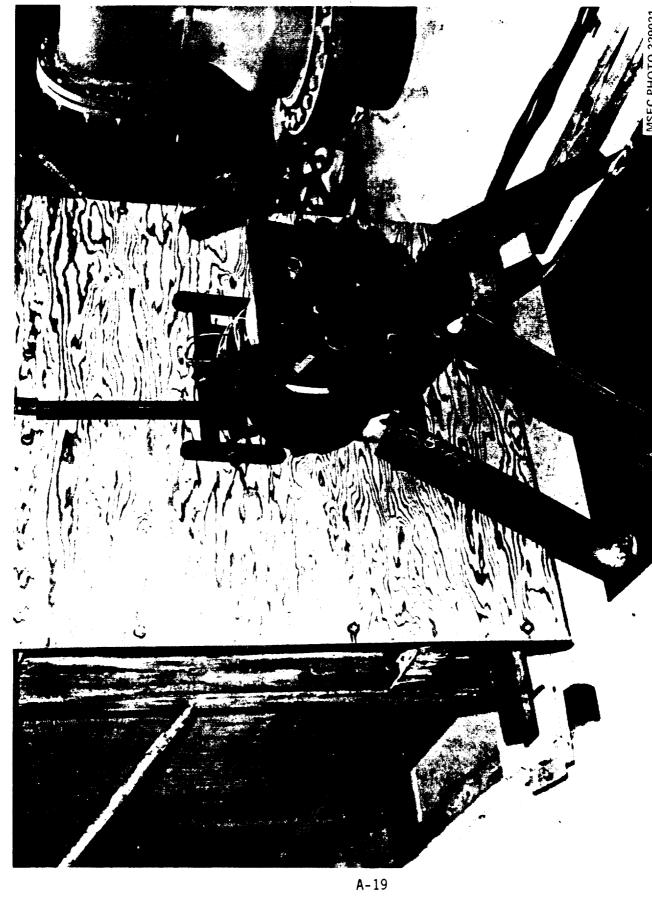
TABLE A-4 DUCT SECTION ORGAN-PIPE MODE RELATIONSHIPS

TEST	TEST	TEMP	TEMP °R	a ft/sec	f Hz	L in/Hz
CONFIGURATION	NO.	°F	K	10/360	114	
BASELINE	1 2 3	65 58 66	52 5 51 8 52 6	1124.5 1117.0 1125.6	31.4 32.0 31.6	107.4 104.8 106.9
	10	77	537	1137.3	32.8	104.0
2 (UNBRACED)	4 5 11	67 69 77	527 529 537	1126.7 1128.8 1137.3	30.6 30.0 30.0	110.5 112.7 113.7
2 (STEEL BRACING)	14 15	76 77	536 537	1136.3 1137.3	29.7 28.8	114.8 118.5
3	6 7	72 68	532 528	1132.0 1127.7	30.3 30.0	112.9 112.8
1	8 9	57 70	517 530	1115.9 1129.9	31.7 31.3	105.7 108.3
STRAIGHT DUCT EXTENSION	13 18	81 47	541 507	1141.6 1105.1	30.3 22.7	113.0 146.0
0.032" MEMBRANE 0.016" MEMBRANE		72 70	532 530	1132.0 1129.9	30.6 31.7	110.9 106.9
4	19 20	59 59	519 519	1118.1	29.7 29.1	112.9 115.3
5	21 22	61 61	521 521	1120.2	30.3 30.8	110.9 109.1
6	24 25	4 5 52	50.5 51.2	1102.9 1110.5	29.7 29.7	111.4 112.7
7	26 27	35 50	495 510	1090.2 1106.6	29.4 30.0	111.2

FIGURE A-1. "OFF-LINE" TEST ARRANGEMENT



A-18



INTERNAL VOLUME = 692.6 IN³

 $R_{C} = 4.47 \text{ IN}$

 $D_N = 2.40 IN$

 $L_N = 6.05 IN$

L_C = 5.13 IN

WHERE SUBSCRIPT N DENOTES THE "POPPER" NOZZLE AND SUBSCRIPT C DENOTES THE "POPPER" CHAMBER

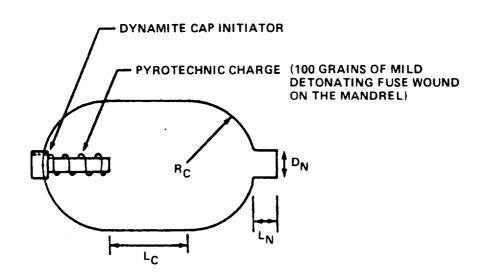
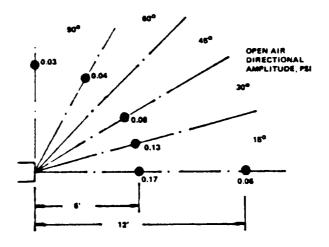


FIGURE A-3 "POPPER" INTERNAL GEOMETRY
AND EXPLOSIVE CHARGE DETAILS



a. PRESSURE FIELD (DELTA P), PSI

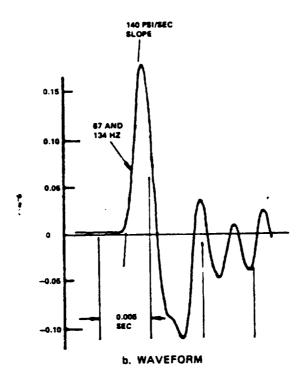
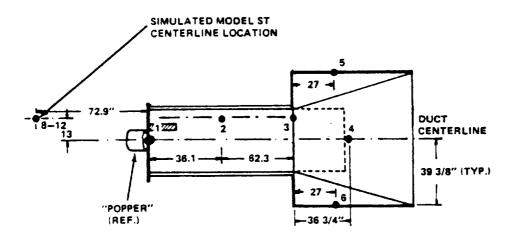
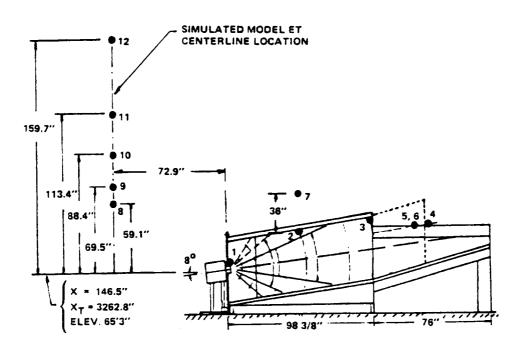


FIGURE A-4 "POPPER" CALIBRATION DATA FROM OPEN-AIR TESTING



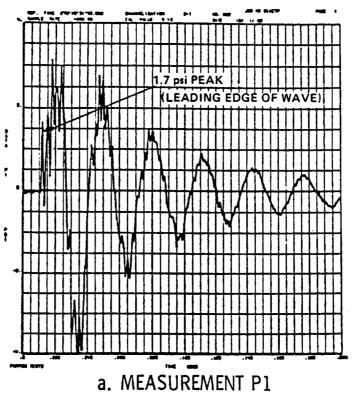
a. PLAN VIEW

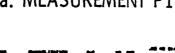
FIGURE A-5. OVERPRESSURE MEASUREMENT LOCATIONS FOR "OFF-LINE" TESTS

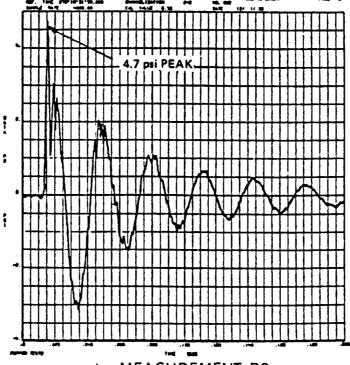


b. ELEVATION VIEW

FIGURE A-5, (CONCLUDED)

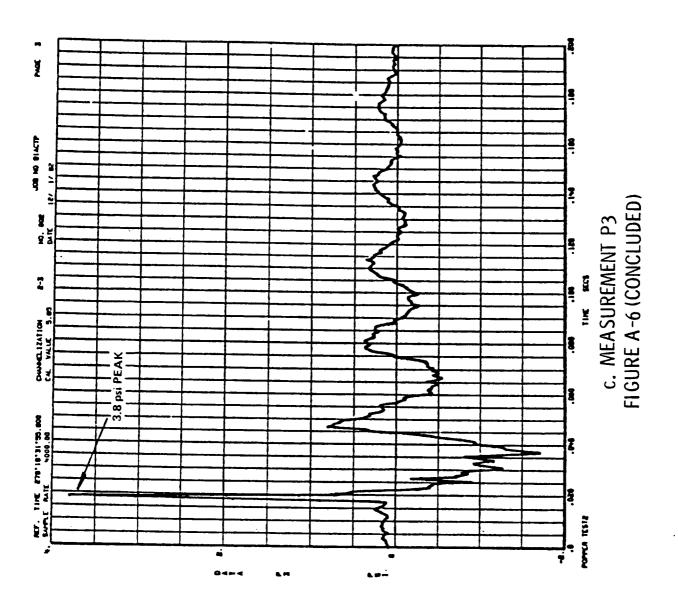




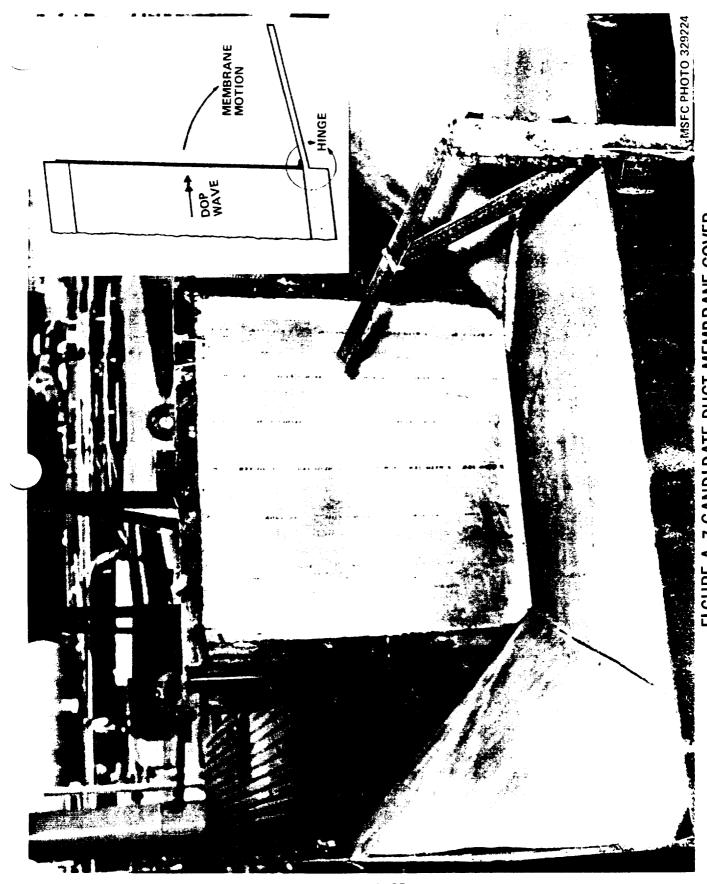


b. MEASUREMENT P2

FIGURE A:-6 TYPICAL "POPPER" OVERPRESSURE WAVE DATA INSIDE THE DUCT SECTION



A-24



A-25



A-25 A

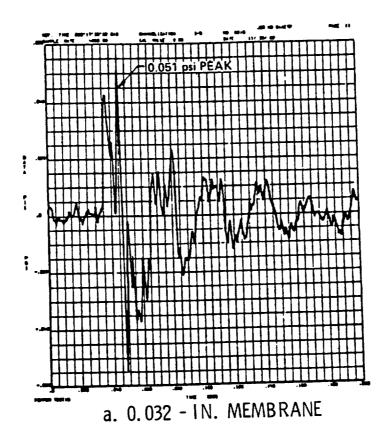


A-26

			·
1			



A-27



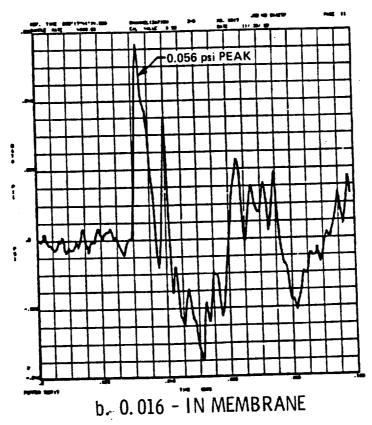
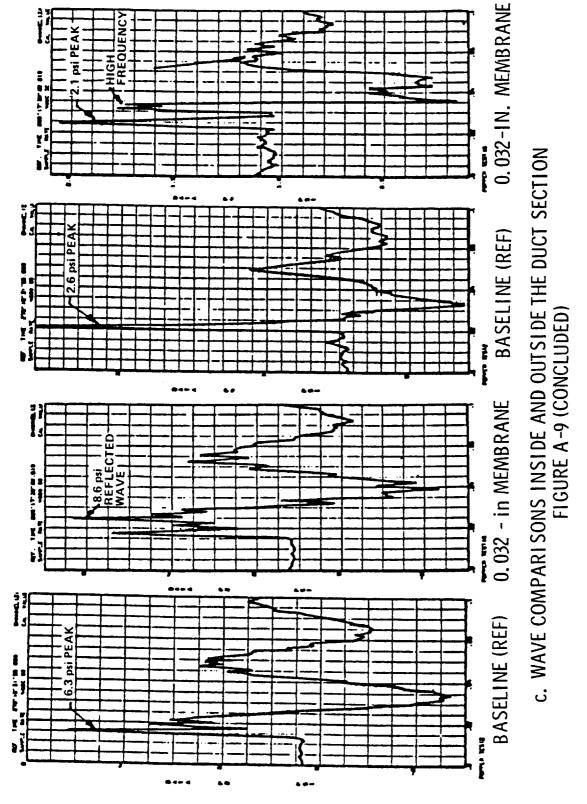


FIGURE A-9 DUCT MEMBRANE COVER TEST DATA
A-28



A-29

NOTE: ALL DIMENSIONS IN INCHES

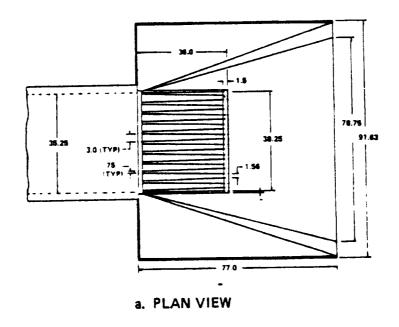
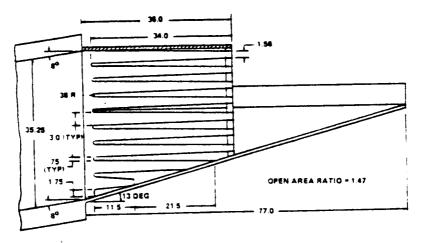
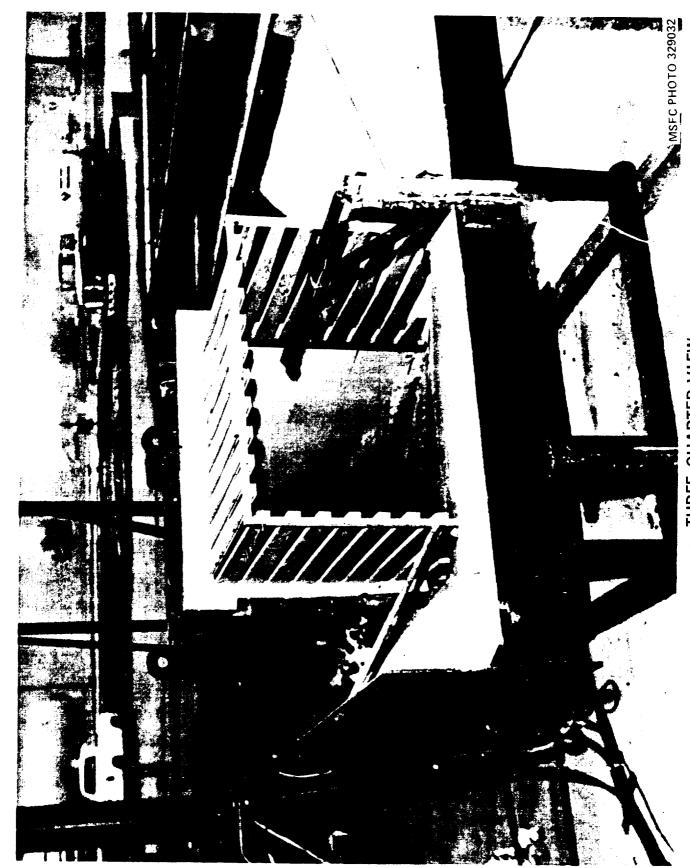


FIGURE A-10. CANDIDATE MUFFLER CONFIGURATION 1



b. ELEVATION VIEW

FIGURE A-10 (CONTINUED)



A-31

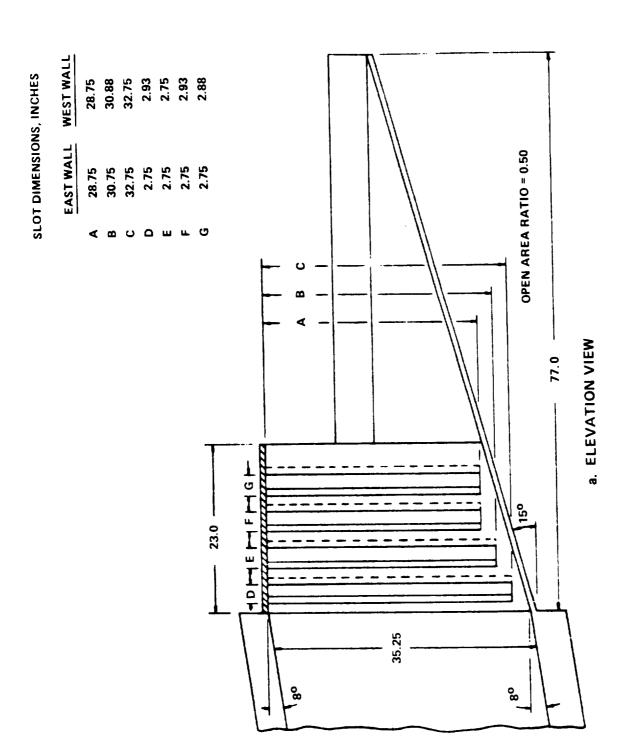
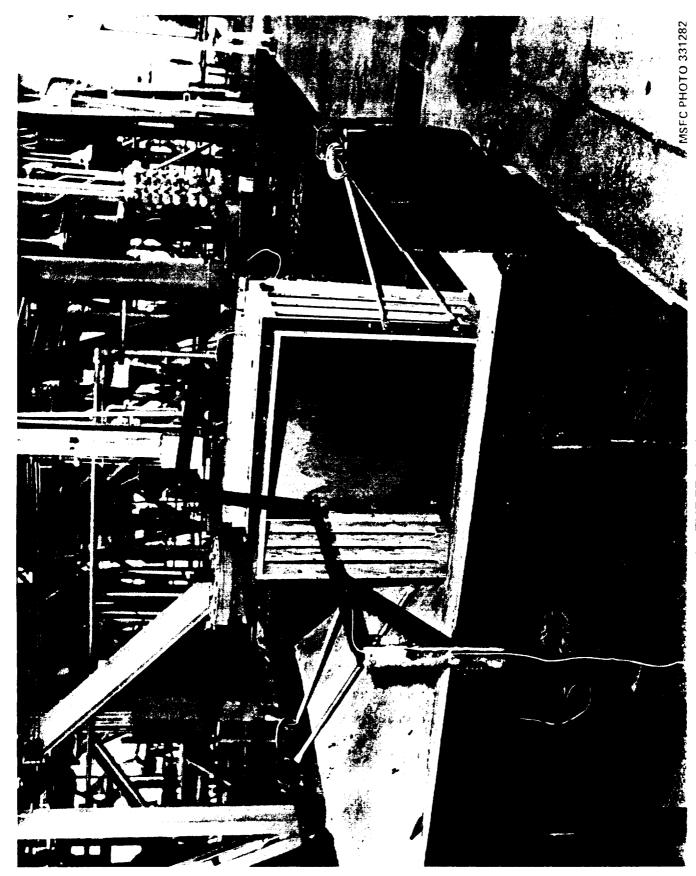


FIGURE A-11 CANDIDATE MUFFLER CONFIGURATIONS



A-33

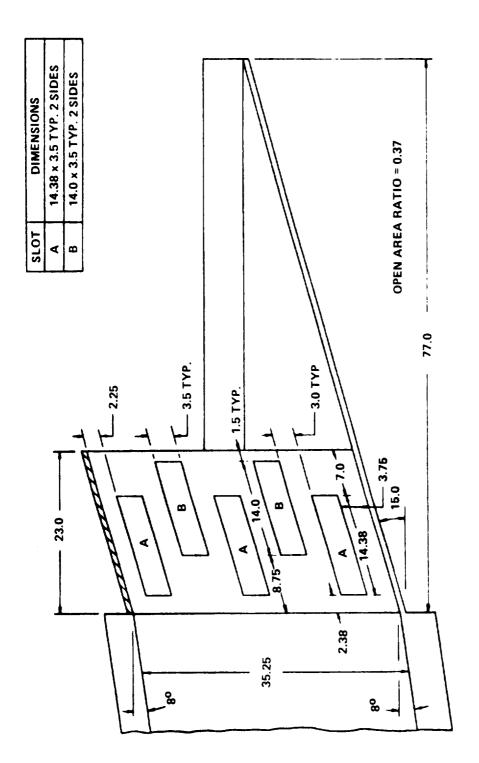
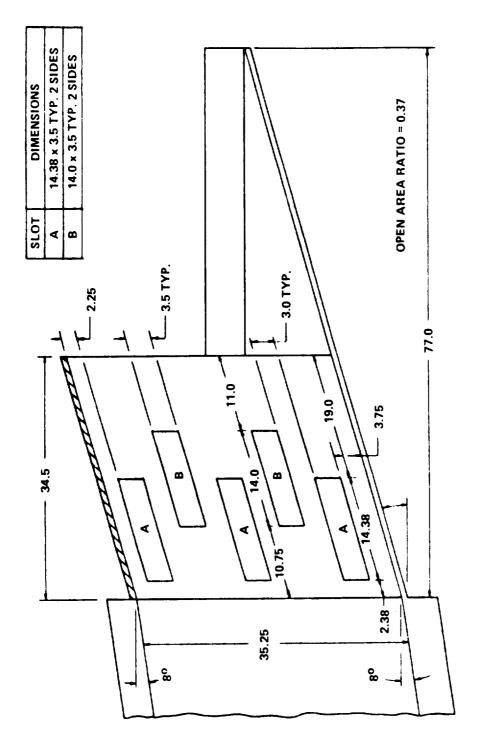
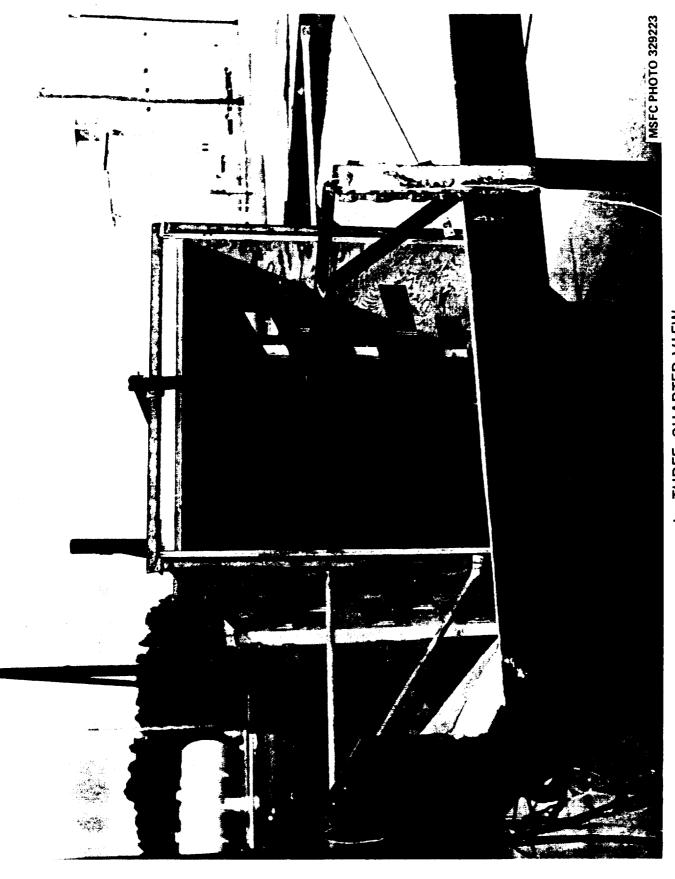


FIGURE A-12. CANDIDATE MUFFLER CONFIGURATION 4



a. ELEVATION VIEW

FIGURE A-13. CANDIDATE MUFFLER CONFIGURATION 2



A-36

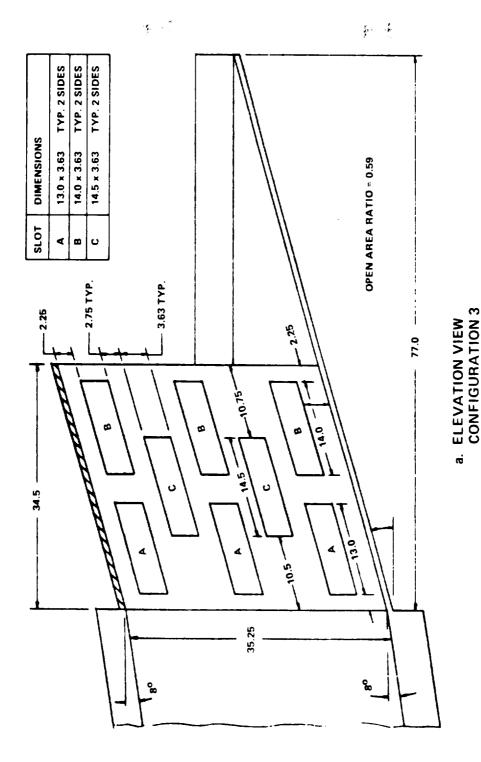


FIGURE A-14. CANDIDATE MUFFLER CONFIGURATION 3

b. THREE-QUARTER VIEW FIGURE A-14 (CONCLUDED)

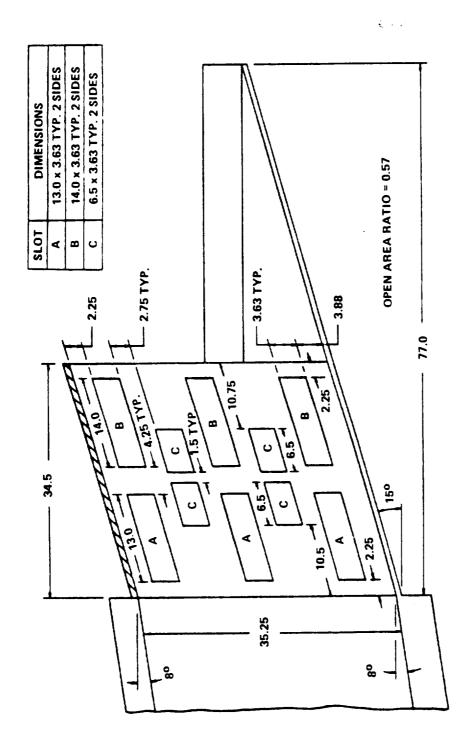


FIGURE A-15. CANDIDATE MUFFLER CONFIGURATION 6

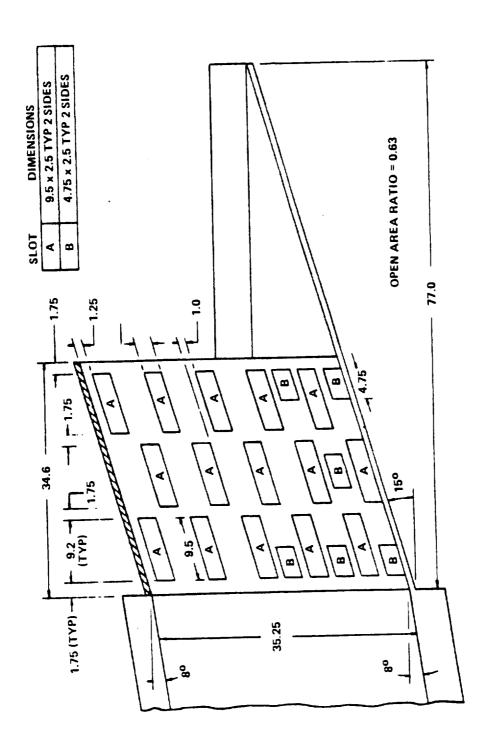
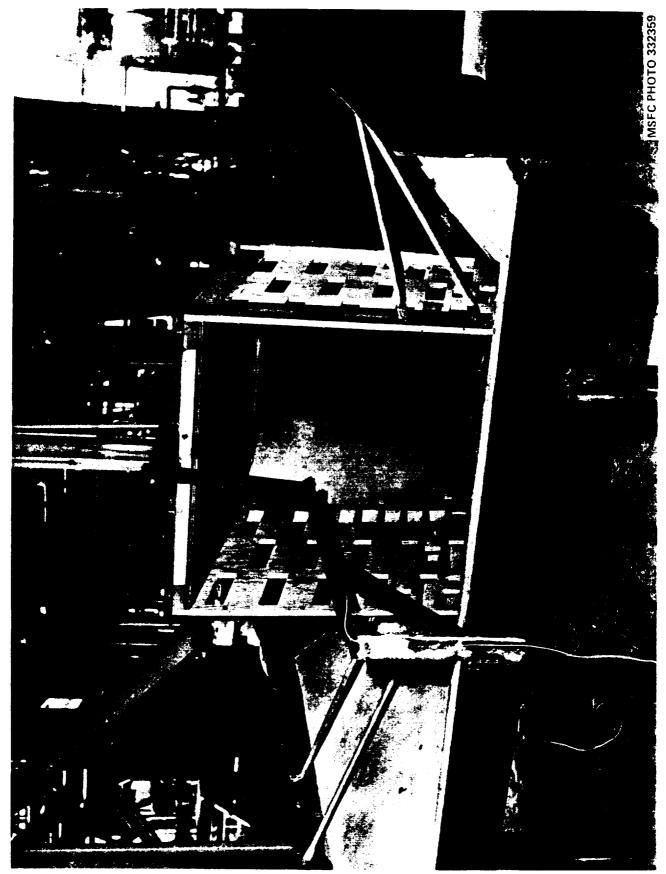


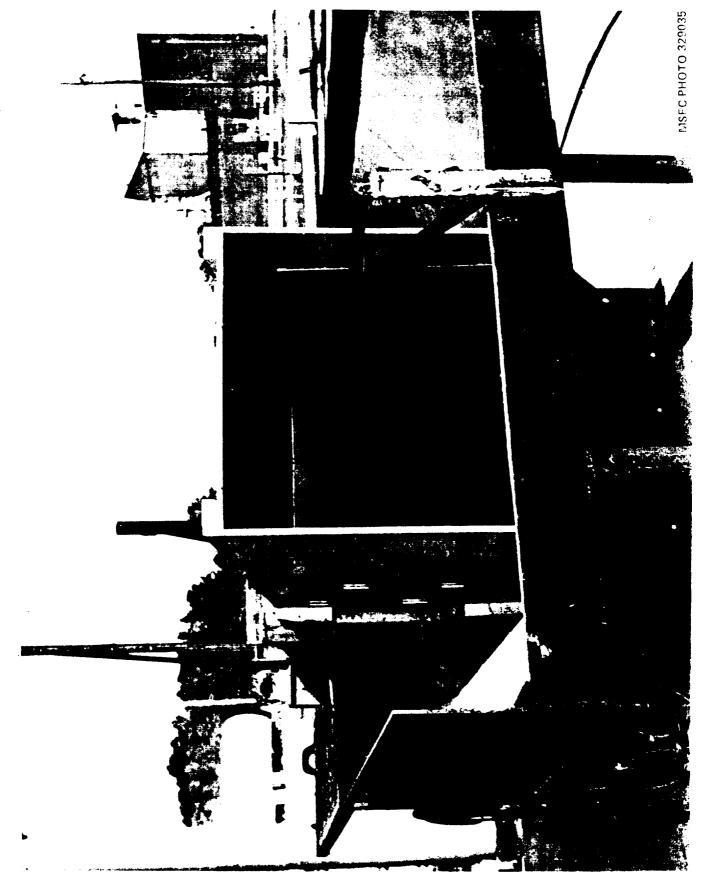
FIGURE A-16. CANDIDATE MUFFLER CONFIGURATION 7



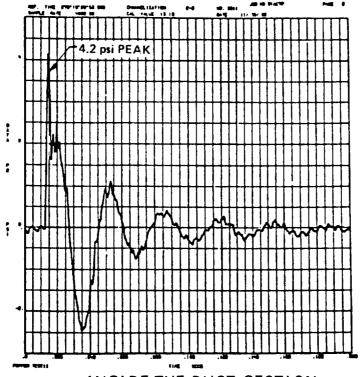
A-41

NOTE: THREE-COLUMN CONCRETE MUFFLER

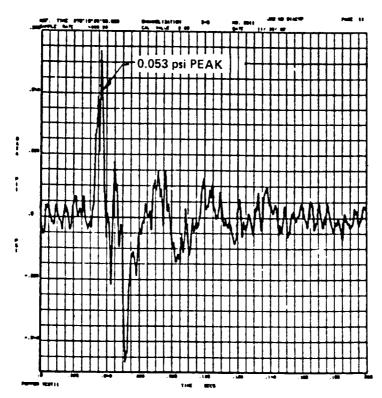
FIGURE A-17 ARTIST'S CONCEPT OF A FULL-SCALE CONFIGURATION 6 MUFFLER IN CONCRETE



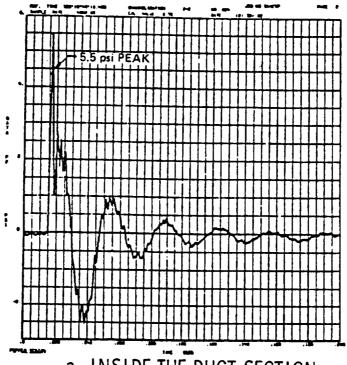
A-43

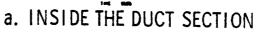


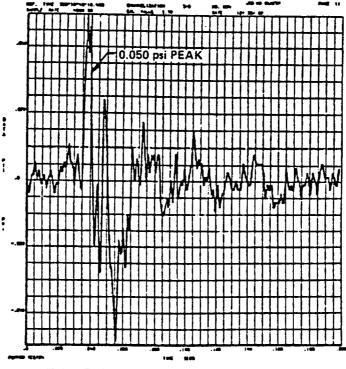




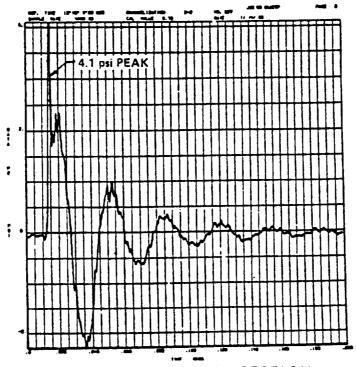
b. AT THE SIMULATED VEHICLE LOCATION
 FIGURE A-19 OVERPRESSURE DATA
 CANDIDATE MUFFLER CONFIGURATION 2



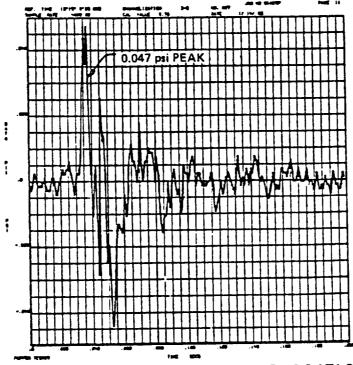




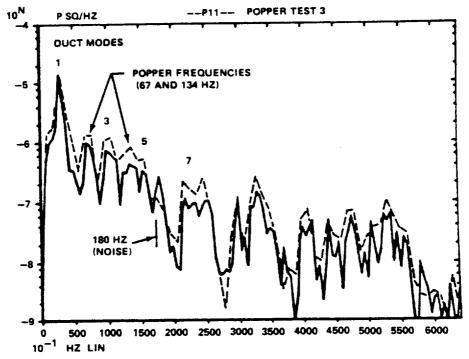
b. AT THE SIMULATED VEHICLE LOCATION
FIGURE A -20 OVERPRESSURE DATA
-- CANDIDATE MUFFLER CONFIGURATION 6



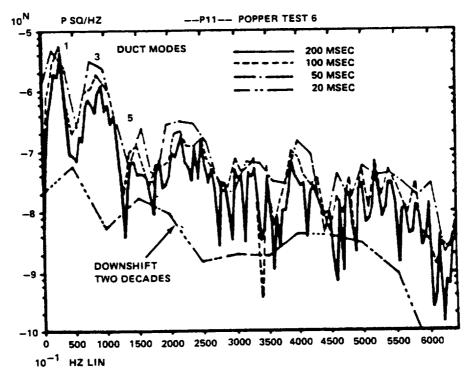




b. AT THE SIMULATED VEHICLE LOCATION FIGURE A-21 OVERPRESSURE DATA -- CANDIDATE MUFFLER CONFIGURATION 7

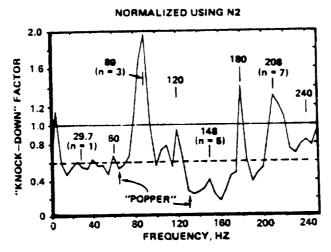




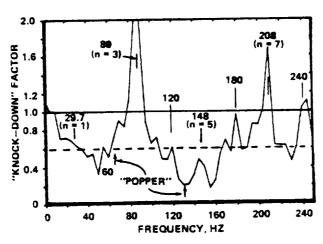


b. MUFFLER CONFIGURATION 3

FIGURE A-22. POWER SPECTRAL DENSITY DATA -- BASELINE AND MUFFLER CONFIGURATION 3 EXAMPLE



a. MUFFLER CONFIGURATION 2



b. MUFFLER CONFIGURATION 6

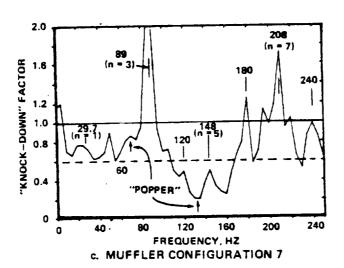
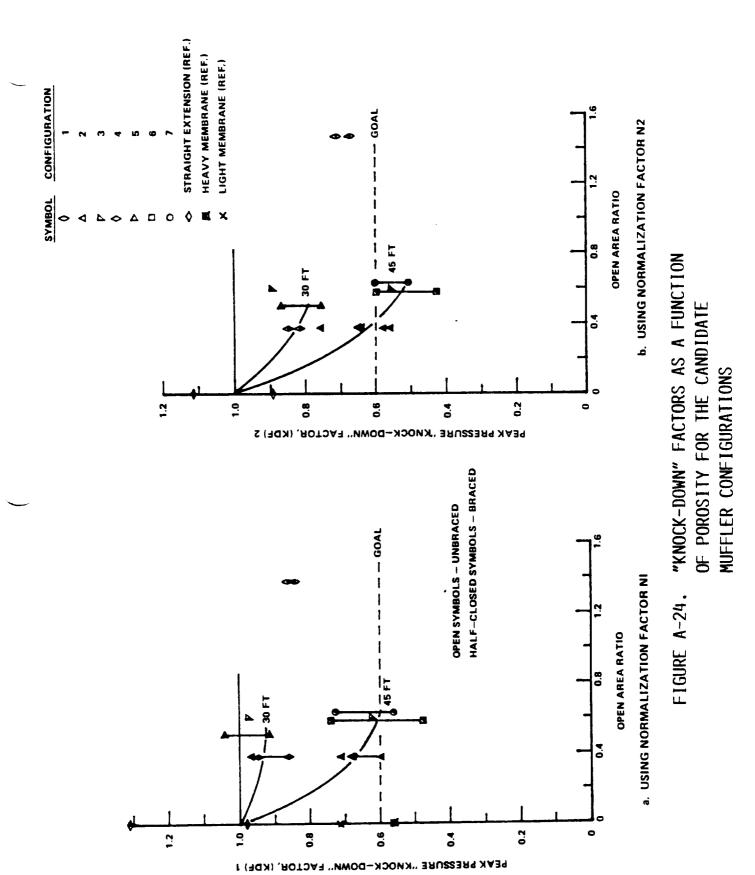
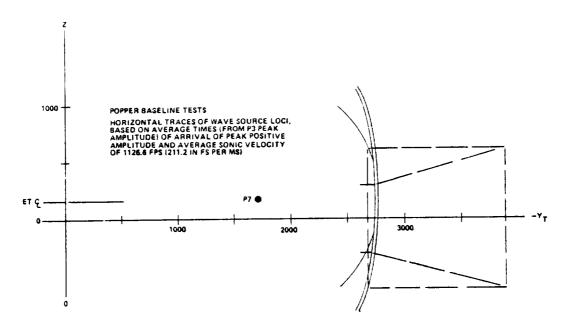


FIGURE A-23. "KNOCK-DOWN" FACTORS AS A FUNCTION OF FREQUENCY FOR THE CANDIDATE MUFFLER CONFIGURATIONS $_{\rm A-48}$

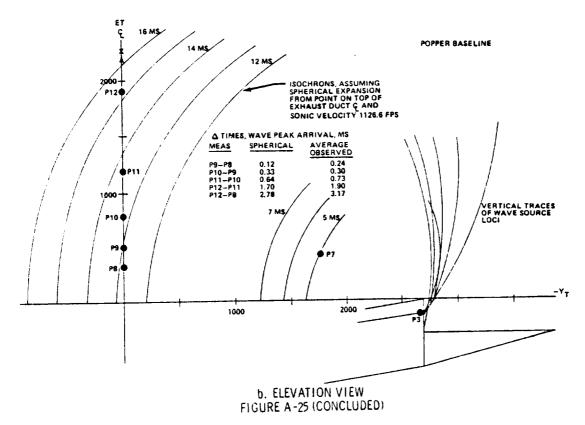


A-49



a. PLAN VIEW
FIGURE A-25 APPARENT WAVE SOURCE LOCATION
DETERMINED FROM WAVE ARRIVAL TIMING
AT THE SIMULATED VEHICLE LOCATION

R-ENG 446



R-ENG 447

APPENDIX B

SRM MODEL IGNITION EXCESSIVE DELAY

•				
				e manifest de la constitución de
				. •
				···· ·
	1			

APPENDIX B

SRM Model Ignition Excessive Delay

The intent of this appendix is to show differences in circumstances for overpressure wave generation that existed in Tests 11 and 13 and inconsistencies in the chamber pressures ignition rise data observed. During a normal Tomahawk motor ignition, the exponentially – decaying igniter pulse has not completely diminished before the ignition-rise-related overpressure is generated and phase coupling of the overpressure with the still-present igniter waves may influence the strength of the overpressure. Ignition rise came 0.642 sec after T_0 in Test 11 and 0.438 sec after T_0 in Test 13. The igniter pulse had diminished in both cases. Instead, there were small motor-generated pressure oscillations in the SRB exhaust duct and evident on the model vehicle with other possibilities for coupling effects than normal ignition cases. These are shown in detail herein. The chamber pressure rise data had unusual characteristics and was unusually high.

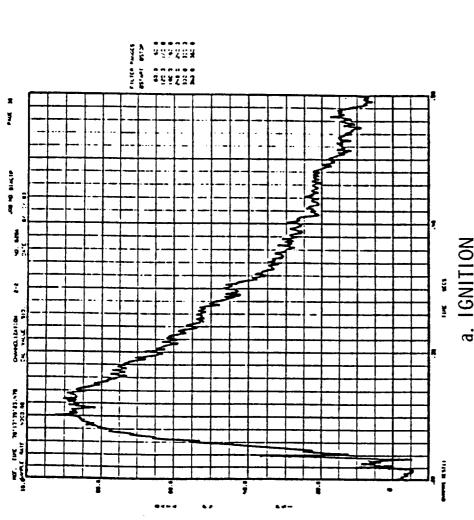
An expanded - scale Tomahawk motor chamber pressure trace for Test 11 is shown in Figure B-1. The chamber pressure rose initially to 88 psig and then decayed down to about 10 psig. Each motor case strain gage recorded a spike when the igniter fired and then oscillations of up to 30 micro inches peak-to-peak in the delay period before the ignition rise occurred as seen in Figure B-2. When the ignition rise did finally occur, the overpressure was generated in a relatively quiescent precursor environment $(\pm 0.005 \text{ psi})$ as seen, for example, in a duct internal measurement in Figure B-3.

The conditions under which the overpressure generated occurred were about the same in Test 13. There was an initial rise to about 27 psig when the igniter fired in Test 13 as seen in Figure B-4. Period oscillations appeared in the motor case strain data as large as 37 microin/in peak-to-peak as seen in Figure B-5. Oscillations with the same frequency (50-to-55 Hz) evident in the motor case strain data appeared in all the model duct and vehicle overpressure data at the same time. The oscillations grew to as large as 0.1 psi peak-to-peak in the duct as seen, for example, in Figure B-6, but had decayed about 20 msec prior to the generation of the ignition - rise overpressure.

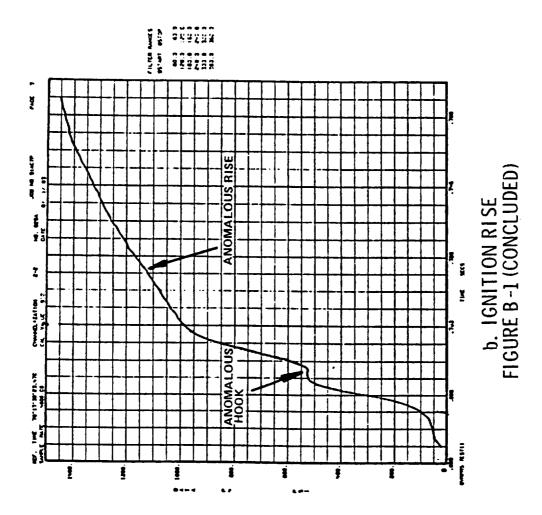
It is further noted about the Test 11 and 13 ignition transients that the first Pcmax peaks in chamber pressure exceeded the second where it is normal for the first to be smaller than the second in Tomahawk motors. This was not true of the head-end strain, the second peak being large as usual. Additionally, there was a hook in the chamber pressure curve instead of a saddle point at the time of maximum strain rate at the nozzle end. The computed derivatives for the chamber pressure and strain data are shown in Figures 8-8 and 8-9 for Tests 11 and 13, respectively. The measured Pcmax values are critical for normalization of overpressure amplitudes to the 50,000 psi/sec reference value. Both the Test 11 and the Test 13 indicated values are unusually high. The head-end strain rate measurements was made as a back-up to the chamber pressure in case the chamber pressure data proved unusable. Whether or not the strain rise rate data should be preferred in these two cases is deferred to trend analysis of the overpressures data. This Appendix serves to point out the inconsistencies observed in the chamber pressure rise rate data.

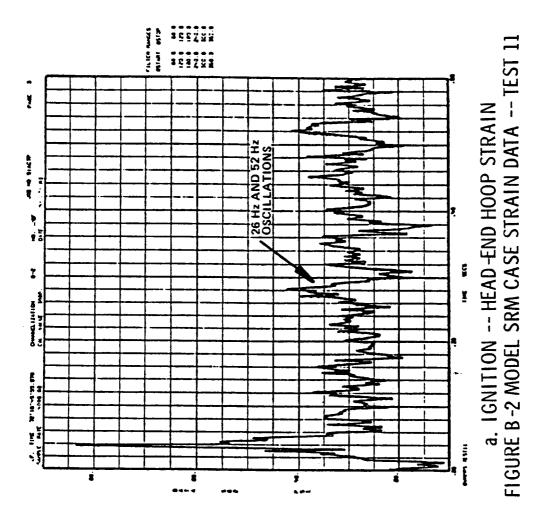
ILLUSTRATIONS

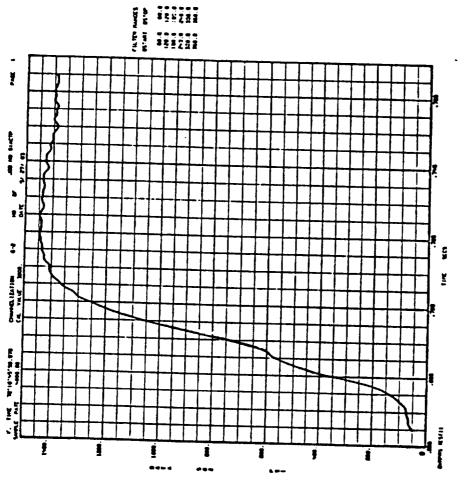
Figure		<u>Page</u>
B-1	Model SRM Chamber Pressure Data Test 11	B-4
B-2	Model SRM Case Strain Data Test 11	B-6
B-3	Model SRB Duct Internal Overpressure Measurement Test 11	B-10
B-4	Model SRM Chamber Pressure Data Test 13	B-11
B-5	Model SRM Case Strain Data Test 13	B-13
B-6	SRB Duct Internal Overpressure Measurement Test 13	B-17
B-7	Typical Overpressure Measurement on the Model Vehicle Test 13	B-18
B-8	Computed Model SRM Chamber Pressure and Case Strain Rise Rate Histories Test 11	B-19
B-9	Computed Model SRM Chamber Pressure and Case Strain Rise Rate Histories Test 13	B - 22



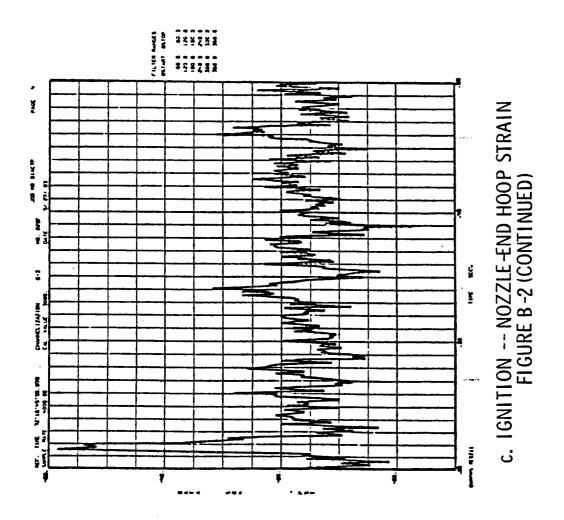
a. IGNITION FIGURE B-1 MODEL SRM CHAMBER PRESSURE DATA-- TEST 11

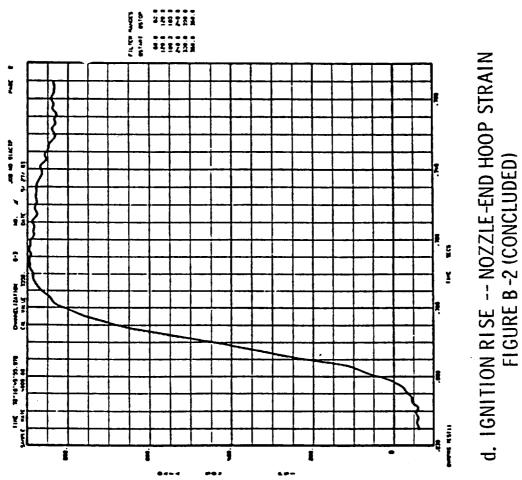


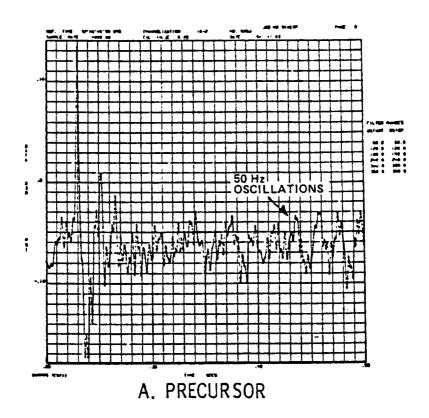




b. IGNITION RISE -- HEAD-END HOOP STRAIN FIGURE B-2 (CONTINUED)







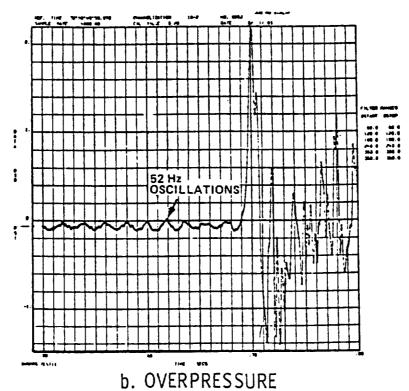
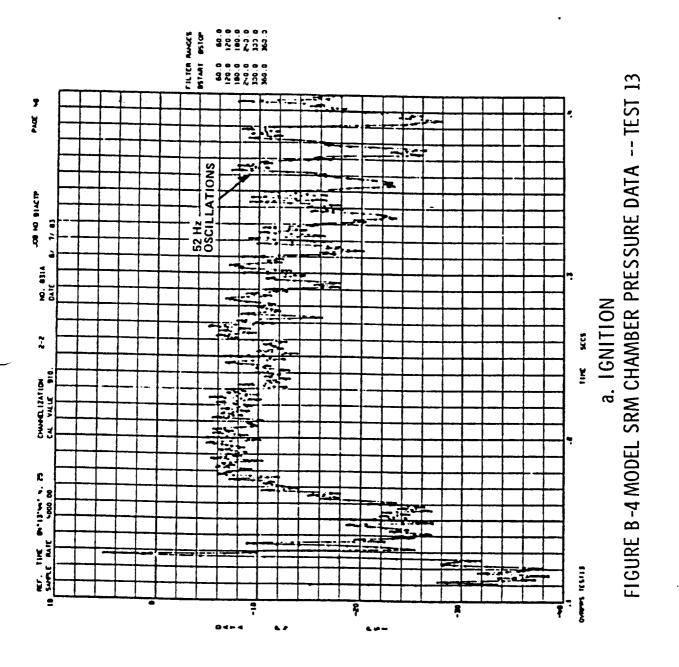
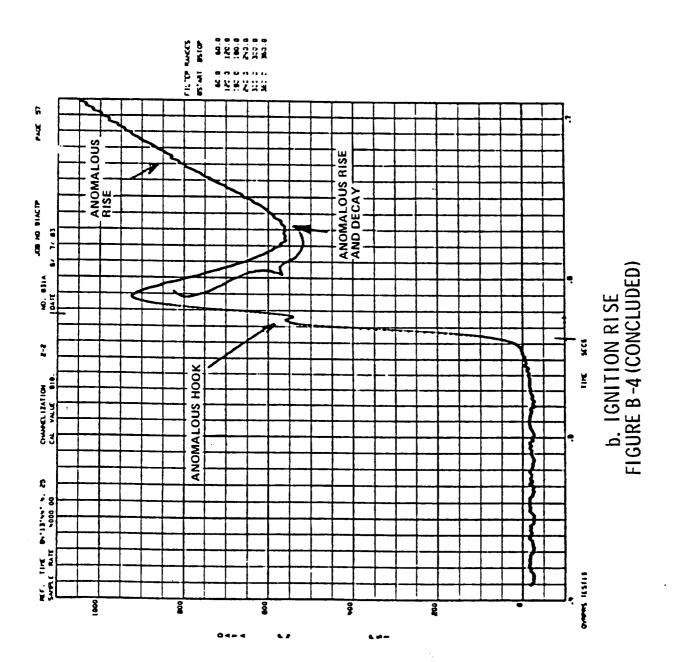
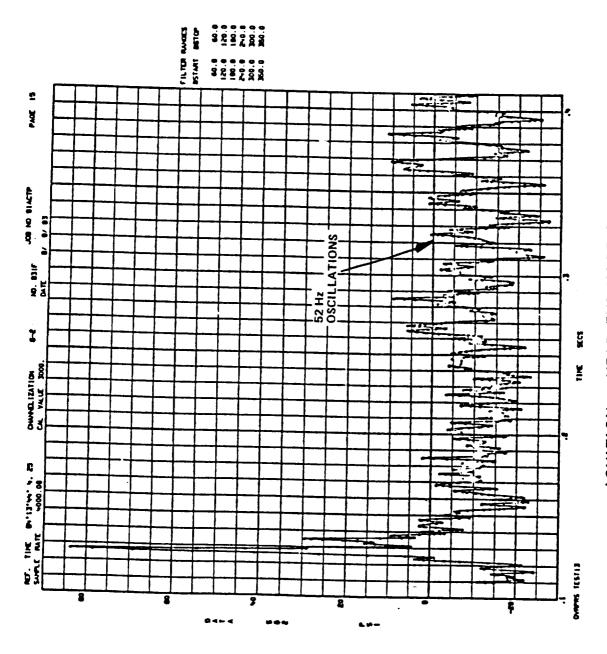


FIGURE B -3 SRB DUCT INTERNAL OVERPRESSURE MEASUREMENT -- TEST 11

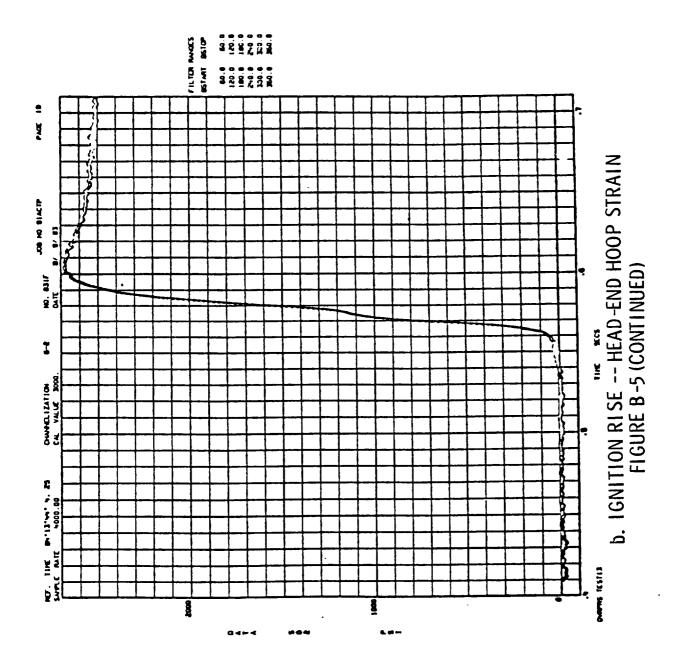


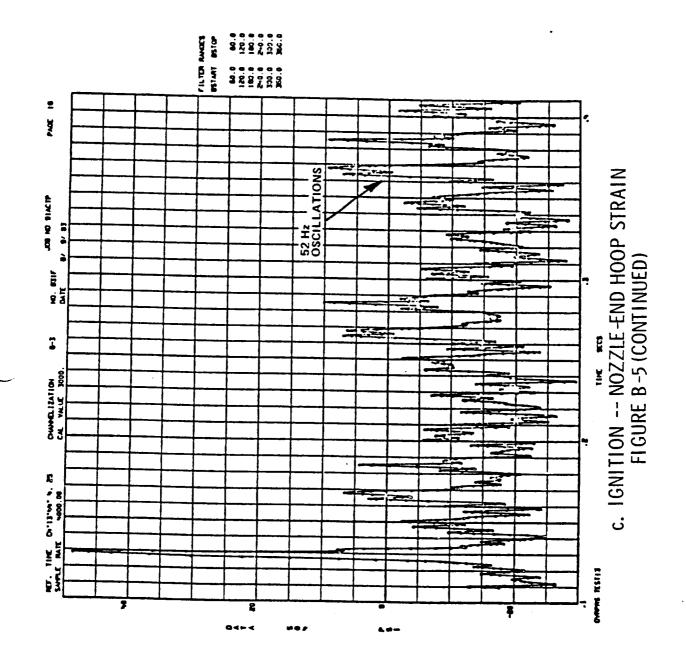


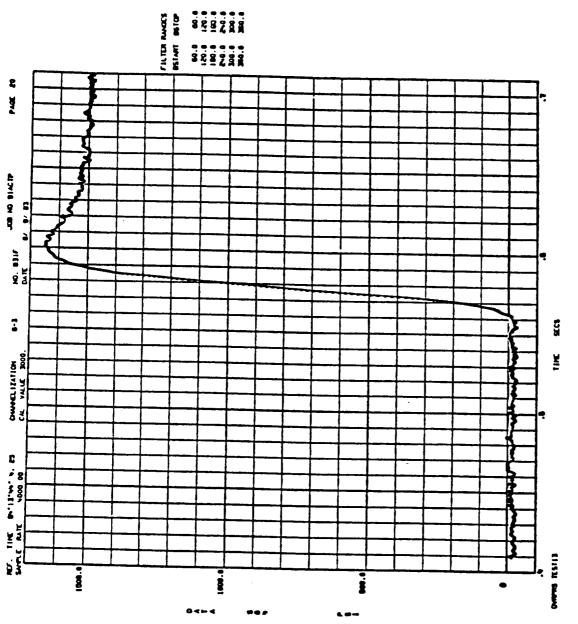
B-12



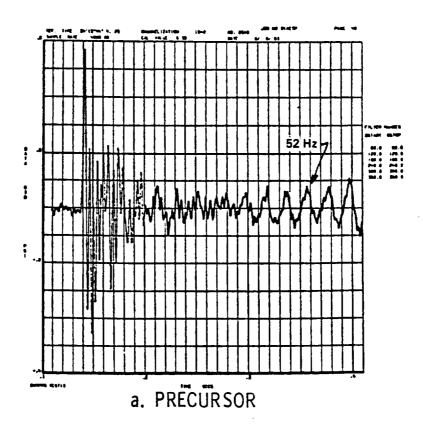
a. IGNITION -- HEAD-END HOOP STRAIN FIGURE B -5 MODEL SRM CASE STRAIN DATA -- TEST 13

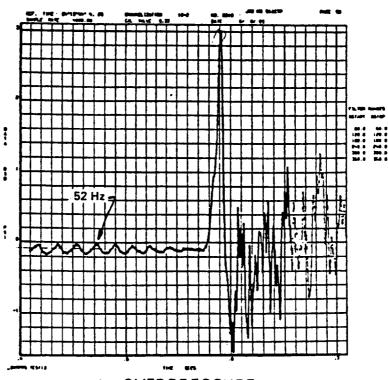




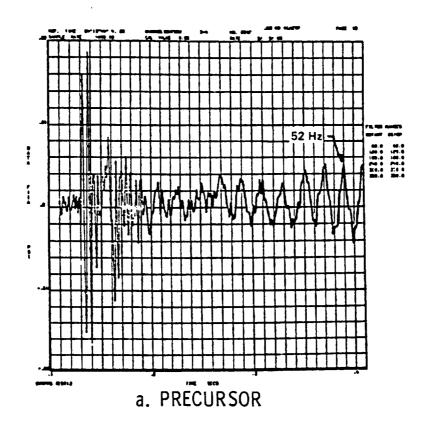


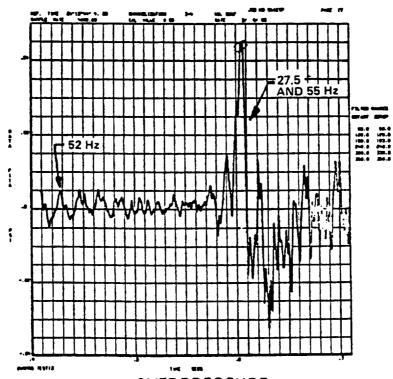
d. IGNITION RISE -- NOZZLE-END HOOP STRAIN FIGURE B-5 (CONCLUDED)



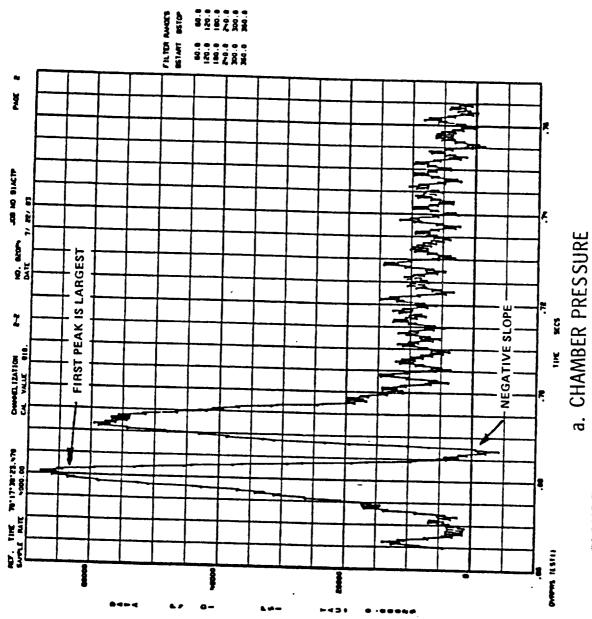


b. OVERPRESSURE
FIGURE B -6 SRB DUCT INTERNAL OVERPRESSURE MEASUREMENT
-- TEST 13
B-17
R-ENG 549

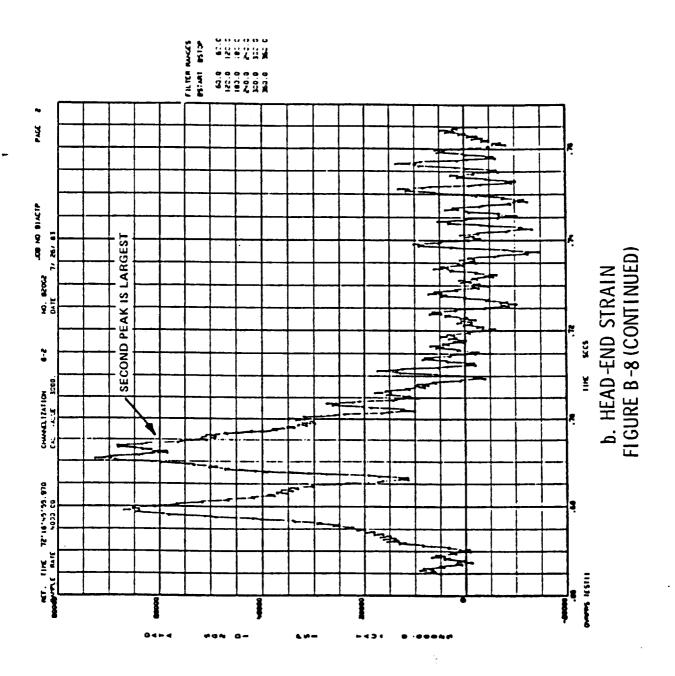


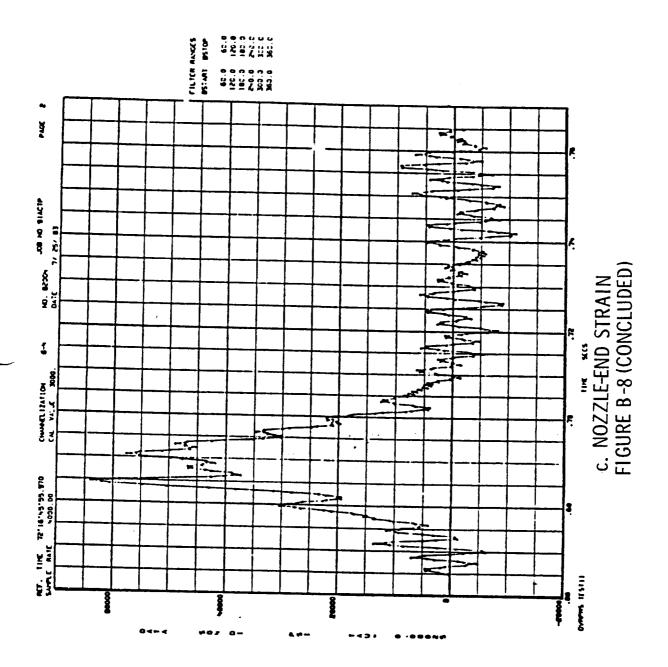


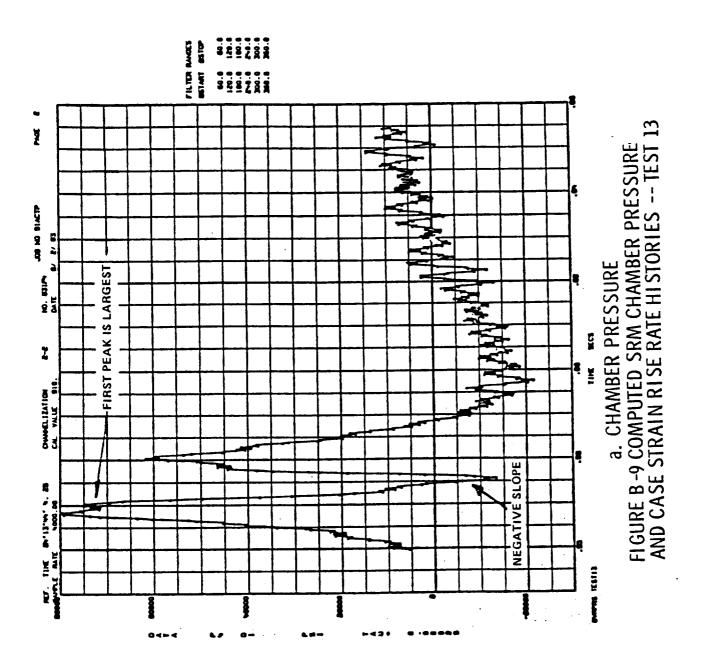
b. OVERPRESSURE FIGURE B-7 TYPICAL OVERPRESSURE MEASUREMENT ON THE MODEL VEHICLE -- TEST 13

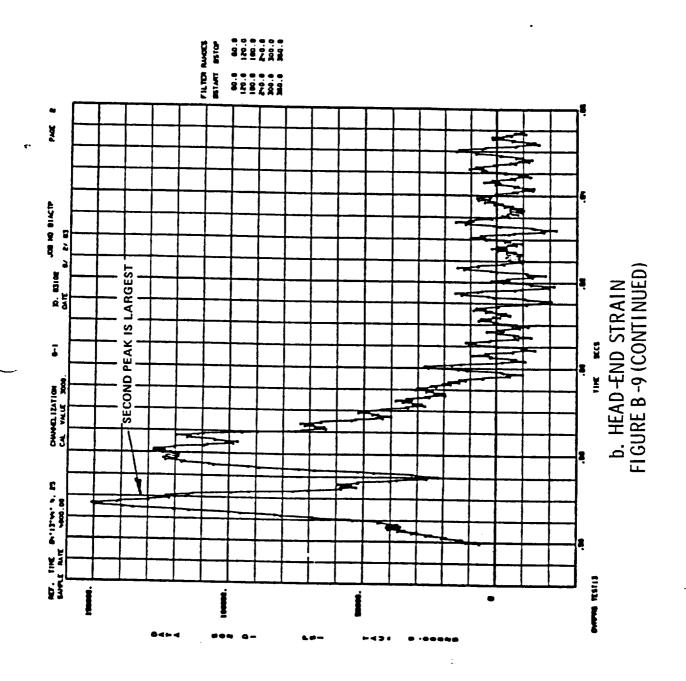


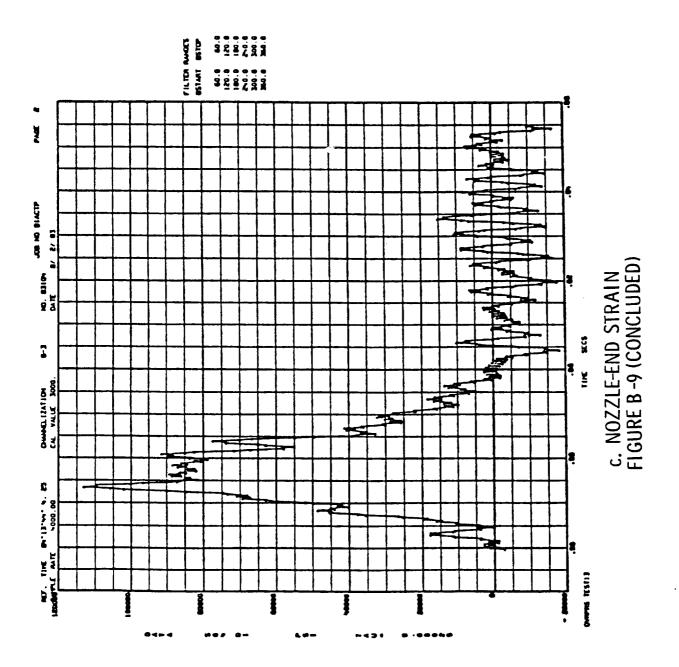
4. CHAMBER PRESSURE
FIGURE B -8 COMPUTED SRM CHAMBER PRESSURE
AND CASE STRAIN RISE RATE HISTORIES -- TEST 11











B-24

APPENDIX C

SPIKES IN MODEL SRM CHAMBER PRESSURE

1			

APPENDIX C

Spikes in Model SRM Chamber Pressure

The ignition transient data presented in this report for many of the SRM overpressure tests performed have interminable pressure rise still indicated after the ignition transient was complete. A less than complete reporting of these data would leave questions about chamber pressure rising to a peak so close after completion of the ignition transient as to how one defines the ignition transient without including such an obvious peak. It is a fact that such peaks were prevalent to the extent they became the rule in the WTR test program, rather than the exception, despite concerted efforts by MSFC's Test Lab to isolate any measurement fault that might explain them. No such spikes occurred in the ETR model test program, Reference 1.

This Appendix shows the terminus in each spike together with the motor case strain and nozzle exit static pressure data, where available. This Appendix also shows the spike to be peculiar to the head-end internal chamber pressure measurement made in each motor and not corroborated by a rise in either the case strain or the nozzle exit static pressure. There was just one spike. It occurred shortly after ignition. It was not totally uncorrelated. It could not be simply dismissed as an instrument fault. It can only be classified as an unexplained anomaly.

The Test 7 Tomahawk motor exhibited a "normal" chamber pressure time history. The Test 7 data are shown in Figure C-1. There are two X's on the time scale in this and subsequent plots; they denote the Water Valves Open Command at time zero and then SRB Ignition Command, respectively. The motor manufacturer's stated nominal thrust and combustion pressure time histories for the Tomahawk motor are shown in Figure C-2 with a maximum peak expected in chamber pressure of 1200 psig corresponding to a maximum thrust of 15,000 lb (for the basic motor without the simulated HPM nozzle extension). Figure C-2 thus shows what is the normal. All the recent ETR model overpressure testing in Reference 1 and three of the WTR Model overpressure screening tests in Reference 2 had normal chamber pressure histories.

The anomaly is peculiar to the recent WTR model tests beginning with Test 4 (Reference 2). This anomaly is not peculiar to tests with the model vehicle at zero elevation. To show that, Test 42 provides an example that the anomaly also occurred with SRM start at 60 ft simulated elevation above the model launch mount.

The time-history data from Tests 5 and 6 are shown in Figures C-3 and C-4, from Tests 8 through 16 in Figures C-5 through C-13, from Test 40 in Figure C-14, and from Test 42 in Figure C-15. The amplitude of the spike and its time of occurrence varied from test to test. Both motors in Test 42 had a spike. Neither hoop-tension strain gage corroborated the chamber pressure spike.

No conclusions are drawn from this appendix. Conclusions are left to subsequent analysis of the data. The purpose here is only to present evidence that an anomaly existed in the chamber pressure data from the majority of the tests performed and that this anomaly could not be dismissed as an instrumentation (transducer, cable, or signal conditioner) fault. These DSU data are shown only in the appendix and are not a part of the final overpressure data packages also appendaged to this report. The DSU data are stored on ASCII tapes on file at MSFC's Test Lab from which the plots presented herein were produced on a Hewlett-Packard 9420 computer.

ILLUSTRATIONS

Figure		Page
C-1	Model SRM Performance Data Test 7	C-4
C-2	Motor Manufacturer's Stated Nominal Performance	C-5
C-3	Model SRM Performance Data Test 5	C-6
C-4	Model SRM Performance Data Test 6	C-7
C-5	Model SRM Performance Data Test 8	C-8
C-6	Model SRM Performance Data Test 9	C-8
C-7	Model SRM Performance Data Test 10	C-9
C-8	Model SRM Performance Data Test 11	C-9
C-9	Model SRM Performance Data Test 12	C-10
C-10	Model SRM Performance Data Test 13	C-10
C-11	Model SRM Performance Data Test 14	C-11
C-12	Model SRM Performance Data Test 15	C-11
C-13	Model SRM Performance Data Test 16	C-12
C-14	Model SRM Performance Data Test 40	C-13
C-15	Model SRM Performance Data Test 42	C-14

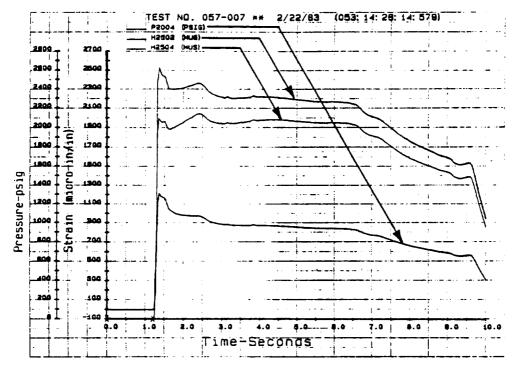


FIGURE C-1 MODEL SRM PERFORMANCE DATA -- TEST 7

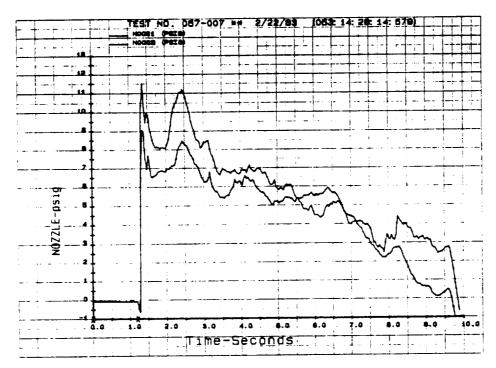


FIGURE C-1 (CONCLUDED)

COURTESY OF MORTON—THIOKOL CORPORATION AT SEA LEVEL AND 60°F AMBIENT TEMPERATURE

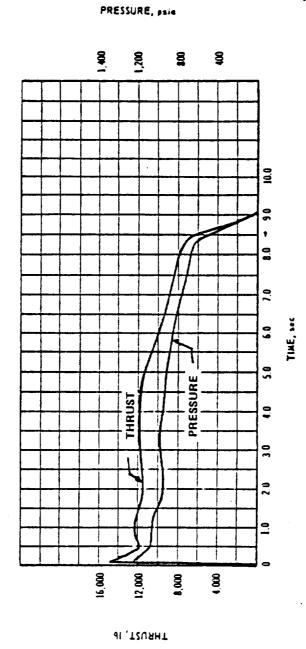


FIGURE C-2 MOTOR MANUFACTURER'S STATED NOMINAL PERFORMANCE

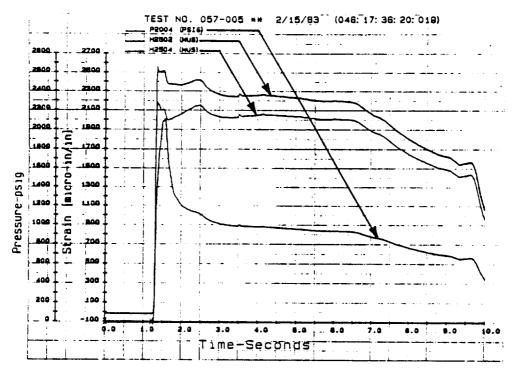


FIGURE C-3 MODEL SRM PERFORMANCE DATA -- TEST 5

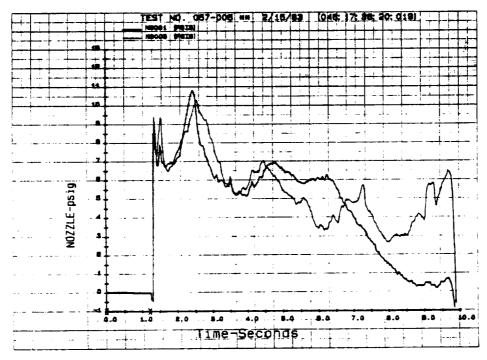


FIGURE C-3 (CONCLUDED)

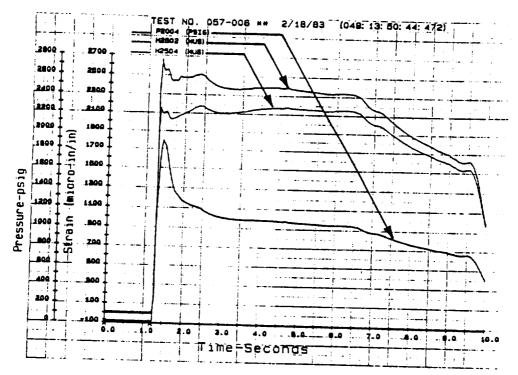


FIGURE C-4 MODEL SRM PERFORMANCE DATA -- TEST 6

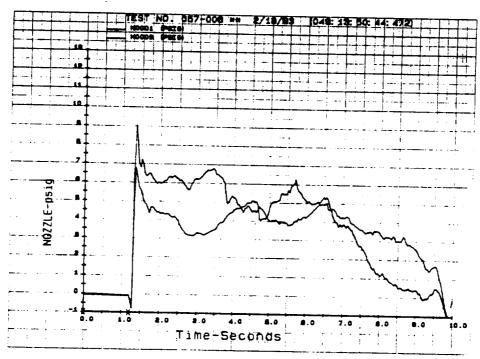


FIGURE C-4 (CONCLUDED)

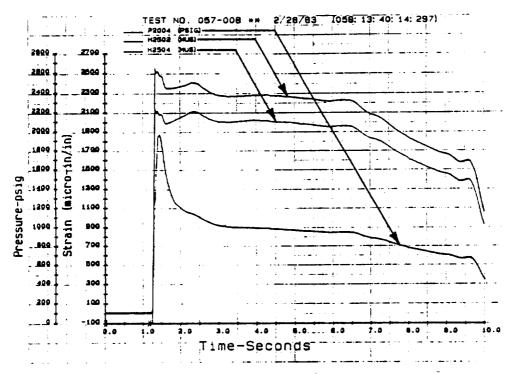


FIGURE C-5 MODEL SRM PERFORMANCE DATA -- TEST 8

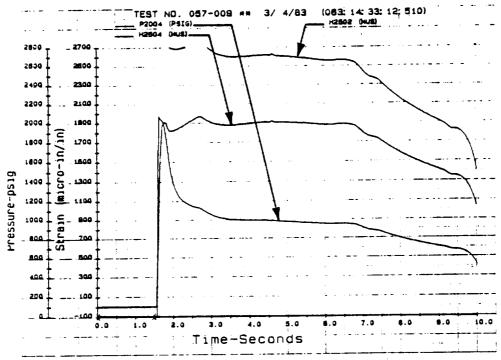


FIGURE C-6 MODEL SRM PERFORMANCE DATA -- TEST 9

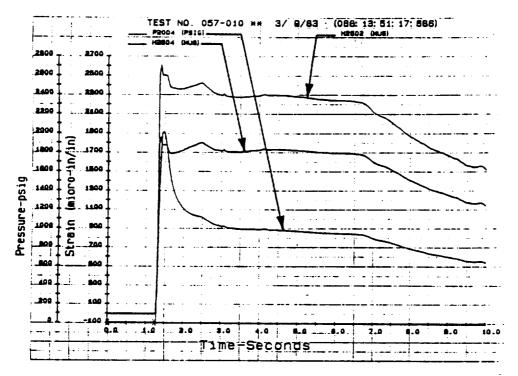


FIGURE C-7 MODEL SRM PERFORMANCE DATA -- TEST 10

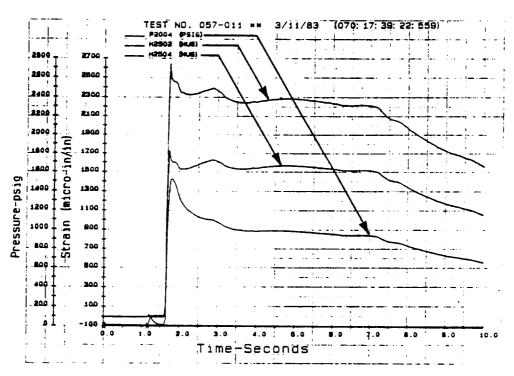


FIGURE C-8 MODEL SRM PERFORMANCE DATA -- TEST 11

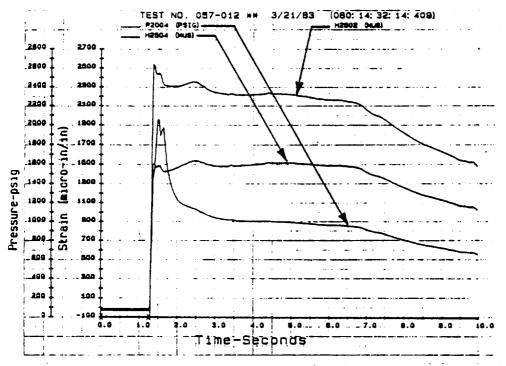


FIGURE C-9 MODEL SRM PERFORMANCE DATA -- TEST 12

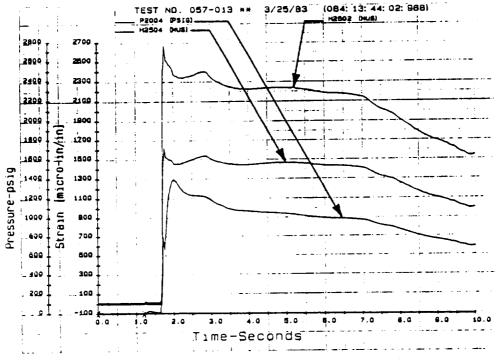


FIGURE C-10 MODEL SRM PERFORMANCE DATA -- TEST 13

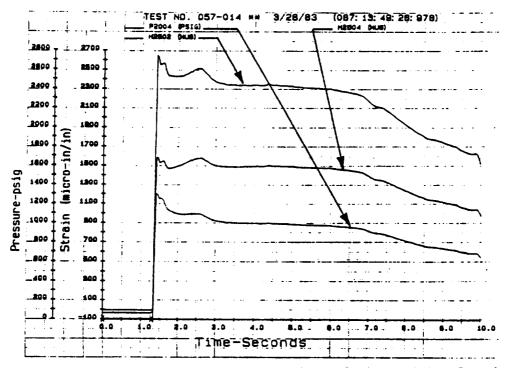


FIGURE C-11 MODEL SRM PERFORMANCE DATA -- TEST 14

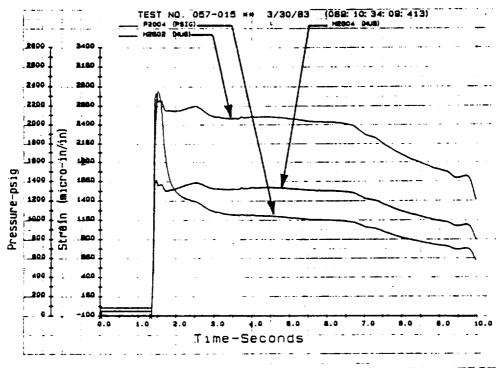


FIGURE C-12 MODEL SRM PERFORMANCE DATA -- TEST 15

C-11

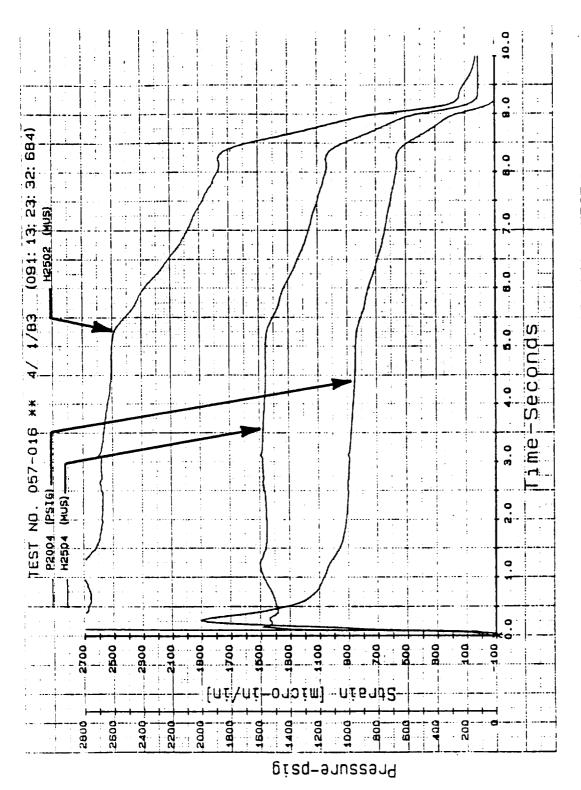


FIGURE C-13 MODEL SRM PERFORMANCE DATA -- TEST 16

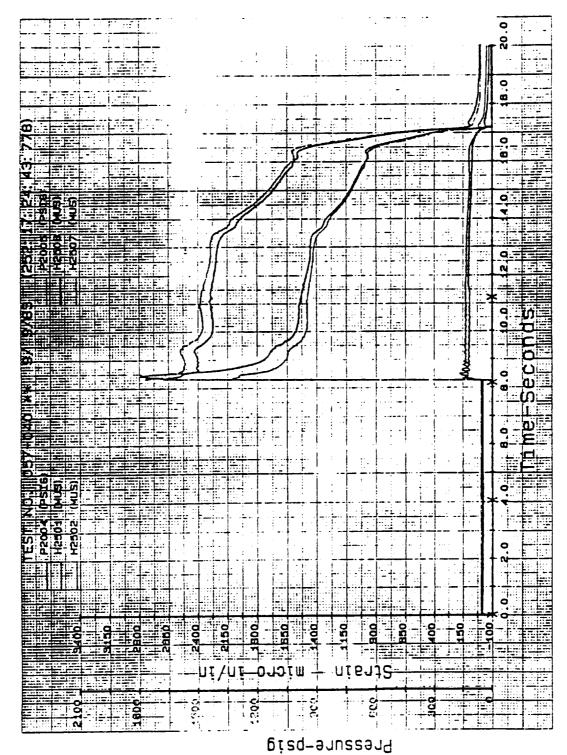


FIGURE C-14 MODEL SRM PERFORMANCE DATA -- TEST 40

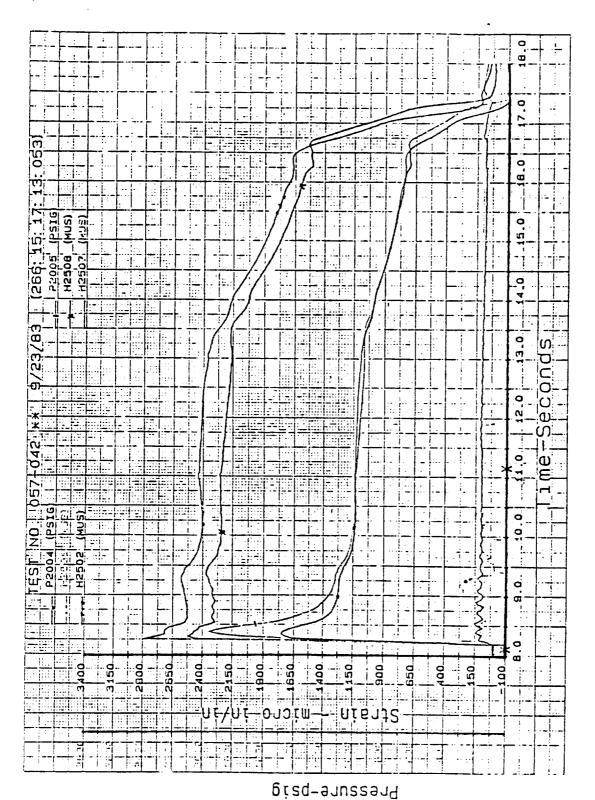


FIGURE C-15. MODEL SRM PERFORMANCE DATA -- TEST 42